

**The Regulatory Role of MtrA and NsrR in
*Streptomyces coelicolor***

Felicity Joy Knowles

Thesis Submitted for the Biomolecular Sciences Research Degree of
Doctor of Philosophy

School of Biological Sciences,
University of East Anglia

March 2014

© This copy of the thesis has been supplied on condition that anyone who consults it is understood to recognise that its copyright rests with the author and that use of any information derived there from must be in accordance with current UK Copyright Law. In addition, any quotation or extract must include full attribution.

Abstract

Streptomyces coelicolor inhabits a harsh soil environment, which it must adapt and respond to; therefore how *S. coelicolor* senses and responds to its environment is of the utmost importance. This project addresses two types of regulation system: the three-component system MtrAB-LpqB and the nitrite-sensitive repressor NsrR. Previous work involving the response regulator MtrA has resulted in the hypothesis that MtrA regulates cell division within actinomycetes. However the role of MtrAB-LpqB within *S. coelicolor* has not been investigated. Therefore it is important to establish whether cell division is disrupted within mutants of the *sco3014-lpqB* operon. Removing components of the MtrAB-LpqB system resulted in actinorhodin production and spore formation being altered. The irregular spore structure seen by scanning electron microscopy (SEM) may be due to the difference in *ftsZ* expression, which could account for the irregularly placed septum and spore size observed. Therefore this work confirms that MtrAB-LpqB is important for cell division within *S. coelicolor*. Work was also carried out on the repressor NsrR to establish its role within *S. coelicolor* as previous findings had primarily focused on the type of Fe-S cluster contained within NsrR. The phenotype of an *nsrR* mutant exhibited a low level of spore production, similar to the distinctive, development whi phenotype. Some Whi proteins function via an [4Fe-4S] cluster, which is also central to NsrR regulation meaning NsrR could be linked to the Whi proteins within *S. coelicolor*. To understand NsrR function further, ChIP-seq was undertaken to identify direct targets; revealing, contrary to prediction studies, NsrR represses only three targets: *hmpA1*, *hmpA2* and *nsrR*. These targets were confirmed by *in vitro* binding studies with purified *S. coelicolor* NsrR. Therefore this work reveals that NsrR undergoes auto-regulation and its sole role is to regulate nitric oxide (NO) stress response via detoxification within *S. coelicolor*.

Table of Contents

	Page
Abstract	1
Abbreviations	7-8
List of Figures and Tables	9-11
Dedication	12
Acknowledgements	13
1. General Introduction	14-29
1.1. Actinobacteria	14-15
1.2. <i>Streptomyces</i>	16-17
1.3 <i>Streptomyces</i> Differentiation	17-25
1.3.1. <i>Streptomyces coelicolor</i> Lifestyle	17-21
1.3.2. Polarised Growth and Cell Division	21-25
1.4. Soil Environment	25-26
1.5. Antibiotic Production	26-27
1.6. Two Projects	28-29
2. Materials and Methods	30-61
2.1. General Methods	30-44
2.1.1. Bacterial Strains and Plasmids	30-32
2.1.2. Solid Media	33-34
2.1.3. Liquid Media	34-36
2.1.4. Antibiotic Concentrations	37
2.1.5. Buffers and Solutions	37-38
2.1.6. Primers	39
2.1.7. Polymerase Chain Reaction (PCR)	40
2.1.8. PCR Purification	40
2.1.9. Restriction Digestion	40
2.1.10. Agarose Gel Electrophoresis	41
2.1.11. Gel Extraction	41
2.1.12. Ligation	41

2.1.13. Transforming Electro-Competent <i>E. coli</i>	41-42
2.1.14. Transforming Chemically-Competent <i>E. coli</i>	42
2.1.15. Storing <i>E. coli</i> Using Glycerol Stocks	42
2.1.16. Storing <i>E. coli</i> Using Microbank Bead Stocks	43
2.1.17. Plasmid Preparation	43
2.1.18. Phenol/Chloroform Extraction	43
2.1.19. Sequencing	43-44
2.2. Generating Mutations in <i>Streptomyces</i>	44-51
2.2.1. Strategy for Producing Mutants in <i>S. coelicolor</i>	44-45
2.2.2. PCR of the Disruption Cassette	45
2.2.3. Transforming <i>E. coli</i> with Cosmid DNA	45
2.2.4. Cosmid Isolation	46
2.2.5. PCR Targeting Cosmids in <i>E. coli</i>	46-47
2.2.6. Conjugation	47
2.2.7. Spore Stocks	48
2.2.8. Spore Quantification	48
2.2.9. Standardised Quantification	48
2.2.10. Chromosomal DNA Isolation from <i>Streptomyces</i>	48-49
2.2.11. Removal of the Apramycin Cassette in <i>nsrR</i> Mutants	49
2.2.12. Complementation of <i>mtrA</i> , <i>mtrB</i> and <i>lpqB</i> Mutations	49-50
2.2.13. Complementation of <i>nsrR</i> Mutation	50-51
2.3. Protein Analysis	51-53
2.3.1. Protein Extraction for SDS-Page Analysis	51
2.3.2. Bradford Assay	51
2.3.3. Protein Preparation for SDS-Page	51
2.3.4. SDS-Page Gel	52
2.3.5. Coomassie Staining	52
2.3.6. MtrA Western	53
2.3.7. α -Flag Western	53

2.4. Microscopy	54-55
2.4.1. Light Microscopy	54
2.4.2. Fluorescence Microscopy	54
2.4.3. Scanning Electron Microscopy (SEM)	55
2.5. Gene Expression	56-57
2.5.1. RNA Isolation from Solid Growth	56
2.5.2. RNA Isolation from Liquid Growth	56-57
2.5.3. qRT-PCR	57
2.6. Actinorhodin and Undecylprodigiosin Assay	57-58
2.6.1. Growth	57
2.6.2. Liquid Chromatography and Mass Spectrometry (LCMS)	57-58
2.6.3. Actinorhodin and Undecylprodigiosin Assay	58
2.7. DNA Binding	58-61
2.7.1. Constructing an <i>nsrR</i> 3XFlag Strain	58
2.7.2. ChIP-seq	59-60
2.7.3. GUS Assay	60-61
2.8. Statistical Analysis	61
3. Introduction for MtrA Project	62-74
3.1. Project Overview	62
3.2. Two-Component Systems (TCS)	63-68
3.2.1. Histidine Protein Kinase (HPK)	63-65
3.2.2. Response Regulators (RR)	65-66
3.2.3. Accessory Proteins	66-68
3.3. MtrAB-LpqB Component System	68-74
3.3.1. MtrB	68-69
3.3.2. MtrA	69-72
3.3.3. LpqB	73
3.3.4. SCO3014	73-74
3.4. Project Aims	74

4. Results for MtrA Project	75-113
4.1. Generation of Mutants	75
4.1.1. Strategy for Producing Mutants	75
4.1.2. Making In-Frame Mutants	75
4.2. Characterisation of <i>sco3014-mtrAB-lpqB</i> Mutants	76-95
4.2.1. Phenotype of <i>sco3014-mtrAB-lpqB</i> Mutants	76-81
4.2.2. Complementing the Mutants	82-87
4.2.3. Scanning Electron Microscopy (SEM)	88-95
4.3. Pigmented Antibiotic Production and Assay	96-102
4.3.1 Pigment Production	96-97
4.3.2 Liquid Chromatography and Mass Spectrometry (LCMS)	97-100
4.3.3. Measuring Pigmented Antibiotic Production	101-102
4.4 Exploring Potential MtrA Targets	103-112
4.4.1. ChIP-seq to Discover Targets	103-104
4.4.2. Is <i>ftsZ</i> a Target of MtrA?	105-107
4.4.3. Localisation of FtsZ	108-112
4.5. Results Summary	112-113
5. Introduction to the NsrR Project	114-129
5.1. Project Overview	114-115
5.2. Rrf2 proteins	115-119
5.2.1. Rrf2 family	115
5.2.2. IscR	115-118
5.2.3. Fe-S Cluster Biogenesis	118-119
5.3. Fe-S clusters	120-121
5.3.1. Function of Fe-S cluster Proteins	120-121
5.4. Nitric Oxide (NO)	121-124
5.4.1. NO and Fe-S Clusters	121-122
5.4.2. NO Sources	122-123
5.4.3. Sensing Nitrosative and Oxidative Stress	123-124
5.5. NsrR	124-128

5.6. Project Aims	129
6. Results for NsrR Project	130-151
6.1. Generation of <i>nsrR</i> Mutants	130-135
6.1.1. Strategy for Producing Mutants	130-131
6.1.2. Phenotype of $\Delta nsrR$ Mutant	131-132
6.1.3. Complementing the <i>nsrR</i> Mutation	133-135
6.2. Scanning Electron Microscopy (SEM)	136-138
6.3. Identifying NsrR Targets in <i>S. coelicolor</i>	139-150
6.3.1. Constructing an NsrR 3XFlag Tagged Strain	139-140
6.3.2. NsrR Targets Identified Using CHIP-seq	141-145
6.3.3. Confirming NsrR Targets	146-149
6.4. Results Summary	150
7. Discussion	151-162
7.1 MtrAB-LpqB Regulates Cell Division in <i>S. coelicolor</i>	152-158
7.2 NsrR Regulates NO Detoxification in <i>S. coelicolor</i>	159-162
8. References	163-177
9. Appendix	178-204
9.1. Results from MtrA Project	178-193
9.1.1. Strategy for Producing Mutants	178
9.1.2. Making In-Frame Mutants	179-182
9.1.3. Complementing the <i>sco3014-mtrAB-lpqB</i> Mutants	183-190
9.1.4. Pigmented Antibiotic Production	191-193
9.2. Results from NsrR Project	194-204
9.2.1. Strategy for Producing an <i>nsrR</i> Mutant	194
9.2.2. Making an <i>nsrR:apr</i> Mutant	195-196
9.2.3. Making an <i>nsrR</i> In-Frame Mutant	197
9.2.4. Complementing the <i>nsrR</i> Mutation	197-200
9.2.5. Making an <i>nsrR</i> 3XFlag Strain	201-202
9.2.6. Constructing pGUS Vectors for Analysing Promoter Activity	203-204

Abbreviations

<i>bld</i>	bald (unable to form aerial hyphae)
bNOS	bacterial nitric oxide synthases
bp	base pairs
BSA	Bovine Serum Albumin
CAA	Casamino acid
ChIP-chip	Chromatin Immunoprecipitation microarray
ChIP-seq	Chromatin Immunoprecipitation sequencing
C-terminal	Carboxyl terminal
DETA	Diethylenetriamine
DMSO	Dimethyl Sulphoxide
DNB	Difco Nutrient Broth
DNICs	dinitrosyl iron complexes
eGFP	Enhanced Green Fluorescent Protein
Fe-S	Iron-Sulphur
<i>filP</i>	Filamentous protein P
FRT	Flp recognition target
EMSA	Electromobility shift assay
GARPO	Goat Anti-Rabbit peroxidase
HPK	Histidine protein Kinase
HTH	Helix-turn-helix
IF	Initiation factor
IscR	Iron-sulphur cluster regulator
LB	Lennox Broth
LCMS	Liquid Chromatography and Mass Spectrometry
LM	Light Microscopy
<i>mce</i>	Mammalian cell entry
Mbp	Mega base pairs
Mtr	<i>Mycobacterium</i> transcriptional regulator
NO	nitric oxide

NsrR	Nitrite sensitive transcription repressor
N-terminal	Amino terminal
PAPA	Propylamine Propylamine
PCR	Polymerised Chain Reaction
qRT-PCR	quantitative real time PCR
RR	Response regulator
RRE	Roussin's red ester
SALPs	SsgA-like proteins
<i>sco</i>	Annotated gene from <i>Streptomyces coelicolor</i>
Scy	<i>Streptomyces</i> cytoskeletal proteins
(S)-DNPA	4-dihydro-9-hydroxy-1-methyl-10-oxo-3-H-naphtho- [2,3-c]-pyran-3-(S)-acetic acid
SDS	Sodium Dodecyl Sulphate
SEM	Scanning Electron Microscopy
SFM	Soya flour Mannitol medium
SMM	Supplemented Minimal Medium
SsgA	Sporulation in <i>Streptomyces griseus</i> protein
TB	tubercule bacillus
TCS	two-component systems
TEM	Transmission Electron Microscopy
TSB	Tryptone Soya Broth
TIPOC	tip organising centre
TSB	Tryptone Soya Broth
UV	Ultraviolet
<i>whi</i>	white (unable to form spores)
Wbl	Whi-B like

List of Figures and Tables

1. General Introduction		Page
Figure 1.1	Model of Spore Compartmentalisation	24
 2. Materials and Methods		
Table 2.1	<i>E. coli</i> Strains	30
Table 2.2	<i>Streptomyces</i> Strains	31
Table 2.3	Plasmids & Cosmids	32
Table 2.4	Antibiotic Concentrations	37
Table 2.5	Primers	39
Table 2.6	Recipe for SDS Page Gel	52
 3. Introduction for MtrA Project		
Figure 3.1	TCS within the <i>S. coelicolor</i> Genome	67
Figure 3.2	<i>M. tuberculosis</i> MtrA Crystal Structure	70
Figure 3.3	<i>C. glutamicum mtrAB</i> Mutant Phenotype	72
 4. Results for MtrA Project		
Figure 4.1	Phenotype of In-Frame $\Delta sco3014-\Delta lpqB$ Mutants at 3 days	79
Figure 4.2	<i>lpqB</i> Grey and White Mutant Phenotype	80
Figure 4.3	Phenotype of In-Frame $\Delta sco3014-\Delta lpqB$ Mutants at 5 days	81
Figure 4.4	Phenotype <i>sco3014-lpqB</i> Complemented Strains at 3 days	83
Figure 4.5	Phenotype <i>sco3014-lpqB</i> Complemented Strains at 5 days	84
Figure 4.6	Complementing <i>mtrA</i> by Overproducing <i>mtrA</i> at 3 days	86
Figure 4.7	Complementing <i>mtrA</i> by Overproducing <i>mtrA</i> at 5 days	87
Figure 4.8	SEM of $\Delta sco3014-\Delta lpqB$ Aerial Mycelium at 3 days	89
Figure 4.9	SEM Showing Spore Chains of $\Delta sco3014-\Delta lpqB$ at 3 days	90
Figure 4.10	Highlighted Spore Structure from Figure 4.12	91
Figure 4.11	SEM of $\Delta sco3014-\Delta lpqB$ Aerial Mycelium at 5 days	93

Figure 4.12	SEM Showing Spore Chains of $\Delta sco3014-\Delta lpqB$ at 5 days	94
Figure 4.13	Highlighted Spore Structure from Figure 4.15	95
Figure 4.14	UV Visible Spectrum of $\Delta mtrA$ and $\Delta mtrB$ Supernatant	98
Figure 4.15	Pigmentation Observed in <i>mtrA</i> & <i>mtrB</i> Mutants	99
Figure 4.16	LCMS of $\Delta mtrB$ Supernatant	100
Figure 4.17	Undecylprodigiosin Production by $\Delta sco3014-\Delta lpqB$	102
Figure 4.18	Immunoblot Detecting MtrA	104
Figure 4.19	MtrA Consensus site Upstream of <i>ftsZ2p</i>	106
Figure 4.20	qRT-PCR Detecting <i>ftsZ</i> Expression in $\Delta mtrA$	107
Figure 4.21	FtsZ Localisation in $\Delta sco3014-\Delta lpqB$ Aerial Mycelium	109
Figure 4.22	FtsZ Localisation in $\Delta sco3014-\Delta lpqB$ Spore Chains	111

5. Introduction to the NsrR Project

Figure 5.1	Fe-S Cluster Assembly Proteins	119
Figure 5.2	Alignment of NsrR Protein Sequences with IscR	125
Figure 5.3	NsrR Regulatory Mechanism	127

6. Results for NsrR Project

Figure 6.1	Genetic Organisation around <i>S. coelicolor nsrR</i>	130
Figure 6.2	Phenotype of $\Delta nsrR$	132
Table 6.1	Comparison of Spore Production in <i>nsrR</i> Strains	133
Figure 6.3	Phenotype of <i>nsrR</i> Complemented Strain	135
Figure 6.4	SEM of $\Delta nsrR$ at 5 days	137
Figure 6.5	SEM of $\Delta nsrR$ at 10 days	138
Figure 6.6	Phenotype of <i>nsrR</i> Flag Strain Constructed for ChIP-seq	140
Figure 6.7	Immunoblot of NsrR Flag	143
Figure 6.8	ChIP-seq of NsrR Targets <i>hmpA1</i> and <i>nsrR</i>	144
Figure 6.9	ChIP-seq of NsrR Target <i>hmpA2</i>	145
Figure 6.10	<i>sco7426</i> , <i>nsrR</i> & <i>hmpA1</i> Promoter Activity	147

Figure 6.11	Promoter Alignment of NsrR Targets	149
-------------	------------------------------------	-----

9. Appendix

Table 9.1	Fragment Sizes of Cosmids Digested with EcoRI	181
Table 9.2	Fragment Sizes of Cosmids Digested with SacI	182
Figure 9.1	DNA Sequence for $\Delta lpqB$ Complementation	185
Figure 9.2	Plasmid Maps for $\Delta lpqB$ Complementation	186
Figure 9.3	DNA Sequence for $\Delta mtrB$ Complementation	187
Figure 9.4	Plasmid Maps for $\Delta mtrB$ Complementation	188
Figure 9.5	DNA Sequence for $\Delta mtrA$ Complementation	189
Figure 9.6	Plasmid Maps for $\Delta mtrA$ Complementation	190
Figure 9.7	Yellow Pigmentation Production	191
Figure 9.8	UV Visible Spectrum of $\Delta mtrA$ and $\Delta mtrB$ at 39 hours	192
Figure 9.9	Actinorhodin Assay Results	193
Figure 9.10	Phenotype of an <i>nsrR:apr</i> Mutant	196
Figure 9.11	Sequencing Result of <i>nsrR</i> for Complementation	199
Figure 9.12	Plasmid Maps for Complementing <i>nsrR</i> Mutant	200
Figure 9.13	Plasmid Maps for $\Delta nsrR$ Complementation	202
Figure 9.14	DNA sequences used to construct pGUS reporters	204

In memory of my brother William Knowles

11th May 1990 – 1st December 2001.

Acknowledgements

I would like to thank a number of people that have been an invaluable help and support throughout this process. First and foremost I would like to thank Matt Hutchings for having the courage to take me on board. His support through the tough days and infectious enthusiasm on the good days really made the process enjoyable.

Next I'd like to thank members of the Hutchings lab for not only their help but also for making the lab a fun and productive workplace. Many thanks goes to Dave Widdick for all your patience in the early days to becoming a great friend whose curries cannot be beaten; Ryan Seipke for your help with the LCMS & for being a hilarious bench buddy; Matt Hicks who taught me the western way; Elaine Patrick for your patience listening to me working out experimental issues, building the GUS constructs and organising lab events; Joerg Barke for teaching me his ethanol ways; Ben Thompson for being good company when I started in the lab; John Munnoch for our chats about bioinformatics; and finally Nicolle Som for being another quirky member of the team.

I'd also like to thank a number of people for their help with this work. Corinne Appia-Ayme for a 'smashing' time with the microarrays to just being a lovely person to work with; Paul Hoskisson for help with fluorescent microscopy; Jay Crack for the EMSA; Neil Holmes for general advice & encouragement; and Kimberly Findlay for making the SEM one of the most exciting data days of the PhD.

I'd also like to thank my family for their love and support throughout this time. Firstly I'd like to thank my parents Paul and Edwina Knowles for their unconditional support; my brother Andrew Knowles for managing to keep me smiling; Keyinde Ajayi for your patience and advice about figure presentation; my Grandma, Jean Knowles whose support and encouragement meant I could complete the PhD; and finally to Chris Wright for your love and understanding - I'm looking forward to the next adventure together.

Chapter 1: General Introduction

1.1. Actinobacteria

The phylum actinobacteria are the high GC branch of Gram-positive bacteria that include both pathogenic and non-pathogenic bacteria. The best studied group of actinobacteria are known as the actinomycetes (Class: actinomycetales) which include the causative agents for tuberculosis, leprosy and diphtheria: *Mycobacterium tuberculosis*, *Mycobacterium leprae* and *Corynebacterium diphtheriae*.

The genus *Mycobacterium* contains species that are mainly free living saprophytes; however some mycobacteria have evolved to become animal pathogens, for which the genus is better known (Cosma *et al.*, 2003, Willey *et al.*, 2008). Pathogenic *Mycobacterium* species include *M. tuberculosis* and *M. leprae*. *Mycobacterium* also contains opportunistic pathogens such as *M. avium*, *M. chelonae*, *M. fulaceum* and *M. kansasii* (Madigan & Martinko, 2006). These pathogens are particularly virulent in immuno-compromised individuals. Vulnerable hosts and the emergence of antibiotic resistant strains means the prevalence of mycobacterial infections has increased (Cole *et al.*, 2001, Kaufmann & McMichael, 2005).

M. tuberculosis (the tubercle bacillus or TB) is the causative agent for tuberculosis. *M. tuberculosis* spreads via respiratory routes, which occurs by inhalation of bacilli-containing droplets (Madigan & Martinko, 2006). Once inhaled, *M. tuberculosis* initiates infection by entering into host macrophages (Schorey *et al.*, 1997). The mammalian cell entry genes (*mce*) play a vital role in infecting macrophages (see p76). There are four *mce* operons encoded in the *M. tuberculosis* genome, which are required at different stages of infection (Cole *et al.*, 1998). Persistence of mycobacterial infections depends on their ability to survive within host macrophages (Warner & Mizrahi, 2007). During infection of macrophages, mycobacteria have to avoid host defences and acquire nutrients to survive.

Obtaining knowledge about how mycobacteria survive and exploit host immune cells may present a new avenue for treating mycobacterial infections.

Another well-known pathogen belonging to the genus is *M. leprae*, which causes leprosy. The interaction between macrophages and *M.leprae* is also vital at the early stages of infection. *M.leprae* is an intracellular pathogen that also grows within the phagosomes of macrophages (Madigan & Martinko, 2006). There are two clinical forms of *M.leprae*; tuberculoid leprosy and lapromatous leprosy (Kindt *et al.*, 2007). In lapromatous leprosy, *M. leprae* cells are widely distributed in macrophages; whereas tuberculoid leprosy involves the formation of granulomas to combat the mycobacterial infection, which results in the majority of the pathogen being removed (Kindt *et al.*, 2007). The removal of *M.leprae* in tuberculoid leprosy results in peripheral nerve damage and characteristic skin lesions. However a few pathogenic bacteria survive and remain in a latent phase within mature granulomas (Grosset, 2003). Therefore genes essential for mycobacterial survival are of interest for combating these infectious pathogens.

Actinomycetes also encompass the genus *Corynebacterium* which includes a number of pathogenic species and organisms important for industrial biotechnology. The acute disease diphtheria is caused by the pathogen *C. diphtheriae*; the diphtheria exotoxin causes an inflammatory response. If the toxin is absorbed into the circulatory system it can damage internal organs, which may eventually result in death. However cases of diphtheria can be prevented by vaccination, meaning the disease mainly affects unvaccinated individuals in poverty stricken areas. One of the most studied corynebacteria is *C. glutamicum*; this is due to its importance for industrial production of amino acids. *C. glutamicum* mutants of metabolic pathways are exploited for their capability of producing glutamic acid and lysine, both of which are used as food additives.

1.2. Streptomyces

Another important genus belonging to the actinomycetes is *Streptomyces*; *Streptomyces spp.* are mostly non-pathogenic organisms that are ubiquitous within the soil environment (Hodgson, 2000). *Streptomyces* are studied because of their unusual developmental life cycle (see section 1.3.) and because they are prolific producers of secondary metabolites, which have numerous uses in human medicine including antibiotics, chemotherapeutics and immunosuppressants. Within the environment, *Streptomyces spp.* produce secondary metabolites to kill competing bacteria. These secondary metabolites have been utilised for medical purposes as antibiotic (daptomycin), antifungal (nystatin), immunosuppressant (rapamycin) and anti-tumour agents (doxorubicin) (Hopwood, 2007a). *Streptomyces* natural products comprise over two thirds of the naturally-derived antibiotics used in medicine (Bentley *et al.*, 2002). Production of these compounds is coordinated with *Streptomyces* development (Hopwood, 2007b) in which the multicellular growth of mycelia, occurring via apical growth and branching, appears more fungal-like than the cell division mechanisms observed in other bacteria (Chater & Losick, 1997, Flärdh & van Wezel, 2003). This differentiation of *Streptomyces* species from a single spore to hyphal filaments is another interesting aspect to study.

The *Streptomyces* genus contains more than 500 known species including antibiotic producers and pathogens (Labeda, 2011); and although most streptomycetes are non-pathogenic a few are associated with plant and human disease. For example the plant pathogen *S. scabies* infects potatoes and beetroot, causing scab disease, which is of economic importance. This is because distinctive lesions caused by the pathogen reduce their market value. Unlike other species, *S. scabies* is capable of infecting crops due to the presence of pathogenicity islands contained within its genome (Kers *et al.*, 2005). The pathogenicity islands encode virulence factors, which are essential for successful infection

of the plant host (Joshi *et al.*, 2007, Loria *et al.*, 2006). Another important factor for *S. scabies* infection is the hyphal growth of the organism, which could be useful in penetrating the host tissues.

1.3. *Streptomyces* Differentiation

1.3.1. *Streptomyces coelicolor* Lifecycle

Streptomyces have a complex lifecycle that originates from a dormant, unicellular spore. This spore, which is resistant to desiccation (Chater *et al.*, 2009), can be dispersed within the environment. This dispersal means that, in nutrient-rich conditions, the spore germinates by swelling and once cell polarity is established forms hyphae via apical growth. Apical growth is unique to actinomycetes, and is achieved by new cell wall being formed only at the poles of the cell or, in the case of *Streptomyces* species, at the hyphal tip. This hyphal tip extension, along with branching of mycelium, results in a network of hyphae known as the vegetative mycelia. While the peripheral regions of the vegetative mycelium are growing, the non-growing regions undertake secondary metabolism and synthesise antibiotics, which are dispersed into the environment. Once the nutrients have been used and depleted within the substrate hyphae, a large number of the substrate mycelia die and release nutrients allowing the few surviving substrate hyphae to form reproductive structures known as aerial hyphae (Miguel *et al.*, 1999). As aerial hyphae grow up and out of the soil they become separated from the subapical stem via a crosswall known as the basal septum. The basal septum provides a base for sporogenic hyphae where FtsZ levels increase causing the formation of sporulation septa (Kwak *et al.*, 2001). These sporulation septa subdivide the apical cell synchronously into unicellular compartments that ultimately gives rise to a chain of spores. These spores are then dispersed and individual spores

germinate and begin the complex lifecycle of *Streptomyces* again. The different developmental stages of *Streptomyces coelicolor* are easily detectable *in vitro* due to the progression of colony phenotypes from smooth and bald (substrate mycelium), to fuzzy and white (aerial mycelium) to grey-brown (spores).

There are two distinct classes of development mutations found within *Streptomyces*, the first being the *bld* genes. The *bld* genes are involved in the progression of growth from vegetative to aerial mycelium and the phenotype of the *bld* (or bald) mutants are smooth colonies as they are unable to form aerial mycelia. The absence of aerial mycelia mean *bld* mutants do not progress to the white, fuzzy phenotype that is seen within a wild type strain producing aerial hyphae (Flärdh & Buttner, 2009, McCormick & Flärdh, 2012). The *bld* phenotype has been shown to be complemented by two different methods; firstly when SapB is introduced to the media or via extracellular complementation. SapB reduces the water surface tension at the colony surface, which in turn facilitates the growth of aerial hyphae (Tillotson *et al.*, 1998). SapB has been shown to complement the bald phenotype as the hydrophobic protein has been shown to coat the aerial mycelium, which allows the erection of hyphae by breaking the surface tension at the colony surface (Tillotson *et al.*, 1998). This hydrophobic sheath has been shown to be important in coating both aerial hyphae and spores; other major components of the sheath are the chaplins and rodlines. Chaplins were found to be important for hydrophobicity and separation of aerial hyphae (Claessen *et al.*, 2006). Rodlins however are located on the outer surface of aerial hyphae and spores forming an insoluble layer (Claessen *et al.*, 2002).

Both Chaplins and Rodlins are regulated by RNA polymerase containing the alternative developmental sigma factor σ^{BldN} (Bibb *et al.*, 2012). Another method for complementing *bld* mutants occurs by proximity complementation; this is where Δbld colonies are grown near other *bld* mutants resulting in mutations being restored back to wild type (Willey *et*

al., 1993). This proximity complementation revealed that the *bld* genes function as a hierarchical cascade. *bldD/bldM* complemented all other *bld* mutants, whereas the *bldJ* mutant that is complemented by any *bld* gene. Therefore by studying these developmental *bld* mutants, a signalling cascade for the erection of aerial hyphae in *Streptomyces* spp. has been demonstrated.

The second distinct class of developmental mutants are in the *whi* genes; unlike the *bld* mutants *whi* (or white) mutants can form aerial mycelium but they are unable to form mature chains of spores. As these *whi* mutants cannot form mature spore chains they do not produce the distinct grey-brown WhiE polyketide pigment associated with mature spore formation in *S. coelicolor* (Davis & Chater, 1990). Therefore these mutants remain characteristically white and are aptly named the *whi* mutants (Flårdh & Buttner, 2009, McCormick & Flårdh, 2012). Each of these *whi* mutants are blocked at different stages of spore formation. Studies exploring the *whi* genes have revealed the complexity of genes required to progress the develop of *Streptomyces* spp. from aerial hyphae to mature spores.

The *whi* genes have been shown to be involved in different stages of aerial mycelium undergoing sporulation; and include early sporulation genes *whiG*, *whiA*, *whiB*, *whiH*, *whiI* and the late sporulation genes *whiD* and *whiE*. (Chater & Chandra, 2006). The involvement of *whi* genes in differentiation begins with the sigma factor σ^{WhiG} that is required at the earliest stages of aerial hyphae development (Chater *et al.*, 1989). Along with *whiG*, *whiJ* has also been implicated in differentiation (Ainsa *et al.*, 2010); however unlike σ^{WhiG} , WhiJ is suggested to function as a repressor of *sco4542* (a putative *bldB* homologue), as simultaneous deletion of *whiJ* suppresses the mutant phenotype. Both σ^{WhiG} and *whiJ* have important roles in the development of aerial mycelium.

The *whi* genes involved in the next section of the lifecycle are *whiA* and *whiB*. *WhiA* has recently been shown to have a number of targets involved in cell division and polarised growth including *ftsZ* and *filP* (Bush *et al.*, 2013). The phenotypes of the *whiA* and *whiB* mutants are very similar; these mutants form very long aerial hyphae that are poor at septating (Ainsa *et al.*, 2000, Bush *et al.*, 2013, Flårdh *et al.*, 1999). *WhiB* belongs to, and was the first discovered member of, the *WhiB*-like (*Wbl*) family of proteins; *Wbl* proteins are small in size but widespread and well conserved within actinomycetes. For example *S. coelicolor* encodes 11 *Wbl* proteins. *Wbl* proteins are transcription factors and exhibit regulatory functions where nitric oxide, and / or redox stress, is sensed by an [4Fe-4S] cluster ligated by four highly conserved cysteine residues (den Hengst & Buttner, 2008, Jakimowicz *et al.*, 2005). The interaction of NO with the Fe-S clusters of *Wbl* proteins is proposed to be important in cell division signalling in the actinomycetes (Crack *et al.*, 2012). Actinobacteria is the only phylum that contains this large family of *Wbl* proteins. These *wbl* genes are thought to have evolved on actinophages and plasmids as *wblN*, *wblO* and *wblP* are still encoded on the plasmid SCP1 (Chandra & Chater, 2013). This, in combination with lateral acquisition in actinomycetes has resulted in a large number of *Wbl* proteins (Saini *et al.*, 2011), which have important roles including the regulation of cell division and drug resistance (Fowler-Goldsworthy *et al.*, 2011, Molle *et al.*, 2000, Morris *et al.*, 2005).

The *whiH* and *whiI* genes encode two regulators that are important in cell division and septation. Both *whiH* and *whiI* appear to be autorepressors where *whiI* also negatively regulates the expression of *whiH* (Ainsa *et al.*, 1999, Ryding *et al.*, 1998). *WhiI* has also been found to influence the expression of three genes involved with normal spore development (Tian *et al.*, 2007, Zhang *et al.*, 2010). This would explain the phenotype of the *whiI* mutant as it is blocked in septation of spores as well as chromosome condensation (Ainsa *et al.*, 1999). Therefore *WhiI* has been proposed to have two different forms, one state required for prespore formation and the other for spore maturation (Tian *et al.*, 2007). The final *whi*

genes, *whiD* and *whiE*, are involved in the later stages of spore formation. WhiD is another Wbl protein that has been shown to be important for correct septa placement and consequently spore formation (Molle *et al.*, 2000). The *whiD* mutants are capable of forming spores but do not produce WhiE spore pigment that is normally associated with mature spore formation in *S.coelicolor* (Davis & Chater, 1990). The number of Whi regulators involved in sporulation reveals the complexity of this process in *S. coelicolor*; these regulators reveal a system of control which is crucial to reaching sporulation and which is still not fully understood.

1.3.2. Polarised Growth and Cell Division

In order to progress through the various stages of the lifecycle *Streptomyces* spp. have to undergo polarised growth. Unlike other bacteria, actinomycetes grow without the use of an MreB cytoskeleton (Flårdh, 2010); instead actinomycete polar growth is achieved by tip extension via the tip organizing centre (TIPOC). The TIPOC is composed of a complex of coiled-coil proteins that include DivIVA and the *Streptomyces* cytoskeletal protein Scy; Scy is proposed to act as a molecular assembler that sequesters DivIVA in order to establish polarity centres and allow *Streptomyces* to proliferate (Holmes *et al.*, 2013, Walshaw *et al.*, 2010). The role of DivIVA as a polarity determinant has been shown using time lapse microscopy where DivIVA is localised to hyphal tips and marks newly emerging hyphal branches on the lateral walls (Hempel *et al.*, 2008, Jyothikumar *et al.*, 2008). This hyphal targeting has been shown to be a result of the N terminus of DivIVA, which determines both function and location of the protein (Letek *et al.*, 2009, Wang *et al.*, 2009); whereas the C-terminus of DivIVA has been shown to interact with Scy via a bacterial two hybrid assay (Holmes *et al.*, 2013). Another important protein linked to the TIPOC in *Streptomyces* is the filament-forming protein FilP (Holmes *et al.*, 2013); which is also occasionally

located at hyphal tips (Bagchi *et al.*, 2008). Further investigation into FilP reveal that mutants exhibit a reduced growth rate and altered hyphal morphology (Bagchi *et al.*, 2008). The interplay between DivIVA, Scy and FilP is important in cell polarity and apical growth in *S. coelicolor*. However while Scy and FilP have important roles, only DivIVA is essential to *S. coelicolor* viability (Grantcharova *et al.*, 2005, Hempel *et al.*, 2012, Moseley & Goode, 2006, Rose *et al.*, 2005). These components of the TIPOC, are important not only for polarized growth but may have a role, albeit direct or indirect, with cell division in *Streptomyces*.

In order to produce unigenomic spores *S. coelicolor* needs to synchronously septate and segregate chromosomal DNA contained within the multigenomic apical cell (Chater, 1999, Flårdh & Buttner, 2009). An essential protein involved in septation is FtsZ; as sporulation is abolished in *ftsZ* mutants (Flårdh *et al.*, 2000, Grantcharova *et al.*, 2003). FtsZ is involved in different types of septal formation within *S. coelicolor* (Schwedock *et al.*, 1997). FtsZ is involved in the formation of crosswalls in vegetative hyphae and the septation of aerial hyphae in order to produce spores. Despite FtsZ being required in different developmental phases there is only one *ftsZ* gene within the *S. coelicolor* genome. However this single *ftsZ* gene is regulated by three separate promoters *ftsZ1p*, *ftsZ2p* and *ftsZ3p*; these promoters have been found to be involved in *ftsZ* expression under different stages of growth. While *ftsZ3p* is important for vegetative growth *ftsZ2p* is upregulated in sporogenic aerial hyphae, which coincides with the onset of sporulation (Flårdh *et al.*, 2000). The sporulation phenotype of the early *whi* mutants has been shown to be restored by the constitutive expression of *ftsZ*, which was detected by the production of grey pigment; where on closer inspection spores were also shown to be viable (Willemse *et al.*, 2012). As *ftsZ* expression restores sporulation to these developmental mutants it highlights the possible control that the early *whi* genes have on processes that result in sporulation in *S. coelicolor*, one of which being the developmental expression of FtsZ (Willemse *et al.*, 2012).

Once expressed FtsZ must localise to the division sites. However the first protein to localise to the septation sites, and hyphal tips, is SsgA; standing for sporulation in S. griseus A, SsgA is required for *Streptomyces* spp. to sporulate in both solid and liquid culture (Kawamoto *et al.*, 1997, van Wezel *et al.*, 2000). SsgA belongs to the SsgA – like protein family (SALPs). This key sporulation protein is independently transcribed by SsgR, instead of by Whi regulatory proteins (Traag *et al.*, 2004). However, microarray studies of an Δ ssgA strain reveal that expression of *whi* and *bld* genes, along with *divIVA*, is influenced by the presence of SsgA (Noens *et al.*, 2007). Once SsgA localises to foci at growing hyphal tips, SsgB then colocalises during early division and has been shown to interact with the cell membrane (figure 1.1). SsgB is required for sporulation as it recruits FtsZ and activates its polymerisation into filaments (Willemse *et al.*, 2011). These FtsZ filaments then assemble at SsgB foci and form the Z rings (figure 1.1) Septation of aerial hyphae by FtsZ is achieved by the remodelling of FtsZ spiral filaments into FtsZ rings (Addinall & Holland, 2002, Errington *et al.*, 2003, Grantcharova *et al.*, 2005, Lutkenhaus & Addinall, 1997, Margolin, 2000, Rothfield *et al.*, 1999). These FtsZ rings need to compartmentalise the segregated chromosome into single copies within the prespore compartments.

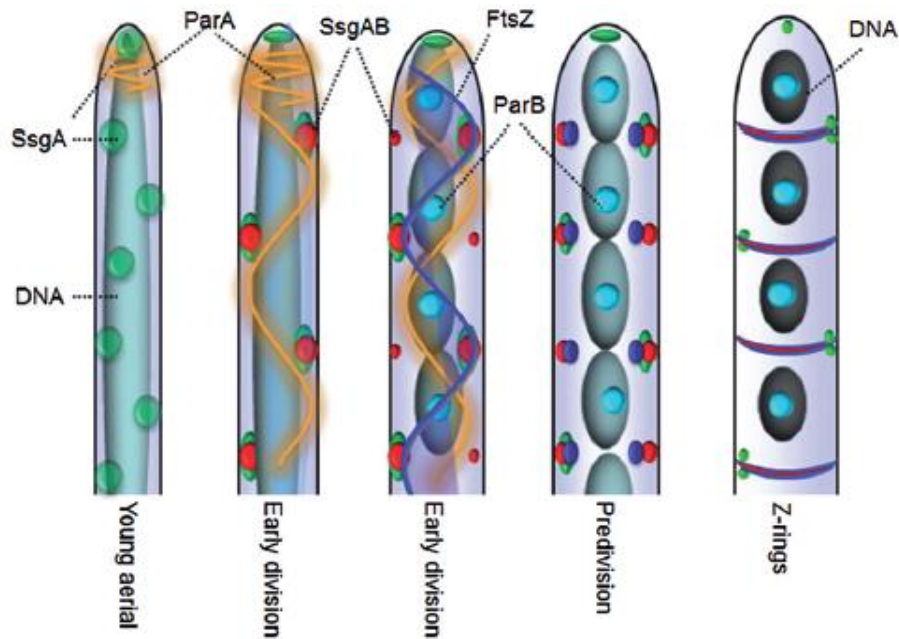


Figure 1.1: Model of spore compartmentalisation due to FtsZ ring formation in *S. coelicolor*. In young aerial hyphae DNA is dispersed throughout while ParA is localised to the hyphal tip and SsgA at focal points along the hyphae. During early division SsgB co-localises to SsgA, ParA extends before FtsZ forms into filaments and ParB is formed. FtsZ filaments form into Z rings, which divide the condensed chromosomes into individual prespore compartments via septation (Jakimowicz & van Wezel, 2012) used with authors permission.

The protein MreB is crucial for cell division in rod-shaped cells, however in actinomycetes MreB is not utilised for polar growth; instead MreB homologues have been implicated in spore compartmentalisation within *Streptomyces* (Heichlinger *et al.*, 2011, Kleinschnitz *et al.*, 2011, Mazza *et al.*, 2006). The main function of MreB in *Streptomyces* appears to be providing stability to the spore wall (Mazza *et al.*, 2006). During tip elongation replicating chromosomes follow the extending hyphal tip (Wolanski *et al.*, 2011); this means the aerial hyphae are multigenomic structures that require efficient chromosome segregation. Chromosome segregation in *S. coelicolor* is controlled by ParA and ParB (Flärth & Buttner, 2009). ParA polymerization is controlled by the TIPOC component Scy (Ditkowski *et al.*, 2013). The ParA-Scy interaction could explain the localization of ParA that functions by forming helical foci at the tips of aerial hyphae; these helices consequently act as a scaffold

for ParB (Jakimowicz *et al.*, 2007) where it is proposed to act as the supplier of energy to ParB (Leonard *et al.*, 2005a, Leonard *et al.*, 2005b). ParB then aligns the condensing chromosomes at regular intervals along the hyphae, which ensures each prespore contains a single copy of the required chromosome (Jakimowicz *et al.*, 2005). Once septation has occurred ParA-ParB disassemble after successful chromosomal segregation (Jakimowicz *et al.*, 2002, Jakimowicz *et al.*, 2005). This results in the formation of unigenomic spores (Jakimowicz *et al.*, 2005).

1.4. Soil Environment

Streptomyces spp. belong to an extensive soil community and have evolved mechanisms to survive this harsh and competitive environment. These saprophytic organisms obtain nutrients from the soil by producing hydrolytic enzymes to break down insoluble, organic remains from organisms such as plants, insects and fungi (Chater *et al.*, 2009). This release of nutrients from organic matter allows the growth of *Streptomyces spp.* within the environment. *Streptomyces* co-habit the environment with many other organisms and they experience competition from these neighbours.

As evolutionary pressure is exerted on *Streptomyces spp.* within their natural environment they produce antibiotics as a survival mechanism. Bacteria that co-habit this niche need to acquire resistance mechanisms to survive against the onslaught of antibiotics. A number of resistance genes promote survival within this environment. The genomes of *Streptomyces spp.* and their cohabiters contain antibiotic resistance genes; the complete collection of these resistance genes in the soil has been called the soil resistome and provides a reservoir of resistance genes for both soil bacteria and for animal pathogens subjected to antibiotic therapy (Wright, 2007).

Even though *Streptomyces spp.* exert stress on their neighbours by antibiotic production they are, also in turn, exposed to secreted primary and secondary metabolites and radicals by other bacteria and fungi within the soil environment. These stresses include nitric oxide (NO), which is a product of microbial denitrification and bacterial nitric oxide synthases (bNOS) (Szukics *et al.*, 2009, Tucker *et al.*, 2010). Therefore *Streptomyces*, like all other soil dwelling bacterial species, are exposed to NO which they need to rapidly detect and metabolise because high concentrations of NO are cytotoxic (Rodriguez-Garcia *et al.*, 2009). Therefore *Streptomyces spp.* encode proteins that rapidly sense and detoxify NO.

1.5. Antibiotic Production

The model organism *S. coelicolor* gets its species name (meaning colour of the sky) from the blue pigmented antibiotic actinorhodin that it produces. A number of pigmented antibiotics are produced by *S. coelicolor*; these include actinorhodin (Bystrykh *et al.*, 1996), the red prodiginines such as undecylprodigiosin (Feitelson *et al.*, 1985) and the recently discovered yellow polyketide coelimycin P1 (Gomez-Escribano, 2012, Gottelt *et al.*, 2010).

Actinorhodin is assembled by a type II polyketide synthase (PKS) and subject to post-PKS modification, all of which is encoded by the 22 gene *act* cluster. One of the precursors for actinorhodin is (S)-DNPA, which is also pigmented; but unlike actinorhodin, (S)-DNPA is yellow. This precursor, (S)-DNPA, has also been implicated in the export of actinorhodin into the external environment (Tahlan *et al.*, 2007, Xu *et al.*, 2012, Willems *et al.*, 2008). The actinorhodin operon *actAB* encodes two export pumps; the expression of these export pumps is repressed by ActR. Both actinorhodin and its precursor (S)-DNPA interacts with ActR, relieving the repression of the actinorhodin export genes (Xu *et al.*, 2012). Therefore (S)-DNPA causes initial de-repression of actinorhodin export pumps, whose expression is

maintained by actinorhodin. This mechanism means actinorhodin production and export are coupled within *S. coelicolor*. Exporting antibiotics into the external environment is an important competition mechanism adopted by *Streptomyces* species. For example the production of the red pigmented, bio active compound undecylprodigiosin has been shown to be increased in the presence of other microorganisms (Luti & Mavituna, 2011, Schaberle *et al.*, 2013). Even though actinorhodin and undecylprodigiosin are well characterised, other less well characterised antibiotic gene clusters are contained within the *S. coelicolor* genome. The product of the *cpk* (cryptic) gene cluster, coelimycin P1 (Gomez-Escribano, 2012), was discovered by removing the *cpk* repressor *scbR2* from the genome. The deletion of *scbR2* resulted in the derepression of the *cpk* cluster such that the uncharacterised coelimycin P1 was produced (Gottelt *et al.*, 2010). Several other studies have shown that manipulating regulatory genes can increase the production of antibiotics from cryptic pathways (Bunet *et al.*, 2008, Rigali *et al.*, 2008, Yang *et al.*, 1995).

The genome of the model strain *Streptomyces coelicolor* A3 (2) was the first streptomycete to be sequenced (Bentley *et al.*, 2002, Donadio *et al.*, 2002). The 8.7 Mbp linear chromosome of *Streptomyces coelicolor* includes 7825 predicted genes and >20 secondary metabolite clusters revealing the potential for bioactive compounds encoded within this genome. The organisation of the chromosome revealed that essential genes are located in the core whereas non-essential genes are encoded within the arms. These chromosome arms are subject to deletions and additions explaining the requirement of essential genes to be maintained in the core genome. However genes within the arms are prone to duplication events, allowing useful flexibility of *Streptomyces spp.* in adapting to their environment. Also the genome sequence revealed a large proportion of genes to have a regulatory role within the *S. coelicolor* genome; this includes 80 two-component systems (TCS), suggesting it is well adapted for survival in the complex and variable soil environment.

1.6. Two Projects

The lifestyle and genome of *S. coelicolor* reveal it is a complex organism that requires highly specialised levels of control, in order to progress through its lifecycle. This lifecycle along with the production of antimicrobials means *S. coelicolor* can thrive within the harsh soil environment. The number of regulators encoded within the *S. coelicolor* genome is disproportionate to its size (Bentley *et al.*, 2002) and this high proportion of regulators likely reflects the desired level of control required to support the lifestyle of *S. coelicolor*. Therefore the roles of encoded regulators are of great interest in understanding the general biology of streptomycetes. Types of regulators encoded in the *S. coelicolor* genome include 67 sigma factors, 184 TCS regulators and hundreds of one-component regulators. The latter belong to regulatory families such as the Wbl protein family and the number and diversity of regulators encoded by the *S. coelicolor* genome is immense. Yet the roles these regulators play in *S. coelicolor* lifestyle are not well understood. Therefore the focus of this project is to understand the roles that two regulatory proteins play during the lifecycle of *S. coelicolor*.

The first regulator studied in this work is encoded by the *sco3013* gene, and is better known as MtrA (after the first discovered homologue *Mycobacterium* transcription regulator A). MtrA belongs to the three-component system MtrAB-LpqB, which has been studied in other actinomycetes including *M. tuberculosis* and *C. glutamicum* where it appears to play a role in regulating cell division. However the role of MtrA in *S. coelicolor* is yet to be established. More detailed information about MtrA is given in chapter 3 of this thesis and the results obtained through studying *S. coelicolor* MtrA are reported in chapter 4.

The second regulator studied in this project, NsrR, is introduced and reported in chapters 5 and 6 of this thesis, respectively. NsrR is an Fe-S containing NO sensing transcription factor

that has not been studied in actinomycetes. *S. coelicolor* is exposed to NO in its natural environment, this exposure to NO has been proposed to act as a signal where the NO stress promotes growth transition within *Streptomyces* (Chandra & Chater, 2013). This NO signal may function via Wbl proteins and other NO sensitive regulators such as NsrR. Therefore the response of *S. coelicolor* to NO, and the role NsrR plays within this response, are of interest.

Chapter 2: Materials and Methods

2.1. General Methods

2.1.1. Bacterial Strains and Plasmids:

The *E. coli* strains used in this study are outlined in Table 2.1. The *Streptomyces coelicolor* strains are displayed in Table 2.2. Also the plasmids and cosmids utilised in this study are shown in table 2.3.

Table 2.1: The *E. coli* strains used in this study

Strain	Genotype	Source
DH5α	F ⁻ λ ⁻ , <i>endA1</i> , <i>glnV44</i> , <i>thi-1</i> , <i>recA1</i> , <i>relA1</i> , <i>gyrA96</i> , <i>deoR</i> , <i>nupG</i> , Φ80 <i>lacZ</i> ΔM15, Δ(<i>lacZYA-argF</i>)U169, <i>hsdR17</i> (<i>r_K⁻m_K⁺</i>)	(Hanahan, 1983)
TOP10	F- <i>mcrA</i> Δ(<i>mrr-hsdRMS-mcrBC</i>) Φ80 <i>lacZ</i> ΔM15 Δ <i>lacX74 nupG recA1 araD139</i> Δ(<i>ara-leu</i>)7697 <i>galE15 galK16 rpsL(StrR)</i> <i>endA1</i> λ-	Invitrogen
BW25113	λ ⁻ , Δ(<i>araD-araB</i>)567, Δ <i>lacZ</i> 4787(:: <i>rrnB-4</i>), <i>lacI</i> p-4000(<i>lacI^q</i>), <i>rpoS</i> 369(<i>Am</i>), <i>rph-1</i> , Δ(<i>rhaD-rhaB</i>)568, <i>hsdR514</i>	(Datsenko, and Wanner, 2000)
BL21	F ⁻ , <i>dcm</i> , <i>ompT</i> , <i>lon</i> , <i>hsdS_B</i> (<i>r_B⁻m_B⁻</i>), <i>gal</i> , λ (DE3)	(Studier & Moffatt, 1986)
ET12567	<i>dam</i> , <i>dcm</i> , <i>hsdS</i> , <i>cmR</i>	(MacNeil <i>et al.</i> , 1992)

Table 2.2: The *Streptomyces* strains used in this study

Strain	Genotype	Source
M145	SCP1 ⁻ SCP2 ⁻ Pgl ⁺	(Hopwood <i>et al.</i> , 1985)
<i>nsrR:apr</i>	M145 <i>nsrR::aac(3)IV</i>	This Study
$\Delta nsrR$	M145 <i>nsrR::scar</i>	This Study
$\Delta nsrR$ (pN26712)	M145 <i>nsrR::scar</i> + pN26712	This Study
$\Delta nsrR$ (pN5112)	M145 <i>nsrR::scar</i> + pN5112	This Study
<i>lpqB:apr</i>	M145 <i>lpqB::aac(3)IV</i>	This Study
<i>mtrB:hyg</i>	M145 <i>mtrB::hyg</i>	This Study
<i>mtrA:apr</i>	M145 <i>mtrA::aac(3)IV</i>	This Study
<i>sco3014:apr</i>	M145 <i>3014::aac(3)IV</i>	This Study
$\Delta lpqB$ grey	M145 <i>lpqB::scar</i>	This Study
$\Delta lpqB$ white	M145 <i>lpqB::scar</i>	This Study
$\Delta mtrB$	M145 <i>mtrB::scar</i>	This Study
$\Delta mtrA$	M145 <i>mtrA::scar</i>	This Study
$\Delta sco3014$	M145 <i>3014::scar</i>	This Study
$\Delta lpqB$ grey (pL11912)	M145 <i>lpqB::scar</i> + pL11912	This Study
$\Delta lpqB$ white (pL11912)	M145 <i>lpqB::scar</i> + pL11912	This Study
$\Delta mtrB$ (pB11912)	M145 <i>mtrB::scar</i> + pB11912	This Study
$\Delta mtrA$ (pA11912)	M145 <i>mtrA::scar</i> + pA11912	This Study
$\Delta mtrA$ (pIJ6883)	M145 <i>mtrA::scar</i> + pIJ6883	(Hong <i>et al.</i> , 2004)

Table 2.3: The plasmids and cosmids used in this study

Plasmid	Genotype	Source
pIJ773	<i>aac(3)IV oriT bla</i>	(Gust <i>et al.</i> , 2002)
pIJ790	<i>araC-P_{araB}, γ, β, exo, cat, repA101ts, oriR101</i>	(Gust <i>et al.</i> , 2002)
pUZ8002	RK2 derivative with a mutation in <i>oriT</i>	(Kieser <i>et al.</i> , 2000)
St6D11	Supercos-1-cosmid with a 41.8 Kbp fragment containing <i>nsrR</i>	(Redenbach <i>et al.</i> , 1996)
StE33	Supercos-1-cosmid with a 33 Kbp fragment containing <i>lpqB, mtrB, mtrA</i> and <i>sco3014</i>	(Redenbach <i>et al.</i> , 1996)
pSET152	<i>oriT, lacZα, apra, lacO, ColE1, int ΦC31, att</i>	(Kieser <i>et al.</i> , 2000)
pMS82	<i>ori pUC18, hyg, oriT RK2, int ΦC31, att</i>	(Gregory <i>et al.</i> , 2003)
pTOPOnsrR	pCRII-TOPO + <i>nsrR</i>	This Study
pN26712	pMS82 + <i>nsrR</i> in KpnI/HindIII	This Study
pUCflagF	pUC19 + 3xFLAG tag (<i>sco</i> optimised)	den Hengst, C. (unpublished)
pN5112	pMS82 + <i>nsrR</i>	This Study
pKF41	<i>ftsZ:eGFP</i>	(Grantcharova <i>et al.</i> , 2005)
pL11912	pSET152 + <i>lpqB</i>	This Study
pB11912	pSET152 + <i>mtrB</i>	This Study
pA11912	pSET152 + <i>mtrA</i>	This Study
pIJ6883	pIJ486 + <i>vanJ</i> promoter	(Hong <i>et al.</i> , 2004)

2.1.2. Solid Media:

SFM also referred to as MS, used to grow and analyse the phenotype of *Streptomyces* strains.

Recipe:	Soya Flour	20 g
	Agar	20 g
	Mannitol	20 g
	tap water	up to 1 L

10 g soya flour and 10 g agar were placed in a 2 L conical flask, while 20 g mannitol was dissolved in 1 L tap water; 500 ml were transferred into each conical flask. These were then autoclaved.

Lennox broth (LB) agar was used to grow *E. coli* strains

Recipe:	tryptone	10 g
	Yeast Extract	5 g
	NaCl	2.5 g
	Agar	10 g
	dH ₂ O	up to 1L

2 g agar was placed in 250 ml conical flask, while the tryptone, yeast extract and NaCl were dissolved in 1 L dH₂O, which was dispensed in 200 ml aliquots into the conical flasks. These were then autoclaved.

LB-NaCl agar:

LB-NaCl was used to grow *Streptomyces coelicolor* in order to quantify spores. It was the same recipe as above, excluding the 5 g NaCl.

Difco Nutrient Broth (DNB) agar:

DNB was used to plate *E. coli* transformed with plasmids conferring hygromycin resistance.

Plates used contained 25 µg/ml hygromycin.

Recipe:	DNB powder	4 g
	dH ₂ O	up to 1 L
	Agar	10 g

DNB was dissolved in 1 L dH₂O and dispensed in 200 ml aliquots into 250 ml conical flasks containing 3 g agar.

2.1.3. Liquid Media:

Lennox broth (LB):

Recipe:	tryptone	10 g
	Yeast Extract	5 g
	NaCl	2.5 g
	dH ₂ O	up to 1L

Used for growing *E. coli* strains. The dissolved mixture was dispensed into 10 ml or 50 ml aliquots and autoclaved.

Tryptone Soya Broth (TSB):

Recipe:	TSB	30 g
	dH ₂ O	up to 1 L

Used for growth of strains to be analysed using the pGUS assay. The mixture was dispensed in 10 ml and 50 ml aliquots and autoclaved.

YEME:

Used to grow *Streptomyces* strains in liquid when in a 1:1 volume with TSB.

Recipe:	yeast extract	3 g
	Peptone	5 g
	Malt extract	3 g
	Glucose	10 g
	dH ₂ O	up to 1L

Once dissolved dispensed in 100 ml volumes into 250 ml conical flasks and autoclaved.

2x YT:

Recipe:	Bactotryptone	16 g
	yeast extract	10 g
	NaCl	5 g
	dH ₂ O	up to 1 L

Once dissolved the solution was dispensed into 10 ml and autoclaved. In order to be used for growing *Streptomyces* strains in liquid.

Supplemented minimal medium (SMM):

Recipe:	PEG ₆₀₀	24.98 g	in 404.5 ml dH ₂ O
	MgSO ₄ ·7H ₂ O	0.3 g	in 12.5 ml dH ₂ O
	TES buffer, pH 7.4	2.865 g	in 50 ml dH ₂ O
	NaH ₂ PO ₄ + K ₂ HPO ₄	0.0173 g + 0.022 g	in 5 ml dH ₂ O
	Glucose	5 g	in 10 ml dH ₂ O
	Glycine	2.5 g	in 12.5 ml dH ₂ O

Each dissolved substance was autoclaved separately. Once autoclaved filter sterilised CAA and Trace elements were added as follows:

Casamino acids (CAA)	1 g	in 5 ml dH ₂ O
Trace elements	1 mg (of each element)	in 10 ml dH ₂ O (store at 4 C)

(Trace elements were MnCl₂·4H₂O, CaCl₂·6H₂O, NaCl, ZnSO₄·7H₂O, FeSO₄·7H₂O)

Once made up to 1 L SMM was dispensed into 50 ml aliquots, which was used for *Streptomyces* growths required for RNA preparation for microarrays and for assaying for Actinorhodin.

2.1.4. Antibiotic Concentrations:

Table 2.4: Antibiotic concentrations used in this study

Antibiotic	Stock concentration (mg/ ml)	<i>Streptomyces</i> working concentration ($\mu\text{g/ml}$)	<i>E. coli</i> working concentration ($\mu\text{g/ml}$)
Apramycin	100	50	50
Carbenicillin	100	-	100
Chloramphenicol	25	-	25
Hygomycin	50	50	25
Kanamycin	100	50	50
Nalidixic acid	25	25	-

2.1.5. Buffers and Solutions:

6 x DNA loading dye: 0.25 % Bromophenol Blue, 0.25 % Xylene Cyanol, 15 % Ficoll (type 400)

10 x TBE: 108 g Tris, 53 g Borate, 9.3 g EDTA, in 1 L dH₂O

TGS: 10 ml 10 % SDS, 3 g Tris, 14.4 g Glycine, in 1 L dH₂O

Laemmli buffer: 950 μl Bio-Rad laemmli buffer, 50 μl β -mercaptoethanol

simplyblue safestain: Invitrogen product

Western 1 x transfer buffer: 25 mM Tris, 192 mM Glycine, 0.1 % SDS and 20 % methanol.

Western blocking solution: 2.5 g skimmed milk powder in 50 ml 1 x TBS + 0.1 % tween

1x TBS: 50 mM Tris Cl pH 7.5, 150 mM NaCl

Solution A: 10 ml 100 mM Tris Cl pH 8.5, 45 µl coumaric acid, 100 µl luminol

Solution B: 10 ml 100 mM Tris Cl pH 8.5, 6 µl 30 % hydrogen peroxide

Solution I: 50 mM Tris HCl pH 8, 10 mM EDTA

Solution II: 930 µl dH₂O, 20 µl 10 M NaOH, 50 µl 20 % SDS

Solution III: 3 M potassium acetate pH 5.5

TE: 10 mM Tris HCl pH8, 1 mM EDTA

10x PBS: 1.37 M NaCl, 27 mM KCl, 100 mM Na₂HPO₄, 18 mM KH₂PO₄

TCB: 100 mM Tris HCl, 50 mM NaCl, 5 mM CaCl₂ pH 7.5

Buffer P1: Qiagen plasmid preparation kit

Buffer B1: Qiagen genomic-tip 100/G kit contents

Buffer B2: Qiagen genomic-tip 100/G kit contents

GUS assay lysis buffer: 50 mM sodium phosphate pH7, 5 mM DTT, 0.1 % Triton X-100, 1 mg/ml lysozyme

GUS assay dilution buffer: 50 mM sodium phosphate pH7, 5 mM DTT, 0.1 % Triton X-100

ChIP lysis buffer: 10 mM Tris HCl pH 8, 50 mM NaCl, 10 mg/ml lysozyme, 1x protease inhibitor

ChIP IP buffer: 100 mM Tris HCl pH8, 250 mM NaCl, 0.5 % Triton X-100, 0.1 % SDS, 1x protease inhibitor

ChIP elution buffer: 50 mM Tris HCl pH7.6, 10 mM EDTA, 1 % SDS

2.1.6. Primers:

Table 2.5: List of primers used for PCR amplification within this study

Primer name	Primer sequence	Role
F25	GGCGAACCTAGCATGCGCATTGATAGCG TCCTGGTGTGATTCCGGGGATCCGTCGACC	<i>ΔnsrR</i> on pIJ773 template DNA
KOR25	GGCCACAGCTCGACGGCCTCAGGGGGCCG CCGCCCCGTCATGTAGGCTGGAGCTGCTTC	<i>ΔnsrR</i> on pIJ773 template DNA
<i>nsrR</i> test F	GCGCATTGATAGCGTCCTGGTGTG	Flanking primers to <i>nsrR</i>
<i>nsrR</i> test R	GGCCTCAGGGGGCCGCCGCCGTC	Flanking primers to <i>nsrR</i>
Apra P1	ATTCCGGGGATCCGTCGACC	Test Apra resistance cassette
Apra P2	TGTAGGCTGGAGCTGCTTC	Test Apra resistance cassette
7427compF	AAGCTTTCAGGTGCCGCCGTTCCGTGT	To complement <i>nsrR</i>
7427compR	TGACGGACCGCCCCTCGGGATGAGGTACC	To complement <i>nsrR</i>
<i>nsrR</i> FLAGf	GGTACCGAGCGGTCCGTGCCGGGGCGGCCG	Primer to insert <i>nsrR</i> into pucFLAGf to form pN5112
<i>nsrR</i> FLAGr	TGACGGACCGCCCCTCGGGAAGGCCT	Primer to insert <i>nsrR</i> into pucFLAGf to form pN5112
<i>sco7426</i> GUSf	TCTAGACGCCTCCTGGGCGTCGCGCA	<i>sco7426</i> promoter fragment for cloning into pGUS
<i>sco7426</i> GUSr	ACACGGAACGGCGGCACCTGGGTACC	<i>sco7426</i> promoter fragment for cloning into pGUS
<i>nsrR</i> GUSf	TCTAGAAGGTACGTCACCCCGTCCGG	<i>nsrR</i> promoter fragment for cloning into pGUS
<i>nsrR</i> GUSr	GCATTGATAGCGTCCTGGTGGTACC	<i>nsrR</i> promoter fragment for cloning into pGUS
<i>hmpA1</i> GUSf	TCTAGACGACCTGGCGCTGCGTTCGC	<i>hmpA1</i> promoter fragment for cloning into pGUS
<i>hmpA1</i> GUSr	CTACCAATTAAGGAGTCGCTGGTACC	<i>hmpA1</i> promoter fragment for cloning into pGUS
M13F	GTAAAACGACGGCCAGT	Sequencing primer
M13R	CAGGAAACAGCTATGAC	Sequencing primer

2.1.7. Polymerase Chain Reaction (PCR):

PCR for amplifying Apramycin cassette: as outlined in the re-direct protocol (Gust *et al.*, 2002).

Bioline TAQ was used for general PCR reactions, therefore the PCR mix and cycle conditions were based on the manufacturer's instructions. The template DNA that was used had a high GC content; this was accounted for by using 5 % DMSO in reactions as well as having an annealing temperature of 55 °C – 71 °C depending on reaction.

The Phusion system was used for high fidelity PCR reactions. Reactions and cycle conditions were based on manufacturer's instructions. The high GC template DNA meant the high GC DNA reaction buffer, 3 % DMSO and an annealing temperature between 55 °C – 71 °C was used.

Primers used for PCR reactions are shown in table 2.5.

2.1.8. PCR Purification:

PCR product was isolated using the Qiagen PCR purification kit, DNA concentration measured using a Nanodrop ND2000c and stored at -20 °C.

2.1.9. Restriction Digestion:

Both Roche and NEB restriction enzymes were used in digests of 20 or 50 µl total volumes in accordance with manufacturer's guidelines. Digests were carried out with optimal buffer, which was outlined by Roche or NEB. Digestion was typically performed at 37 °C for 2 hours. Digests were then analysed by gel electrophoresis, desirable bands were excised and gel extracted.

2.1.10. Agarose Gel Electrophoresis:

DNA fragments were typically analysed on 1 % (w/v) agarose gels containing 1x TBE and 1 µl ethidium bromide at 10 mg/ml. Samples were mixed with 6x DNA loading buffer then loaded gels were run at 100 V for approximately 45 minutes in 1x TBE. DNA was visualised by exposing the gel to UV light.

2.1.11. Gel Extraction:

Bands of interest were excised from the agarose gel and placed in a bijoux. This was weighed and a Qiagen gel extraction kit was used to extract the DNA from the gel slice. DNA concentration measured using a Nanodrop ND2000c and stored at -20 °C.

2.1.12. Ligation:

A 3:1 molar ratio of insert:vector was used for all ligation reactions. Along with insert and vector DNA the ligation reaction consisted of 4 µl ligation buffer, 1 µl ligase, and made up to 20 µl with sigma dH₂O. Reactions were then placed in room temperature water overnight and left at 4 °C. Reactions were used to transform *E.coli* Top10 cells.

2.1.13. Transforming Electro-Competent *E. coli*:

10 ml LB was inoculated with the required *E. coli* strain and placed at 37 °C, shaking at 200 rpm overnight. 100 µl overnight culture was then subcultured in 10 ml LB at 37 °C until the O.D.₆₀₀ was at 0.6. The culture was pelleted at 2 500 g for 5 minutes and resuspended in 10 ml ice-cold 10 % glycerol. A further centrifugation step was carried out (15 120 g, 1 minute,

4 °C) and the resulting pellet was resuspended in 1 ml ice-cold 10 % glycerol. This was repeated four times. Finally the pellet was resuspended in 0.5 ml ice-cold 10 % glycerol. 100 µl aliquots were frozen in liquid nitrogen and stored at -80 °C. To transform cells 100 µl aliquot was thawed on ice and mixed with 2 µl plasmid or cosmid DNA (~200 µg/µl) and placed in an ice-cold electroporation cuvette. This was electroporated in a BioRad Electroporator set at: 200 Ω, 2 µF, 2.5 kV. 1 ml ice-cold LB was immediately added to the transformed cells. These were placed in a microfuge tube, at 30 °C 200 rpm for 1 hour before plating on LB-agar containing relevant antibiotics, which was incubated at 37 °C overnight.

2.1.14. Transforming Chemically-Competent *E.coli*:

10 ml LB was inoculated with *E. coli* and placed at 37 °C, 200 rpm overnight. 100 µl overnight culture was then subcultured in 10 ml LB at 37 °C until the O.D.₆₀₀ was at 0.6, then centrifuged at 2 500 g for 4 minutes. The cell pellet was then resuspended in 5 ml ice-cold 100 mM CaCl₂ and stored on ice for 30 minutes. Centrifugation was repeated at 4 °C and the pellet was resuspended in 0.5 ml ice-cold 100 mM CaCl₂. 100 µl aliquots were frozen in liquid nitrogen and then stored at -80 °C. For transformation 100 µl CaCl₂ competent cells were mixed with 3 µl plasmid DNA (~200 ng/µl) and plated on 37 °C prewarmed LB plates containing the required antibiotic. Plates were incubated at 37 °C overnight.

2.1.15. Storing *E. coli* Using Glycerol Stocks:

Strains were grown overnight, then pelleted at 15 120 g for 1 minute. The pellet was then resuspended in 0.5 ml 40 % glycerol and 0.5 ml LB and stored at -20 °C

2.1.16. Storing *E. coli* Using Microbank Bead Stocks:

Colonies were stored in accordance to procedure outlined by ProLab diagnostics Microbank storage systems (<http://www.pro-lab.com/literature/microbank-www-portfolio.pdf>).

2.1.17. Plasmid Preparation:

E. coli strains containing desired plasmids were grown overnight at 37 °C 200 rpm. The 10 ml culture was then pelleted and a Qiagen plasmid preparation kit was used to isolate the desired plasmid, which was stored at -20 °C.

2.1.18. Phenol/Chloroform Extraction:

DNA was precipitated by adding 1/10 volume 3 M sodium acetate to sample and mixed by inversion. 1:1 phenol/chloroform was added to equal volume. This was vortex mixed for 2 minutes, 15 120 g for 5 minutes. Upper phase was removed and 1 ml 100 % ethanol was added and placed on ice for 10 minutes. 15 120 g for 5 minutes and pellet was washed in 200 µl 70 % ethanol, 15 120 g for 5 minutes to remove ethanol. Pellet was then air dried and resuspended in 50 µl TE buffer and stored at -20 °C.

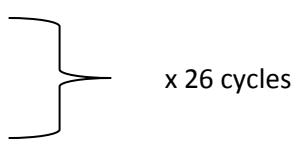
2.1.19. Sequencing:

The sequencing reaction consisted of:

1 µl (150-300 ng/µl) plasmid, 1 µl 32 pM/µl primer M13F or M13R, 1 µl BDV 3.1 dye, 1.5 µl buffer, 5.5 µl dH₂O

The sequencing reaction before sending off samples was:

96 °C for 1 minute
 96 °C for 10 seconds
 50 °C for 5 seconds
 60 °C for 4 minutes
 60 °C for 10 seconds



x 26 cycles

Samples were then sent to TGAC or Source Bioscience for sequencing.

2.2. Generating Mutations in *Streptomyces*

2.2.1. Strategy for Producing Mutants in *S. coelicolor*:

Protocols for producing mutations in *Streptomyces coelicolor* were applied from the Redirect PCR based system (Gust *et al.*, 2002). PCR was used to amplify a resistance cassette, in this project Apramycin from pIJ773, with oligonucleotides containing extensions of 39 nucleotides homologous to the flanking regions of the genes of interest. These PCR products were used to PCR target to supercos-1 cosmids containing the genomic region of interest from *S. coelicolor* in an *E. coli* strain (BW25113) expressing the λ Red recombinase system. *E. coli* BW25113 containing a phage lambda red recombinase was electroporated with the amplified resistance cassette, resulting in the resistance gene replacing the desired gene via homologous recombination. The knock out (Δ) cosmid can then be conjugated into *Streptomyces coelicolor* from *E. coli* strain ET12567 containing the driver plasmid pUZ8002 due to the presence of an oriT site present in the resistance cassette. The resistance cassette also contain flp recombinase (flp) recognition target sequences (FRT) that allow an in-frame mutation to be produced by introducing the Δ cosmid into an *E. coli* strain containing the flp recombinase expressing plasmid BT340. These mutations were then complemented by reintroducing the gene into the mutant

strain. The removed gene was inserted (*in trans*) onto a plasmid containing an integration site, which reinserted the gene into the chromosomal DNA.

2.2.2. PCR of the Disruption Cassette:

An apramycin knockout cassette was generated by using EcoRI/HindIII fragment of pIJ773 as the template DNA. Primers used for PCR reactions are shown in Table 2.5. The primers used for the apramycin cassette (along with *oriT*, flp recombinase sites and the upstream and downstream regions of *nsrR* including the start/stop codon, respectfully) were F25 and KOR25. The PCR cycle used had an initial annealing at 50 °C for 45 seconds followed by a second annealing 55 °C for 45 seconds for 15 cycles. 5 µl of PCR product was mixed with 6x loading buffer then gel electrophoresis was undertaken. The remaining 45 µl of samples were then extracted using a Qiagen PCR purification kit.

2.2.3. Transforming *E. coli* with Cosmid DNA:

A colony of BW25113 / pIJ790 was placed in 10 ml LB with 10 µl chloramphenicol and grown at 30 °C 200 rpm overnight. 100 µl overnight BW25113 / pIJ790 was then subcultured in 10 ml LB with 10 µl chloramphenicol and grown at 30 °C 200 rpm for 5 hours. Electrocompetant cells were prepared and transformed with the 2 µl of cosmid DNA (~200 µg/µl), which was then spread on LB plates containing carbenicillin and chloramphenicol for 30 °C overnight.

2.2.4. Cosmid Isolation:

BW25113 / pIJ790 (this plasmid was temperature sensitive so the strain was grown at 30 °C) containing the wild-type cosmid was grown overnight in 10 ml LB with 10 µl carbenicillin (100 µg/ml), kanamycin (50 µg/ml) and chloramphenicol (25 µg/ml) at 30 °C, 200 rpm. 1 ml overnight culture was centrifuged at 15 120 g for 1 minute and resuspended in 100 µl solution I (50 mM Tris HCl pH 8, 10 mM EDTA), 200 µl solution II (930 µl dH₂O, 20 µl 10 M NaOH, 50 µl 20 % SDS) was immediately added and the tube was inverted 10 times. Then 150 µl solution III (3 M potassium acetate pH 5.5) was added and the tube was inverted 5 times and then centrifuged at 15 120 g for 5 minutes. The supernatant was transferred to a fresh microfuge tube and phenol/chloroform extracted. The DNA pellet was resuspended in 50 µl TE buffer + RNase and 10 µl cosmid DNA was used for checking by restriction digestion with BamHI or SacI. The size of fragments obtained by digestion was predicted by identifying the restriction sites within the cosmid.

2.2.5. PCR Targeting Cosmids in *E. coli*:

An colony of BW25113 / pIJ790 containing the cosmid of interest was inoculated into 10 ml LB containing 10 µl carbenicillin, 10 µl chloramphenicol and 10 µl kanamycin then placed at 30 °C 200 rpm overnight. 100 µl overnight cultured was then subcultured in 10 ml LB containing 10 µl (100 µg/ml) carbenicillin, 10 µl chloramphenicol, 10 µl kanamycin and 100 µl 1 M L-arabinose and grown at 30 °C 200 rpm for approximately 3.5 hours until the O.D.₆₀₀ was 0.4. Cells were then pelleted at 2 500 g for 5 minutes, resuspended in 10 ml ice-cold 10 % glycerol, centrifuged repeated at 4 °C, resuspended in 5 ml ice-cold 10 % glycerol pelleted at 4 °C. Pellet was resuspended in 100 µl ice-cold 10 % glycerol of which 50 µl was mixed with 1 µl PCR product (approximately 200 ng). The mixture was placed in an ice-cold

electroporation cuvette, placed in a Biorad Electroporator set at: 200 Ω , 2 μ F, 2.5 kV. 1 ml ice-cold LB was immediately added to shocked cells. These were placed in a 1.5 ml micro-centrifuge tube, at 30 °C 200 rpm for 1 hour. 500 μ l of the mixture was then spread on LB agar plates containing carbenicillin, kanamycin and chloramphenicol for 37 °C overnight. Transformant colonies were cultured and DNA was extracted and used to transform DH5 α . DNA was then extracted again and tested by restriction digestion with EcoRI or SacI.

2.2.6. Conjugation:

A colony of *E. coli* ET12567 / pUZ8002 was cultured in 10 ml LB with 10 μ l each of chloramphenicol and kanamycin then placed at 30 °C at 200 rpm overnight. 100 μ l overnight culture was then subcultured in 10 ml LB containing 10 μ l carbenicillin, 10 μ l chloramphenicol, 10 μ l kanamycin and grown at 30 °C 200 rpm to an O.D.₆₀₀ of 0.4. Cells were pelleted at 2 500 g for 5 minutes, all supernatant was removed and cells were resuspended in 10 ml LB. This was repeated twice and pellet was resuspended in 1 ml LB. 500 μ l ET12567 / pUZ8002 cells were added to 10 μ l M145 spore stock, which was plated on SFM containing 10 mM MgCl₂ and placed at 30 °C for 16-20 hours. After 16-20 hours plates were overlaid with 1 ml water containing 20 μ l nalidixic acid, 25 μ l apramycin. Exconjugants were then replica plated on LB nalidixic acid containing kanamycin and apramycin, respectively. These were grown at 30 °C for 2-3 days. Colonies that grew on apramycin but not on kanamycin were of interest. Successful mutants were confirmed by PCR using primers nsrRtestF and nsrRtestR (See table 2.5).

2.2.7. Spore Stocks:

Successful *Streptomyces* strains were picked and representative single colonies (6) were streaked on 20x SFM plates, supplemented with specific antibiotics, to produce lawns. These were incubated at 30 °C for 7-10 days. Any mutant phenotypes that arose were excised from plates using a sterile blade. Each plate then had 2 ml 20 % glycerol added & colonies were gently rubbed with a sterile cotton bud to release spores. All spores were collected in a 15 ml tube then filtered through a syringe, containing sterilised cotton wool, into a new 15 ml tube. Once filtered spores were centrifuged at 2 500 g for 10 minutes and resuspended in approximately 2-3 ml residual glycerol. Spores were then dispensed into 0.5 ml aliquots and stored at -80 °C.

2.2.8. Spore Quantification:

Spore stocks were serial diluted 5 µl in 995 µl water, then 10 µl stock 1 in 990 µl water, 100 µl stock 2 in 900 µl water and 100 µl to 900 µl water in subsequent dilutions. On 100 µl dilution 5 and 6 were spread plated.

2.2.9. Standardised Quantification:

Previously quantified spore stocks were diluted and 1000 spores were plated on 10x SFM plates, which were placed at 30 °C for 5 days. Spore were then stocked and re-quantified.

2.2.10. Chromosomal DNA Isolation from *Streptomyces*:

10 ml 1:1 TSB/YEME containing apramycin and nalidixic acid was inoculated with a sterile spring and 50 µl spores for 30 °C 200 rpm overnight. The overnight culture was then

pelleted at 2 500 g for 5 minutes. The pellet was then resuspended in 0.5 ml buffer P1, 10 μ l 30 mg/ml lysozyme, 10 μ l 10 μ g/ml RNase A and placed at 37 °C for 1 hour. 5 μ l 20 % SDS was added then a phenol/chloroform extraction was undertaken (See section [2.1.18](#)).

2.2.11. Removal of the Apramycin Casette in *nsrR* Mutants:

A colony of *E. coli* DH5 α /BT340 was inoculated in 10 ml LB with 10 μ l chloramphenicol and placed at 30 °C 200 rpm overnight. 100 μ l overnight culture was subcultured in 10 ml LB with 10 μ l chloramphenicol and placed at 30 °C 200 rpm until O.D.₆₀₀ was 0.4. Then centrifuged at 2 500 g for minutes at 4 °C and resuspend in 10 ml ice-cold 10 % glycerol, repeat centrifugation and resuspension. After final centrifugation cell pellet was resuspended in 100 μ l ice-cold 10 % glycerol, all 100 μ l were then mixed with 2 μ l Δ cosmid DNA. The mixture was placed in an ice-cold electroporation cuvette, placed in a Biorad Electroporator set at: 200 Ω , 2 μ F, 2.5 kV. 1 ml LB was immediately added to shocked cells. These were placed in a microfuge tube, at 30 °C 200 rpm for 1 hour. After 1 hour cell were plated on LB with apramycin and chloramphenicol, then placed at 30 °C for 2 days. Successful transformants were streaked on LB agar and placed at 42 °C overnight. Colonies were then screened on LB + kanamycin and LB + apramycin respectively. Colonies sensitive to apramycin but grown on kanamycin were of interes. Further screening was then carried out by PCR to ensure that a double cross over had ocured.

2.2.12. Complementation of *mtrA*, *mtrB* and *lpqB* Mutations:

mtrA, *mtrB* and *lpqB* were synthesised in pUC57 by Genscript under the control of the *sco3014* promoter. These were excised using EcoRI and XbaI and sub-cloned into pSET152 also cut with EcoRI and XbaI, which was then dephosphorylated by adding 5.83 μ l buffer I

(in kit) and 2.5 µl phosphorylase to 50 µl restriction reaction. Subclones were tested by digesting with EcoRI and XbaI. Successful plasmids were renamed pA11912, pB11912 and pL11912 respectively then conjugating into corresponding mutant strains to produce the complemented strains $\Delta mtrA$ (pA11912), $\Delta mtrB$ (pB11912), $\Delta lpqB$ grey (pL11912) and $\Delta lpqB$ white (pL11912).

2.2.13. Complementation of the *nsrR* Mutation:

The primers used were 7427comp F and R, displayed in Table 2.5 and the cosmid 6D11 was the template used. Phusion was used and PCR mix was set up in accordance with manufacturer instructions. The PCR cycle used had an initial denaturation at 98 °C for 30 seconds. 25 cycles of 98 °C for 10 seconds, 66 °C for 30 seconds, 72 °C for 30 seconds, completed by a final extension of 72 °C for 5 minutes. 50 µl of PCR product was mixed with 6x DNA loading buffer then run on a 1 % agarose gel in 1 x TBE with 1 µl ethidium bromide, at 100 V for 45 minutes. DNA was then visualised by exposure to UV light. The band was then excised and DNA was obtained using a Qiagen gel extraction kit. 6 ng PCR product was sent to source bioscience for sequencing. A TOPO cloning kit was then used where 7.5 µl PCR product was added to 1 µl BioTaq NH₄ buffer, 0.5 µl Taq polymerase, 1 µl 10 mM dATP and placed at 72 °C for 10 minutes. Then 4 µl of this product was added to 1 µl salt solution, 1 µl TOPO vector and left at room temperature for 5 minutes. 2 µl of the ligation reaction was added to 100 µl TOPO cells and left on ice for 30 minutes before placing at 42 °C for 30 seconds. Cells were then placed on ice and 250 µl LB was added and incubated at 37 °C 200 rpm for 1 hour. Cells were plated on LB agar containing kanamycin, and overlaid with 40 mg/ml X-gal to promote blue white selection, and placed at 37 °C overnight. DNA was isolated and sequenced from potential white transformant colonies. The *nsrR* gene was excised from the TOPO vector and sub-cloned into pMS82 by digesting both with KpnI

and HindIII, and the resulting plasmid (pN26712) was then conjugated into the $\Delta nsrR$ strain to form the complemented strain $\Delta nsrR$ (pN26712).

2.3. Protein analysis

2.3.1. Protein Extraction for SDS-PAGE Analysis

1.5 ml overnight culture, grown in 10 ml 2x YT at 30 °C 200 rpm, was centrifuged at 15 120 g for 1 minute. The pellet was resuspended in 1 ml TCB + 5 μ l 14x protease inhibitor. Sonicated 7x at 50 Hz for 10 seconds with 1 minute intervals on ice, then 15 120 g for 5 minutes.

2.3.2. Bradford Assay

200 μ l Bradford reagent (Bio-Rad), 2 μ l protein sample and 798 μ l water, were standardised against 0-5 μ g BSA at 2 μ g/ μ l. Optical density was then measured at 595 nm.

2.3.3. Protein Preparation for SDS-Page

50 μ l whole cell extract + 50 μ l laemmli buffer and placed at 90 °C for 5 minutes. 20 μ g protein run for each sample on a SDS page gel.

2.3.4. SDS-page gel

Table 2.6: Recipe used for Resolving and Stacking gel components of 2 x SDS page gels.

	4 % Stacking Gel (5 ml)	15 % Resolving gel (10 ml)
0.5 M Tris pH 6.8	0.5 ml	-
1.5 M Tris pH 8.8	-	2.5 ml
30 % Acrylamide	0.67 ml	5 ml
20 % SDS	0.02 ml	0.02 ml
dH ₂ O	3.75 ml	2.37 ml
TEMED	0.01 ml	0.01 ml
25 % APS	0.05 ml	0.1 ml

Using the mini protean 3 system as to manufacture's (Bio-Rad) instructions a 15 % resolving gel for SDS was poured between two glass plates and topped with 70 % ethanol before the gel set. Once polymerization occurred the ethanol was removed and replaced with a 4% stacking gel and a comb was placed before polymerization had occurred. Once set the comb was removed and the SDS page gels were placed in a Bio-Rad electrophoresis tank containing 1x TGS. Gels were loaded with 20 µg protein sample and ran at 100 V for 15 minutes then 200 V for an hour. If NsrR protein were run 10 mM DTT was added to the 1x TGS running buffer.

2.3.5. Coomassie Staining

The SDS PAGE gel was transferred to water for 10 minutes and washed twice before placing in simplyblue safestain overnight. The gel was then destained with 3x 10 minutes washes with water.

2.3.6. MtrA Western

Once run the gel was transferred onto a 8.5 cm x 5.5 cm membrane, which was soaked briefly in methanol, then 1 x transfer buffer. The transfer was from the 15 % SDS page gel to the membrane at 10 V for 1 hour. The membrane was then placed in a 5 % milk solution overnight. The membrane was then placed in 10 ml 5 % milk solution with 2 μ l MtrA TB3 primary antibody and left shaking for 1 hour. After incubation the membrane in washed 3 x in 10 ml 1x TBS + 0.1 % tween for 10 minutes. Incubation with 10 ml 1x TBS + 0.1 % tween with 3 μ l secondary antibody GARPO was left shaking for 1 hour. Finally the membrane was washed twice in 10 ml 1 x TBS + 0.1 % tween for 10 mins and imaged. Imaging occurred by placing mixing solution A and solution B and placing 4 ml on the membrane for 1 minute, then wrapping the membrane in cling film to expose the membrane to photographic film, which was developed.

2.3.7. α -Flag Western

The primary antibody that was used was α -flag, HRP conjugated antibody from Sigma. So only one 5 % milk wash was required.

2.4. Microscopy

2.4.1. Light Microscopy

Growths for imaging:

Serial dilutions were carried out for samples and grown on SFM, LB without salt at 24 h time points from 48 h to track colonies over a number of days depending on the experiment carried out.

Imaging:

Brightfield images were obtained using a Zeiss M2 Bio Quad SV11 stereomicroscope. Colonies were illuminated with a halogen lamp and images taken with an attached AxioCam HRc CCD camera. Axiovision software (Carl Zeiss, Welwyn Garden City, UK) was used to view and save images as tiff and jpeg files. Scale bars were then calculated dependent on magnification and burnt into the images.

Following acquisition of images files were transferred to adobe photoshop where brightness and contrast were adjusted.

2.4.2. Fluorescence Microscopy

M145, $\Delta lpqB$ grey, $\Delta lpqB$ white, $\Delta mtrB$, $\Delta mtrA$, $\Delta sco3014$, $\Delta nsrR$ were conjugated with pKF41. Successful conjugates were then spore stocked, plated and sent to Dr. Paul Hoskisson at Strathclyde for imaging.

2.4.3. Scanning Electron Microscopy (SEM):

Growths for SEM:

Spore stocks were serially diluted 5 µl in 995 µl water, then 10 µl stock 1 in 990 µl water, 100 µl stock 2 in 900 µl water and 100 µl to 900 µl water in subsequent dilutions. On SFM 100 µl dilution 5 and 6 were spread plated.

MtrA strains were M145 *ΔlpqB* grey, *ΔlpqB* white, *ΔmtrB*, *ΔmtrA* and *Δsco3014* grown for 3 days and 5 days on SFM. NsrR strains were M145 and *ΔnsrR* grown for 5 days and 10 days on SFM.

Fixing samples:

Representative colonies were excised from the SFM plate with a blade and attached to the aluminium slide with tissue tek (BDH laboratory supplies, Poole, UK). Once all samples were attached they were submerged in liquid nitrogen it was transferred to the Cryostage of an ALTO 2500, cryo transfer system (Gatan, Oxford, UK). Then sublimation of surface frost was carried out at -95 °C for 3.5 minutes, -125 °C for 2 minutes before coating in platinum for 3 minutes at 10 mA and prior to placement in the microscope chamber of the Zeiss Supra 55 VP FEG scanning electron microscope.

SEM imaging:

Sample was held at approximately -130 °C and imaged with an EHT beam at 3 KV. To image brightness was fixed around 50 % and high current selected. Images were taken 6-7 mm from the lens and saved.

2.5. Gene Expression:

2.5.1. RNA Isolation from Solid Growth:

1 x 10⁴ spores were grown on SFM with cellophanes at 30 °C for 48 hours, isolated and stored at -80 °C. RNA was isolated by submerging mycelium samples in liquid nitrogen and ground vigorously for 30 seconds resulting in mycelium becoming powder. Then 0.7 ml buffer RLT (from QIAGEN RNeasy kit) and 0.25 g sterile sand were added to powdered mycelium and vortexed for 90 seconds. Samples were centrifuged at 15 120 g for 4 minutes then applied to a QIAGEN RNeasy column. A QIAGEN RNeasy mini kit was then used to isolate RNA. Once RNA was isolated an Ambion DNase treatment was applied for 30 minutes at 37 °C. Samples were then stored at -20 °C. Samples were quantified using a nanodrop and checked by gel electrophoresis.

2.5.2. RNA Isolation from Liquid Growth:

1 x 10¹⁰ spores were inoculated in 10 ml 2 x YT + spring and placed at 30 °C, 200 rpm for 7 hours. Germlings were harvested at 2 500 g for 5 minutes and resuspended in 5 ml SMM. Then sonicated at 25 Hz for 1 second before inoculating into 50 ml SMM + spring and placed at 30 °C 200 rpm for 15 hours. 10 ml phenol ethanol was added (5 % phenol, 95 % EtOH) and placed on ice for 30 minutes. Cells were pelleted at 2 500 g for 10 minutes at 4 °C and pellets were stored at -80 °C. Pellets were resuspended in 1 ml TE buffer and 15 mg/ml lysozyme and incubated at room temperature for 1 hour, then placed at 37 °C for 30 minutes. 4 ml RLT buffer and 40 µl β-mercaptoethanol were added to each sample and sonicated for 3x 0.5 second cycles at 18 Hz and stored on ice for 1 minute before repeating sonication. Samples were then phenol/chloroform extracted and applied to RNeasy midi columns from a Qiagen RNeasy midi kit. Samples were quantified using a nanodrop and

checked by using a Bio-Rad RNA Experion and run in accordance with Bio-Rad's instructions.

2.5.3. qRT-PCR:

qPCR primers were designed to amplify fragments at 90-110 bp, and an annealing temperature of 58-60 °C. Bioline sensimix was used and the reaction within each well consisted of 10 µl sensimix, 0.2 µl forward primer, 0.2 µl reverse primer, 8.1 µl sigma dH₂O then 1.5 µl template DNA. The plate was sealed and centrifuged at 1500 rpm for 3 minutes at 4 °C, then placed in the Bio-Rad real time thermocycler. The cycle undertaken was outlined in the manufacturer's guidelines.

2.6. Actinorhodin and Undecylprodigiosin Assay

2.6.1. Growth:

Spores were quantified and 1×10^9 spores were inoculated in 10 ml 2 x YT with a spring and placed at 30 °C, 200 rpm overnight. Mycelia were harvested at 2 500 g for 10 minutes then resuspended in 1 ml SMM. Then sonicated at 25 Hz for 1 second and placed in 50 ml SMM with a spring. These were grown at 30 °C 200 rpm. Samples were then taken at 20 and 39 hours.

2.6.2. Liquid Chromatography and Mass Spectrometry (LCMS):

5 ml culture was spun at 2 500 g for 10 minutes and supernatant was stored at -20 °C. 0.5 ml sample were mixed with 0.5 ml methanol and placed in a Liquid Chromatography mass

spectrometer with a C₁₈ column running a gradient of 70 % dH₂O / 30% acrylamide to 5 % dH₂O / 95 % acrylamide for 15 minutes. UV visible spectrum was also taken of the supernatants.

2.6.3. Actinorhodin and Undecylprodigiosin Assay:

Undecylprodigiosin was assayed by pelleting 1 ml culture. Resuspending the pellet in 1 ml methanol with 20 µl 1.5 M HCL, vortexed and centrifuged at 15 120 g for 1 minute. Samples was then placed in a cuvette and the optical density was measured at 530 nm. For calculations a molar coefficient value of 100 500 M⁻¹cm⁻¹ was used.

Actinorhodin was assayed by taking 667 µl broth and adding 333 µl 2 M KOH, vortexed and centrifuged at 15 120 g for 1 minute. The optical density used was 640 nm and for calculation the molar coefficient value of 25 320 M⁻¹cm⁻¹ was used. Protein concentration was measured as described in section 2.3.2.

2.7. DNA Binding

2.7.1. Constructing an *nsrR* 3XFlag Strain

PCR the *nsrR* gene along with its native promoter (but excluding a stop codon), was cloned into the plasmid pUCflagF via KpnI and StuI. The plasmid pUCflagF was used as it contained a 3XFlag tag with optimised GC rich codon for use in *Streptomyces spp.* Prospective plasmids were checked with restriction digestion and PCR; fragments were subcloned with KpnI and HindIII (so *nsrR* along with the in-frame 3XFLAG tag would be excised) and inserted into a KpnI/HindIII digested pMS82. Successful plasmids were checked by restriction digestion, PCR and sequencing. Successful plasmids were named pN5112.

2.7.2. ChIP-seq:

Equilibrating 50 % protein A sepharose beads:

Protein A beads set up: 0.125 g washed with 0.5x IP buffer (excluding protease inhibitor) for 15 minutes then centrifuged at 2 500 g for 3 minutes. Four washes undertaken at room temperature for beads to swell to four times original weight.

1×10^8 spores were inoculated on 20 SFM plates with cellophanes for M145 at 30 °C for 48 hours, *ΔnsrR* (pN5112) strain at 30 °C for 48 hours. Cellophanes were then removed and flipped so mycelium were directly placed in 10 ml 1 % formaldehyde solution, within the petri dish lids, for 20 minutes at room temperature. Cellophanes were then transferred to a new petri dish containing 10 ml 0.5 M glycine for 5 minutes. Mycelia were harvested, kept on ice, centrifuged at 2 500 g for 10 minutes at 4 °C. Mycelia were washed twice with 25 ml ice cold PBS (1x PBS pH 7.4) and were pelleted or removed with a spatula. Then resuspended in 1 ml lysis buffer and incubated at 25 °C for 25 minutes. Samples were then placed on ice and incubated for 2 minutes once 1 ml IP buffer was added. Samples were then sonicated at 50 Hz for 15 seconds for 7 intervals then centrifuged at 15 120 g for 10 minutes at 4 °C. Supernatants were transferred to a new tube and centrifugation was repeated. 1 ml sample was used for IP, 25 μl for total DNA and excess was stored at -20 °C. The 1 ml IP sample was pre cleared using 1/10 volume (100 μl) equilibrated 50 % protein A sepharose beads and incubated at 4 °C for 1 hour on a rotating wheel. Then centrifuged at 15 120 g for 15 minutes at 4 °C. Supernatant was transferred to a new and 1/10 volume (100 μl) 10 mg (sigma α-flag) antibody was used and incubated overnight at 4 °C on a rotating wheel. Then 1/10 volume (100 μl) equilibrated protein A sepharose beads were added and incubated for 4 hours at 4 °C on a rotating wheel. Then centrifuged at 1 100 g

for 5 minutes and washed twice with 1 ml 0.5x IP buffer for 15 minutes with gentle agitation then twice with 1 ml 1x IP buffer for 15 minutes with gentle agitation. Then each sample was split into two separate tubes containing 0.5 ml sample, 1 100 g for 5 minutes to remove all supernatant. 150 μ l elution buffer was added, 10 μ l for the total DNA samples, and incubated at 65 °C overnight. Tubes were then inverted seven times and centrifuged at 15 120 g for 5 minutes. Supernatant was transferred to a new tube and 50 μ l TE (pH 7.8) was added to the beads, placed at 65 °C for 5 minutes then 15 120 g for 5 minutes. Supernatant was then pooled with previous 150 μ l, centrifuged at 15 120 g for 1 minute and transferred to a new tube. The 2 μ l 10 mg/ml proteinase K was added to each eluate and placed at 55 °C for 1.5 hours. Then 200 μ l phenol/chloroform was added, vortexed for 3 minutes then centrifuged for 3 minutes at 15 120 g. Upper phase was stored and the organic phase was re extracted with 100 μ l TE (pH 7.8). Samples were then purified using a QiaQuick kit and eluted with 50 μ l sigma water, and re eluted with the eluate. DNA was then quantified using a nanodrop.

2.7.3. GUS Assay

Cloning:

The 500 bp promoter region of *ftsZ*, *mce (sco2422)*, *sco7426*, *nsrR* and *hmpA1* were fused to the β -glucuronidase gene in pGUS by PCR. Products were then cloned into pGEMT and identified by blue/white selection and vectors were digested to test for the 500 bp inserts. Then cloned into a KpnI and XbaI digested pGUS. Successfully clones were tested by restriction digestion and sequencing.

Liquid assay:

10 μ l spore stock were inoculated in 10 ml TSB and placed at 30 °C, 200 rpm for 16 hours. 1 ml was sub-cultured in 100 ml TSB and placed at 30 °C, 200 rpm for 24 hours. Then mycelia were harvested at 2 500 g for 10 minutes, resuspended in 3 ml lysis buffer and placed at 37 °C for 1 hour. Lysates were centrifuged at 2 500 g for 10 minutes, then 0.5 ml lysate was mixed with 0.5 ml dilution buffer and 5 μ l 0.2 M *p*-nitrophenyl- β -D-glucuronide. Samples were incubated at 37 °C for 20 minutes before the optical density at 415 nm was measured.

Standardisation:

Samples were standardised using a Bradford assay. 2 μ l lysate was added to 200 μ l Bradford reagent and 798 μ l water. Optical density was measured at 595 nm.

2.8 Statistical Analysis

All graphs were generated from Microsoft Excel; the statistical analysis was carried out on data using GraphPadPrism5. For comparison of two samples a t-test was used; for more than two samples a one way analysis of variance (ANOVA) was carried out followed by a Tukey post-test.

Chapter 3: Introduction to the MtrA Project

3.1. Project Overview

The MtrA project focuses on the role of the highly conserved actinobacterial three-component system MtrAB-LpqB in *Streptomyces coelicolor*. This three component system contains one of the signature actinobacteria proteins LpqB along with the response regulator MtrA and the histidine kinase MtrB. The response regulator MtrA was first characterised in the actinomycete *Mycobacterium tuberculosis* (Mycobacterium tuberculosis regulator A). MtrAB-LpqB has been studied within a number of mycobacterial species and in *C. glutamicum* to try and understand the importance of this system. MtrA-LpqB is highly conserved in actinomycetes and has a probable role in regulating cell division within actinomycetes such as *M. tuberculosis* and *C. glutamicum*.

In *M. tuberculosis* MtrA is essential for survival; however in *C. glutamicum* the *mtrAB* genes have been successfully deleted resulting in a mutant with a pleiotropic phenotype. When the *mtrAB* genes are absent, irregular septation is observed within *C. glutamicum*; therefore MtrA is assumed to regulate cell division in *Corynebacterium spp.*

MtrAB-LpqB, function has not been well investigated in *S. coelicolor*, which has been proposed to be an excellent model for studying cell division since many cell division genes are non-essential in streptomycetes. In addition it is of interest to determine whether the function of MtrA-LpqB, previously observed in the more closely related corynebacteria and mycobacteria, is conserved in filamentous actinomycetes. This project aims to characterise mutations in the MtrAB-LpqB multiple-component system and in doing so explore the possible targets of *S. coelicolor* MtrA.

3.2. Two-Component Systems (TCS)

A major way that bacteria sense, and respond to, their environment is via TCS (Hoch and Silhavy 1995). TCS are composed of a histidine protein kinase and a cytoplasmic response regulator; which in prokaryotes are typically transcribed from a single operon. When a signal is detected by the sensor domain of the histidine protein kinase (HPK) it causes autophosphorylation of a histidine residue within the cytoplasmic domain (Hoskisson & Hutchings, 2006). This phosphate is then transferred to an aspartate residue in the receiver (REC) domain of the cognate response regulator. The phosphorylated response regulator is usually the active form and brings about a response to the original signal, usually by modulating the target genes.

3.2.1. Histidine Protein Kinase (HPK)

Histidine protein kinases (HPKs) are assumed to have arisen in bacteria; this is due to their wide distribution within bacterial genomes (Koretke *et al.*, 2000). They exist in all major branches of bacteria and archaea and in plants and fungi but are absent from the animal kingdom (Grebe & Stock, 1999). HPKs are a large family of signal-transduction enzymes that mostly act as trans-membrane receptors due to their hydrophobic, membrane-spanning sequences. The conserved sequence of the kinase core defines which sub-family each HPK belongs to (Grebe & Stock, 1999). The HPK family consists of different subgroups and are classified into 11 subfamilies accordingly.

As HPKs are usually located within the membrane with extracellular sensing domains they have a major role in bacteria adapting to their surrounding environment. Conditions that HPKs have been shown to sense include external nutrients, osmotic conditions and chemoattractants to name a few (Amemura *et al.*, 1990, Bentley *et al.*, 2003, Burbulys *et*

al., 1991, Fuqua *et al.*, 2001, Kanamaru *et al.*, 1989). HPKs detect these extracellular signals via the highly diverse sensing domain; where signal transduction through the HPK typically results in gene expression being altered accordingly by the cognate response regulator. This transduction occurs when an extracellular signal is detected by the sensory domain and induces kinase activity (Hakenbeck & Stock, 1996). Activated HPKs catalyse the transfer of a phosphate from ATP to a conserved histidine residue in their cytoplasmic domains, creating a high-energy phosphohistidine. The high-energy phosphohistidine acts as a substrate for phosphotransfer to the cognate response regulator. Some HPKs also have the ability to dephosphorylate the RR, this bifunctional activity is mediated by the dimerization domain (Hoch & Silhavy, 1995, Perego & Hoch, 1996). HPKs are widely abundant in prokaryotes and are the primary mechanism used for signal transduction (Wolanin *et al.*, 2002).

HPKs generally function as homodimers and consisting of different domains. The HAMP domain transduces signal from the activated sensor domain to the cytoplasmic kinase domain. The two α -helices that comprise the HAMP domain are vital to this signal transduction process. The HAMP domain is thought to transduce signal by either a two or three state mechanism (Gushchin *et al.*, 2013, Stewart, 2014). The two state mechanism is a change in conformation being either loosely or tightly packed helices. Whereas the three state mechanism is multiple conformations of this HAMP bundle, which has been proposed to function via oscillation between the loosely and tightly packed states (Parkinson, 2010). The change in conformational state of the HAMP helices transduces signal from the sensor domain to consequently activate the cytoplasmic kinase domain.

The number of HPK within bacterial genomes varies dramatically. For example *Escherichia coli* and *Bacillus subtilis* contain 25 HPKs; whereas *Streptomyces coelicolor* contains 84 (Hutchings *et al.*, 2004) and the *Helicobacter pylori* genome contains only 4 HPKs.

Organisms that contain more HPKs within their genome can, as a general rule, live in a wide range of environmental conditions. This adaptation is due to the HPKs functioning as sensors to accommodate for the change in environmental conditions. The number of HPKs detected within a genome roughly reflects the number of cognate TCS encoded by each bacterium. HPKs have been found to evolve by horizontal gene transfer, gene duplication or domain shifting (Alm *et al.*, 2006). The prominent mode of HPK evolution in *Streptomyces coelicolor* is lineage-specific expansion of existing HPK families (Alm *et al.*, 2006). Forming new HPKs through gene duplication means that they are often formed without a paired response regulator; therefore HPKs are less likely to co-evolve with the cognate response regulators in a single duplication event (Alm *et al.*, 2006). However orphan HPKs are often found in close proximity to cognate response regulators, where it is assumed cross-regulation of response regulations occurs with the additional kinase.

3.2.2. Response Regulators (RR)

Response regulators (RRs) are paired with HPKs by the N-terminal receiver domain, which is phosphorylated by the cognate HPK (Hakenbeck & Stock, 1996); once activated the C-terminal domain of some RR can interact with DNA in order to alter transcription. Phosphorylation of the RR is achieved by transfer of the phosphate from the HPK to an aspartate within the response regulator receiver domain and is catalysed by the RR (Brocker *et al.*, 2011); (Friedland *et al.*, 2007). This phosphorylation state results in a conformational change in the RR that allows the helix-turn-helix DNA binding domain to bind to its DNA binding site at target gene promoters and bring about a response to the original signal.

MtrA can be assigned to the OmpR/PhoB family of RRs due to a number of distinct features. The OmpR/PhoB family is the most populated subfamily containing approximately one third of identified RRs (Galperin, 2006). The features of the OmpR/PhoB family include a highly conserved N-terminal sequence composed of α 4- β 5- α 5 deemed the receiver domain; as well as the definitive winged helix-turn-helix DNA binding domain (Gao *et al.*, 2007). Regulatory diversity is seen within OmpR/PhoB regulators due to the variety of interaction exhibited between the receiver and DNA binding domains; examples of these regulators include DrrB, PrrA, and DrrD (Robinson *et al.*, 2003, Buckler *et al.*, 2002, Nowak *et al.*, 2006). The interaction between the two domains results in a variation of regulation as well as the inactive state being maintained. The orientation of key residues within the receiver domain results in either an inactive or active state. The orientation of these residues is altered by phosphorylation, which causes a common active dimer to be formed and stabilised by phosphorylation.

3.2.3. Accessory Proteins

Studies have also shown that auxiliary proteins can sometimes interact with either the HPK or RR of the TCS resulting in a multiple-component system. The auxiliary proteins that have been shown to interact with the sensor domains of HPKs include lipoproteins in Gram-positive bacteria and periplasmic proteins in Gram-negatives. Lipoproteins in Gram-positive bacteria have been described as the equivalent of periplasmic proteins in Gram-negative bacteria (Nielsen & Lampen, 1982). Lipoproteins are cell envelope proteins that are anchored to the outer surface of the cell membrane via a membrane phospholipid covalently attached to the N-terminus (Hutchings *et al.*, 2009, Sutcliffe & Russell, 1995). Some lipoproteins are located within the operon of TCS and have therefore been proposed to interact with the HPK on the outside of the cell (Hoskisson & Hutchings, 2006).

Streptomyces coelicolor contains 67 paired (i.e. co-encoded) TCS; of which 6 encode lipoproteins within the same gene cluster (figure 3.1). These are likely to use the lipoprotein as an accessory to control the HPK activity and likely feed in additional, as yet unknown, signals.

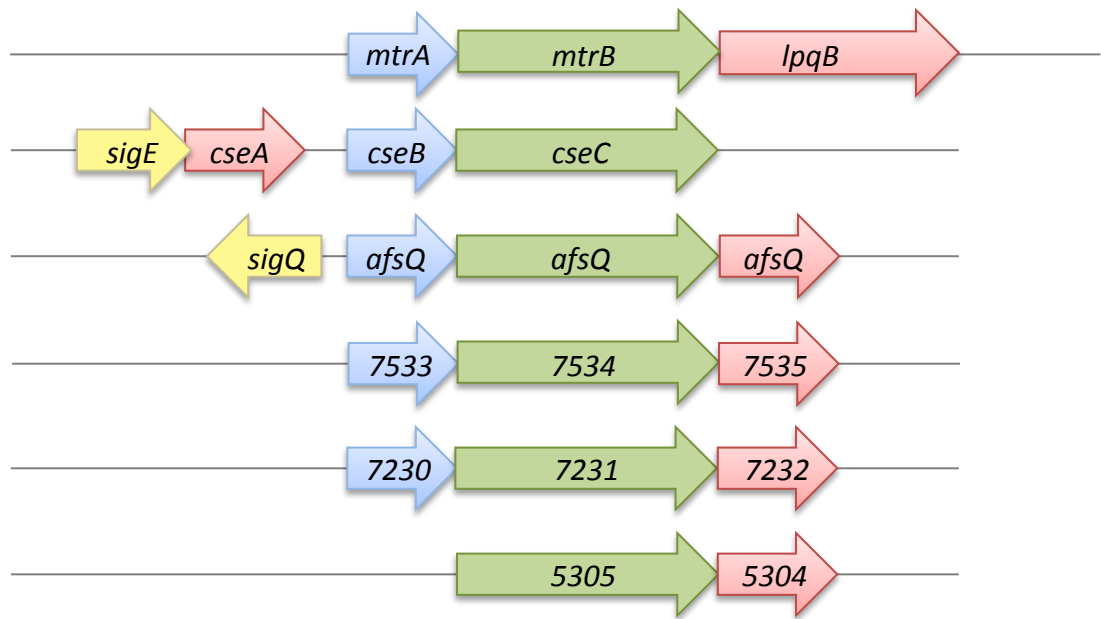


Figure 3.1: Two-component system operons contained within the *Streptomyces coelicolor* genome that encode lipoproteins. The sigma factors are in yellow, response regulators in blue, HPKs are green and lipoproteins are red. Adapted from (Hoskisson & Hutchings, 2006).

Multiple-component systems have been reported in other bacteria in which lipoproteins assist or modify the activity of the TCS via the HPK. One example is the KdpED system that exhibits a primary response to osmotic stress by targeting *kdpFABC* expression. To investigate the function of the KdpED component system in *M. tuberculosis* and *M. smegmatis* a yeast two-hybrid screen was undertaken. This screen identified lipoproteins, LprJ and LprF, which interact with the sensing domain of the HPK, KdpD (Steyn *et al.*, 2003). As these lipoproteins interact with the sensing domain they were proposed to influence HPK signal detection within this multiple-component system (Steyn *et al.*, 2003). Another

proposed multiple-component system is YycFG within the phylum Firmicutes; where the membrane proteins YycH and YycI, encoded within the *yycFG* operon, have been shown to negatively regulate the HPK YycG (Szurmant *et al.*, 2007b, Szurmant *et al.*, 2005). These auxiliary proteins are involved in expression of peptidoglycan modification genes and also regulate cell division in *Bacillus subtilis* via *ftsAZ* (Fukuchi *et al.*, 2000, Fukushima *et al.*, 2008, Szurmant *et al.*, 2007a). The YycFG system has been proposed as being analogous to the actinobacterial MtrAB-LpqB three-component system (Hoskisson & Hutchings, 2006, Winkler & Hoch, 2008). This multiple-component system contains the lipoprotein LpqB, which also has been found to interact with the HPK MtrB in *Mycobacterium smegmatis* (Nguyen *et al.*, 2010).

3.3. MtrAB-LpqB Component System

3.3.1. MtrB

The MtrAB-LpqB system is highly conserved in actinobacteria and regulates a range of cellular processes. In *C. glutamicum*, MtrB is activated by various compounds; including sugars, amino acids and polyethylene glycols (Möker *et al.*, 2007b). As the stimulating compounds vary drastically in structure the hydration state, instead of solute binding, has been proposed to activate *C. glutamicum* MtrB. As MtrB detects changes in hydration state it may act as an osmosensor, that can sense the intensity of osmotic stress experienced by the cell (Kramer, 2009, Möker *et al.*, 2007a, Möker *et al.*, 2007b, Möker *et al.*, 2004).

Stimulation of *C. glutamicum* MtrB by these changes in hydration state was shown to occur at the cytoplasmic domain (Möker *et al.*, 2007b) while the extracellular domain may sense an alternative extracellular signal. The trans-membrane domain therefore anchors MtrB to the cell membrane (Kramer, 2009). MtrB is composed of two trans-membrane domains

connected by an extracellular loop, a HAMP linker domain, the dimerization domain and a catalytic domain. The dimerization domain and catalytic domain of HPKs are comprised of clusters of highly conserved residues known as homology boxes (Grebe & Stock, 1999). The trans-membrane domain of MtrB has recently been shown to be lipid associated, which influences the activity of MtrB (Nguyen *et al.*, 2010).

MtrB has been shown to localise to the cell division septa and poles in *M. tuberculosis* and *M. smegmatis* cells (Plocinska *et al.*, 2012). This septal localisation is independent of phosphorylation and occurs after FtsZ ring formation; therefore the localisation of MtrB to the septa could be linked to FtsZ formation. As MtrB is linked to septation in *M. tuberculosis*, it has been proposed that MtrB could be activated by synthesis of the division septa (Plocinska *et al.*, 2012).

3.3.2. MtrA

The MtrA response regulator is conserved within all members of the phylum Actinobacteria with the exception of *Troperyma whipplei* (Hoskisson & Hutchings, 2006, Bentley *et al.*, 2003).

The solved structure of MtrA from *M. tuberculosis* (figure 3.2) reveals that MtrA, like other members of the OmpR/PhoB family, has a N-terminal regulatory domain and a definitive C-terminal winged helix-turn-helix DNA binding domain (Friedland *et al.*, 2007). The intermolecular interactions of $\alpha 4$ - $\beta 5$ - $\alpha 5$ of the regulatory domain allow the C-terminal DNA binding domain to recognise target sites when MtrA is in its active form. An interdomain hydrogen bond between tyrosine residue 102 (tyr102) and aspartate residue 190 (asp190) means that there is a bias for the inactive form of the MtrA protein (Barbieri *et al.*, 2010), meaning the rate of phosphorylation is reduced. The dominant inactive state accounts for

the low phosphorylation rate of MtrA; when compared to other members of the OmpR/PhoB family (Barbieri *et al.*, 2010).

The phosphorylation of the aspartate residue 56 (Asp56), in the N-terminal regulatory domain of MtrA, modulates its activity (figure 3.2). Activation within the regulatory domain of MtrA involves two highly conserved residues. These vital residues are threonine 83 (thr83) in the C terminus of β 4 and tyrosine 102 (tyr102) in the β 5 of the regulatory domain (figure 3.2).

The orientation of these residues differs in active or inactive conformations. This change of orientation in both the active and inactive form of MtrA is seen with the Tyr102 residue. In the active form Tyr102 extends outwards whereas in the active state Tyr102 is buried within the domain. The orientation of Tyr102 is vital to bonding with the Asp190 of the DNA binding domain. In the inactive form of MtrA (figure 3.2) a hydrogen bond is formed; whereas in the active state the inward orientation of Tyr102 disrupts this bond and weakens this inactive interface.

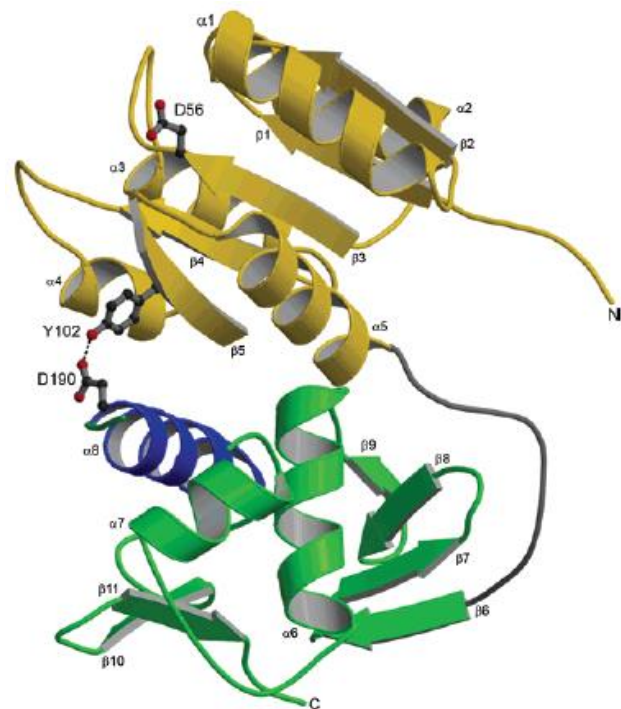


Figure 3.2: The structure of MtrA from *M. tuberculosis*. The regulatory domain is depicted in gold and the DNA binding domain in green. The phosphorylation site (Asp56), interdomain bond (between Tyr102 and Asp190) are shown in ball and stick format (Friedland *et al.*, 2007) used with authors permission.

Another important residue within the regulatory domain is Thr83. In the inactive state the hydroxyl group of the Thr83 residue points away from the active site; but points towards the active site when in the active state. Therefore within the active state the hydroxyl

group of Thr83 can interact with the phosphorylated Asp56 residue. These two states exist in equilibrium where phosphorylation of the Asp56 residue shifts this equilibrium towards an active state (Volkman *et al.*, 2001).

The winged helix-turn-helix (HTH) of MtrA defines it not only as a member of the OmpR/PhoB family but also a transcriptional regulator. This C-terminus of MtrA interacts with DNA, and the N-terminus interacts with MtrB; when bound to MtrB, DNA binding is inhibited (Li *et al.*, 2010a). The *mtrAB* genes were first identified in *M. tuberculosis* when hybridized with a *Pseudomonas aeruginosa phoB* probe (Via *et al.*, 1996). This work showed that MtrA cannot be deleted in *M. tuberculosis*, which suggests that MtrA function is essential in *M. tuberculosis* (Curcic *et al.*, 1994, Via *et al.*, 1996, Zahrt & Deretic, 2000). The expression of *mtrA* was observed within both the virulent *M. tuberculosis* and the *M. bovis* vaccine strain. This direct comparison of *mtrA-gfp* expression *in vivo* revealed that, unlike the avirulent strain, *mtrA* is constitutively expressed in *M. tuberculosis* (Zahrt & Deretic, 2000).

Unlike *M. tuberculosis* the *mtrAB* genes were successfully removed from the *C. glutamicum* genome revealing MtrA is not essential (Möker *et al.*, 2004). The viable *C. glutamicum* $\Delta mtrAB$ mutant exhibits elongated cell morphology, shown in figure 3.3, and is susceptible to some antibiotics (Möker *et al.*, 2004). As well as being elongated the *C. glutamicum* $\Delta mtrAB$ mutant cells were segmented and irregular septation was detected by transmission electron microscopy (TEM). Therefore the MtrAB-LpqB system is likely to have a role in *C. glutamicum* cell division.

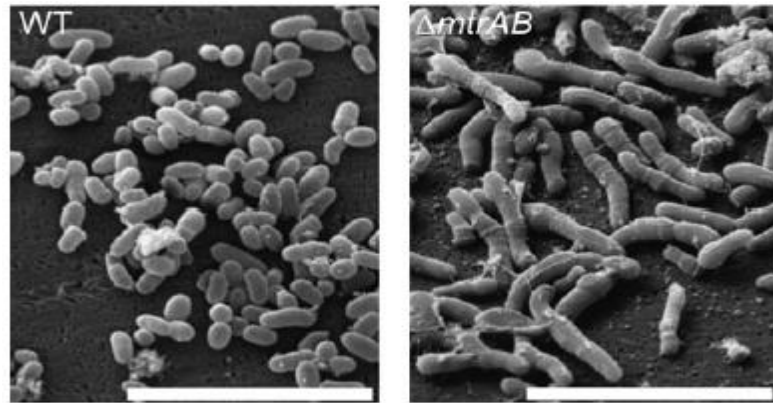


Figure 3.3: Scanning electron microscopy (SEM) identifying the phenotype of WT and $\Delta mtrAB$ *C. glutamicum* where the white line is 10 μ M. The mutant phenotype suggests potential targets of MtrA within *C. glutamicum*, both the phenotype and potential targets are important in comparison with other actinomycetes including *S. coelicolor*. (Möker *et al.*, 2004) used with authors permission.

The phenotype of the *C. glutamicum* $\Delta mtrAB$ mutant suggested MtrA targets in this species might include genes involved in cell wall metabolism, and microarray and ChIP-chip experiments identified *mepA* and *nlpC* (cell wall peptidases) and *proP* and *betP* (solute carriers) to be MtrA targets (Brocker *et al.*, 2011, Möker *et al.*, 2004).

In mycobacterial species a complete MtrA regulon has not been defined but the *mce* genes are targets of MtrA and the *dnaA* gene is a direct target of MtrA in *M. tuberculosis* suggesting a role for MtrA in regulating the initiation of DNA replication (Fol *et al.*, 2006). This may explain why MtrA proves to be essential in *M. tuberculosis* but not in *C. glutamicum*.

DNA replication and cell division are linked within the bacterial cell cycle (Greendyke *et al.*, 2002) and DnaA also functions as a transcription factor in bacteria; possible targets of DnaA include genes involved in cell division: *ftsK*, *ftsL*, *ftsY* and *ftsQ* (Fol *et al.*, 2006, Greendyke *et al.*, 2002). This adds further support to the theory that the MtrAB-LpqB component system regulates cell division in actinomycetes.

3.3.3. LpqB

The *lpqB* gene is located immediately downstream of the *mtrA* and *mtrB* genes in all actinobacteria which encode this signal transduction system. *lpqB* encodes a lipoprotein that was proposed to mediate signal transduction through the MtrAB TCS from the outside of the cell (Hoskisson & Hutchings, 2006). In *C. glutamicum* the expression of *lpqB* is increased in an *mtrAB* mutant strain, but the *lpqB* gene itself cannot be disrupted, suggesting it might be essential (Möker *et al.*, 2004).

Interaction between LpqB and MtrB was first demonstrated in *M. smegmatis* using a bacterial two-hybrid assay. This worked showed that LpqB interacts with the extracellular domain of MtrB and affects the phosphorylation state of MtrA, presumably by modulating MtrB activity (Nguyen *et al.*, 2010). The increased phosphorylation state of MtrA, by interaction of LpqB with MtrB, causes the increased expression of MtrA targets. Therefore LpqB positively regulates MtrAB activity by changing the phosphorylation state of MtrA via its interaction with MtrB.

The role of LpqB was examined further in mycobacteria by successfully creating a *lpqB* mutant in *M. smegmatis*; this *M. smegmatis lpqB* mutant exhibits branched filamentous growth reminiscent of *Streptomyces* spp. and in stark contrast to wild type, rod-shaped *M. smegmatis* cells (Nguyen *et al.*, 2010).

3.3.4 SCO3014

Immediately upstream of *mtrA* is the gene *sco3014*, where the protein sequence is similar to that of an initiation factor (IF) belonging to the IF 2 subfamily. This could mean that SCO3014 is an important component of the *sco3014-mtrAB-lpqB* operon. Phenotypic analysis of the *sco3014* mutant will be important to establish whether the phenotype is

similar to other mutants from the *sco3014-mtrAB-lpqB* operon. However it is important to note that although *sco3014* is contained within many *Streptomyces* spp. it is absent from the *S. venezuelae* genome.

3.4. Project Aims

Using end-point RT-PCR the *mtrA*, *mtrB* and *lpqB* genes have been shown to form a single transcript in *S. coelicolor*, along with *sco3014* which is upstream of *mtrA* (unpublished). In order to understand the MtrAB-LpqB system in *Streptomyces coelicolor* a number of questions need to be addressed within this project. Firstly as some components of the MtrAB-LpqB system have been shown to be essential in other actinomycetes, are any of the encoding genes also essential in *S. coelicolor*? In order to test this, single in-frame mutations will be made in *sco3014*, *mtrA*, *mtrB* and *lpqB* to determine whether any components of the system are essential in *S. coelicolor*. If these mutants are viable their effects on growth and development will be investigated using both light microscopy and Scanning Electron Microscopy (SEM). Finally potential targets of the MtrAB-LpqB system will be investigated using qRT-PCR analysis and GUS reporter assays. These experiments were conducted to investigate whether the MtrAB-LpqB component system is involved in regulating differentiation and cell division in *S. coelicolor* and to further our understanding of the role of this system in the actinobacteria.

Chapter 4: Results for MtrA Project

4.1. Generation of Mutants

4.1.1. Strategy for Producing Mutants

Prior to working on this project the cosmid StE33, containing *sco3014*, *mtrA*, *mtrB* and *lpqB* had already been targeted using the redirect system to replace each gene with an apramycin or hygromycin resistance cassette and make the marked knock out cosmids: *sco3014:apr*, *mtrA:apr*, *mtrB:hyg*, and *lpqB:apr*. These mutant cosmids had been conjugated into *S. coelicolor* M145 and double crossovers had been isolated but the phenotypes of the mutants had not been investigated.

4.1.2. Making In-Frame Mutants

The previously made knock out cosmids, constructed using the cosmid StE33, were used to transform *E. coli* BT340 and grown to induce flp recombinase expression. The Flp recombinase removed the apramycin or hygromycin cassette using the flanking FRT sites. Once plated double cross overs were identified and colonies were then screened for apramycin or kanamycin sensitivity due to the desired loss of the resistance cassette. Potential candidates, which were sensitive to apramycin or hygromycin but resistant to kanamycin, were confirmed by isolating and digesting the cosmids.

4.2. Characterisation of *sco3014-mtrAB-lpqB* Mutants

4.2.1. Phenotype of *sco3014-mtrAB-lpqB* Mutants

The phenotypes of all unmarked mutants were observed (figure 4.1); after three days growth wild type *S. coelicolor* has formed aerial mycelium and was beginning to sporulate. Normally when selecting potential successful mutants to screen a dominant phenotype is observed. However figure 4.2 revealed that when producing the *lpqB:apr* mutant strain, this was not the case. Instead a grey and white phenotype was observed. Therefore in this case both grey and white strains were tested by PCR using primers 3011 test forward and reverse (figure 9.2). Therefore due to both $\Delta lpqB$ grey and $\Delta lpqB$ white being correct mutants both were used for experiments.

The production of both grey and white colonies occurred when *lpq:apr* and $\Delta lpqB$ mutant cosmids were introduced into *S. coelicolor*, which produced double crossovers. Continuation of growth grey colonies mutated to form white colonies; but once white colonies were formed they did not mutate to grey colonies. The proposed reasoning for the formation of white colonies by the *lpqB* mutants is explored in section 7.1.

The *mtrB:hyg* mutant was smaller than the wild type strain and produced both blue and red pigment. Also the *mtrA:apr* mutant exhibited a similar phenotype to *mtrB:hyg* and had begun to form aerial mycelium. Finally the *sco3014:apr* mutant looked similar to wild type M145, but appeared to sporulate earlier than the wild type.

When the marked *mtrA:apr*, *mtrB:hyg* and *lpqB:apr* mutants were produced and plated out to check their colony phenotypes they looked genetically stable, that is individual colonies looked the same within each strain. However when spores of the *lpqB:apr* mutant were plated onto SFM they consistently formed a mixture of grey or white colonies, as shown in

figure 4.2. In subsequent experiments therefore both grey and white *lpqB:apr* mutants were tested alongside the *sco3014:apr*, *mtrA:apr* and *mtrB:hyg* mutants.

The variation in phenotypes observed in the mutants could be effected by the introduction of an antibiotic resistance cassette because it might have polar effects on the downstream genes. Therefore the only way to be certain that the phenotype is a result of the removal of genes was to create in-frame mutations in each gene (deemed Δ). These mutations were made by removing the resistance cassette by the flanking *flp* recombination sites to produce an in frame 'scar'.

The phenotypes of the in-frame (Δ) *sco3014* *mtrA* *mtrB* and *lpqB* mutants are shown in figures 4.1 and 4.3. Colonies of the Δ *mtrB* and Δ *mtrA* strains were consistently much smaller than the wild type and produced actinorhodin and undecylprodigiosin pigment. The Δ *sco3014* strain was sporulating earlier (or more) than the *wild-type*. Therefore figure 4.1 revealed that the phenotypes seen in the Δ *sco3014*, Δ *mtrA* and Δ *mtrB* were due to the loss of those genes and not the not due to introduction of the resistance cassette having a polar effect on downstream genes.

The Δ *lpqB* mutant remained separated into grey and white phenotype (figure 4.2). These two Δ *lpqB* lineages could possibly be at different stages of the lifecycle. In order to establish whether the Δ *lpqB* grey and Δ *lpqB* white strains were sporulating SEM was required. However the difference in colony morphology of the Δ *lpqB* mutants was depicted in figure 4.3 where the strains have progressed further in their development.

Figure 4.3 revealed that at 5 days growth the wild type strain M145 had sporulated, along with Δ *lpqB* grey and Δ *sco3014*. In comparison to both wild type and Δ *lpqB* grey, it is unclear whether the Δ *lpqB* white strain had formed spores without further investigation. Also at 5 days growth the Δ *mtrB* and Δ *mtrA* strains have just begun to sporulate. The size of the

mutant strains varied in that both $\Delta lpqB$ strains are a similar size to the wild type, and $\Delta sco3014$ colonies are larger. Figure 4.3 revealed the phenotypes caused by removing the individual genes *sco3014*, *mtrA*, *mtrB* and *lpqB* in the *sco3014-mtrAB-lpqB* operon. In order to confirm these findings, these mutants were complemented by re-inserting the deleted genes *in trans* (section 4.2.2).

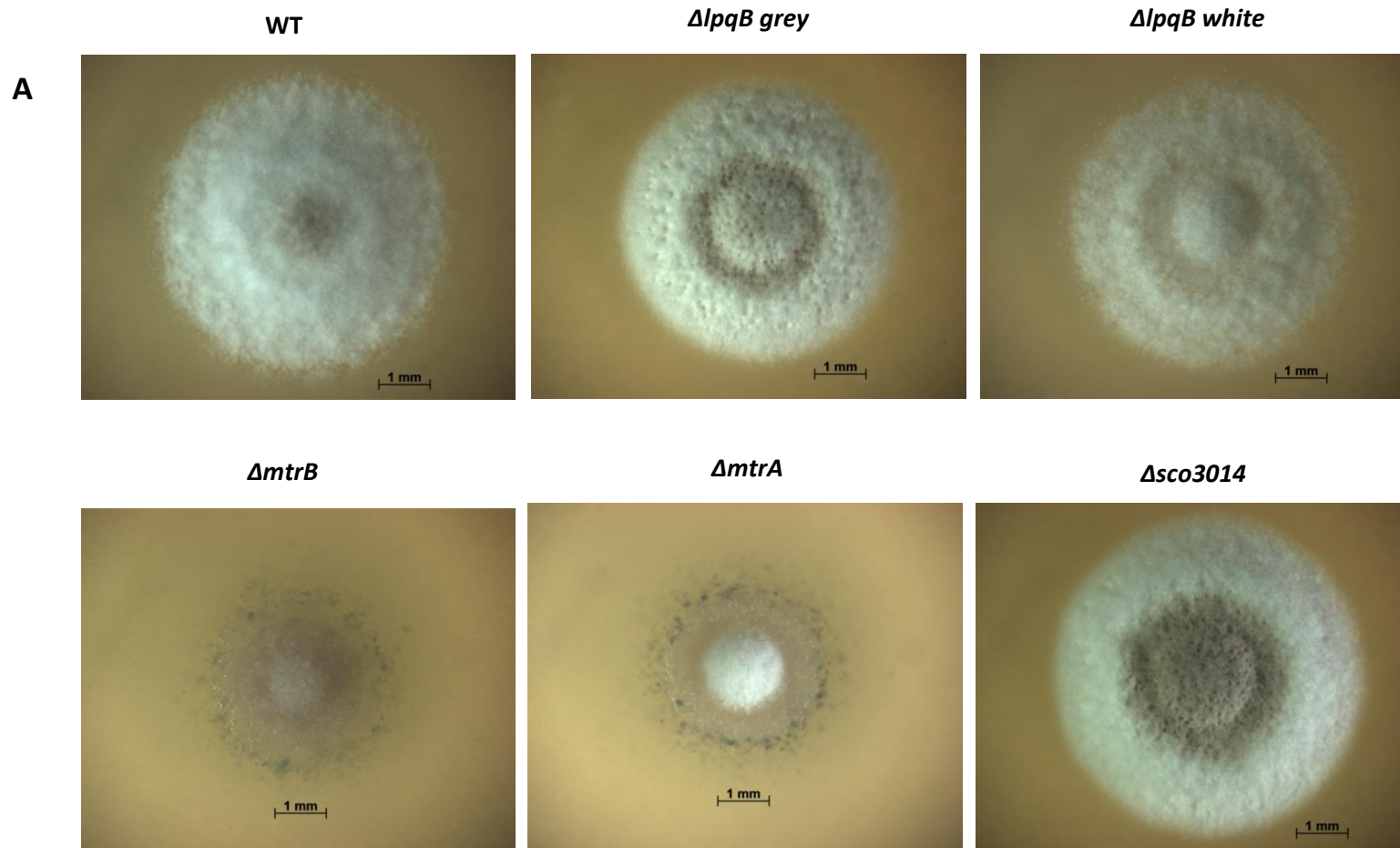


Figure 4.1: Phenotypic comparison of *Δsco3014-mtrAB-lpqB* mutants when grown on SFM for 3 days at 30 °C in relation to wild type *Streptomyces coelicolor* M145. (A) Light microscopy of *S. coelicolor* M145, *ΔlpqB* grey, *ΔlpqB* white, *ΔmtrB*, *ΔmtrA* and *Δsco3014*. At this stage of growth developmental progression may be effected by removal of genes within the mutant strains. The *ΔmtrB* and *ΔmtrA* strains also exhibit a smaller, stressed phenotype. (B) Genetic organisation of the *S. coelicolor* 3014-*mtrAB-lpqB* operon.

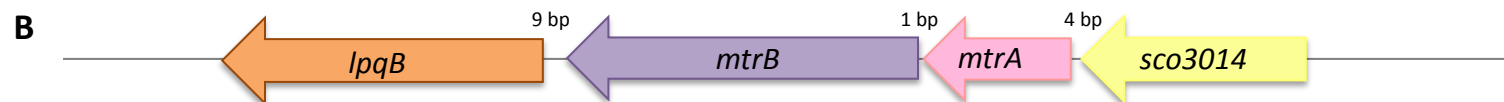




Figure 4.2: The grey / white phenotype which arose in apramycin resistant double cross over mutants when introducing the *lpqB:apr* cassette into *S. coelicolor* and remained within the in-frame *lpqB* mutants. Photographic representation of an entire SFM plate inoculated with $\Delta lpqB$ and grown for 5 days at 30 °C revealing both grey and white colonies.

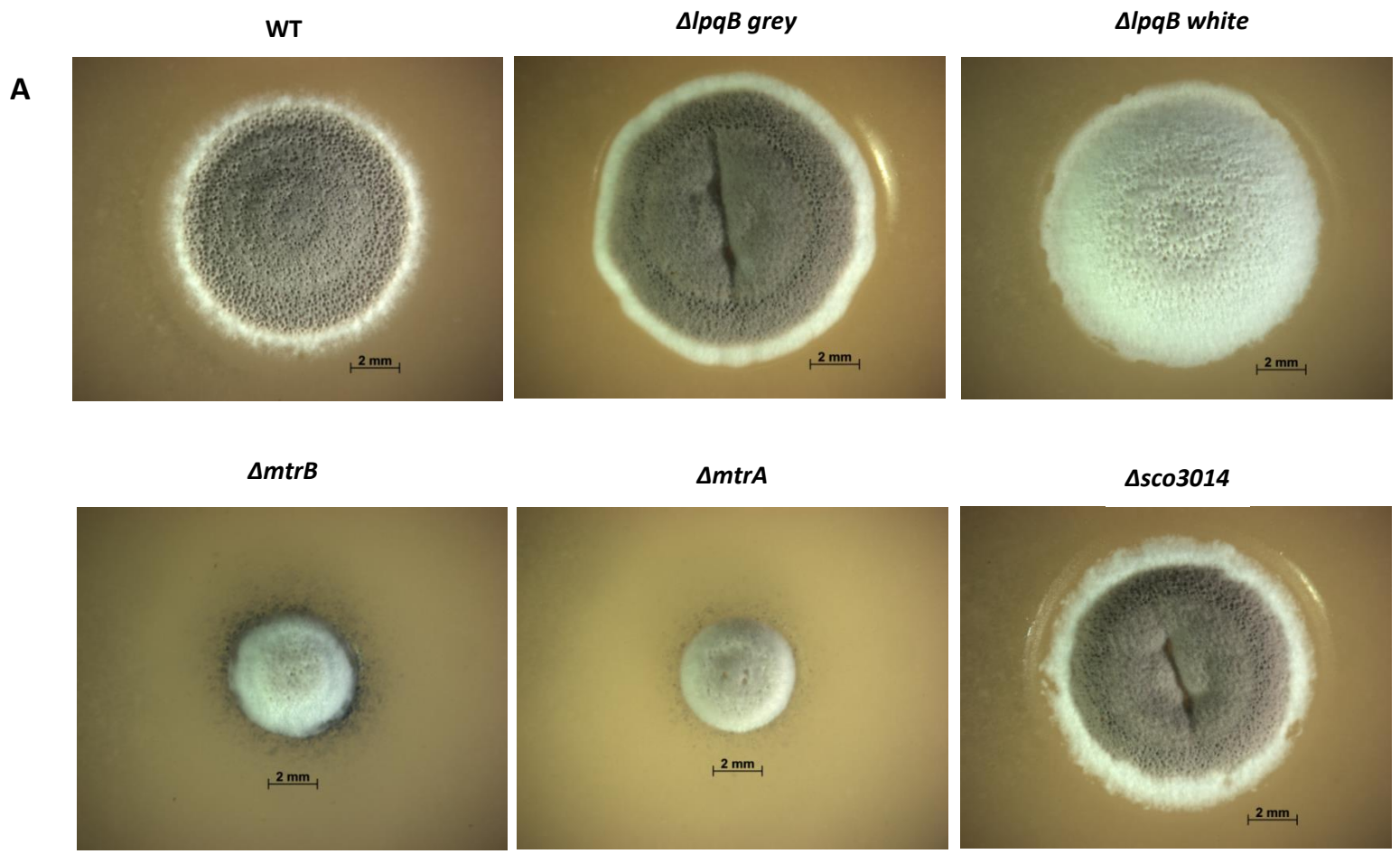
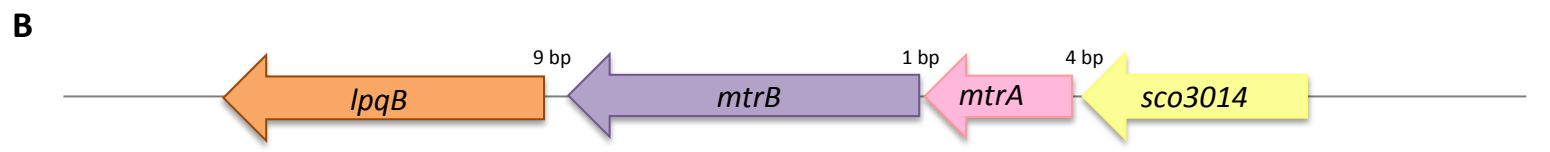


Figure 4.3: Phenotypic comparison of $\Delta sco3014$ -*lpqB* mutants when grown on SFM for 5 days at 30 °C in relation to wild type *Streptomyces coelicolor* M145. (A) Light microscopy of *S. coelicolor* M145, $\Delta lpqB$ grey, $\Delta lpqB$ white, $\Delta mtrB$, $\Delta mtrA$ and $\Delta sco3014$. At this stage of growth the grey / white phenotype of the $\Delta lpqB$ strain can be seen. The $\Delta mtrB$ and $\Delta mtrA$ mutants remain small in comparison to wild type *S. coelicolor*. (B) Genetic organisation of the *S. coelicolor* 3014-*lpqB* operon.



4.2.2 Complementation of the Mutants

Removal of the resistance cassette from the $\Delta sco3014$, $\Delta mtrA$, $\Delta mtrB$ and $\Delta lpqB$ strains prevented any polar effects meaning the phenotype observed was due to the loss of the gene. To prove that a phenotype was due to the deletion of a single gene it was therefore necessary to complement the mutation by re-introducing that gene under the control of its native promoter (appendix, page 183-190). To achieve this each gene was synthesised by Genscript with the *sco3014* promoter region at the 5' end and flanked by 5' EcoRI and 3' XbaI sites. The position of the restriction sites in relation to the *lpqB*, *mtrB* and *mtrA* can be seen in appendix, pages 185-190.

Once the complementation plasmids (appendix, pages 186, 188, 190) were successfully conjugated the resulting strains were referred to as $\Delta lpqB$ grey (pL11912), $\Delta lpqB$ white (pL11912), $\Delta mtrB$ (pB11912) and $\Delta mtrA$ (pA11912) (figure 4.4 and 4.5) and their phenotypes were compared to those of their parent mutant strains. If wild-type phenotype was successfully restored then the change in phenotype could be confirmed as due to the loss of the gene of interest.

Complementation of the *lpqB* white strains with the *lpqB* gene had no obvious effect on the colony morphologies, which suggested that the white phenotype was due to secondary mutation(s). When *lpqB* is reintroduced into the *lpqB* grey mutant the instability of forming white colonies no longer occurs.

The small colony phenotype of the *mtrB* mutant was fully complemented by re-introduction of *mtrB* *in trans*. However, the phenotype of $\Delta mtrA$ cannot be complemented, which suggests that putting the *mtrA* gene into a separate locus has somehow affected mRNA copy number or phosphorylation of MtrA by MtrB (Figure 4.5).

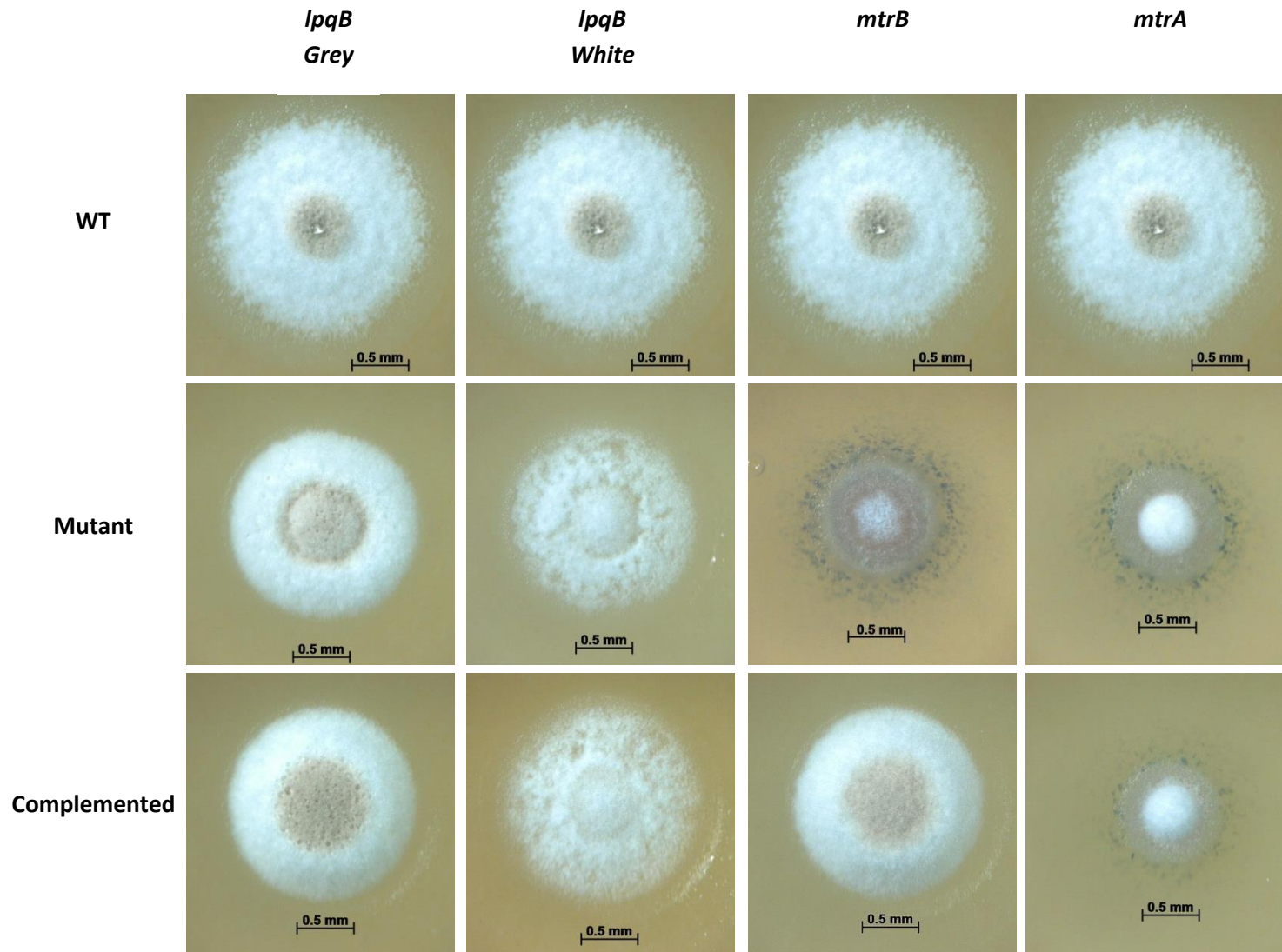


Figure 4.4: Light microscopy of complemented *lpqB* grey, *lpqB* white, *mtrB* and *mtrA* in comparison to wild type and mutant strains grown on SFM for 3 days at 30 °C. At this stage of growth the phenotype of the *mtrB* mutant has been restored to wild type. Unlike *mtrB* the $\Delta mtrA$ (pA11912) strain has not been restored to wild type.

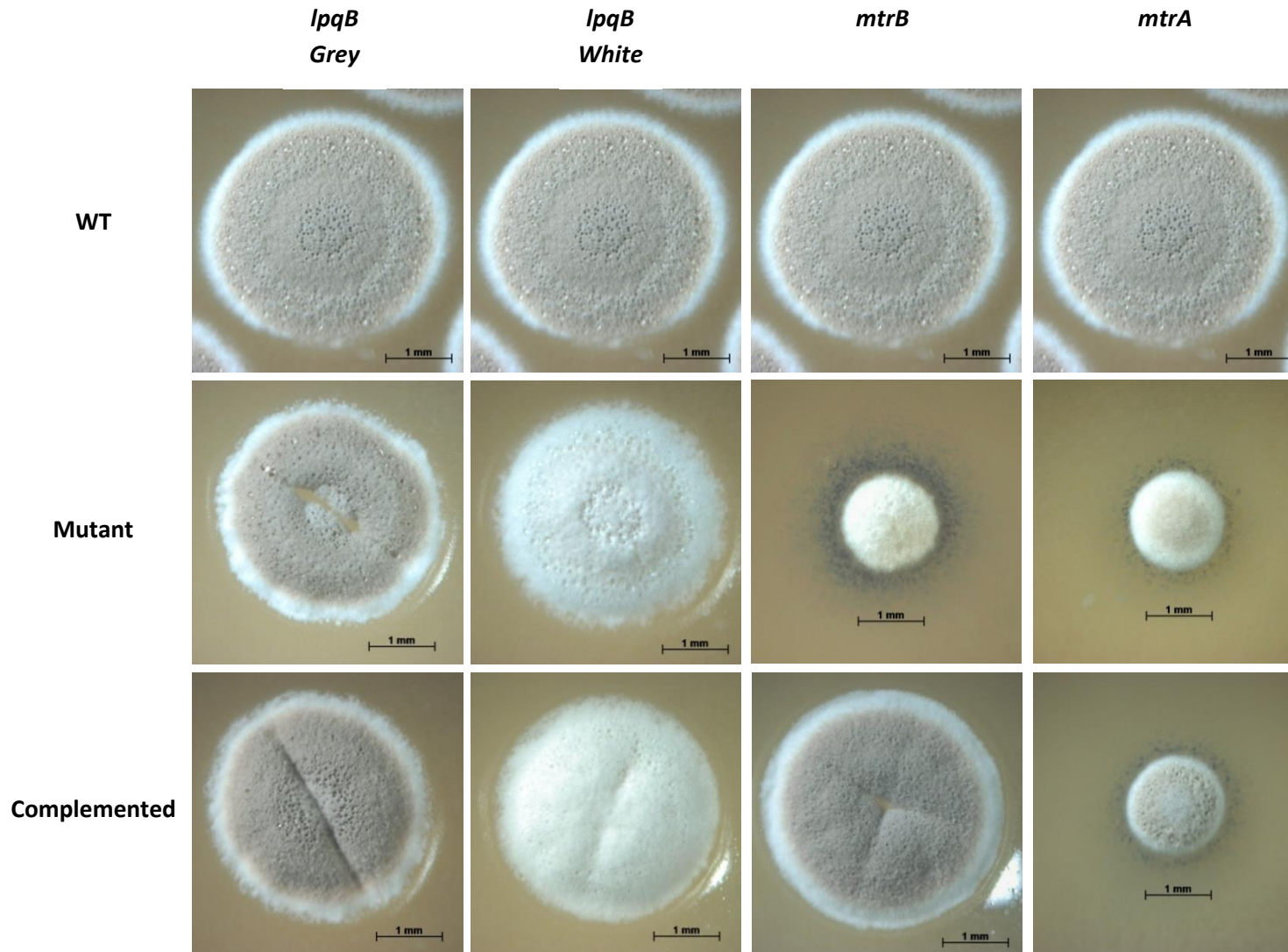


Figure 4.5: Light microscopy of complemented *lpqB grey*, *lpqB white*, *mtrB* and *mtrA* in comparison to wild type and mutant strains grown on SFM for 5 days at 30 °C. At this stage of growth the $\Delta mtrB$ (pB11912) strain is fully restored to wild type, which cannot be said of $\Delta mtrA$ (pA11912) meaning further experimentation was required (figure 4.6). The $\Delta lpqB$ grey (pL11912) strain no longer exhibits grey / white instability, yet the $\Delta lpqB$ white (pL11912) strain does not restore to wild type phenotype.

In order to explore this further *mtrA* was placed under the control of the *vanJ* promoter, where expression of *mtrA* was dependent on the addition of vancomycin (figures 4.6 and 4.7). The results show that when Vancomycin was increased the $\Delta mtrA$ phenotype was partially complemented. At five days the $\Delta mtrA$ strain carrying *vanJp-mtrA* formed aerial mycelium and grey pigmentation was seen, however the colony size remained smaller than that of wild-type *S. coelicolor*. The $\Delta mtrA$ phenotype was therefore only partially complemented by the *vanJp-mtrA* expression construct. These results suggested that the lack of complementation was possibly due to the location of the *mtrA* gene in the complemented strain rather than secondary mutations.

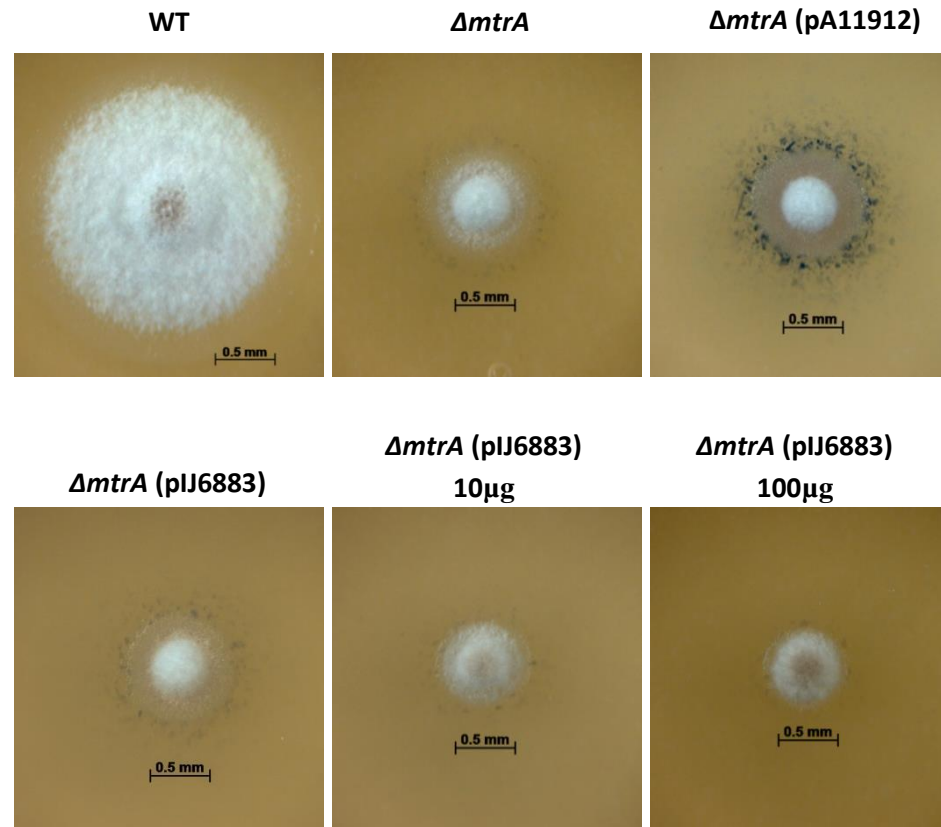


Figure 4.6: Complementation of the $\Delta mtrA$ by overexpressing *mtrA* under the control of the *vanJ* promoter grown on SFM or SFM supplemented with Vancomycin, to induce the *vanJ* promoter and subsequently *mtrA* expression, for 3 days. The $\Delta mtrA$ (pIJ6883) strain grown on SFM supplemented with either 10 μ g or 100 μ g Vancomycin exhibit grey pigmentation in comparison to $\Delta mtrA$ (pA11912) and $\Delta mtrA$ (pIJ6883) grown on SFM. Overexpression of *mtrA* restores pigmentation back to wild type however mutant colony size remains unaltered suggesting partial complementation by overexpressing *mtrA*.

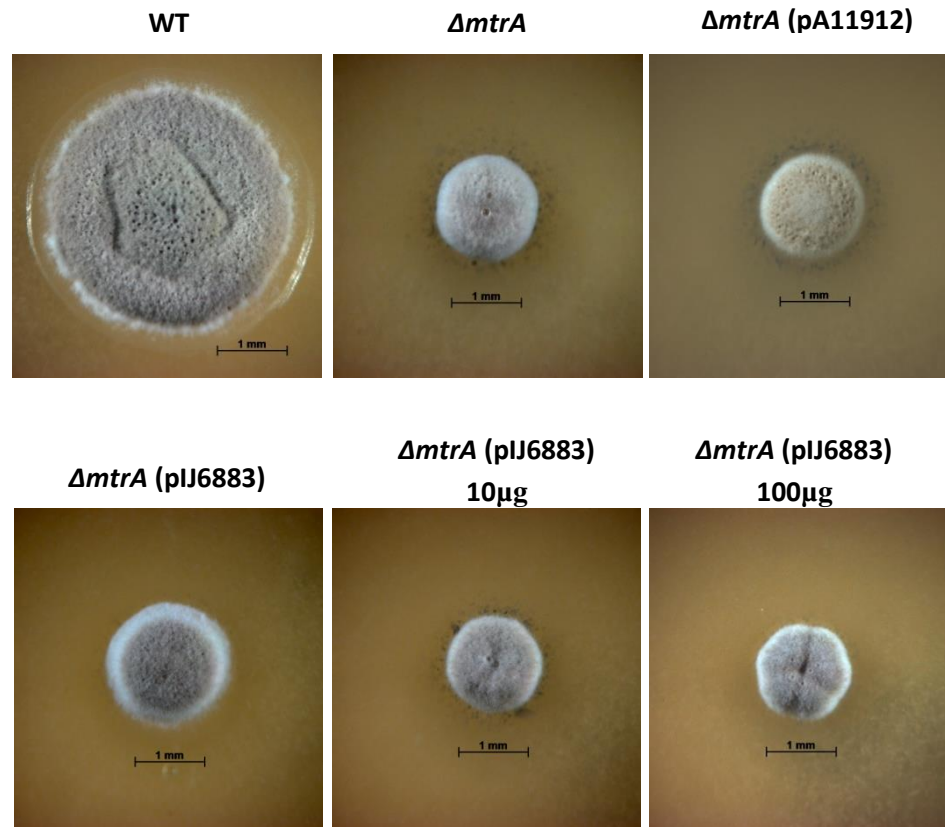


Figure 4.7: Complementation of the $\Delta mtrA$ by overexpressing *mtrA* under the control of the *vanJ* promoter grown on SFM or SFM supplemented with Vancomycin, to induce the *vanJ* promoter and subsequently *mtrA* expression, for 5 days. The $\Delta mtrA$ (pIJ6883) strain grown on SFM supplemented with either 10 μ g or 100 μ g Vancomycin exhibit grey pigmentation in comparison to $\Delta mtrA$ (pA11912) grown on SFM. Overexpressing *mtrA* appears to restore the development phenotype to wild type, however colony size remains small.

4.2.3. Scanning Electron Microscopy (SEM)

Once distinctive phenotypes had been documented in the mutant strains Scanning Electron Microscopy (SEM) was undertaken with wild type and the in-frame $\Delta sco3014$, $\Delta mtrA$, $\Delta mtrB$ and $\Delta lpqB$ strains. This was in order to identify whether single mutations in the *sco3014-mtrAB-lpqB* operon affected the structure of the aerial mycelium or spores.

The SEM images are shown in figure 4.8, where the mutant strains were compared to wild type *S. coelicolor* M145. This SEM revealed that at three days growth the wild type aerial hyphae had begun to coil, this can also be seen in the $\Delta lpqB$ grey, $\Delta lpqB$ white and $\Delta sco3014$ strains. However the mycelium in both $\Delta mtrB$ and $\Delta mtrA$ strains was linear instead of coiled, which suggested that both these strains exhibited a delayed development in comparison to the wild type, which was also observed using light microscopy (figure 4.1) at the same time point.

When the magnification was increased the spore structure could be seen, which is displayed in figure 4.9. This image revealed that wild type *S. coelicolor* spores were uniform and that $\Delta lpqB$ grey, $\Delta lpqB$ white and $\Delta sco3014$ strains had formed variable sized spores (figure 4.10). This revealed that in $\Delta lpqB$ grey, $\Delta lpqB$ white and $\Delta sco3014$ the spores were not compartmentalised as they were in the wild type. This phenotype could be caused by a change in assembly of the *ftsZ* ring which could in turn cause irregular spacing of the cell division septa, which would account for the varied spore sizes. Therefore the conclusions from the work so far were that a possible connection between deleting *lpqB* and *sco3014* and *ftsZ* expression needs to be investigated further. This phenotype was not seen in the $\Delta mtrB$ and $\Delta mtrA$ strains at this stage because, unlike wild type, they had not begun to form spores.

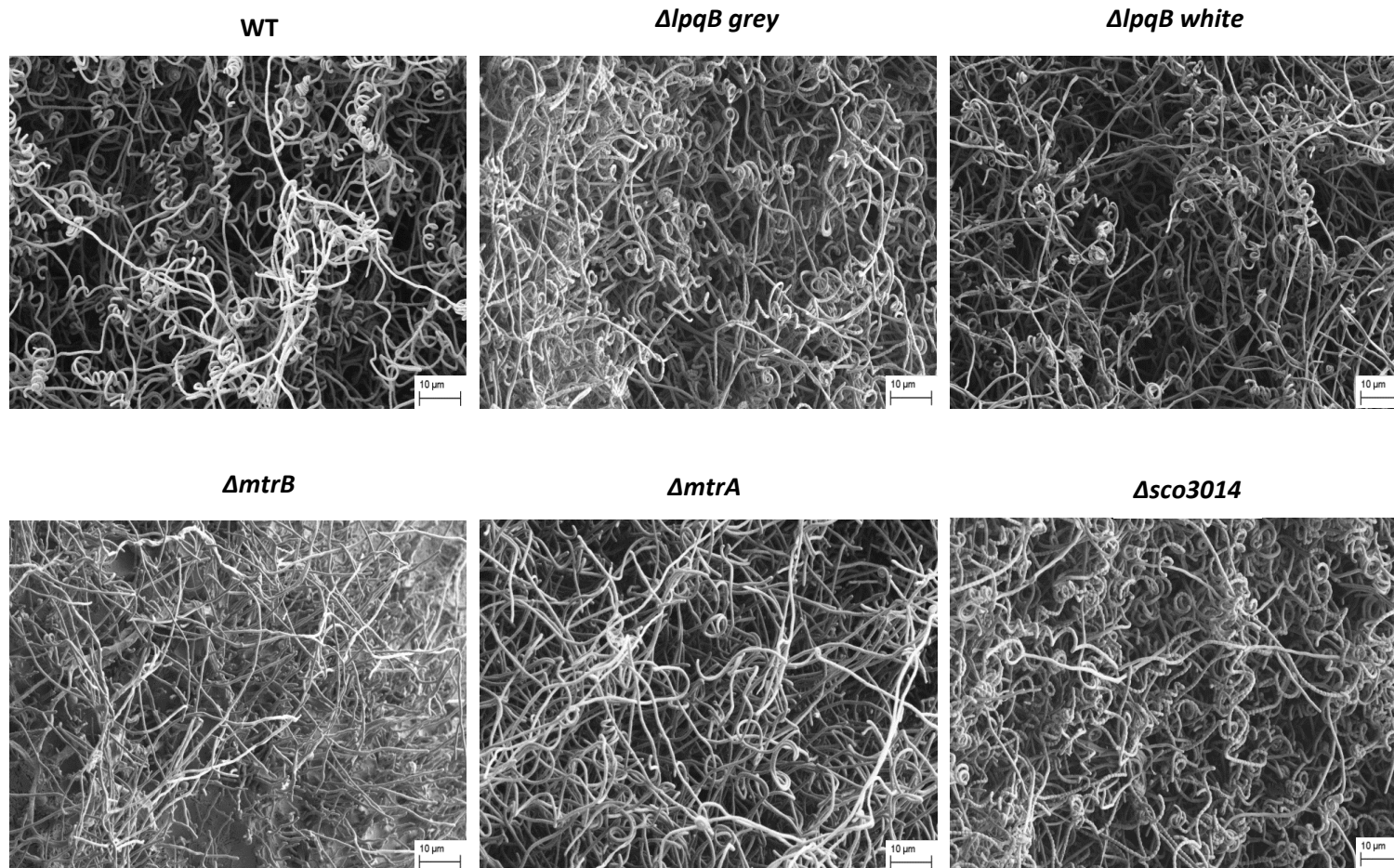


Figure 4.8: Scanning electron microscopy (SEM) showing mycelial growth of wild type and mutant *Streptomyces coelicolor* when grown on SFM at 30 °C for 3 days. The wild type, *ΔlpqB grey*, *ΔlpqB white* and *Δsco3014* mycelia are coiled at this stage of growth. However aerial mycelia of the *ΔmtrB* and *ΔmtrA* mutants have not begun to coil at this stage of growth.

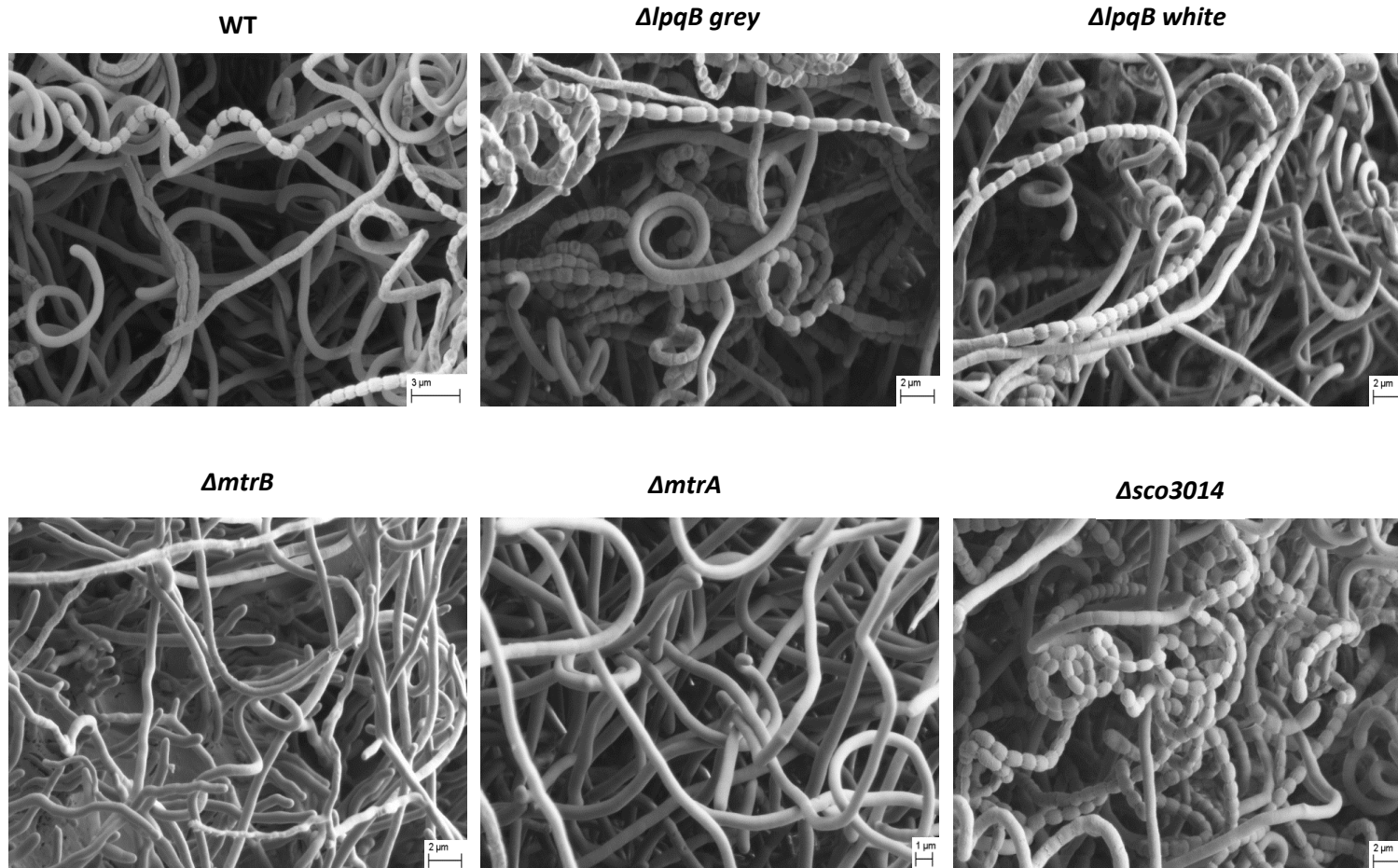


Figure 4.9: Scanning electron microscopy (SEM) showing spore chains of *Streptomyces coelicolor* wild type and mutant strains when grown on SFM at 30 °C for 3 days. Irregular spore sizes are observed in *lpqB* and *sco3014* mutant strains in comparison to wild type.

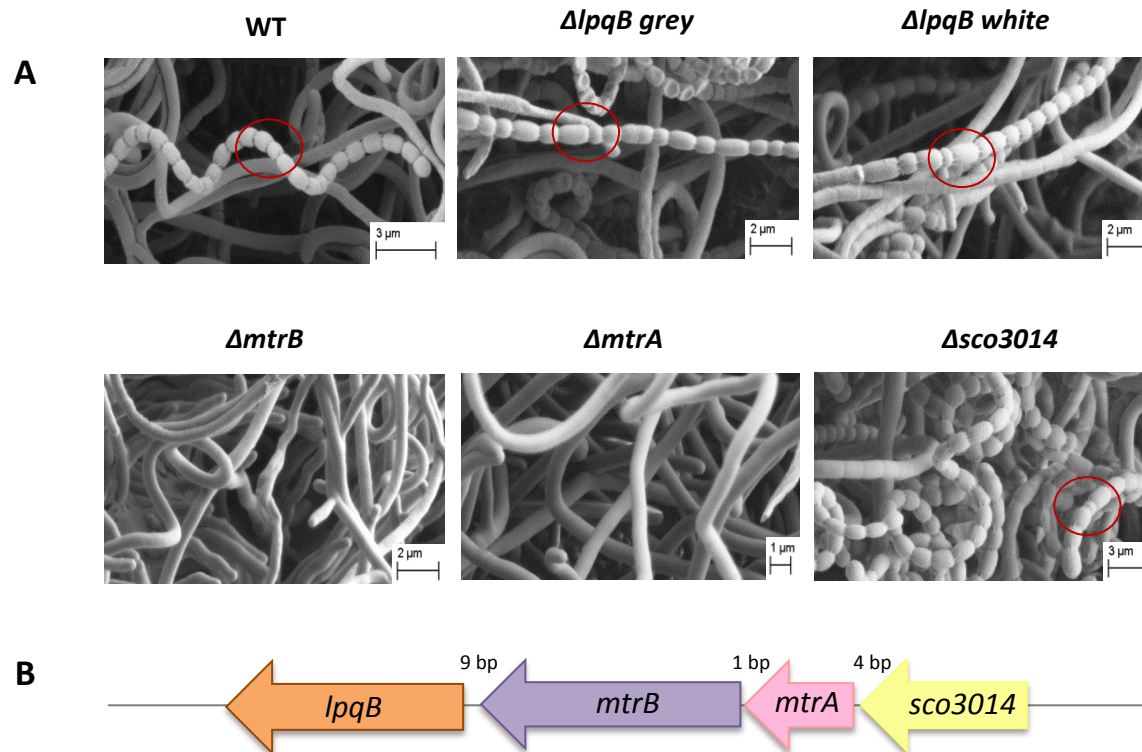


Figure 4.10: Highlighted spore structure of $\Delta sco3014$ -*mtrAB*-*lpqB* compared to wild type *S. coelicolor* when grown on SFM for 3 days at 30 °C and visualised by SEM. (A) The spore structure of wild type and mutant *S. coelicolor* strains are highlighted with red circles. Comparison of the $\Delta sco3014$, $\Delta lpqB$ grey and $\Delta lpqB$ white reveal irregular spores are formed in these strains in comparison to wild type *S. coelicolor*. The $\Delta mtrA$ and $\Delta mtrB$ mutant strains are not sporulating at this time point. (B) Genetic organisation of the *S. coelicolor* *sco3014*-*mtrAB*-*lpqB* operon.

SEM images were also taken of the wild type and mutant strains at five days growth in order to view phenotypes at this later stage of development. The images obtained can be seen in figures 4.11-4.13.

Figures 4.11 and 4.12 revealed the structure of wild type *S. coelicolor* mycelium in comparison to the mutant strains after 5 days growth on SFM. However unlike at three days growth where no coiling was seen both $\Delta mtrB$ and $\Delta mtrA$ exhibited some curling and spore chains had formed. Spore chains can be seen in all the strains and $\Delta sco3014$ seemed to exhibit a higher density of spores, than that of the wild type, consistent with the whole colony images identified by light microscopy. Therefore mutating the individual genes in the *sco3014-mtrAB-lpqB* operon did not completely inhibit sporulation. However, at 5 days growth the spore structure of wild type *S. coelicolor* was uniform whereas the $\Delta lpqB$ grey and $\Delta lpqB$ white strains still had irregular sized spores.

At five days growth both $\Delta mtrB$ and $\Delta mtrA$ also formed irregular sized spores compared to the wild type (figure 4.13). This suggested that the division machinery involved in forming regular cell division septa might be affected by mutating any (and all) of the four genes within the *sco3014-mtrAB-lpqB* operon. These results led to the hypothesis that mutations in the *sco3014-mtrAB-lpqB* operon all ultimately affect the activity of MtrAB which in turn affects expression of *ftsZ* expression and that this might affect Z ring formation and could therefore account for the observed mutant phenotypes. The connection between the *sco3014-mtrAB-lpqB* operon and the expression of *ftsZ* therefore requires further investigation.

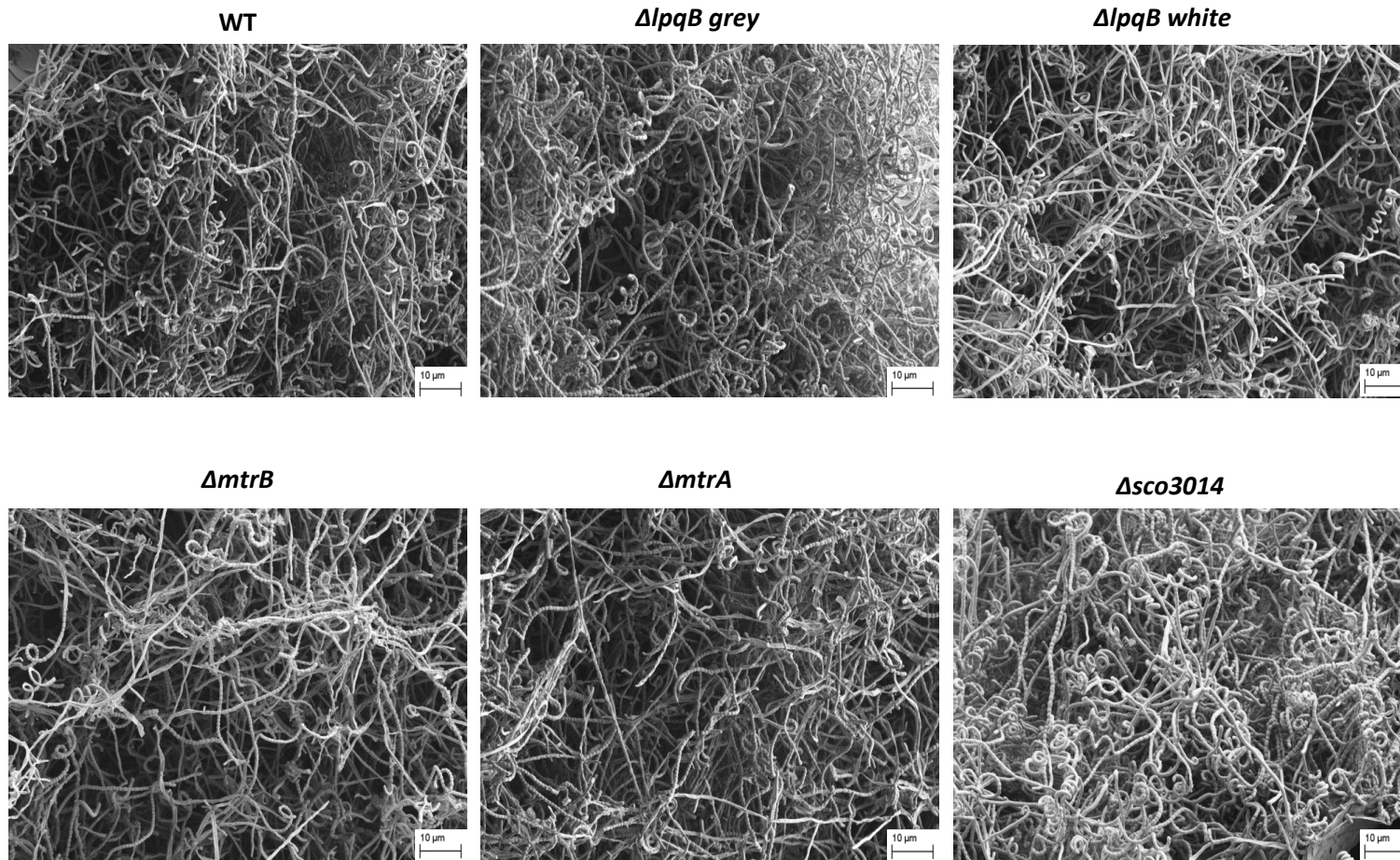


Figure 4.11: Scanning electron microscopy (SEM) showing mycelial growth of wild type and mutant *Streptomyces coelicolor* when grown on SFM at 30 °C for 5 days. At this stage of growth all strains have formed spore chains, which can be seen at higher magnification in figure 4.12.

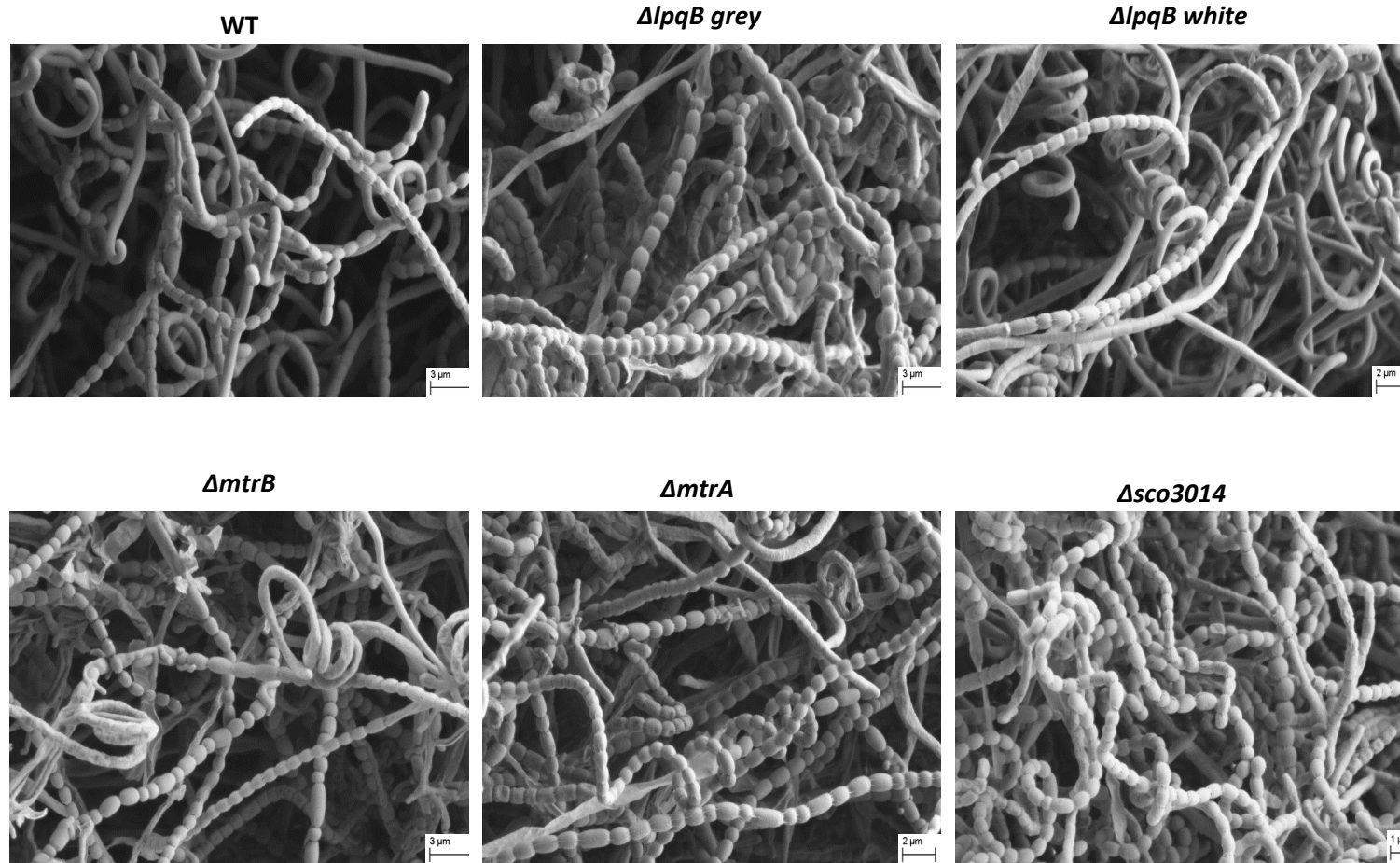


Figure 4.12: Scanning electron microscopy (SEM) of spore chains of wild type and mutant *S. coelicolor* strains grown on SFM for 5 days at 30 °C. The spore sizes of the sco3014-mtrAB-lpqB mutants are irregular when compared to wild type *S. coelicolor*.

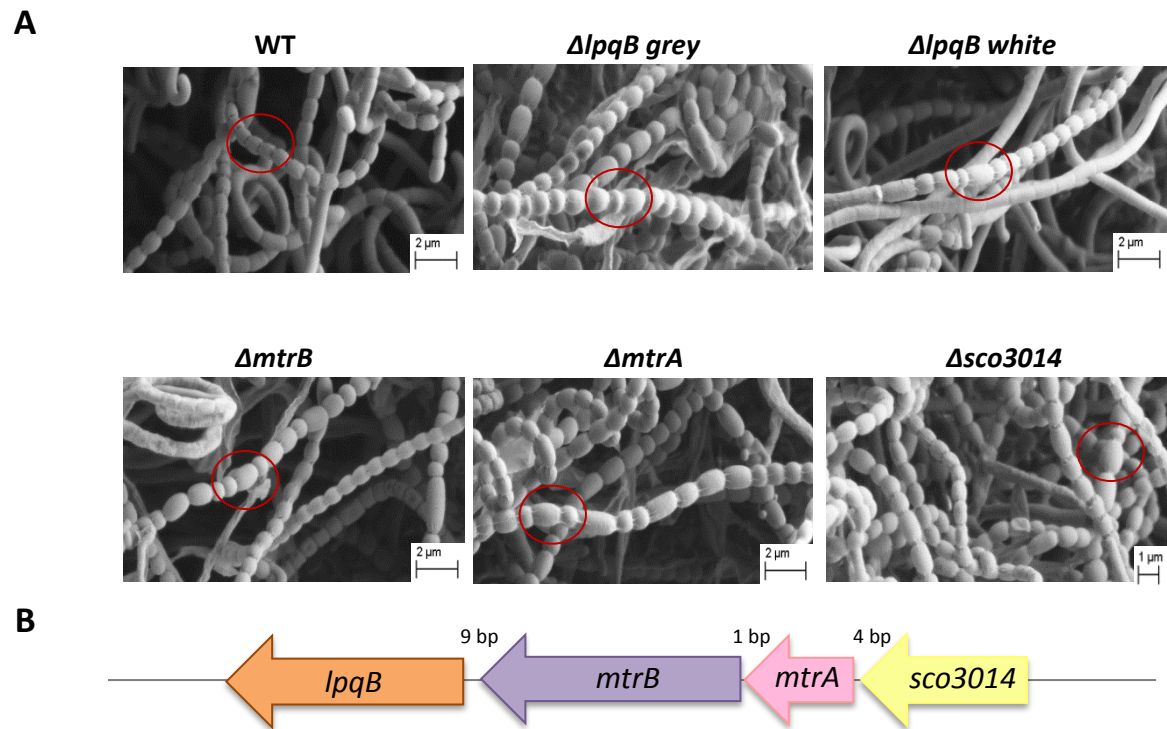


Figure 4.13: Highlighted spore structure of $\Delta sco3014$ - $mtrAB$ - $\Delta lpqB$ compared to wild type *S. coelicolor* when grown on SFM for 5 days at 30 °C and visualised by SEM. (A) The spore structure of wild type and mutant *S. coelicolor* strains. Single mutants of the *sco3014*-*mtrAB*-*lpqB* operon all exhibit irregular spore formation, which is highlighted in red. (B) Genetic organisation of the *sco3014*-*mtrAB*-*lpqB* operon.

4.3. Pigmented Antibiotic Production and Assay

4.3.1 Pigment Production

While growing cultures of the wild-type and mutant strains on solid media the production of pigmented antibiotic was observed. Growing the wild type and mutant strain in liquid SMM (supplemented minimal medium) a yellow pigment was observed of which onset was earlier in both the $\Delta mtrA$ and $\Delta mtrB$ cultures (appendix, p224). One possibility was that the compound was the rare polyketide coelimycin P1 (CPK), which has been reported to be yellow in colour (Gottelt *et al.*, 2010). To determine whether this might be the case a UV visible spectrum (4.14) was taken of the supernatants in figure 4.15 in order to compare them with the UV visible spectrum of CPK, which is known to exhibit a peak at 460 nm (Gottelt *et al.*, 2010). The UV visible spectrum of the yellow $\Delta mtrA$ and $\Delta mtrB$ culture supernatants, shown in figure 4.14, did not contain the distinctive 460 nm peak.

The absorbance traces for the yellow $\Delta mtrA$ and $\Delta mtrB$ culture supernatants were therefore not consistent with them containing CPK. Therefore another possibility was that the yellow compound could be the actinorhodin precursor (*S*)-DNPA, which is yellow pigmented (see section 1.5). This could be due to a high level of actinorhodin production in both the $\Delta mtrA$ and $\Delta mtrB$ mutants.

Pigmentation was observed in mutant strains grown in SMM are shown in figures 4.15 and reveal the production of pigmented antibiotics by the mutant strains. The purple colour produced by marked and in-frame mutants could be a mixture of Undecylprodigiosin and Actinorhodin. As with the yellow supernatant UV absorbance readings were taken in order to measure pigment production and determine whether the distinctive 460 nm peak, consistent with CPK production, could be identified (appendix, page 192). However the 460 nm peak was absent from all supernatant UV spectrums (figure 4.14 and appendix, pages

191-193). Therefore to be certain that CPK was not produced by these mutant strains further investigation was required.

4.3.2 Liquid Chromatography and Mass Spectrometry (LCMS)

To determine whether the $\Delta mtrA$ and $\Delta mtrB$ mutants are producing CPK, LCMS was carried out using the wild-type control and the $\Delta mtrB$ strain, which consistently produced more pigmented compounds in both liquid and solid media. Following ethyl acetate extraction the yellow pigment remained in the aqueous phase so samples were diluted in methanol and separated on a C_{18} column. Figure 4.16 reveals two extracted ion chromatogram peaks with m/z 349 and m/z 351. However even though these peaks were similar to those seen for CPK the retention time of both peaks is very different to CPK. When eluting with 100 % methanol CPK eluted at a retention time of 20 minutes but the yellow pigment produced by $\Delta mtrB$ eluted after only two minutes suggesting they are different compounds.

The difference between CPK and the yellow pigment produced by $\Delta mtrB$ can be seen further in figure 4.16. The UV visible spectrum of the yellow pigment revealed a lambda max of approximately 220 nm; whereas CPK exhibits a lambda max of 360 nm. Therefore the yellow pigment produced by both $mtrB$ and $mtrA$ mutant strains cannot be CPK. This means that the yellow pigment could be the Actinorhodin precursor (S)-DNPA, which is rarely seen.

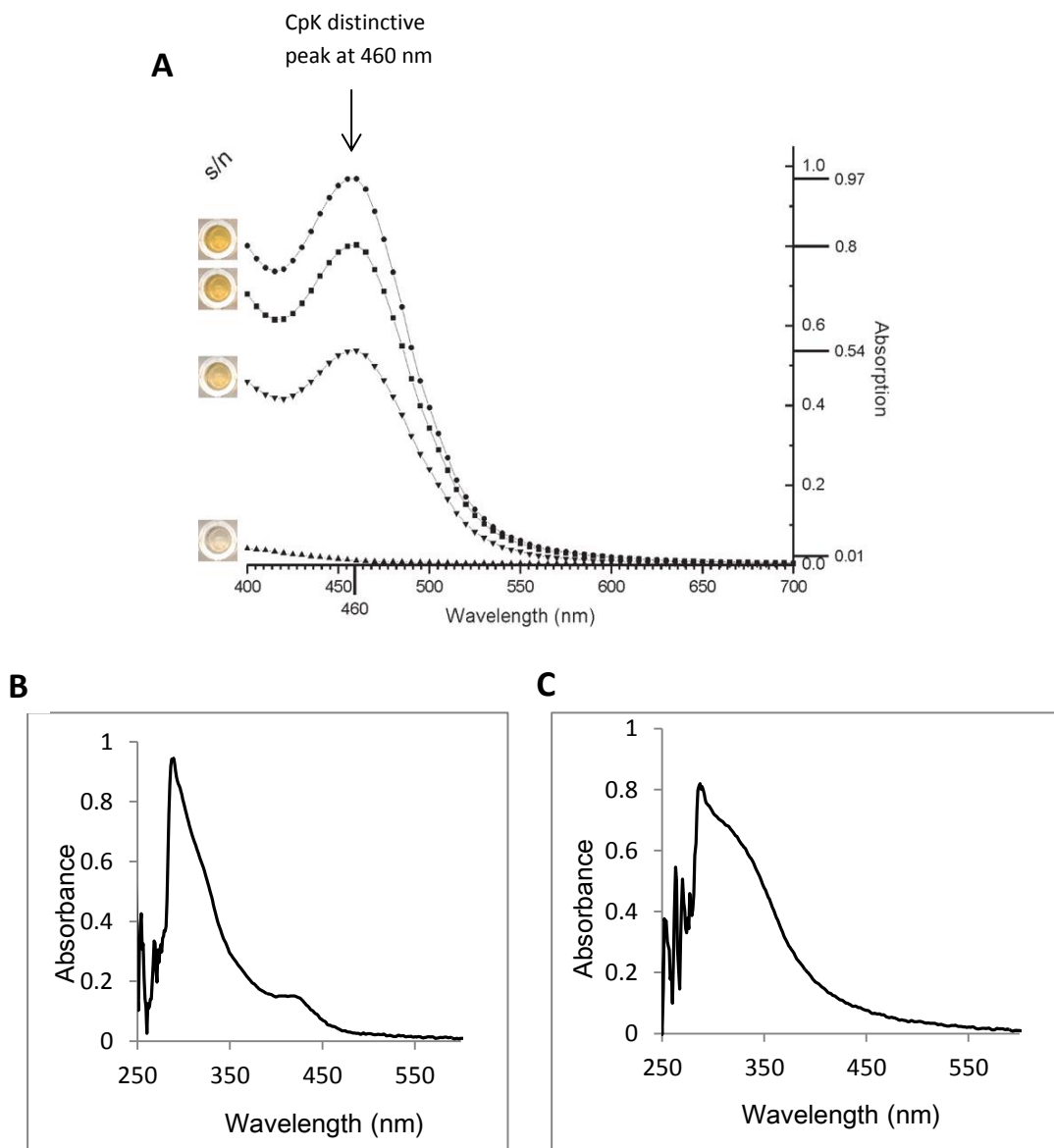


Figure 4.14: UV visible spectrum of yellow pigmented supernatant produced by $\Delta mtrB$ and $\Delta mtrA$ strains grown for 20 hours in liquid SMM at 30 °C, in comparison to UV visible spectrum of CpK producing strains that exhibit a distinctive 460 nm peak. (A) UV visible spectrum detected from supernatants of $\Delta scbR2$, wild type, $\Delta act\Delta red$ and Δcpk (Gottelt *et al.*, 2010). The distinctive peaks at 460 nm can be seen in the CpK producing strains. (B) UV visible spectrum of supernatant from the $\Delta mtrB$ strain, where no 460 nm peak can be seen. (C) UV visible spectrum of supernatant from the $\Delta mtrA$ strain where no 460 nm peak can be seen in comparison to the CpK producing strains.

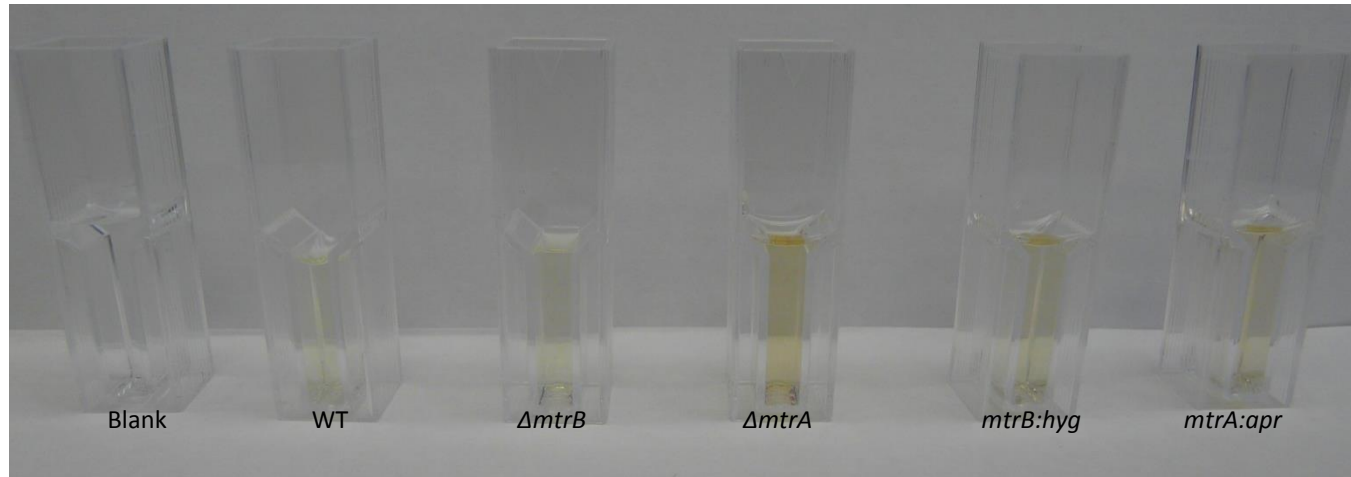
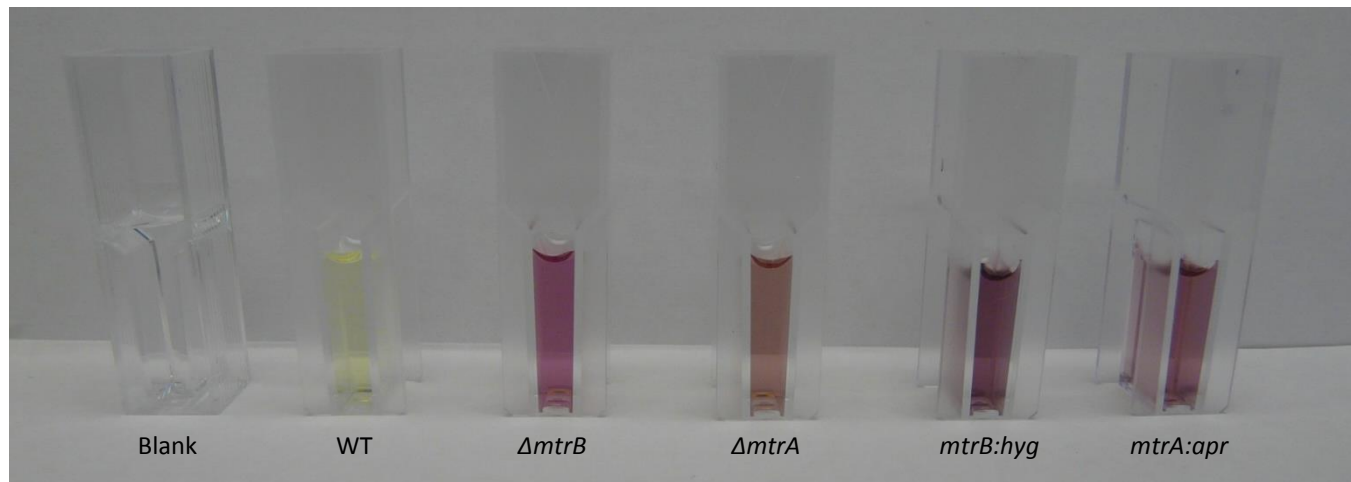
A**B**

Figure 4.15: Supernatant of *S. coelicolor* strains when grown in liquid SMM at 30 °C 200 rpm, where colour pigmentation was observed under these conditions. (A) Wild type, $\Delta mtrB$, $\Delta mtrA$, *mtrB:hyg* and *mtrA:apr* grown for 20 hours, where yellow pigmentation was observed within the mutant strains. (B) Wild type, $\Delta mtrB$, $\Delta mtrA$, *mtrB:hyg* and *mtrA:apr* grown for 39 hours. A delayed onset of yellow pigmentation was observed in wild type, at this stage mutant strains were undergoing further pigmentation.

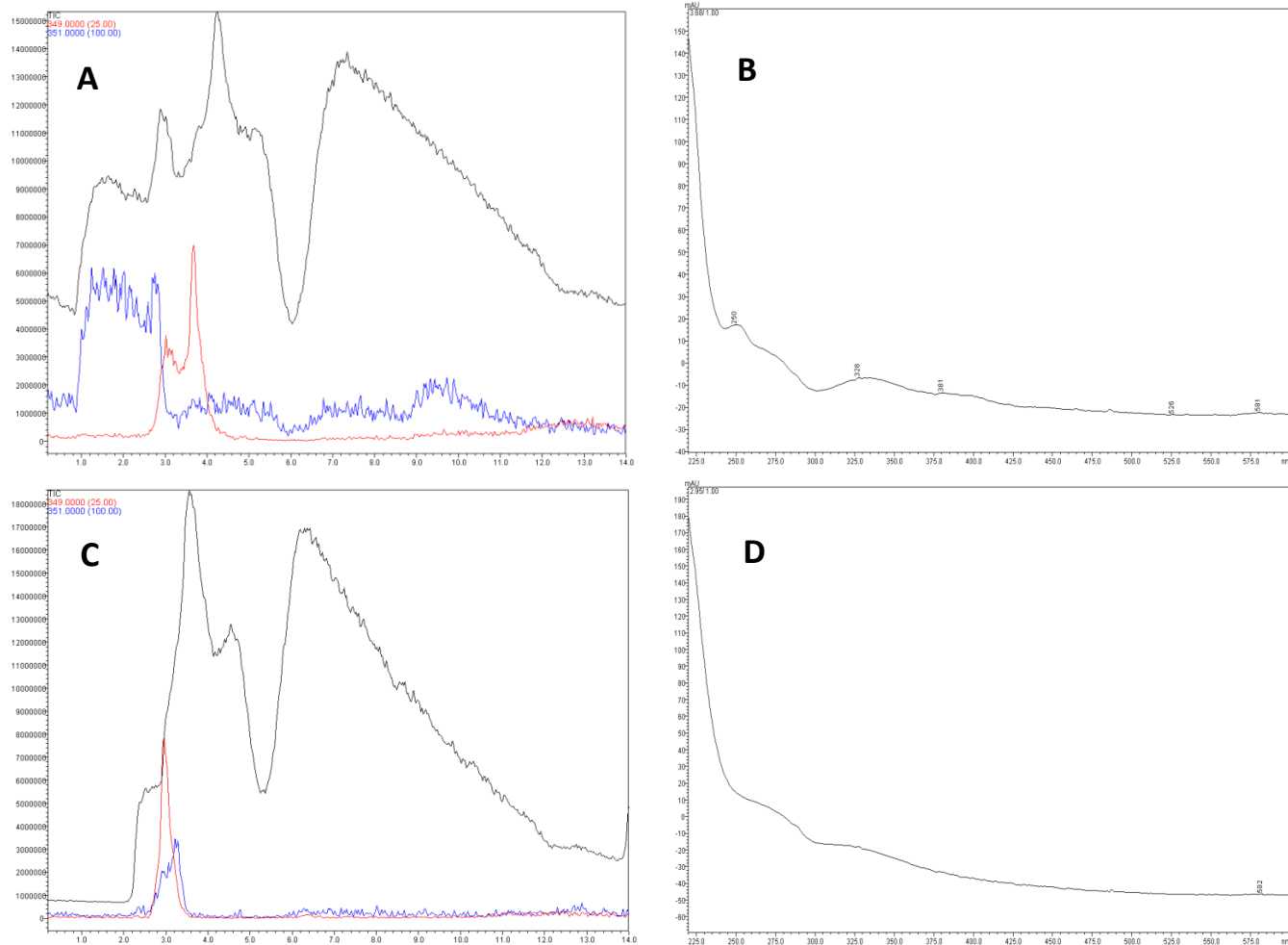


Figure 4.16: LCMS and UV visible spectrum of wild type and $\Delta mtrB$ grown in liquid SMM for 20 hours. (A) LCMS results of wild type *S. coelicolor* when yellow pigment was seen. (B) UV visible spectrum of wild type *S. coelicolor*. (C) LCMS results of $\Delta mtrB$ when yellow pigment was seen. (D) UV visible spectrum taken of $\Delta mtrB$ supernatant.

4.3.3. Measuring Pigmented Antibiotic Production

To further investigate pigment production (or over-production) by the mutants strains, undecylprodigiosin assays were undertaken on the wild-type and all the mutant strains. All of the mutant strains produced more undecylprodigiosin than the wild-type (Figure 4.17); and production of undecylprodigiosin from the $\Delta lpqB$ and $\Delta sco3014$ strains was significantly higher in comparison to the wild type *S. coelicolor*.

The amount of actinorhodin produced was not successfully quantified by undertaking an actinorhodin assay in liquid culture (appendix, page 193), however as actinorhodin production is linked to sporulation the results from the actinorhodin assay were not representative of the actinorhodin production observed on solid media.

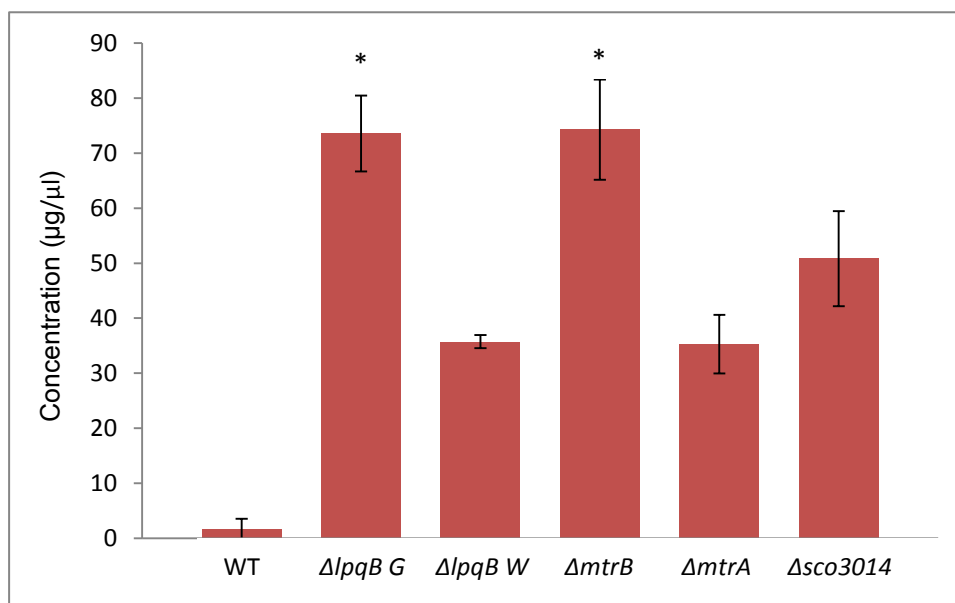


Figure 4.17: Undecylprodigiosin concentration produced by wild type, $\Delta lpqB$ grey, $\Delta lpqB$ white, $\Delta mtrB$, $\Delta mtrA$ and $\Delta sco3014$ strains. Undecylprodigiosin production was higher in all single mutants of the *sco3014-mtrAB-lpqB* operon. This higher production was significant in the *lpqB* grey and *mtrB* mutant strains (as indicated by a *).

4.4 Exploring Potential MtrA Targets

4.4.1 ChIP-seq to Discover Targets

In order to identify direct targets of MtrA ChIP-seq was carried out on both wild type *S. coelicolor* and $\Delta mtrA$ using polyclonal antiserum raised against purified *S. coelicolor* MtrA protein. An immunoblot with this antibody against whole cell extracts of the *S. coelicolor* strains is shown in figure 4.18. This revealed an absence of a band in the $\Delta mtrA$ strain, which runs at around 30 kDa in size, consistent with the absence of MtrA from this mutant. However the whole cell extract from the $\Delta mtrB$ strain did not cross react at all, probably as a result of low protein yields due to the growth defects previously seen.

This immunoblot also revealed a number of cross-reacting bands detected by the polyclonal MtrA antibody, which may explain why no targets were enriched from the wild type versus $\Delta mtrA$ sample in the ChIP-seq experiment. Therefore the ChIP-seq needs to be repeated with an improved antibody, for example by tagging MtrA with a 3xFlag tag and using a corresponding monoclonal antibody against that tag for more acute detection and enrichment of targets.

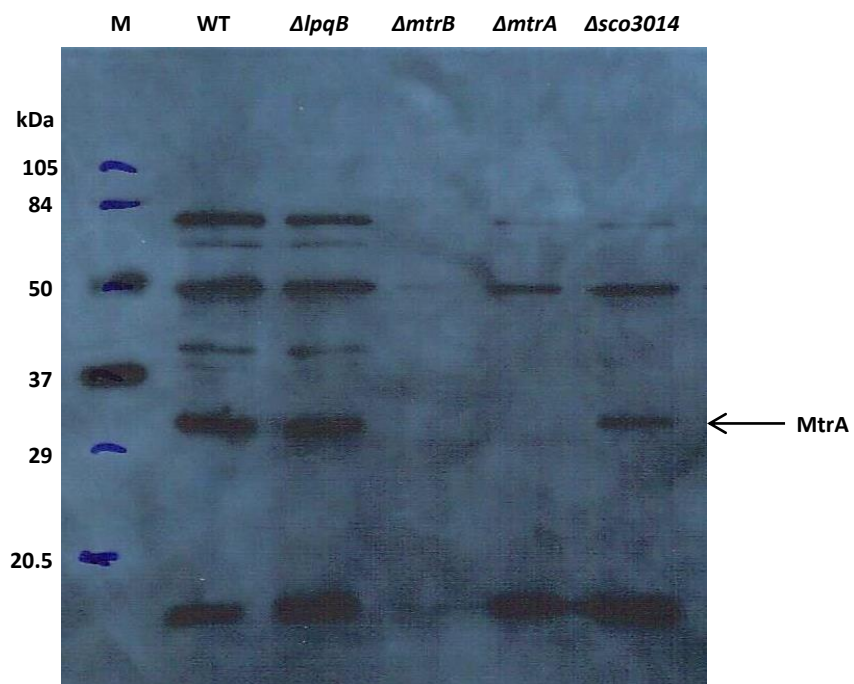


Figure 4.18: Immunoblot using a polyclonal antibody raised against purified *S. coelicolor* MtrA. Whole cell extracts were tested for the presence of MtrA.

MtrA is detected in wild type, *lpqB*, *sco3014* extracts and not seen in the *mtrA* mutant strain. Cross reacting bands can also be seen.

No bands are detected in the *mtrB* mutant extract, which is possibly due to low protein yield from this strain.

4.4.2. Is *ftsZ* a Target of MtrA?

Given the sporulation defects of deletion mutants in the *sco3014-mtrAB-lpqB* operon it was hypothesised that *ftsZ* might be a target for MtrA. The *ftsZ* gene has three promoters, the second of which (P2) is developmentally regulated and required for sporulation specific FtsZ production (Flardh *et al.*, 2000). Notably, there is also a perfect inverted match to the proposed MtrA binding sequence in mycobacteria and corynebacteria (CGGCGTG) immediately upstream of the -35 region of the *ftsZP2* promoter (Figure 4.19) (Li *et al.*, 2010b). The irregular spores formed by the mutants could be due to irregular septation and could be due to aberrant FtsZ production in aerial hyphae. This is also consistent with the fact that Δ *ftsZ* mutants over produce actinorhodin (McCormick *et al.*, 1994).

In order to explore whether *ftsZ* was a target of MtrA qRT-PCR was conducted. Strains were grown on solid medium before RNA isolation, because *S. coelicolor* differentiates on solid medium.

The data show that deletion of *mtrA* negatively affected *ftsZ* expression (figure 4.20) and add evidence to support the hypothesis that MtrA regulates *ftsZ* expression (either directly or indirectly) in *S. coelicolor*. This may be because *ftsZP2* is a target for MtrA but might also be due to the growth and developmental defects observed in the Δ *mtrA* strain. Direct binding will have to be demonstrated *in vitro* and *in vivo* to prove that *ftsZ* is directly regulated by MtrA.

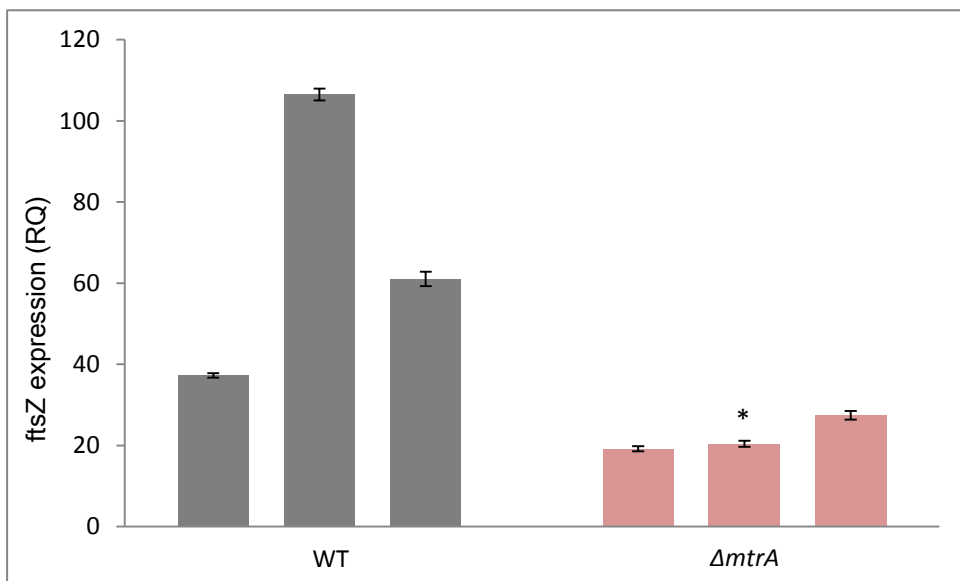


Figure 4.20: qRT-PCR results testing *ftsZ* expression in $\Delta mtrA$ in comparison to wild type *S. coelicolor* grown on SFM with cellophanes for 48 hours at 30 °C. Expression of *ftsZ* in wild type *S. coelicolor* is significantly higher in comparison to the *mtrA* mutant. The separate columns represent individual biological replicates. The significant difference (as indicated by a *) was shown when comparing the second biological replicates and the entire group sets of wild type and $\Delta mtrA$ *S. coelicolor*.

4.4.3. Localisation of FtsZ

In order to observe FtsZ localisation, the wild-type and mutant strains were conjugated with *E. coli* containing a plasmid encoding a translational FtsZ-eGFP fusion and fluorescence microscopy was used to examine the localisation of FtsZ. Microscope images were taken at 3 days and 5 days growth.

Figure 4.21 revealed that regularly spaced FtsZ ladders had begun to form in the wild type aerial hyphae whereas in the $\Delta lpqB$ grey strain expressing *ftsZ-egfp* the FtsZ was irregularly placed, which appeared to be due to overproduction of FtsZ. This overproduction causes irregular foci, which in turn could cause the uneven spores seen using SEM. Figure 4.21 showed that this apparent overproduction of FtsZ also occurred within the *lpqB white* mutant. As well as irregular foci being formed, higher concentration of FtsZ forming larger foci could be seen.

The $\Delta mtrB$ mutants formed irregular Z rings, possibly because growth and development was delayed. However, in the $\Delta mtrA$ mutant no FtsZ could be detected, possibly because FtsZ production prior to sporulation is dependent on MtrA activity, consistent with *ftsZP2* being dependent on MtrA (figure 4.19).

Finally the level and localisation of FtsZ in the $\Delta sco3014$ mutant in comparison to the wild type is shown in figure 4.21. This figure revealed that FtsZ is spaced at regular intervals, resulting in even spore formation, within the $\Delta sco3014$ strain at this stage of growth consistent with the LM and SEM images that show normal, or even precocious, sporulation in the $\Delta sco3014$ strain.

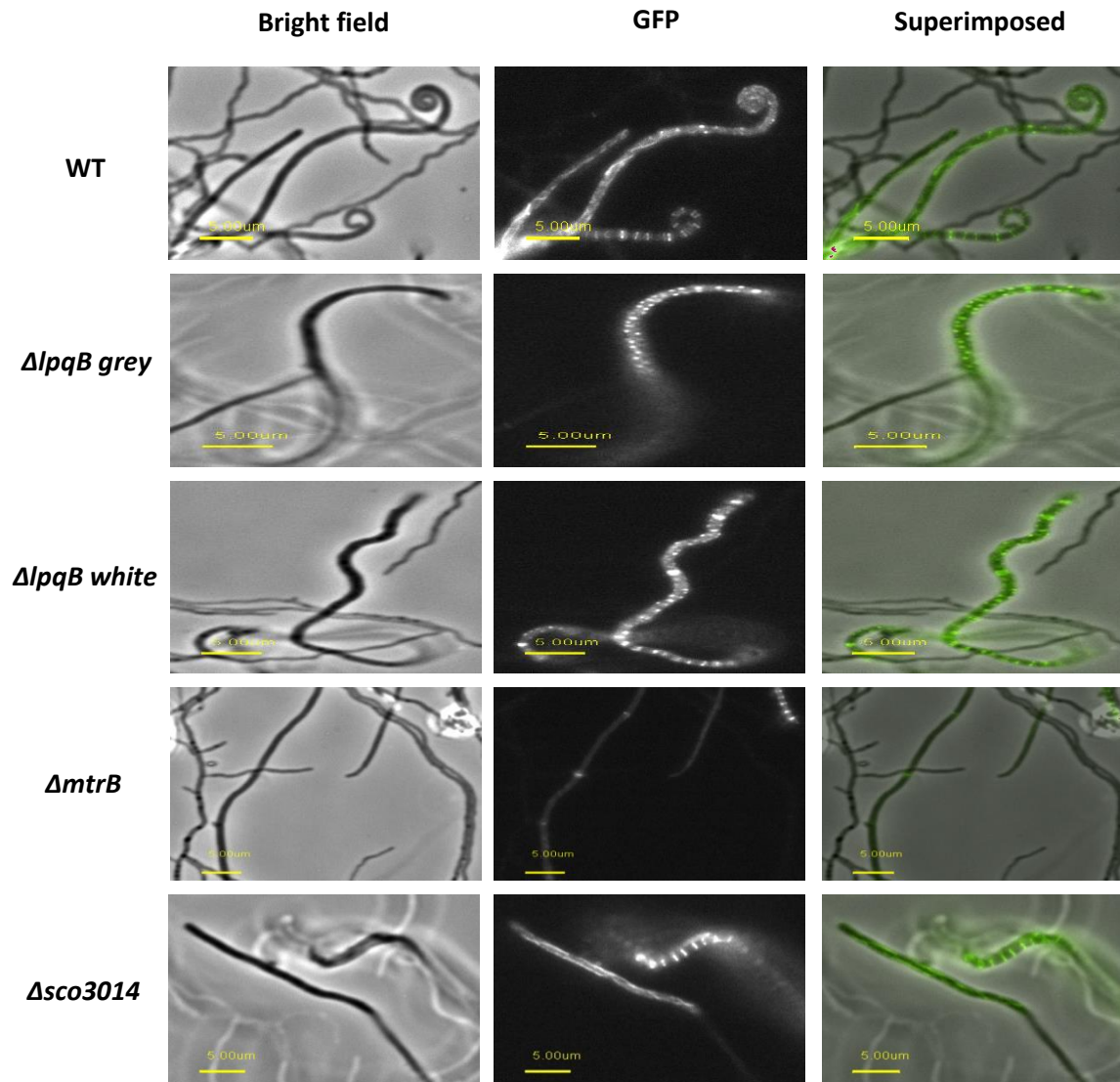


Figure 4.21: FtsZ localisation within wild type and mutant *S. coelicolor* aerial mycelium. Fluorescence microscopy of wild type, *ΔlpqB grey*, *ΔlpqB white*, *ΔmtrB* and *Δsco3014* containing pKF41. The expression of *ftsZ* could not be visualised in the *ΔmtrA* mutant. Overproduction of *ftsZ* is seen within the *lpqB* mutants.

After FtsZ-eGFP had been visualised in strains during aerial mycelial growth the next step was to observe the concentration and localisation of FtsZ in spore chains. The first comparison between spore structure and FtsZ expression is displayed in figure 4.22 where *ΔlpqB grey* was compared to wild type *S. coelicolor*. This data confirmed that irregular spore formation had occurred within the *ΔlpqB grey* strain in comparison with wild type and higher expression of FtsZ within the *ΔlpqB grey* strain could still be seen at this stage of growth (figure 4.22). Irregular spore sizes were also detected in the *ΔlpqB white* mutant strain (figure 4.22); however, unlike the *ΔlpqB grey* strain the *ΔlpqB white* strain was no longer focally expressing FtsZ-eGFP, which suggests no new spore chains were being produced.

At the spore chain stage of growth no FtsZ-eGFP signal could be detected in the *ΔmtrA* strain containing the pKF41 plasmid but some spores could be detected (image not shown). The FtsZ expression in the *ΔmtrB* strain could be seen and are displayed in figure 4.22. This showed FtsZ flanking the formed spores within the spore chain. However it was difficult to identify the spore sizes at this level of magnification.

In figure 4.22 the FtsZ signal appeared to be dispersed within the *Δsco3014* spore chain. However it was inconclusive whether irregular spore formation could be detected within this strain. Meaning spore formation may only be affected in *mtrAB-lpqB* strains.

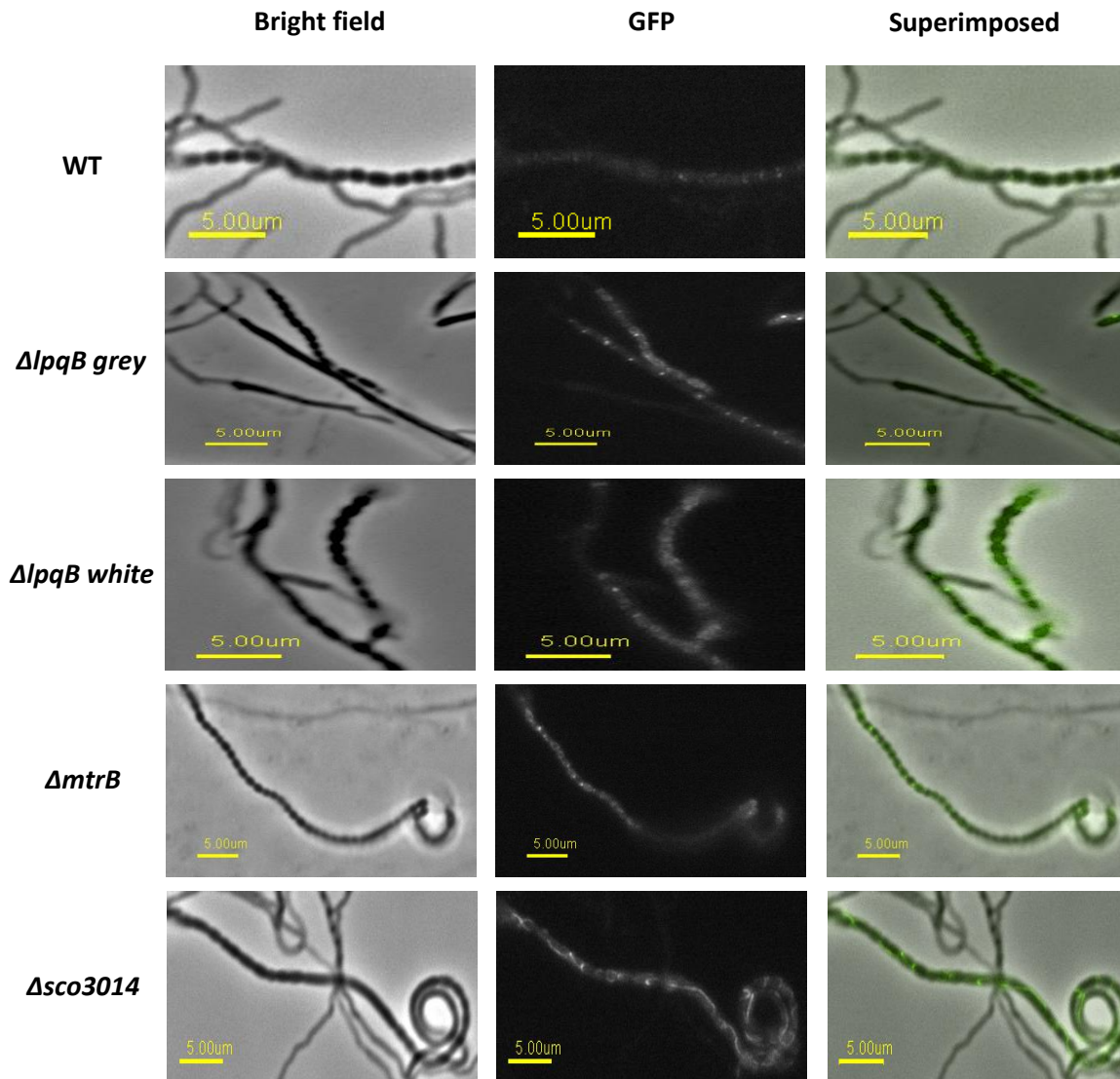


Figure 4.22: FtsZ localisation within wild type and mutant *S. coelicolor* spore chains. Fluorescence microscopy of wild type, *ΔlpqB grey*, *ΔlpqB white*, *ΔmtrB* and *Δsco3014* containing pKF41. The expression of *ftsZ* could not be visualised in the *ΔmtrA* mutant. Irregular spore formation occurs within the *lpqB* mutants. FtsZ is seen at the poles of the spores, which were identified as irregular by SEM.

The images produced from the fluorescence microscopy alongside the SEM images revealed that FtsZ formation was not uniform within mutants in the *mtrAB-lpqB* system. This irregularity appeared to be due to over- or under-expression of FtsZ within the mutant strains. This aberrant expression likely causes the irregular spore phenotype of either double or half spores, as observed using the SEM. Despite this, and the qRT-PCR data alluded to *ftsZ* being a target of MtrA further *in vitro* work is required to identify whether the *ftsZ* promoter is a direct target of MtrA. If this is the case then FtsZ expression and growth in *S. coelicolor* is controlled by the MtrAB-LpqB component system.

4.5 Results summary

This chapter describes the characterisation of the conserved actinobacterial MtrAB-LpqB signal transduction system in *S. coelicolor* along with a co-encoded protein, SCO3014, of unknown function, which is present in some but not all streptomycetes *mtrAB-lpqB* operons. The results provide some indication that FtsZ production is controlled by MtrA in *S. coelicolor* and suggest that the MtrAB-LpqB system regulates cell division in filamentous actinomycetes as it does in unicellular mycobacteria and corynebacteria. Intriguingly however, FtsZ is not a target for MtrA in those genera. Further work is required to determine whether MtrA binds directly to the *S. coelicolor* *ftsZ* P2 promoter, as indicated by a putative MtrA binding site upstream of the -35 region. Crucially, this future work should include CHIP-seq experiments using a tagged copy of MtrA to define the complete regulon of MtrA-regulated genes. It will then be necessary to determine where MtrA fits into the hierarchy of Bld and Whi regulators in the complex regulation of differentiation in *Streptomyces* species. It seems likely that LpqB regulates MtrB activity, as reported in mycobacteria, and the results presented here show a clear effect on FtsZ-eGFP production

and localisation in the absence of *lpqB*. Although FtsZ-eGFP could not be detected in an *mtrA* mutant this strain does form some spores so there must be FtsZ present but perhaps FtsZ-eGFP is produced at levels below the threshold required for visualisation. FtsZ-eGFP is visible in the *mtrB* mutant which suggests that MtrA can be activated in the absence of MtrB, most likely by acetyl phosphate (for which there is precedence in *S. coelicolor*, e.g. VanRS). Deletion of *sco3014* appears to increase the amount of spores produced and this may be due to increased expression of *mtrAB-lpqB*. A role for SCO3014 in regulating MtrAB-LpqB seems unlikely since it is missing from many streptomycetes and all other actinobacterial genera.

Chapter 5: Introduction to the NsrR Project

5.1. Project Overview

In the environment bacteria are exposed to a number of stresses which they need to survive. One example of stress is the highly reactive molecule nitric oxide (NO), which is generated by microbes living in the soil. Therefore bacteria that inhabit this environment, such as *S. coelicolor* must be exposed to NO produced by denitrifying microbes. NO is also produced by the bacterial nitric oxide synthases (bNOS) enzymes encoded by some Gram-positive soil bacteria. Since NO is cytotoxic at high concentrations, bacteria must sense and then rapidly detoxify NO before it becomes lethal. In order to do this *S. coelicolor* and other bacteria encode regulators that sense NO and switch on the expression of NO detoxification systems in order to survive. The focus of this project is on one of these regulators, NsrR, which belongs to the Rrf2 family of regulators and is encoded by *S.coelicolor* and by numerous other bacteria.

NsrR senses NO via an iron sulphur (Fe-S) cluster and previous work on *S. coelicolor* NsrR has focused on identifying the type of Fe-S cluster it contains and how it reacts with NO. However in this work the focus is on the role of NsrR in *S. coelicolor* survival. An in-frame *nsrR* mutant was constructed in order to observe any changes in colony morphology or sensitivity to NO which might give an insight to the role of NO and NsrR within *S. coelicolor* since it has been suggested that NO may act as a transient signalling molecule regulating cell division in *S. coelicolor* (Chandra & Chater, 2013).

The aim of this work was also to identify the complete regulon of NsrR target genes in *S. coelicolor* and roles they play in responding to NO stress. Targets of *S.coelicolor* NsrR have previously been predicted using a computationally derived binding site which suggested a regulon of more than 300 target genes, whereas NsrR target genes have been identified

experimentally in other bacteria, including *Salmonella enterica* serovar Typhimurium, *Bacillus subtilis* and *Escherichia coli*. In comparison, the study of NsrR in *Streptomyces coelicolor* is still in its infancy and during this project *S.coelicolor* NsrR targets will be identified using chromatin immunoprecipitation followed by sequencing (ChIP-seq).

5.2. Rrf2 Proteins

5.2.1. Rrf2 Family

The Rrf2 superfamily of transcriptional repressors is named after the first discovered member, the Rrf2 protein. Rrf2 was investigated with Rrf1, which was found to regulate the *hmc* operon within the bacterium *Desulfovibrio vulgaris* (Keon *et al.*, 1997), which encodes enzymes that are involved in electron transfer during respiration in *D. vulgaris* (Keon *et al.*, 1997). The Rrf2 protein family also includes the transcriptional regulators RirA, CymR, IscR and NsrR. RirA, *Rhizobium* iron regulator A, has been shown to negatively regulate over eighty transcripts in both *Rhizobium* and *Sinorhizobium* when iron is depleted (Johnston *et al.*, 2007, Todd *et al.*, 2005) while CymR regulates cysteine metabolism in *Bacillus subtilis* (Tanous *et al.*, 2008). In *Escherichia coli* the Rrf2 protein IscR, iron sulphur cluster regulator is involved in regulating the biogenesis of Fe-S clusters (Schwartz *et al.*, 2001).

5.2.2. IscR

IscR was initially characterised in *E.coli* and shown to contain a [2Fe-2S] cluster (Schwartz *et al.*, 2001). Assembly of the [2Fe-2S] cluster within IscR is encoded by the *isc* operon, which consists of *iscRSUA*, *hscBA* and *fdx*. The role that these *isc* components have in Fe-S biogenesis is described in section 5.2.3.

The *isc* operon is negatively regulated by IscR, therefore IscR autoregulates itself and the assembly of Fe-S clusters via the Isc pathway (Schwartz *et al.*, 2001). As a result IscR also maintains Fe-S homeostasis within the cell since this occurs primarily through the Isc pathway (Giel *et al.*, 2013). IscR has been shown to have over 40 possible targets, which it may directly or indirectly regulate (Giel *et al.*, 2006). Other target promoters that IscR has been found to repress include those of the *hya*, *hyb* and *nap* operons. Genes within these operons encode for hydrogenases and nitrite reductase, which utilise Fe-S clusters during anaerobic respiration (Giel *et al.*, 2006).

IscR has also been found to positively regulate some of its targets, for example the *suf* operon (Giel *et al.*, 2006, Yeo *et al.*, 2006, Lee *et al.*, 2008), which encodes an alternative Fe-S cluster biogenesis pathway. The Suf Fe-S biogenesis pathway functions under stress conditions such as iron limiting conditions as well as oxidative and nitrosative stress (Justino *et al.*, 2005, Mukhopadhyay *et al.*, 2004, Outten *et al.*, 2004). This is in contrast to the Isc system, which is proposed to be involved in housekeeping of Fe-S biogenesis under normal conditions (Johnson *et al.*, 2005, Py & Barras, 2010, Py *et al.*, 2011). IscR has been shown to regulate these targets via a different mechanism (Giel *et al.*, 2006, Nesbit *et al.*, 2009). The cluster containing, holo-form of IscR has been found to negatively regulate the *isc* operon while the apo-form positively regulates the *suf* operon (Nesbit *et al.*, 2009, Yeo *et al.*, 2006). IscR has also been shown to activate the *suf* operon (Rincon-Enriquez *et al.*, 2008). Even though the Isc pathway is primarily responsible for ligating the cluster into IscR, recent work has shown that when expression of the Suf pathway is elevated it can also ligate the [2Fe-2S] cluster into IscR; meaning it can be substituted for the Isc pathway in *E. coli* (Giel *et al.*, 2013). Therefore IscR can sense the Fe-S status of the cell and adjust the expression of either Fe-S biogenesis pathway accordingly.

IscR senses the Fe-S status within the cell due to the presence or absence of its own [2Fe-2S] cluster (Giel *et al.*, 2013). Both apo and holo forms of IscR function as homodimers (Nesbit *et al.*, 2009) and the Fe-S cluster is ligated by the Cys92, Cys98, C104 and His107 residues resulting in the holo form of the protein. This ligation scheme is uncommon in metalloproteins but when compared to other [Fe-S] proteins that adopt the (Cys)₃(His)₁ ligation pattern they appear to function as sensors (Fleischhacker *et al.*, 2012).

As IscR is proposed to sense intracellular Fe-S status (Giel *et al.*, 2013) the regulation of *isc* occurs via negative feedback due to the cellular requirements of Fe-S. IscR is more sensitive to Fe-S requirements under aerobic conditions (Giel *et al.*, 2013). This is probably due to the sensitivity that Fe-S clusters exhibit towards oxygen (Imlay, 2006, Imlay, 2008) and therefore the demand for replacing Fe-S clusters in aerobic conditions is greater within the cell. Therefore IscR is a global regulator of [Fe-S] cluster biogenesis within the cell.

IscR has been found to regulate two types of target promoters; these have been classified into type 1 (*iscR*, *yhgl* and *yadR*) and type 2 (*sufA*, *ydiU* and *hyaA*). Type 1 promoters are only bound by the holo-IscR; whereas type 2 promoters are bound by both holo and apo IscR (Giel *et al.*, 2006, Lee *et al.*, 2008, Nesbit *et al.*, 2009, Yeo *et al.*, 2006, Fleischhacker *et al.*, 2012). Holo-IscR has been found to bind to two type 1 sites, deemed site A (-65 to -41) and site B (-40 to -16), in order to repress *isc* (Giel *et al.*, 2013, Giel *et al.*, 2006). The intensity of this repression is increased by cluster occupancy. Cluster occupancy is not involved with type 2 sites as IscR does not require the cluster to regulate these targets (Nesbit *et al.*, 2009, Yeo *et al.*, 2006). Recently the cluster has been proposed to reorientate key residues away from the major groove of DNA; which would allow the holo-form to bind to type 1 sites (Rajagopalan *et al.*, 2013). The key residue in apo-IscR binding is Glu43, which was shown by mutating this residue in both holo and apo-IscR; resulting in a reversal in type 1 binding (Rajagopalan *et al.*, 2013, Zeng *et al.*, 2008). Meaning the apo-IscR E43A

could bind to type one sites whereas holo-IscR E43A could not. This residue highlights the mechanism by which IscR can regulate different sites in both its forms.

5.2.3. Fe-S Cluster Biogenesis

Biogenesis of an Fe-S cluster is composed of two main processes. The first being the assembly of an Fe-S cluster onto a scaffold protein, then transferred from the scaffold onto the target apo-protein where it becomes incorporated into the structure.

Both the Isc machinery and Suf machineries for Fe-S cluster biogenesis are shown in figure 5.1. The Isc assembly machinery is found within bacteria and mitochondria. Biosynthesis with the Isc system initially uses the cysteine desulphurase IscS and the iron donor CyaY to procure the components required for cluster assembly. IscS generates persulphide attachment to a cysteine residue while the iron donor CyaY is thought to function as an iron dependant regulator that inhibits IscS (Adinolfi *et al.*, 2009). The electron transfer occurs in this system via Fdx, which is displayed in figure 5.1. The Fe-S cluster is then assembled onto the scaffold protein IscU or IscA (figure 5.1). IscU and IscA are highly conserved and contains three cysteine residues (Raulfs *et al.*, 2008), which allow the cluster to be ligated onto the protein. Once constructed the Fe-S cluster is then transferred to the recipient apo-protein; the chaperones involved with cluster transfer within the Isc system are HscA and HscB. The chaperone HscB is thought to function by changing the structure of IscU, which causes cluster dissociation from the scaffold (Bonomi *et al.*, 2008, Chandramouli & Johnson, 2006). When the Fe-S cluster is dissociated it can then be incorporated into the apo-protein to form the holo-form.

The other system used in bacteria is Suf, which is also used by plastids. The cysteine desulphurase is SufS which transfers sulphur from a conserved cysteine residue within SufE. However unlike the Isc system the iron and electron donors are unknown in the Suf system. There are three possible scaffold proteins SufB, SufU and SufA. The scaffold proteins SufU and SufA are similar to IscU and IscA, respectively. The scaffold SufB has been found to contain conserved cysteines that ligate the Fe-S cluster (Ayala-Castro *et al.*, 2008, Fontecave & Ollagnier-De-Choudens, 2008). The Scaffold SufB forms a stable complex with SufC and SufD (Loiseau *et al.*, 2003, Nachin *et al.*, 2003, Outten *et al.*, 2003); where SufC is an ATPase that dissociates the Fe-S cluster from SufD. Therefore SufC is assumed to transfer the Fe-S cluster to the desired apo-protein. All of these possible scaffolds may ligate the Fe-S cluster into the apo form of the protein resulting in the active holo Fe-S cluster protein.

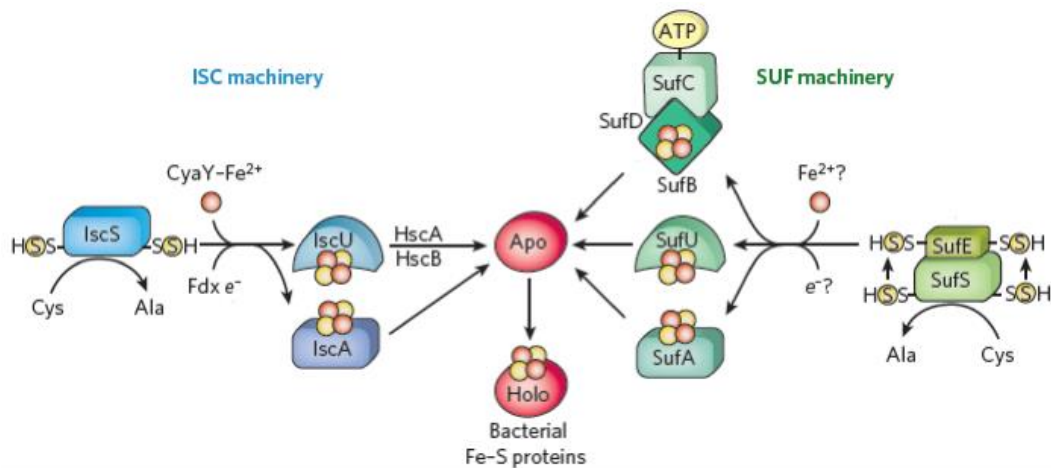


Figure 5.1: The bacterial Fe-S cluster assembly machinery's ISC and Suf. Bacteria adopt either the ISC, Suf or both systems in order to produce fully functional [Fe-S] cluster proteins. The ISC machinery functions under normal conditions in *E.coli*. This ISC system consists of IscS (a cysteine desulphurase), IscU and IscA (scaffold proteins). The Suf system operates under oxidative stress and iron limiting conditions. The Suf system consists of SufS (cysteine desulphurase), possible scaffolds: SufU, SufA and SufB (Lill, 2009) used with authors permission.

5.3. Fe-S Clusters

Fe-S clusters are essential cofactors in a number of proteins that have a variety of functions from electron transfer to transcription factors. The most common cluster forms are either the rhombic [2Fe-2S] or cubane [4Fe-4S] cluster, which have been proposed to have evolved when both iron and sulphur were highly abundant on Earth, up until two billion years ago (Meyer, 2008). Since then rarer types of Fe-S cluster have emerged when both iron and sulphur resources are limited. These rarer Fe-S cluster types include the [3Fe-4Fe] cluster, which has been hypothesised to be a modification of the primitive [4Fe-4S] cluster (Meyer, 2008, Rao & Holm, 2004) or a degradation product of the [4Fe-4S] cluster (Crack *et al.*, 2012).

Fe-S clusters commonly ligate into proteins via cysteine residues (Hutchings *et al.*, 2002, Rousset *et al.*, 2008). However other residues including histidine (Martins *et al.*, 2004), glutamine (Zeng *et al.*, 2008), and arginine have also been found to ligate Fe-S cluster within proteins. The presence or absence of the Fe-S within the protein impacts its function within the cell.

5.3.1. Functions of Fe-S cluster Proteins

Function and activity of proteins that exhibit Fe-S cofactors are extremely diverse and well established. Fe-S cluster proteins are involved in a number of processes including electron transfer, catalysis and sensing ambient conditions (Lill, 2009). The most common use of Fe-S cluster proteins is electron transfer (Johnson, 1994, Lovenburg, 1973); this is due to the capability of iron to switch between oxidative states +2 and +3 (Beinert *et al.*, 1997). A physiological example of this is that Fe-S proteins function as vital components of photosynthesis (Karrasch *et al.*, 1996).

Fe-S clusters have been found to be involved in other processes, such as sensing both iron and oxygen levels in order to switch between different oxidative states (Beinert *et al.*, 1997). Also these catalytic cofactors have been shown in a number of enzymes such as L-serine dehydratase (Burman *et al.*, 2004), biotin synthase and lipoate synthase (Hewitson *et al.*, 2000, Ollagnier-de Choudens *et al.*, 2000).

Finally, and most relevant to this project, Fe-S clusters have been found within transcriptional regulator proteins. These Fe-S cluster-containing regulators sense environmental or intracellular stress conditions and regulate expression of target genes accordingly. Transcription factors that rely on an Fe-S cluster include FNR, IscR (described above), SoxR and NsrR. These regulators have been shown to both positively and negatively regulate target gene expression. This activity of the regulator is controlled by the presence or absence of the Fe-S cluster; or as in SoxR the redox state of the [2Fe-2S] cluster (Imlay, 2008).

Once Fe-S clusters are ligated into proteins modifications can occur resulting in cluster conversion or even the loss of cluster from the protein. This is due to the Fe-S cluster dissociating from the protein; this dissociation can occur due to environmental conditions, such as exposure to redox-active gases such as molecular oxygen or nitric oxide (Crack *et al.*, 2008).

5.4. Nitric Oxide (NO)

5.4.1. NO and Fe-S Clusters

NO is a lipophilic radical that diffuses into the cell and reacts with Fe-S cluster proteins within the cell (Crack *et al.*, 2012). NO is a highly potent antimicrobial because it is highly

reactive with transition metals such as iron, copper and zinc. Iron is a vital component of many cofactors within enzymes and regulators (Jones-Carson *et al.*, 2008).

Reaction of NO with iron centres gives rise to nitrosyl complexes; and when NO reacts with Fe-S clusters dinitrosyl iron complexes (DNICs) are formed (Crack *et al.*, 2011). This DNIC means that the cluster becomes bound to the NO instead of the cysteine ligands in the protein. Therefore DNICs cause the Fe-S cluster to dissociate and the protein returns to its apo-form. Another way in which Fe-S clusters can degrade in response to NO is into Roussin's red ester (RRE) (Butler *et al.*, 1988). When two RREs combine they form a tetranuclear octanitrosyl cluster (Crack *et al.*, 2012).

5.4.2. NO Sources

The potency of NO is a threat that bacteria are exposed to in a range of environments. One such environment is within the soil. NO is produced by denitrifying bacteria that reside in soils (Tucker *et al.*, 2010). Denitrification is an important aspect of the nitrogen cycle where NO is produced (Richardson *et al.*, 2009, Payne, 1983). This alternative respiration pathway, produces NO as an intermediate in the conversion of nitrate to nitrogen gas (Butler & Nicholson, 2003). This means that non denitrifying bacteria are exposed to NO in their environment due to their denitrifying neighbours (Watmough *et al.*, 1999).

NO is also produced by bacterial nitric oxide synthases (bNOS). NOS are multidomain metalloproteins that catalyse the oxidation of arginine citrulline and generate NO. Most bacterial NOS lack the essential reductase domain; instead they recruit cellular reductases in order to produce NO *in vivo* (Gusarov *et al.*, 2008, Crane *et al.*, 2010). bNOS produce NO endogenously and have been found in an array of soil microorganisms including some

Gram-positive bacterial species Therefore bacteria that inhabit the soil must have NO defence mechanisms in order to survive.

5.4.3. Sensing Nitrosative and Oxidative Stress

NO and other nitrosating agents are known as reactive nitrogen species (RNS). RNS are compounds that when combined with oxidizers, act as nitrosating agents (Membrillo-Hernandez *et al.*, 1999); RNS include NO and peroxyxynitrite. When bacteria are exposed to NO or other RNS it causes nitrosative stress (Flatley *et al.*, 2005, Justino *et al.*, 2005, Mukhopadhyay *et al.*, 2004). Another group of compounds that are stressful to bacteria are reactive oxygen species (ROS). ROS are dangerous bi-products of aerobic respiration, due to incomplete reduction of O₂ (Crack *et al.*, 2012). ROS include O₂, superoxide, hydrogen peroxide and hydroxyl radicals.

Bacteria are exposed to RNS and ROS in a number of environments (Choi *et al.*, 2006, Fang, 2004, Jones-Carson *et al.*, 2008) and this is problematic because they cause intracellular damage; such as thiol S-nitrosylation, thiol N-nitrosylation of some amino acids, oxidative DNA damage; as well as reacting with metal cofactors, including Fe-S clusters. Therefore when NO is present within the cell it needs to be rapidly sensed and detoxified.

Many of the proteins which sense and response to RNS and ROS contain Fe-S clusters (Crack *et al.*, 2012, Mukhopadhyay *et al.*, 2004). These regulators include FNR, SoxR, IscR, NsrR and WhiB-like (Wbl) proteins. The integrated Fe-S cluster acts as a sensor within these proteins, allowing them to detect environmental conditions. Conditions, such as NO levels, cause the integrated Fe-S cluster to dissociate from the protein, which leads to a variation in target gene expression. IscR has been shown to repress or activate a different set of

targets in its apo or holo forms such that cluster occupancy influences gene expression, which can be adjusted to deal with environmental conditions accordingly (Lill, 2009).

5.5. NsrR

Like IscR, the nitrite-sensitive repressor NsrR also belongs to the Rrf2 protein family. NsrR was first discovered in *Nitrosomonas europaea* where it is encoded upstream of, and regulates, the gene encoding the nitrite reductase NirK (Beaumont *et al.*, 2004). Once NsrR was discovered a number of target DNA-binding motifs were predicted in different bacteria in order to indicate the genes under NsrR control (Rodionov *et al.*, 2005). NsrR binds to target sequences using an N-terminal helix-turn-helix DNA binding motif (figure 5.2). The prediction of NsrR binding sites revealed a generalised consensus sequence for NsrR in γ -proteobacteria, β -proteobacteria and also within *Streptomyces* and *Bacillus* species (Rodionov *et al.*, 2005). Experiments in *E. coli* also revealed that NsrR regulates target genes by binding to either a single 11bp motif or two inverted repeats of the 11bp sequence separated by a single base pair (Partridge *et al.*, 2009). The predicted targets of NsrR binding were validated experimentally within a number of organisms including *E.coli*, *Salmonella enterica* serovar Typhimurium, *Neisseria meningitidis*, *Bacillus subtilis* amongst others (Bodenmiller & Spiro, 2006, Gilberthorpe *et al.*, 2007, Anjum *et al.*, 2002, Rogstam *et al.*, 2007, Overton *et al.*, 2006).

Helix-turn-Helix

```

IscR  MRLTSKGRYAVTAMLDVALNSEA-GPVPLADISERQGISLSYLEQLFSRRLRNKGLVSSVRGPGGGYLLGKDASSIAVGEVISA
Bsu   MCLTNYTDYSLRVLIFLAAERPG-ELSNIKQIAETYSISKNHLMKVIYRLGQLGYVETIRGRGGGIRLGMDPEDINIGEVVRK
Eco   MQLTSFTDYGLRALIYMASLPEG-RMTSISEVTDVYGVSRNHMVKIINQLSRAGYVTAVRGKNGGIRLGKPAASAIRIGDVVRE
Sco   MRLTKFTDLALRSLMRLAVVRDGEPLATREVAEVVGPYTHAAKAITRLQHLGVVEARRGRGGGLTLDLGRRVSVGWLVRE
Sen   MQLTSFTDYGLRALIYMASLPGD-RMTSISEVTEVYGVSRNHMVKIINQLSRAGFVTAVRGKNGGIRLGKPAANTICIGDVVRE
Vvu   MQLTSFTDYALRTLIIYLASLPDN-EQTNITDVTELVGVSRNHMVKIINRLGQLNYIQTVRGKNGGIRLNRPAKTILVGEVVRD
Ype   MQLTSFTDYGLRALIYMASLPGD-QMTSISQVTEVYGVSRNHMVKIINQLSRVGLVTAVRGKNGGIRLGKPADQILIGDVVVRQ

IscR  VDESVDATFCQ--GKGCCQGGDFCLTHALWRDLSDRLTGFLNNTLGELVNNQEVLDVSGRQHTHDAPRTRTQDAIDVKLRA
Bsu   TEDDFNIVECFDANKNICVISPVCGLKHVLEALLAYLAVLDKYTLRDLVKNKEDIMKLLKMKKE-----
Eco   LEP-LSLVNCs---SECHITPACRLKQALSKAVQSFLTELDNYTLADLVEENQPLYKLLLVE-----
Sco   LEGEAEVVDC--GDNECPLRGACRLRRALRDAQEAFYAALDPLTVTDLVAAAPTGPVLLGLTDRPSG-----
Sen   LEP-LSLVNCs---SECHITPACRLKQALSKAVQSFLKELDNYTLADLVEENQPLYKLLLVE-----
Vvu   LEP-LDLVNCs---VECHITPACRLKERLYRAKLAFLAELDDCSIAELDDNAELLILLQKA-----
Ype   MEP-LTLVNCs---SDCHITPACRLKQVLNQAVQSFLKELDNYTLADMVKDNSPLYKLLLVE-----

```

Figure 5.2: Alignment of protein sequences comparing NsrR from different bacterial species against *E. coli* IscR. NsrR sequences displayed from the following bacterial species: *Bacillus subtilis* (Bsu), *E. coli* (Eco), *Streptomyces coelicolor* (Sco), *Salmonella enterica* (Sen), *Vibrio vulnificus* (Vvu) and *Yersinia pestis* (Ype). The DNA binding helix-turn-helix motif (bold) and conserved cysteine residues (outlined) have been highlighted (Tucker *et al.*, 2008) used with authors permission.

Microarray studies in *E. coli* revealed that NsrR repressed nine operons, including the most highly regulated transcripts: *hcp-hcr*, *hmpA* and *ytfE* (Filenko *et al.*, 2007). Microarray studies in *E. coli* showed the nitrosative stress response genes *ytfE*, *hmpA* and *ygba* changed expression due to the absence of NsrR (Bodenmiller & Spiro, 2006) NsrR has also been shown to regulate *ytfE*, *ygba* *hcp* and *hmpA* in *Salmonella enterica* serovar Typhimurium (Gilberthorpe *et al.*, 2007, Rodionov *et al.*, 2005). Among these targets, *hmpA* encodes an NO dioxygenase which is upregulated in the presence of NO (Crawford & Goldberg, 1998, Poole *et al.*, 1996, Membrillo-Hernandez *et al.*, 1999). *hmp* is also predicted to be an NsrR target in *S. coelicolor* which encodes two copies of HmpA (1 and 2) (Tucker *et al.*, 2008). Therefore *hmp* appears to be one of the most conserved targets of NsrR in diverse species of bacteria, this includes soil bacteria in which HmpA has been shown to be vital for NO detoxification (Rogstam *et al.*, 2007, Poole, 2005).

The *hmpA* gene in *E. coli* is expressed under both aerobic and anaerobic conditions (Poole *et al.*, 1996). Under these conditions HmpA has been shown to catalyse different reactions to detoxify NO; HmpA functions as a dioxygenase under aerobic condition to convert NO to nitrate whereas under anaerobic conditions HmpA reduces NO to nitrous oxide (Gardner *et al.*, 1998). In *Neisseria meningitidis* NsrR regulates the nitric oxide reductase gene *norB* rather than *hmpA*, to reduce NO to nitrous oxide (Rock *et al.*, 2007, Anjum *et al.*, 2002).

dnrN, that repairs nitrosative damage to Fe-S clusters, has also been found to be regulated by *Neisseria meningitidis* and *N. gonorrhoeae* NsrR (Heurlier *et al.*, 2008, Isabella *et al.*, 2009). However genes related to Fe-S clusters and NO metabolism are not the only NsrR targets. Chromatin immunoprecipitation followed by microarray (ChIP-chip) within *E. coli* revealed that NsrR also regulates target genes that also involved in motility, stress response, metabolism and transport processes (Partridge *et al.*, 2009). These additional processes may be involved in taxis either towards or away from NO.

NO was first to shown to nitrosylate the Fe-S cluster of purified NsrR *in vitro* using the *S. coelicolor* protein, and this nitrosylation removes the DNA binding activity of NsrR thereby derepressing target genes including *hmpA* (figure 5.3) (Tucker *et al.*, 2008). The Fe-S cluster of NsrR was initially reported to be a [2Fe-2S] cluster in *S. coelicolor* NsrR (ScNsrR) when aerobically purified from *E. coli*. This aerobically purified ScNsrR was shown to bind to the promoters of *S. coelicolor hmpA1* and *hmpA2* (Tucker *et al.*, 2008).

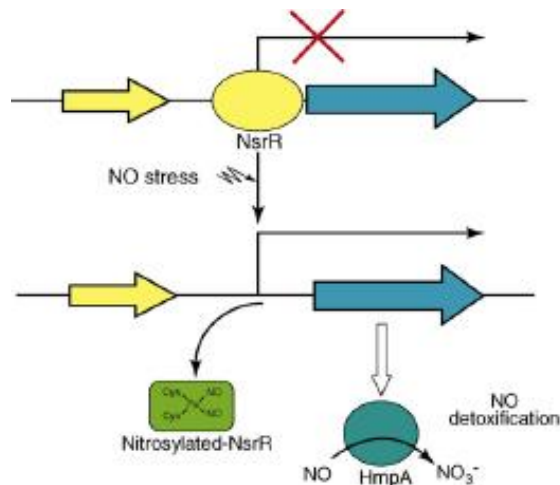


Figure 5.3: Diagrammatic representation of NsrR regulatory mechanism. Target genes, such as *hmpA* (blue) in *Streptomyces coelicolor*, are repressed by the holo form of NsrR (yellow); however when NsrR is exposed to stress from nitric oxide the cluster within NsrR becomes nitrosylated, which consequently affects NsrR function (green) allowing target genes to be transcribed. The products of these target genes then operate to detoxify NO and allow the bacteria to survive (Tucker *et al.*, 2010) used with authors permission.

More recently it has been shown that *S. coelicolor* NsrR can be purified anaerobically with a [4Fe-4S] cluster and that this form has high affinity for target sites, including *hmpA1* and *hmpA2* (J. Crack, personal communication), suggesting the initial experiments were done with a mixture of [2Fe-2S] and [4Fe-4S] forms. The biological significance of the two forms (if any) is as yet unclear. The activity of the [4Fe-4S] form of ScNsrR agrees with the report that *B. subtilis* NsrR (BsNsrR) contains a [4Fe-4S] cluster when anaerobically purified from *E. coli* (Yukl *et al.*, 2008). This [4Fe-4S] form of BsNsrR was also found to produce dinitrosyl iron complexes in response to NO exposure and, when exposed to oxygen, to degrade to an intermediate [3Fe-4S] and [2Fe-2S] cluster (Yukl *et al.*, 2008). The work in *B. subtilis* was extended to show that BsNsrR containing a [4Fe-4S] cluster bound to its known target *nasD* (Kommineni *et al.*, 2012, Kommineni *et al.*, 2010).

E. coli and *B. subtilis* NsrR appears to bind to either half (11bp) or full (23bp – 11 bp inverted repeat) sites at its target gene promoters (Henares *et al.*, 2014, Partridge *et al.*, 2009). This difference in binding site has been proposed to influence binding affinity of NsrR, with, low affinity binding at half sites and high affinity binding at full sites (Henares *et al.*, 2014). NsrR targets *nasD* and *hmpA* have full sites, meaning they are tightly regulated by NsrR. Half sites appear to be more diverse and genes containing such sites are possibly controlled by a number of regulators (Kommineni *et al.*, 2012).

The proposed residues involved with ligating the cluster in NsrR are thought to be three conserved cysteines. These cysteine residues are similar to the ligation pattern seen in the Rrf2 protein IscR (figure 5.2) (Yeo *et al.*, 2006, Giel *et al.*, 2006). These three cysteines are conserved in NsrR from a number of bacterial species and also in IscR (figure 5.2). The fourth ligand is currently unknown. The preferred ligand for [Fe-S] ligation is cysteine; however other residues such as histidine, arginine or glutamine are also used (Meyer, 2008). These conserved residues influence the function of NsrR due to their role of the ligation of the [Fe-S] cluster within NsrR. This was seen when the conserved cysteines (C90, C97 and C103) were substituted for alanines in order to observe the effect on the ability of NsrR to bind to DNA (Isabella *et al.*, 2009). These substitutions resulted in the reduction or even inhibition of the DNA-binding capability of NsrR in *Neisseria gonorrhoeae* (Isabella *et al.*, 2009). The derepression of NsrR target genes was also seen in *B. subtilis* by substituting individual cysteines in NsrR for alanines (Kommineni *et al.*, 2010). These studies have all confirmed that NsrR activity is dependent on the ligation of the Fe-S cluster contained within the holo-form.

5.6. Project Aims

In order to extend understanding of the role of NsrR in bacteria and specifically in *S. coelicolor* a number of questions needed to be addressed by this project. Firstly as NsrR has been shown to be involved in NO detoxification and survival, what are the effects of removing NsrR on *S. coelicolor*? This will be investigated by deleting the *nsrR* gene and observing any changes in phenotype in the presence and absence of NO.

The other important objective of this project is to experimentally determine the targets of NsrR in *S. coelicolor*. In order to identify these targets NsrR will be flag tagged for ChIP-seq experiments. Once NsrR targets are identified then a consensus binding motif will be generated. This binding motif might reveal other possible targets through in silico analysis that could be regulated by the Fe-S cluster containing, holo-form of NsrR that are not captured by ChIP. Targets will be validated *in vitro* by carrying out electromobility-shift assays (EMSAs). These experiments will extend our understanding of NsrR and the role it has in *S. coelicolor*.

Chapter 6: Results for NsrR Project

6.1. Generating *nsrR* Mutants

6.1.1. Strategy for Producing Mutants

The *nsrR* gene (figure 6.1) was deleted first by replacing the gene with an apramycin resistance cassette using the Redirect PCR targeting technique and then removing the cassette with Flp recombinase to leave an in-frame unmarked *nsrR* mutation with an 81 bp scar (see section 2.2).

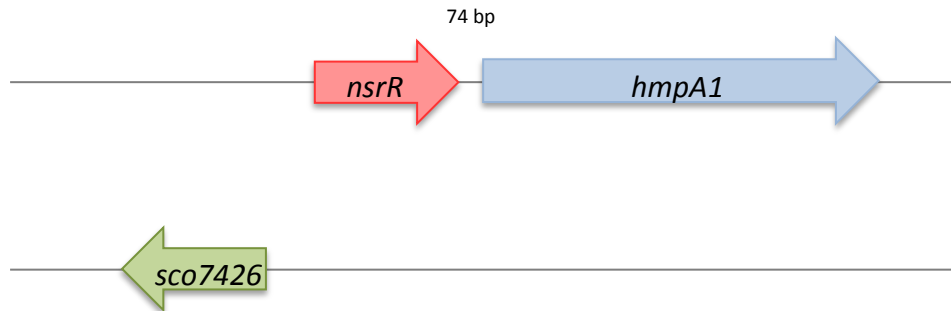


Figure 6.1: Genetic organisation of *S. coelicolor nsrR* and its surrounding genes. The chromosome of which the genes are encoded are displayed and the 74 bp intergenic region between *nsrR* and the downstream target gene *hmpA1*.

This was achieved by amplifying the apramycin cassette with flanking sequence to the *nsrR* gene (appendix, pages 194-196) and using it to PCR target the St6D11 cosmid. The *apra* marked cosmid was checked by both restriction digest and PCR. This PCR test amplified either the presence of the apramycin cassette in the knockout cosmid or the *nsrR* gene in the wild type cosmid. The *St6D11nsrR::apra* cosmid was then conjugated into wild-type *S. coelicolor* to isolate an M145 *nsrR:apra* strain which was checked by PCR. The in-frame mutant was made by removing the apramycin resistance cassette from the *St6D11nsrR::apra*

cosmid using Flp recombinase. An origin of transfer was introduced by PCR targeting, the cosmid was conjugated into the M145 *nsrR::apr* strain and in-frame *S. coelicolor nsrR* mutants were selected and checked by PCR.

6.1.2. Phenotype of the $\Delta nsrR$ Mutation

The $\Delta nsrR$ mutant was grown on MS agar and compared to wild-type parent strain M145 using light microscopy (figure 6.2). This revealed that the *nsrR* mutant is delayed in sporulation since, after 5 days of growth, it was clear that the wild type strain produced spores due to the production of grey-brown WhiE spore pigment, while the *nsrR* strain produced 13X less spores (figure 6.2 and table 6.1). The emergence of this phenotype was initially seen when isolating double crossover *nsrR:apra* mutants. Tests of three independently isolated *nsrR:apra* double crossover mutants were found to be correct and exhibited the same phenotype (appendix, p196). The apramycin cassette was later removed to form the $\Delta nsrR$ mutant, which exhibited the same phenotypic delay of sporulation. Spores were isolated from these mutants and aliquots of spore stocks were stored and used as the parental stock. Isolating and storing parental stocks prevented the requirement of numerous generations having to be re-isolated from individual colonies; this consequently reduced the chance of secondary mutations being introduced. Once mutant strains were constructed a representative mutant strain was used for all experiments.

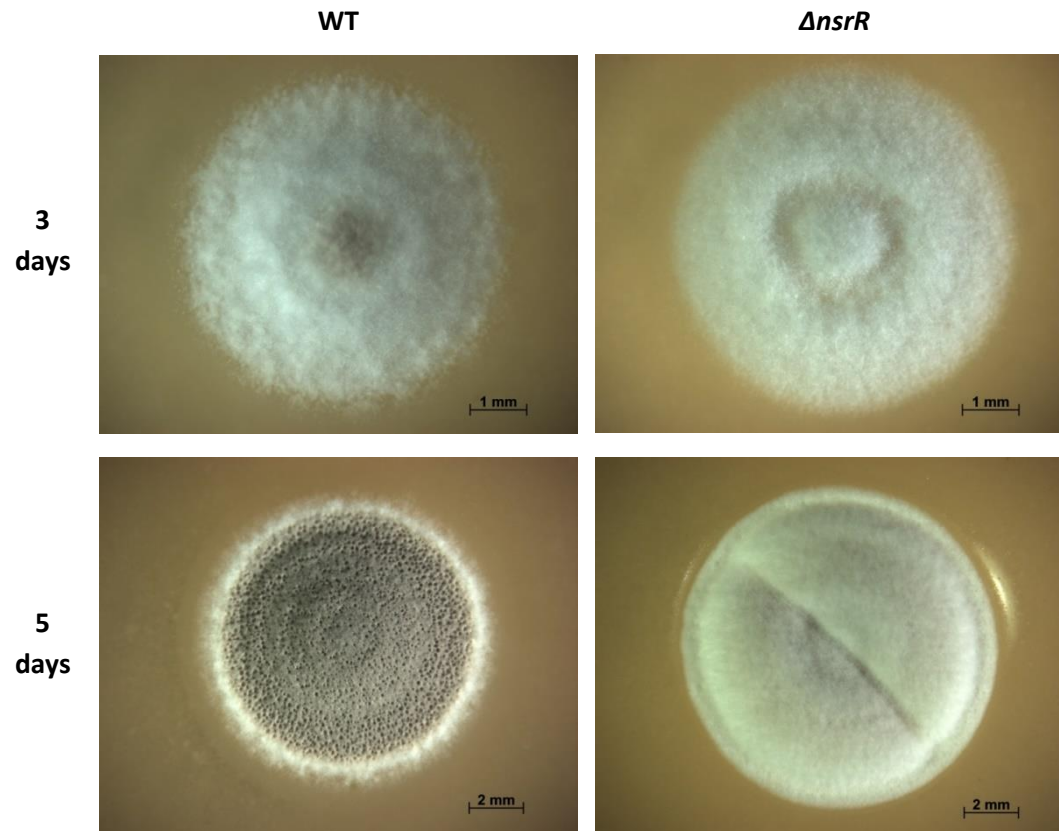


Figure 6.2: Phenotypic comparison of *S. coelicolor* wild type and $\Delta nsrR$ strains grown on SFM at 30 °C for 3 and 5 days then images by light microscopy. A drastic difference in phenotype was seen in the *nsrR* mutant in comparison to wild type *S. coelicolor*. This white phenotype was first seen when isolating the double crossover over *nsrR:apra* mutants. This white phenotype required further investigation as it was unsure whether white colonies meant a change in sporulation within the *nsrR* mutant at this stage.

6.1.3. Complementing the *nsrR* Mutation.

In order to complement the *nsrR* mutant the *nsrR* gene and upstream region were amplified (appendix, pages 197-200) and cloned into pCRII-TOPO, where successful candidates were identified by blue/white selection and sequenced (appendix, page 199), before sub-cloning into pMS82 (appendix, page 200). This complementation plasmid (pN26712) was conjugated into the $\Delta nsrR$ strain, but only partially complemented the mutant phenotype and did not restore sporulation to wild-type levels (figure 6.3).

In order to clarify whether $\Delta nsrR$ (pN26712) produced more spores than the mutant the number of spores produced by these strains was quantified and the results are displayed in table 6.1. These data show that the wild-type produced more spores than both the mutant and complemented mutant strain and that complementation had very little effect on spore production by the *nsrR* mutant. Spore production in the *nsrR* mutant is 13-fold lower than that of the wild type.

Table 6.1: Number of spores isolated from a standardised growth of the wild type, $\Delta nsrR$ and complemented *nsrR* strains. The number of spores isolated from *nsrR* mutant strains was 13-fold lower of that isolated from wild type *S. coelicolor*, this reduction in sporulation was only partially restored in the *nsrR* complemented strain $\Delta nsrR$ (p26712)

Strain	Spore quantity
<i>S. coelicolor</i> wild type M145	1.3×10^{11}
<i>S. coelicolor</i> $\Delta nsrR$	1.0×10^{10}
<i>S. coelicolor</i> $\Delta nsrR$ (p26712)	1.6×10^{10}

Table 6.1 also reveals the quantity of spores produced by the *nsrR* comp strain. This spore quantification revealed that the level of spore production in the complemented strain was only 1.6-fold higher than the *nsrR* mutant. However spore production was not at the same level of that of the wild type. Therefore this data in combination with the phenotype seen in figure 6.2 showed that reintroducing *nsrR* into the mutant only partially restored the wild type phenotype.

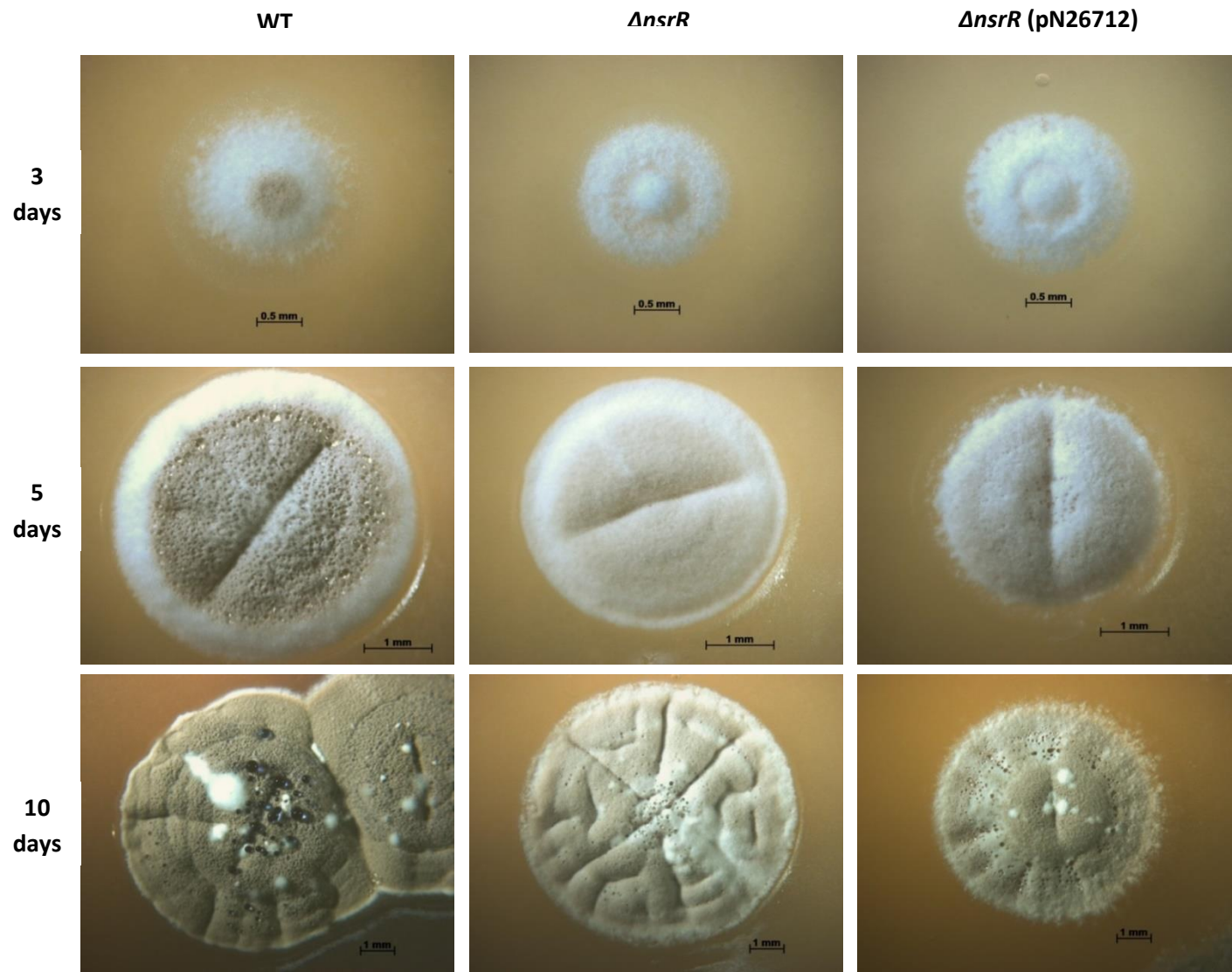


Figure 6.3: Phenotype of comparison of wild type, *ΔnsrR* and complemented strain *ΔnsrR* (pN26712) grown on SFM at 3, 5 and 10 days. Grey pigmentation appears reduced within the *nsrR* mutant at this level of microscopy; however SEM was required to visualise the effect removing *nsrR* had on the mutant strain. The grey pigmentation appears partially complemented in the *ΔnsrR* (pN26712) strain however further investigation would be required to confirm whether sporulation is truly effected within this strain.

6.2 Scanning Electron Microscopy (SEM)

To further analyse the sporulation defect in the *nsrR* mutant scanning electron microscopy (SEM) was carried out on both the wild type and *nsrR* strains in order to visualise the aerial hyphae and spores (figure 6.4).

The wild-type aerial hyphae were coiled but not as dense as those in the *nsrR* mutant. At 5 days growth less spores were visible in the *nsrR* strain in comparison to the wild type but both strains were forming spores. At this magnification a number of germ tubes have collapsed in the *nsrR* mutant. This lower quantity of spores and collapsing of mycelium explains the lack of spore pigment seen when the *nsrR* strain was viewed using a light microscope.

SEM was also conducted on strains after 10 days of growth on SFM agar (figure 6.5), and a drastic difference in developmental phenotype was seen between the two strains. The majority of wild type mycelium was coiled with uniform spore chains. In comparison the *nsrR* mycelium was not coiled and produced a lower yield of spores in comparison to the wild type.

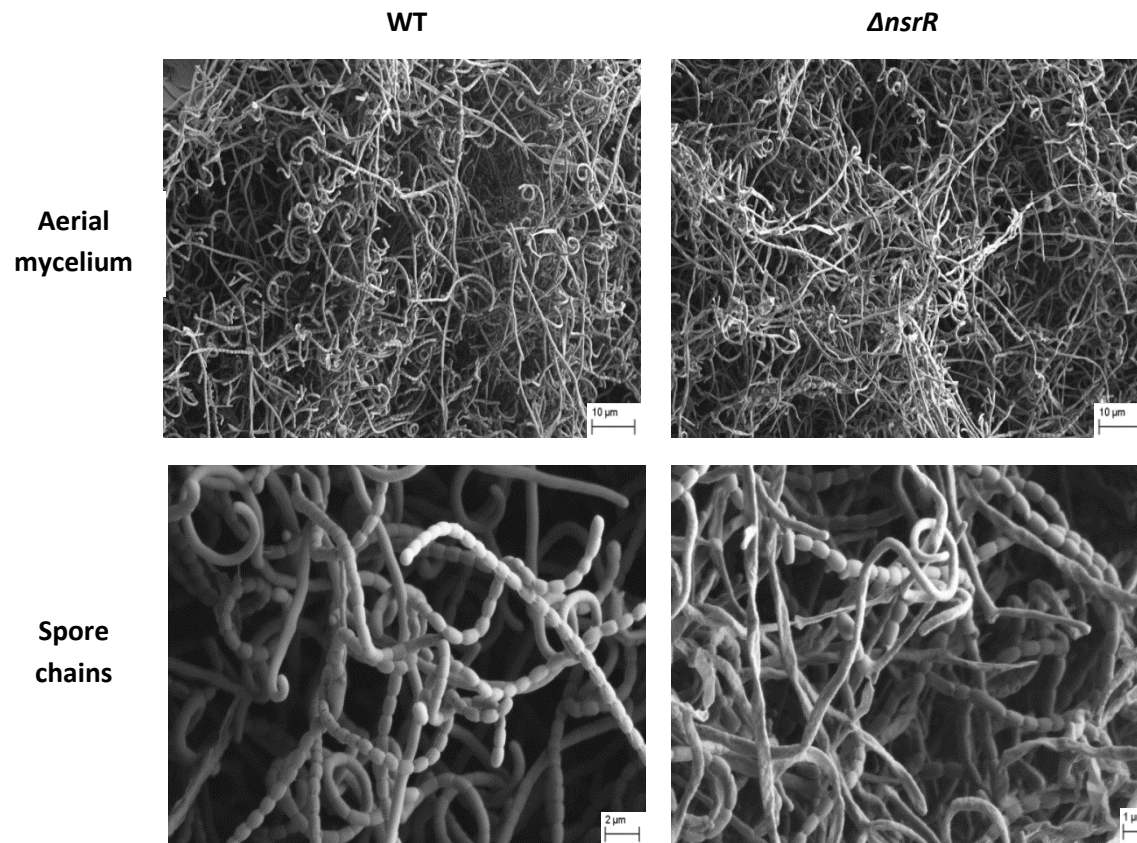


Figure 6.4: Scanning electron microscopy images of wild type and *ΔnsrR S. coelicolor* grown on SFM at 30 °C for 5 days. At this time point both the wild type and mutant strain are producing spores, however the *ΔnsrR* mutant appears to produce fewer spores and a number of collapsed germ tubes were visualised at this stage of growth.

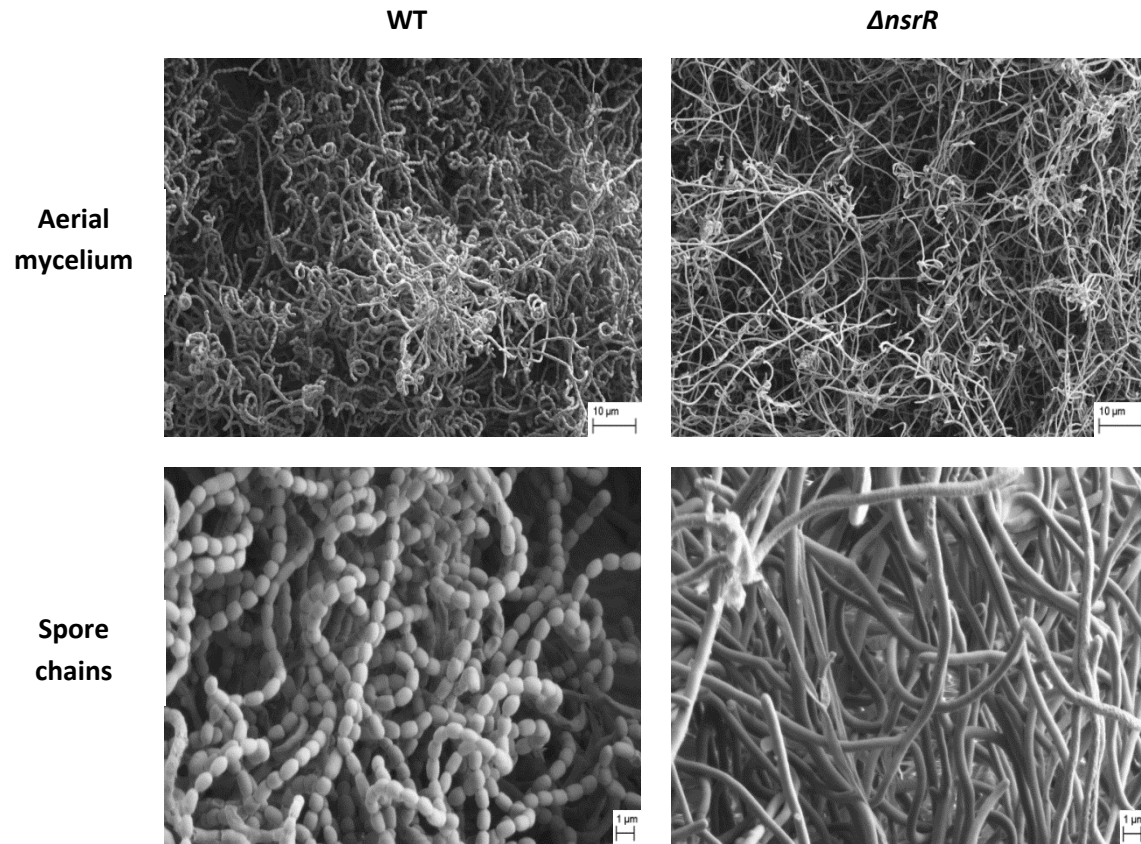


Figure 6.5: SEM images of wild type and *ΔnsrR S. coelicolor* grown on SFM at 30 °C for 10 days. At this time point wild type mycelia is coiled and sporulation occurs within the wild type strain. In comparison the representative figures of the *ΔnsrR* mutant visualised by SEM showed a difference in phenotype where only a few spores could be identified in the mutant strain at this time point.

6.3. Identifying NsrR Targets in *S. coelicolor*

6.3.1. Constructing an NsrR-3xFlag Tagged Strain

In order to identify the targets of NsrR *in vivo* a *S. coelicolor* strain expressing NsrR with a 3xFlag tag was constructed by amplifying the *nsrR* gene along with its native promoter, excluding the stop codon and cloned into pUCflagF by digestion with KpnI and NdeI in order to incorporate the DNA sequence encoding a C-terminal 3xflag tag. Prospective plasmids were then tested by restriction digestion. These vectors were designated pUCflagF *nsrR* (appendix, page 202). When *nsrR* is inserted into the pUCflagF plasmid a 3xflag tag was downstream of the gene. The in-frame flag tag from pUCflagF had optimised GC codon for *S. coelicolor* instead of *E.coli*. This construct was then subcloned into pMS82, renamed pN5112 (appendix, page 202), and integrated into the chromosome of the *nsrR* mutant strain to express NsrR from its native promoter but with a C-terminal 3xFlag tag (see section 2.7.1 and appendix, pages 200-202).

Before ChIP-seq analysis was carried out the phenotype of the *nsrR* mutant expressing the *nsrR*-FLAG was of interest (figure 6.6). Like the *nsrR* complemented strain the $\Delta nsrR$ (pN5112) strain expressing the *nsrR*-3xFlag only partial complemented the mutant phenotype.

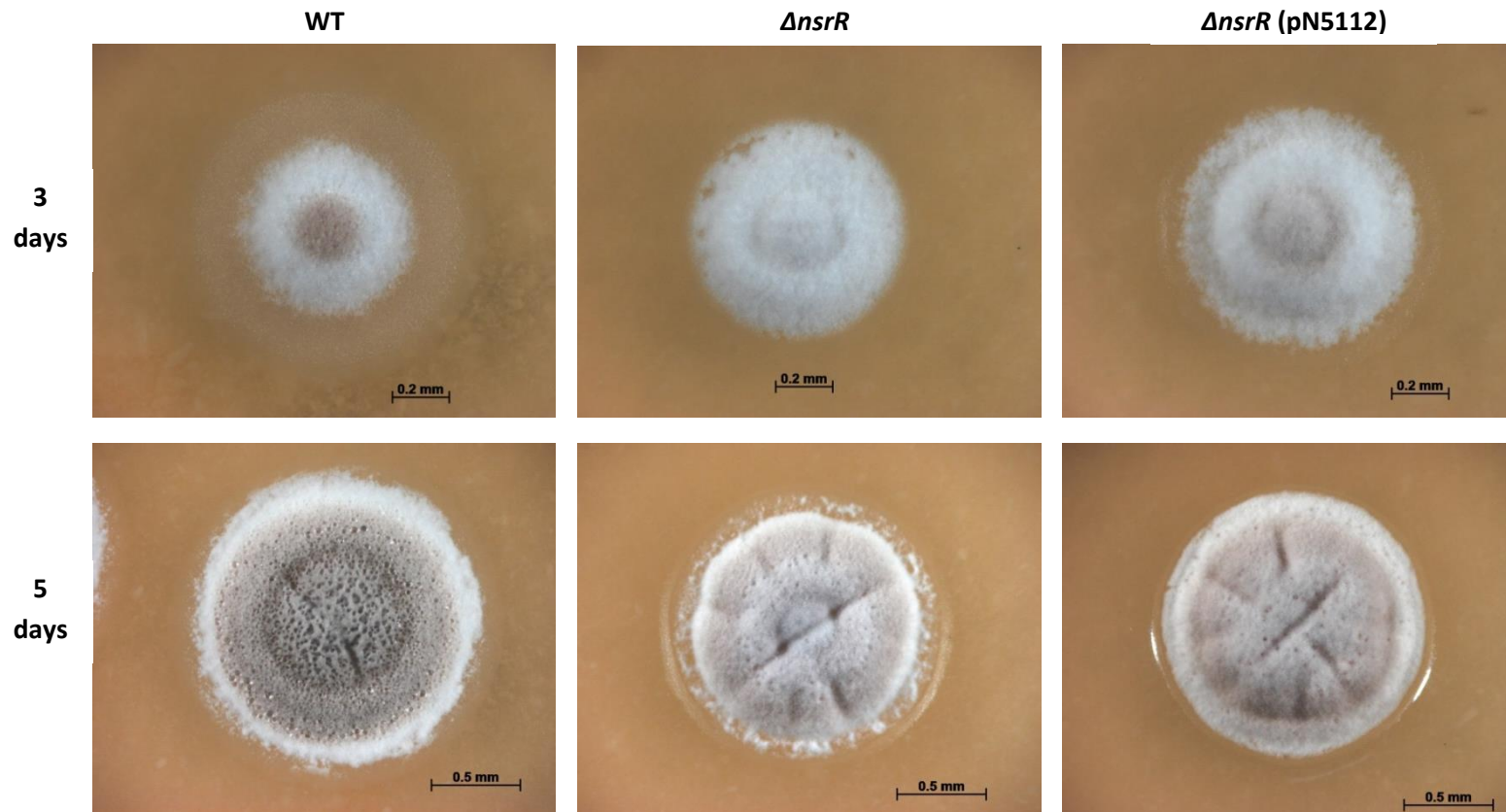


Figure 6.6: Colonies of wild type, $\Delta nsrR$ mutant and *nsrR*-Flag *S. coelicolor* strains grown on SFM at 30 °C on SFM for 3 or 5 days and imaged by a light microscope. Grey pigmentation appears reduced in the $\Delta nsrR$ strain, which is partially complemented in the $\Delta nsrR$ (pN5112) strain expressing *nsrR*-Flag. Further investigation would be required to establish whether sporulation was effected within these strains.

6.3.2. NsrR Targets Identified Using ChIP-seq.

Once the NsrR-3xFlag strain was constructed, the NsrR-3xFlag protein was detected by immunoblot using anti-Flag antibodies (figure 6.7). The immunoblot in figure 6.7 depicted the expression of *S.coelicolor* NsrR-3XFlag at 12 hour intervals for 3 days. This immunoblot was used to identify what time point to grow *S. coelicolor* strains required for ChIP-seq analysis. As NsrR-3xFlag is constitutively expressed in the $\Delta nsrR$ (pN5112) strain and $\Delta nsrR$ the control strain, 48 hours was the time period chosen for the growth of *S. coelicolor* strains in order to conduct ChIP-seq analysis. ChIP-seq was carried out on the *nsrR* mutant strains with and without the NsrR-3xFlag construct grown on cellophane disks placed on top of SFM agar plates in order to isolate mycelium. Once the strains had grown the cellophane disks were removed and DNA and proteins were cross linked using formaldehyde and used for ChIP with an α -flag antibody (see section 2.7.1). The isolated DNA was sequenced using Illumina and the sequence data was analysed using CLC workbench 4, which was used to identify ChIP-seq peaks present in the NsrR-3xFlag expressing strain but absent in the *nsrR* mutant control strain (figure 6.8). In order to identify peaks with CLC workbench 4 the $\Delta nsrR$ mutant was used as the control and sequencing results were aligned to the M145 genome. Peaks were seen in both the control strain and *nsrR* flag strain $\Delta nsrR$ (pN5112) however peaks were only called once control peaks were subtracted from the $\Delta nsrR$ (pN5112) peaks. Successful peaks were identified by the CLC workbench 4 by using a false discovery rate of 5%.

The biggest ChIP peaks (blue) were detected at the promoter regions of the *nsrR* (*sco7427*) and *hmpA1* (*sco7428*) genes, which are shown in yellow (figure 6.8). As the *nsrR* promoter is divergent from the *sco7426* promoter further tests were required to identify which promoter was the target of bound NsrR-3xFlag (see section 6.3.3).

A smaller ChIP-seq peak, with about 1.5 fold enrichment, was detected at the *hmpA2* promoter (figure 6.9) which is a previously validated NsrR target in *S. coelicolor* but no other significant peaks were detected. Therefore the only NsrR target genes identified by this ChIP-seq experiment were the previously identified *hmpA1* and *hmpA2* promoters; and a previously unknown target, the *nsrR* promoter. This is strikingly different to the >300 predicted ScNsrR target genes and suggests the computationally derived consensus for ScNsrR is incorrect.

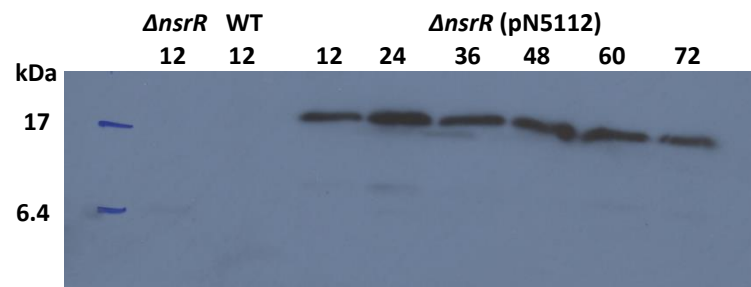


Figure 6.7: Immunoblot using α -FLAG to detect the expression of NsrR-Flag. *S. coelicolor* $\Delta nsrR$ (pN5112) was tested for 12 – 72 hours when grown at 30 °C on SFM. The control strains used to test NsrR-Flag expression were $\Delta nsrR$ and wild type *S. coelicolor* grown for 12 hours at 30 °C on SFM. This immunoblot showed that the $\Delta nsrR$ (pN5112) strain constitutively expressed NsrR-Flag and 48 hours was the determined time point used for CHIP-seq experimentation.

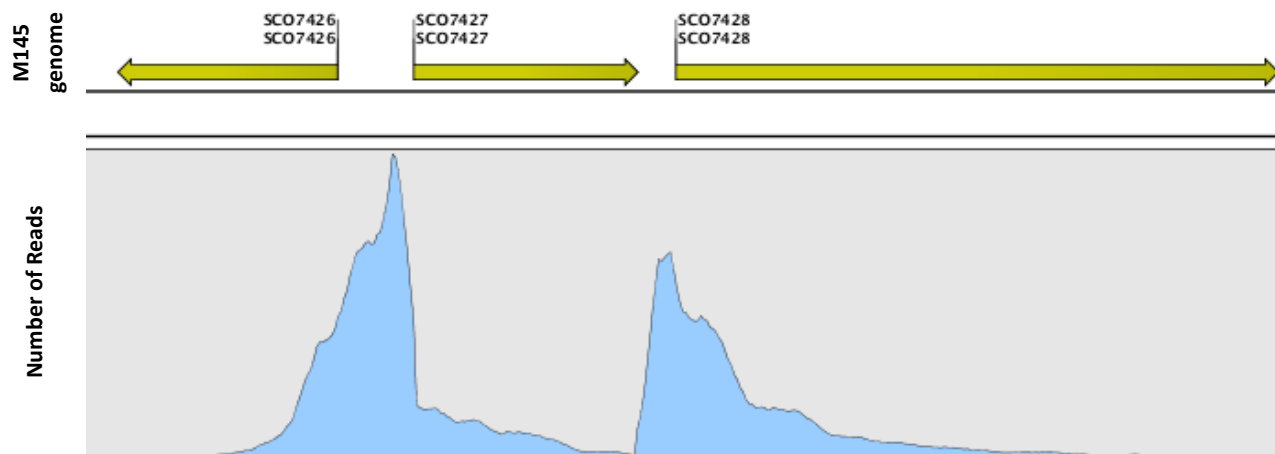


Figure 6.8: ChIP-seq peaks detecting the binding of NsrR to target promoters *nsrR* (*sco7427*) and *hmpA1* (*sco7428*). The peaks displayed in this figure were the two main peaks identified by ChIP-seq. The ChIP-peak within the intergenic region of *sco7426* and *nsrR* was confirmed to be a peak for the *nsrR* promoter due to further experimentation. Whereas the peak at the *hmpA1* promoter was clear and this target was previously established. The only other NsrR target identified by ChIP-seq was *hmpA2* (figure 6.9). All ChIP-seq targets were identified by the difference in the number of reads detected of target promoters (coverage) isolated from the $\Delta nsrR$ (pN5112) strain in comparison to the control strain.

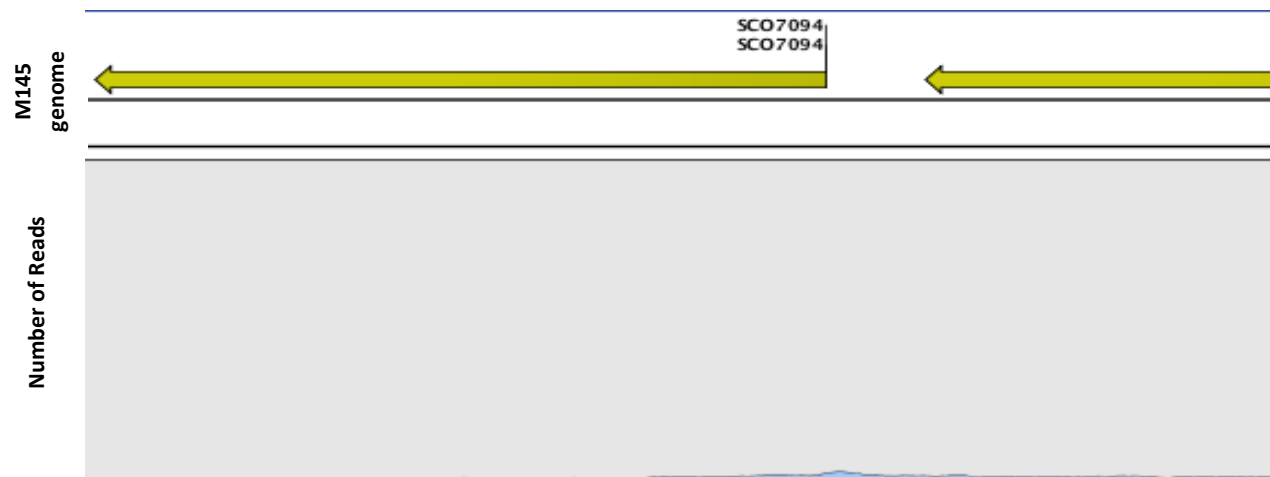


Figure 6.9: ChIP-seq peak detecting the binding of NsrR to target promoter *hmpA2* (*sco7094*). The ChIP-peak is at the same scale as figure 6.8 as *hmpA1* and *nsrR* were the two main targets identified by ChIP-seq, *hmpA2* was also identified due to the difference in the number of reads detected of target promoters (coverage) isolated from the $\Delta nsrR$ (pN5112) strain in comparison to the control strain.

6.3.3. Confirming NsrR Targets

After *nsrR*, *hmpA1* and *hmpA2* were shown to be targets of NsrR *in vivo* by CHIP-seq the next thing was to confirm these targets. This confirmation was achieved firstly by using a GUS reporter assay to detect the activity of the target promoters (figure 6.10). In order to achieve this the *nsrR* and *hmpA1* promoters were inserted upstream and in-frame of the β -glucuronidase gene in the vector pGUS (see section 2.7.3) using PCR (Myronovskyi *et al.*, 2011). After fragments were amplified for *sco7426*, *nsrR* and *hmpA1* promoters these were cloned into pGEMT. Prospective transformants were identified by blue/white screening and vectors were tested for the presence of the 500 bp inserts; which were ligated into KpnI and XbaI digested pGUS. Possible pGUS vectors were isolated and tested using restriction digestion. Successful pGUS *sco7426*, pGUS *nsrR* and pGUS *hmpA1* vectors were then conjugated into wild type and $\Delta nsrR$ *S. coelicolor* so a GUS assay could be conducted to allow a direct comparison of promoter activities in both the presence and absence of NsrR.

The results of this target expression test are shown in figure 6.10 and revealed the only significant difference in promoter activity between wild-type and *nsrR* mutant strains was observed for the *hmpA1* promoter. Since NsrR binds to its own promoter *in vivo* but *nsrR* promoter activity was unaffected by *nsrR* deletion this suggested that additional levels of regulation exist at the *nsrR* promoter. The *sco7426* gene is divergent from *nsrR* so it is feasible from the CHIP-seq data that NsrR could also regulate this promoter but since *sco7426* was unaffected in expression by deletion of *nsrR* we conclude that *sco7426* is not an NsrR target gene. The *nsrR*, *hmpA1* and *hmpA2* promoters are bound *in vitro* by Fe-S containing NsrR but not apo NsrR (J. Crack, personal communication). The binding efficiency of NsrR to these targets varies with *hmpA1* being the most tightly regulated target (J. Crack, personal communication). Therefore the *nsrR* promoter is a target of NsrR, which consequently undergoes auto regulation.

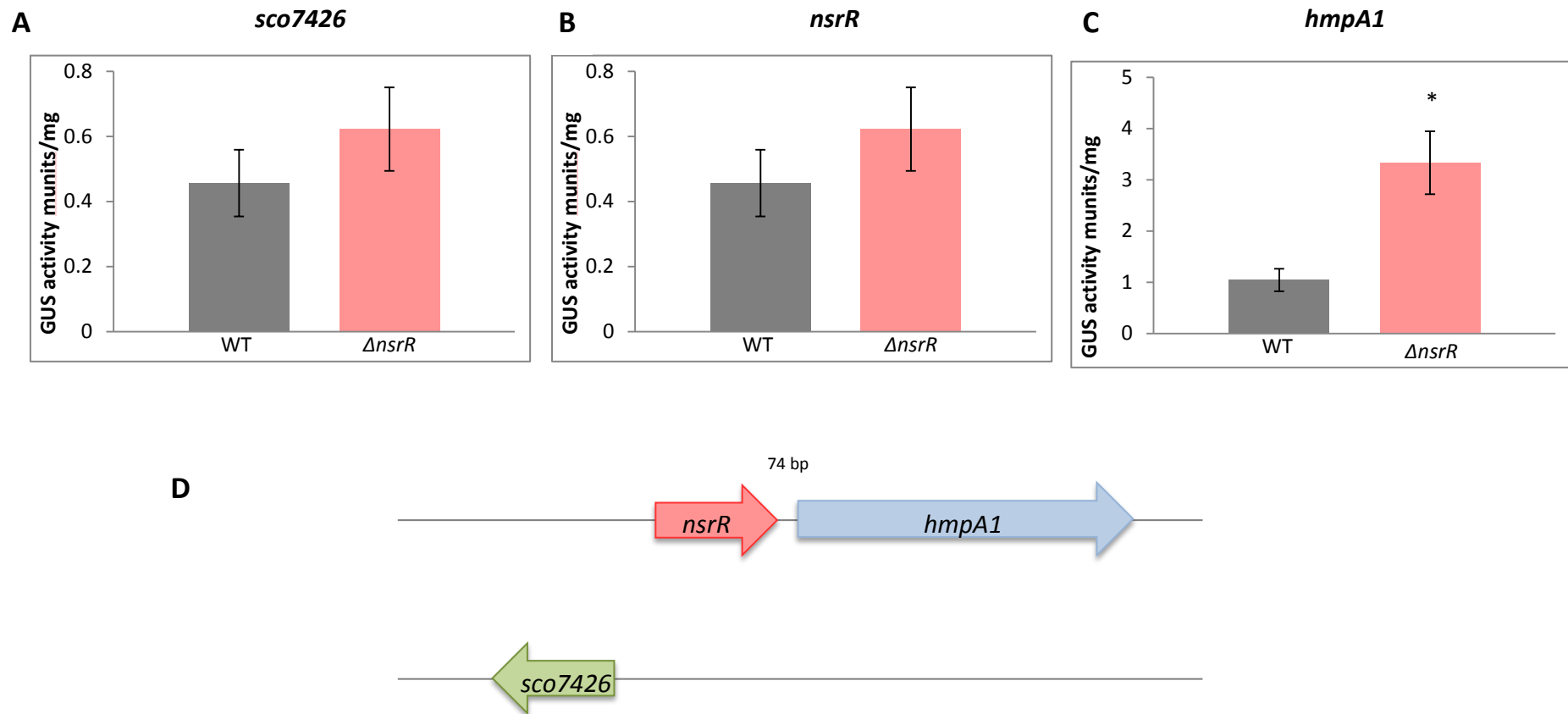


Figure 6.10: GUS assay to determine promoter activity of potential NsrR targets *sco7426*, *nsrR* and *hmpA1* in both the wild type and $\Delta nsrR$ strains. (A) Results of a GUS assay measuring promoter activity of *SCO7426* where no significant difference was detected. (B) GUS assay comparing promoter activity of *nsrR* in the presence and absence of the proposed regulator NsrR where no significant difference was seen meaning further experimentation was required. (C) GUS assay confirmed *hmpA1* is a target of NsrR and the significant difference was indicated by a *. (D) Genetic organisation of potential NsrR targets within the *S. coelicolor* genome. The GUS reporter construct could never be made for *hmpA2*.

Once NsrR was proven to bind to the targets, discovered by ChIP-seq analysis, an NsrR binding consensus was of interest. In order to identify this binding motif the promoter regions, 200 bp upstream of the start codon, were compared using MEME analysis. The results of this analysis are shown in figure 6.11.

Once the promoter sequences were aligned by MEME analysis (figure 6.11) the results showed that the target promoters aligned and contained conserved motif region. This region in combination with the ChIP-seq data revealed that the NsrR regulon may in fact only regulate *nsrR*, *hmpA1* and *hmpA2*. Therefore further work may be required to confirm that NsrR does not regulate any other predicted targets.

A

Predicted motif:

[AT]AAA[CG][AG][CA]G[AC]A[TC][CA]T[ACG][AG][CGT][AC]T[ACG]
C[CG][AC][AG]TT

>SCO7428 (*hmpA1*) promoter (8242155 to 8242395)

GCGGCGTGCCTGCGCGACGCCAGGAGCGTTCTACGCGGCACTCGACCCACTGACCGT
GACCGACCTGGTGGCCGCACCGACCGGCCGGTTCTGCTCGGCCTGACGGACCGCCCCTC
GGGATGACGGGCGGCGGCCCTGAGGCCGTGAGCTGTGGCTAAAACACGAATATCAT
CTACCAATTAAGGAGTCGCTGTGCTCTCCGAACAGTCCGTTCCCGTGGTCCGAGCCACCC

>SCO7094 (*hmpA2*) with 200 flanks (7884551 to 7886162)

AGCCCAGGGAGTCGTCCGCGGACCCCGGAACCCATAGCTCCGGCGCCCGGTCTCCGGCTT
ACCCGTCGTCCGTCAGCGGCCGGTCTGACATCGCGTCACAAGTCCGGCCGCTGTCCGG
TCTCACTGAGAAGACGGGCCGCACAGACGGTCCGTGGCACGTCGAAAACAAGCATCTGA
GATCCAGTTTCGGAGTAGGCATGCTCTCCAGTCAGTCGGCCAGATCGTCCGCGACACGC

>SCO7427 (*nsrR*) promoter (8241635 to 8241875)

GGGGAGGGGAGGGCCCGCAGTGCCCGGGGAGCCCGCTTCCGCTGCCATCAGGTGCCG
CCGTTCCGTGTGCCCGACCGTGCCCGTACGCCGCCCGTTGAGCGGTCCGTGCCGGGGCG
GCCGGTCCAGTGACGCACCGCACAGGCTCAGTACCCGGGTAAAGGCGAACCTAGCATGC
GCATTTGATAGCGTCCTGTGTGTCGGTTGACGAAGTTCACCGACCTGGCGCTGCGTTCGC

B

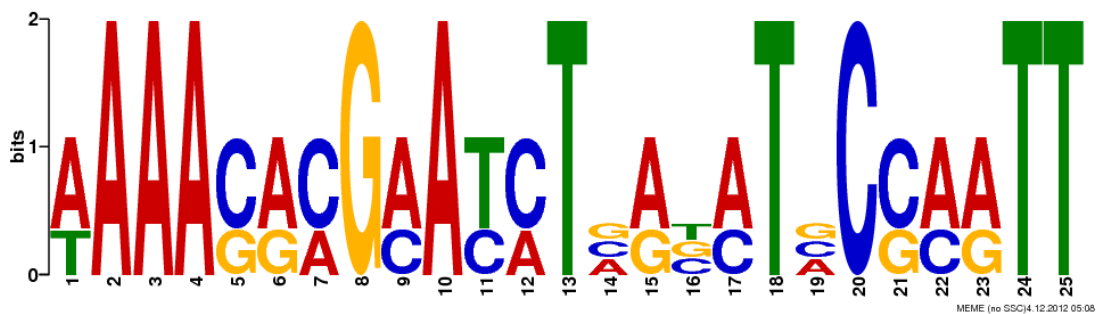


Figure 6.11: Alignment of NsrR target promoter sequences *hmpA1*, *hmpA2* and *nsrR* discovered by ChIP-seq analysis. (A) Promoter sequences from the ChIP-seq targets *hmpA1*, *hmpA2* and *nsrR* were aligned using MEME which predicted conserved motifs at all three (underlined). These include the NsrR binding sequences (in red) at both *hmpA* promoters which were previously validated using analytical ultracentrifugation (Tucker et al 2008). (B) WebLogo generated using the MEME predicted NsrR binding sites at the *hmpA1*, *hmpA2* and *nsrR* promoters.

6.4. Results Summary

This chapter explores the role of the nitric oxide sensing regulator NsrR within *S. coelicolor*. Binding of NsrR to the targets *hmpA1* and *hmpA2* had been observed (Tucker *et al.*, 2008) but numerous other targets had been predicted *in silico* (Rodionov *et al.*, 2005). Therefore to study *S. coelicolor* function *nsrR* was removed from the genome, causing a phenotype that could only be partially complemented. The creation of an *nsrR* mutant meant *nsrR* could be reintroduced into the mutant containing a 3XFlag tag, so ChIP-seq could be undertaken. The ChIP-seq results along with binding studies show despite numerous targets being predicted for ScNsrR only three were found: *hmpA1*, *hmpA2* and the newly discovered target *nsrR*. Therefore this work revealed that NsrR undergoes auto-regulation.

Chapter 7: Discussion

The aim of this work was to investigate the function of the MtrAB-LpqB three-component system and the NO sensitive repressor NsrR in the model organism *S. coelicolor*. The ability to rapidly respond to environmental changes by modulating gene expression is essential for *S. coelicolor* to survive within its harsh soil environment and previous studies in other bacteria have suggested important roles for both MtrA and NsrR in bacterial stress response.

7.1. MtrAB-LpqB Regulates Cell Division in *S. coelicolor*.

Investigating the role of the MtrAB-LpqB three-component system within *S. coelicolor* was undertaken because it is highly conserved in the phylum Actinobacteria and it has been implicated in the regulation of cell division in *M. tuberculosis* and *C. glutamicum* but never completely characterised in any species. The aim of this project was to explore the effect removing components of the *sco3014-mtrAB-lpqB* operon on *S. coelicolor* growth and differentiation, where *sco3014* is a transcriptionally linked gene found only in streptomycetes. This work revealed that all mutants in the *sco3014-mtrAB-lpqB* operon are viable (in contrast to *M. tuberculosis* and *C. glutamicum*) but the individual *mtrA*, *mtrB* and *lpqB* mutants showed a severe growth defect. The phenotypes of these mutants led to the hypothesis that MtrA might regulate FtsZ production in *S. coelicolor* and this was further analysed as a potential target gene.

Removing *mtrA* from the *S. coelicolor* genome resulted in a drastic phenotype (section 4.2.1); where pigmented antibiotic production was seen within a smooth colony. This production revealed that the vegetative mycelia of the *mtrA:apr* mutant was already producing undecylprodigiosin and actinorhodin. This finding is surprising because

actinorhodin biosynthesis is usually coupled to differentiation into aerial mycelium and spores in *S. coelicolor*. Deletion of *mtrA* causes the production of actinorhodin to be uncoupled from development, the question is why? Recent work involving a branched TCS in *S. coelicolor*, AbrC 1/2/3, has found to be linked to antibiotic production in *S. coelicolor*, where removing the RR of the system caused a decrease production of actinorhodin and undecylprodigiosin because actinorhodin is a direct target (Rico *et al.*, 2014). However the increase of actinorhodin and undecylprodigiosin seen within the *mtrA:apr* mutant could be an indirect effect caused by stress. As the *mtrA:apr* mutant exhibits both a growth defect and pigmented antibiotic production removing individual components of the *mtrAB-lpqB* system are viable but *S. coelicolor* differentiation is affected. In order to investigate this further, unmarked mutants were produced in each of the four genes in the *sco3014-mtrAB-lpqB* operon to investigate the role of each component in *S. coelicolor*.

When single mutants were produced for *sco3014-mtrAB-lpqB* significant growth defects were observed (displayed in section 4.2.1). Previous studies involving *C. glutamicum* and *M. tuberculosis* revealed that the MtrA and MtrB are important for cell viability and cell division; a single *mtrA* mutant could not be constructed in *M. tuberculosis* without introducing a second copy of *mtrA* suggesting that MtrA is essential in this organism (Zahrt & Deretic, 2000). Mutations in *mtrAB* could be produced in *C. glutamicum* but the *lpqB* gene could not be deleted (Möker *et al.*, 2004). Unlike the rod-shaped wild type cells, the $\Delta mtrAB$ double mutant in *C. glutamicum* exhibited elongated cell morphology (section 3.3.2, figure 3.7); which appears to be more like the mycelial growth observed in *Streptomyces* spp..

Phenotypic analysis of the in-frame mutants showed that removal of individual genes from the *sco3014-mtrAB-lpqB* operon caused defects in *Streptomyces* differentiation and, as discussed above, antibiotic production (section 4.2.1). The $\Delta mtrA$ and $\Delta mtrB$ mutants both

grow as much smaller colonies than the wild-type and they over-produce pigmented antibiotics. Crucially this analysis has shown that, unlike in *M. tuberculosis*, MtrA is not essential in *S. coelicolor*. However like *C. glutamicum* removing *mtrA* or *mtrB* appears to drastically change the growth phenotype of *S. coelicolor*.

In *M. smegmatis*, the accessory lipoprotein LpqB, has been shown to interact with the sensor domain of MtrB using an *E. coli* two hybrid assay (Nguyen *et al.*, 2010). The phenotype of *S. coelicolor* Δ *lpqB* suggests that *Streptomyces* differentiation is affected by removal of LpqB; in fact the Δ *lpqB* mutant exhibits two forms of growth: grey and white, the latter apparently arising through spontaneous mutation of the grey *lpqB* mutant to block cell division (figure 4.2). This divergence of phenotype has not been described for any of the classical *bld* or *whi* developmental mutants (Willemse *et al.*, 2012). When the Δ *lpqB* mutant formed white mutants they maintained their white phenotype upon restreaking suggesting the *lpqB* white phenotype is more stable. Whole genome sequencing and analysis of these strains and their parent strain will be required to identify and understand these secondary mutation(s). The conclusions drawn from this work is that removal of LpqB results in over-production of FtsZ (as observed using an FtsZ-eGFP fusion) which has an adverse effect on cell division. In order to survive the *lpqB* mutants spontaneously mutate to block cell division and thus generate white colonies.

When the mutants were examined using SEM the formation of aerial hyphae and spores could be visualised (section 4.2.2). In wild type *S. coelicolor* sporulation is a synchronised event in which septa are evenly spaced in the aerial hyphae. The *sco3014-mtrAB-lpqB* single mutants however exhibited non-uniform compartments, due to irregular spacing of the septa. Which suggested FtsZ production and or localisation might be affected. In contrast to the wild-type, at three days growth the Δ *mtrA* and Δ *mtrB* strains had not begun to sporulate and only aerial hyphae could be detected using SEM (figure 4.9); however the

ΔlpqB and *Δsco3014* strains were forming irregular spore compartments at this stage of growth (figure 4.10). The irregular spore formation exhibited by these mutants was eventually seen in the *ΔmtrA* and *ΔmtrB* mutants when they began sporulating after five days growth (figure 4.12). The irregular spacing of septum seen in the *sco3014-mtrAB-lpqB* single mutants suggests the mechanism of cell division is perturbed by the removal of these genes from the *S. coelicolor* genome. Meaning the MtrAB-LpqB three-component system could be linked, either directly or indirectly, with spore division and therefore formation in *S. coelicolor* and perhaps suggesting a role for SCO3014 in *S. coelicolor* also. The irregularity of septum placement seen within the mutants appears to form a 2x or 0.5x normal spore size (figures 4.10 and 4.12). The irregularity of septum placement within mutants is most likely due to the irregular placement of FtsZ rings; meaning components of the divisome such as SsgA, SsgB, ParA, ParB or FtsZ could be targets of MtrA. Furthermore, a putative MtrA binding site (identified in corynebacteria and mycobacteria) was identified upstream of the -35 region at the developmental P2 promoter at the *ftsZ* gene. Therefore, further studies into the link between *sco3014-mtrAB-lpqB* mutations and FtsZ expression and production were carried out in this study.

As spore formation appears altered in all of the individual *sco3014-mtrAB-lpqB* mutants the partitioning of chromosomes within these altered compartments would be of interest and transmission electron microscopy (TEM) could be used to determine whether chromosomal condensation and partitioning is altered within these mutants. If each spore does not each contain a complete genome the viability of the spores will be affected. TEM studies as well as DAPI staining of the chromosome for fluorescence microscopy would reveal if irregular septation in *sco3014-mtrAB-lpqB* mutants has consequently affected DNA arrangement within spores.

The MtrAB-LpqB component system has already been implicated in cell division in mycobacteria as MtrB was found to localise to septa and cell poles in *M. smegmatis* (Plocinska *et al.*, 2012). This localisation of MtrB was found to be FtsZ dependant but MtrB and FtsZ do not interact directly. This supports the idea that correct placement of FtsZ requires the MtrAB-LpqB component system in at least some actinobacteria; although the direct mechanisms of action of MtrA appear to differ even between closely related genera like *Mycobacterium* and *Corynebacterium*. Further investigation into this in *S. coelicolor* would require co-localisation experiments in strains expressing *ftsZ-eGFP* and *mtrB-mCherry* translational fusions within *S. coelicolor* wild type, Δ *ftsZ*, Δ *sco3014*, Δ *mtrA*, Δ *mtrB* and Δ *lpqB* strains. Co-localisation studies would reveal the position(s) of MtrB in *S. coelicolor* and its co-dependence on FtsZ. Since MtrA does not directly regulate *ftsZ* expression in *Mycobacterium tuberculosis* the situation appears to be slightly different from *S. coelicolor* since there is evidence presented here that MtrA activity affects *ftsZ* expression.

Another important phenotype seen in *mtrA* and *mtrB* mutant strains was the overproduction of pigments, specifically undecylprodigiosin (red) and a yellow pigmented compound that was detected in liquid growth (appendix, page 191). One yellow pigmented antibiotic, CPK, is a target of the PhoP-PhoR and AfsQ1/Q2 TCS (Allenby *et al.*, 2012, Shu *et al.*, 2009); where targets of PhoP included CPK and genes involved in *S. coelicolor* differentiation. Therefore in order to establish whether CPK was produced by *sco3014-mtrAB-lpqB* mutants, and possibly a target of MtrA, a number of tests were performed (section 4.3). These experiments revealed that CPK was not being produced by the Δ *mtrA* or Δ *mtrB* mutants and we propose that the yellow compound is likely to be the actinorhodin precursor (S)-DNPA. However (S)-DNPA had not been detected in high enough abundance for the yellow pigmentation to be observed (communication with Prof David Hopwood). Therefore in order for the yellow pigmented antibiotic to be (S)-DNPA,

actinorhodin had to be overexpressed within the $\Delta mtrA$ and $\Delta mtrB$; therefore an assay to determine the quantity of actinorhodin and undecylprodigiosin, produced by the mutants, was conducted (section 4.3.3). The MtrAB-LpqB component system could be involved in regulating actinorhodin production, via repression until *Streptomyces* have developmentally progressed into forming aerial mycelium. The overexpression of MtrA lower the production of actinorhodin observed on solid media. The antibiotic production by the single mutants is most likely due to stress.

As cell division is altered within the *sco3014-mtrAB-lpqB* mutant strains the potential targets of MtrA are of great interest. Unfortunately ChIP-seq using a polyclonal antibody against MtrA was unsuccessful. This is likely to be due to the cross reaction of the MtrA polyclonal binding to MtrA but also non-specific proteins (figure 4.18). With hindsight it would have been preferable to undertake the ChIP-seq by Flag tagging MtrA and using a monoclonal α -FLAG antibody for ChIP-seq analysis.

The results presented in chapter 3 suggest that the MtrAB-LpqB component system is involved in regulating *ftsZ* expression and / or localisation of the FtsZ protein, due to the irregular placement of cell division septa observed by SEM. Since we predict that the developmental *ftsZP2* promoter is regulated by MtrA this is not likely to be detected in liquid culture so expression of *ftsZ* was measured in solid (agar) grown cultures using qRT-PCR. The qRT-PCR revealed a significant decrease in *ftsZ* expression in the $\Delta mtrA$ strain in comparison to wild type (figure 4.20). As this change in expression is not seen within the $\Delta lpqB$ mutant the irregular septal spacing cannot solely be due to changes in *ftsZ* expression. Therefore the MtrAB-LpqB system may play a role in both regulating FtsZ production and localisation, although further work is required to support this hypothesis. One interesting point to note is when *ftsZ* is removed from the *S. coelicolor* genome actinorhodin is overexpressed, as seen in an MtrA deficient strain (McCormick *et al.*, 1994).

FtsZ production and localisation in the wild-type and individual mutants in the *sco3014-mtrAB-lpqB* mutants was investigated using an *ftsZ-egfp* translational fusion and fluorescence microscopy. FtsZ-eGFP signal was detected in all strains apart from $\Delta mtrA$; this absence of signal may be due to the significantly low *ftsZ* expression seen in this strain which means that the FtsZ-eGFP does not reach the threshold required for observation with fluorescence microscopy. The localisation of *ftsZ-egfp* was visualised at different stages of *S. coelicolor* growth. Within aerial mycelium the distribution of FtsZ-eGFP appeared to be overexpressed with the $\Delta lpqB$ mutant strains (figures 4.21); and organised into spiral filaments within the $\Delta mtrB$ strain (figure 4.21). FtsZ ladders are only observed within the $\Delta sco3014$ mutant at this stage of growth (figure 4.21), which may be due to the further progression of development seen within this strain.

Fluorescence microscopy of mutant spores revealed that FtsZ-eGFP is placed at the poles of spores; however distance between FtsZ-eGFP placement in strains (figure 4.21) appears irregular. This irregular placement of FtsZ-eGFP could account for the irregular sized spores seen in the SEM data. Therefore the organisation of divisome components resulting in FtsZ placement in *sco3014-lpqB* mutants is of great interest. Observing *ftsZ* placement in these mutant strains by time-lapse microscopy for future experiments would be of interest; this and Förster resonance energy transfer and fluorescence lifetime imaging microscopy (FRET-FLIM) to observe FtsZ interaction with components of the MtrAB-LpqB system and whether these irregular spores are viable.

Other future directions to consider when working on the MtrAB-LpqB system include testing cell wall viability of the mutants. Another interesting aspect of this system is to fully investigate the involvement of co-encoded, unknown protein SCO3014 with MtrAB-LpqB. In order to investigate this, a bacterial two hybrid assay could be performed to determine if SCO3014 directly interacts with any component of MtrAB-LpqB. To investigate whether the

intergenic regions within the *sco3014-mtrAB-lpqB* operon contain intergenic promoters 5'
RACE or reverse transcription of intergenic regions could be used.

7.2. NsrR Regulates NO Detoxification in *S. coelicolor*.

Previous work with purified NsrR from *S. coelicolor* had primarily focused on the presence and role of the Fe-S cluster but the function of NsrR within the organism itself had not been addressed experimentally. Over 300 targets had been predicted by genome scanning *S. coelicolor* using a computationally derived NsrR binding site for *Streptomyces* species (Rodionov *et al.*, 2005), and these included the *hmpA1* and *hmpA2* in *S. coelicolor*. Both *hmpA* promoters were shown to bind Fe-S containing ScNsrR *in vitro* using EMSAs and analytical ultracentrifugation and binding was abolished by NO (Tucker *et al.* 2008). Therefore the aims of this project were to delete the *nsrR* gene in *S. coelicolor* to observe any changes in phenotype, to look at the effects of NO on *S. coelicolor* growth and sporulation and to define the ScNsrR regulon using ChIP-seq. Identifying the ScNsrR target regulon *in vivo* is crucial to understanding the role of the protein in *S. coelicolor*

The phenotype of the *nsrR* defective mutant appeared to be a defect or delay in sporulation, since the *nsrR* mutant makes 10-fold less spores than the wild-type strain in the same age colonies (figure 6.2 and table 6.1). The white phenotype appears similar to that of the classical *S. coelicolor whi* mutants that are able to form aerial hyphae but cannot sporulate. There are a number of *whi* genes contained within the *S. coelicolor* genome; including *whiB* and *whiD*. Like NsrR, WhiB and WhiD also contain a [4Fe-4S] cluster that is vital to their function but they belong to the Wbl (WhiB-like) family and are not Rrf2 proteins like NsrR (Crack *et al.*, 2011, Crack *et al.*, 2009).

SEM of the wild-type and *nsrR* mutants revealed that spores are formed by the *nsrR* mutant strain, however some of these spores appear to be germinating (figure 6.4) and the majority of biomass appears to be aerial hyphae (figure 6.5). The dominance of aerial hyphae within the *nsrR* mutant accounts for the white colony phenotype since no spores, or spore pigment, is formed. Despite this NsrR cannot be classified as a *whi* mutant because

the *nsrR* mutant is still capable of forming spores albeit at a 13-fold lower yield than wild type *S. coelicolor*.

Once the sporulation phenotype was observed for the *nsrR* mutant the question was could this mutation be complemented. Figure 6.3 shows that only partial complementation occurs when *nsrR* was reintroduced. This partial complementation is also shown by quantification of the spores (table 6.1); the *nsrR* mutant exhibited a 13 fold decrease in spore production in comparison to wild type which was only increased to approximately 1.6 fold in the complemented strain. This means restoring *nsrR* into the mutant does only partially complement the white phenotype. The most likely possibility is that the *nsrR* mutant has either acquired a secondary mutation(s), or the phenotype is due to a possible target of the apo-protein, which contributes to the observed defect in sporulation. It is important to note that although not fully complemented back to wild-type levels inserting *nsrR* does increase the yield of spores. NsrR may be linked with the *whi* genes not via regulation of sporulation specific genes but by detoxifying NO resulting in holo-WhiB and WhiD proteins. In order to establish the most likely scenario direct targets were identified using ChIP-seq (see below) and this revealed only three targets, which are dedicated to sensing and detoxifying NO and have no obvious role in development.

An interesting aspect to investigate would be the impact of NO on different stages of the *S. coelicolor* lifecycle. The effect of NO on the *S. coelicolor* lifecycle is of future interest. This could be investigated further by observing how the transcriptional profile of *S. coelicolor* changes when exposed to NO at different stages in the lifecycle using RNA seq. Especially as NO signalling is emerging as an important feature of *Streptomyces* growth (Chandra & Chater, 2013).

The intracellular targeting of NO and its consequences are an emerging area of investigation; in order to understand the complexity of NO targeting within *S. coelicolor* a

number of experiments would be advantageous. These include observing NO targeting using an NO sensitive dye (CuFL) (Schreiber *et al.*, 2011), which would allow observation of NO positioning with fluorescent microscopy. The intracellular levels of NO within *S. coelicolor* could also be measured by using a fluorescent probe to quantify NO by flow cytometry (Xian *et al.*, 2013); this technique could be adopted to identify the levels of NO throughout the *S. coelicolor* cycle as NO has been proposed to be an important stress in the transition of growth (Chandra & Chater, 2013). Therefore further studies on the impact of NO on *S. coelicolor* development are of great importance.

Data obtained from ChIP-seq analysis revealed only three targets of NsrR in *S. coelicolor*: *hmpA1*, *nsrR* and *hmpA2* (figures 6.8 and 6.9). These identified targets were substantially lower than the >300 predicted targets that were identified as having the putative NsrR consensus binding sequence (Rodionov *et al.*, 2005). As these targets were only computationally predicted it is clear from our analysis that the predicted binding site is wrong although, intriguingly, it does overlap with the real binding site at the *hmpA1* and *hmpA2* promoters. It was also possible that the ChIP-seq experiment didn't identify all of the targets, but this is unlikely as, scanning the genome with the experimentally generated NsrR consensus binding site and testing putative targets using EMSAs failed to identify any other NsrR target genes (J. Munnoch, personal communication). Thus, the conclusion from these experiments is that ScNsrR controls only its own expression and that of HmpA to sense and detoxify NO. This further leads to the hypothesis that other regulators mediate the NO induced block in sporulation and these are most likely to be WhiB, and / or WhiD plus possible other unknown regulators in *S. coelicolor*. It is also possible that apo-NsrR regulates alternative sites but there is no evidence to support this hypothesis in any of the bacterial species in which NsrR has been studied.

The three direct targets of NsrR that were identified by ChIP-seq in this study were *nsrR*, *hmpA1* and *hmpA2*. Both *hmpA1* and *hmpA2* had been previously identified as targets of NsrR (Tucker *et al.*, 2008); however it was not known that NsrR was autoregulated and this was confirmed using EMSA. However, the activity of the *nsrR* promoter was not significantly increased in an *nsrR* mutant suggesting additional regulators control *nsrR* expression (figure 6.10).

MEME analysis was undertaken to align the 200 bp of DNA upstream of the *nsrR* *hmpA1* and *hmpA2* genes and identify putative regulatory sites (figure 6.14), and this revealed that the consensus sequence actually differs from that presented by Rodionov *et al.* (Rodionov *et al.*, 2005). This variation accounts for the difference in predicted targets (>300) in comparison with the three actually identified in this study. So almost all of the predicted targets are not real targets of ScNsrR *in vivo*.

The fact that *S. coelicolor* and presumably other streptomycetes dedicate an Fe-S regulator to controlling only its own expression and that of HmpA NO dioxygenase activity reflects the importance of NO to these bacteria, and in particular the danger of being exposed to an excess of NO in the soil. Clearly NO has a drastic effect on sporulation but presumably at even higher levels it is cytotoxic and would kill *S. coelicolor*. If NO acts as a signalling molecule to control sporulation, as has been suggested, via one or more of the Wbl proteins then NsrR is there to make sure NO levels do not get so high that they kill the cell, or perhaps is there to keep NO at the right levels for sporulation signalling to occur effectively. Clearly there is a lot still to learn about NO signalling in these bacteria and the next logical step would be to investigate the functions and targets of the WhiB and WhiD proteins *in vivo* and their responsiveness to NO.

Chapter 8: References

- Addinall, S.G. & B. Holland, (2002) The tubulin ancestor, FtsZ, draughtsman, designer and driving force for bacterial cytokinesis. *J Mol Biol* **318**: 219-236.
- Adinolfi, S., C. Iannuzzi, F. Prischi, C. Pastore, S. Iametti, S.R. Martin, F. Bonomi & A. Pastore, (2009) Bacterial frataxin CyaY is the gatekeeper of iron-sulfur cluster formation catalyzed by IscS. *Nature structural & molecular biology* **16**: 390-396.
- Ainsa, J.A., N. Bird, N.J. Ryding, K.C. Findlay & K.F. Chater, (2010) The complex whiJ locus mediates environmentally sensitive repression of development of *Streptomyces coelicolor* A3(2). *Antonie van Leeuwenhoek* **98**: 225-236.
- Ainsa, J.A., H.D. Parry & K.F. Chater, (1999) A response regulator-like protein that functions at an intermediate stage of sporulation in *Streptomyces coelicolor* A3(2). *Mol Microbiol* **34**: 607-619.
- Ainsa, J.A., N.J. Ryding, N. Hartley, K.C. Findlay, C.J. Bruton & K.F. Chater, (2000) WhiA, a protein of unknown function conserved among gram-positive bacteria, is essential for sporulation in *Streptomyces coelicolor* A3(2). *J Bacteriol* **182**: 5470-5478.
- Allenby, N.E., E. Laing, G. Bucca, A.M. Kierzek & C.P. Smith, (2012) Diverse control of metabolism and other cellular processes in *Streptomyces coelicolor* by the PhoP transcription factor: genome-wide identification of in vivo targets. *Nucleic Acids Res* **40**: 9543-9556.
- Alm, E., K. Huang & A. Arkin, (2006) The Evolution of Two-Component Systems in Bacteria Reveals Different Strategies for Niche Adaptation. *PLoS Computational Biology* **2**: 1329-1342.
- Amemura, M., K. Makino, H. Shinagawa & A. Nakata, (1990) Cross talk to the phosphate regulon of *Escherichia coli* by PhoM protein: PhoM is a histidine protein kinase and catalyzes phosphorylation of PhoB and PhoM-open reading frame 2. *J Bacteriol* **172**: 6300-6307.
- Anjum, M.F., T.M. Stevanin, R.C. Read & J.W.B. Moir, (2002) Nitric oxide metabolism in *Neisseria meningitidis*. *Journal of Bacteriology* **184**: 2987-2993.
- Ayala-Castro, C., A. Saini & F.W. Outten, (2008) Fe-s cluster assembly pathways in bacteria. *Microbiology and Molecular Biology Reviews* **72**: 110-+.
- Bagchi, S., H. Tomenius, L.M. Belova & N. Ausmees, (2008) Intermediate filament-like proteins in bacteria and a cytoskeletal function in *Streptomyces*. *Mol Microbiol* **70**: 1037-1050.
- Barbieri, C.M., T.R. Mack, V.L. Robinson, M.T. Miller & A.M. Stock, (2010) Regulation of Response Regulator Autophosphorylation through Interdomain Contacts. *THE JOURNAL OF BIOLOGICAL CHEMISTRY* **285**: 32325-32335.
- Beaumont, H.J., S.I. Lens, W.N. Reijnders, H.V. Westerhoff & R.J. van Spanning, (2004) Expression of nitrite reductase in *Nitrosomonas europaea* involves NsrR, a novel nitrite-sensitive transcription repressor. *Mol Microbiol* **54**: 148-158.
- Beinert, H., R.H. Holm & E. Munck, (1997) Iron-sulfur clusters: Nature's modular, multipurpose structures. *Science* **277**: 653-659.
- Bentley, S.D., K.F. Chater, A.M. Cerdeno-Tarraga, G.L. Challis, N.R. Thomson, K.D. James, D.E. Harris, M.A. Quail, H. Kieser, D. Harper, A. Bateman, S. Brown, G. Chandra, C.W. Chen, M. Collins, A. Cronin, A. Fraser, A. Goble, J. Hidalgo, T. Hornsby, S. Howarth, C.H. Huang, T. Kieser, L. Larke, L. Murphy, K. Oliver, S. O'Neil, E. Rabinowitsch, M.A. Rajandream, K. Rutherford, S. Rutter, K. Seeger, D. Saunders, S. Sharp, R. Squares, S. Squares, K. Taylor, T. Warren, A. Wietzorrek, J. Woodward, B.G. Barrell, J. Parkhill & D.A. Hopwood, (2002) Complete genome sequence of the model actinomycete *Streptomyces coelicolor* A3(2). *Nature* **417**: 141-147.

- Bentley, S.D., M. Maiwald, L.D. Murphy, M.J. Pallen, C.A. Yeats, L.G. Dover, H.T. Norbertczak, G.S. Besra, M.A. Quail, D.E. Harris, A. von Herbay, A. Goble, S. Rutter, R. Squares, S. Squares, B.G. Barrell, J. Parkhill & D.A. Relman, (2003) Sequencing and analysis of the genome of the Whipple's disease bacterium *Tropheryma whippelii*. *Lancet* **361**: 637-644.
- Bibb, M.J., A. Domonkos, G. Chandra & M.J. Buttner, (2012) Expression of the chaplin and rodlin hydrophobic sheath proteins in *Streptomyces venezuelae* is controlled by sigma(BldN) and a cognate anti-sigma factor, RsbN. *Mol Microbiol* **84**: 1033-1049.
- Bodenmiller, D.M. & S. Spiro, (2006) The yjeB (nsrR) gene of *Escherichia coli* encodes a nitric oxide-sensitive transcriptional regulator. *J Bacteriol* **188**: 874-881.
- Bonomi, F., S. Iametti, A. Morleo, D. Ta & L.E. Vickery, (2008) Studies on the mechanism of catalysis of iron-sulfur cluster transfer from IscU[2Fe2S] by HscA/HscB chaperones. *Biochemistry* **47**: 12795-12801.
- Brocker, M., C. Mack & M. Bott, (2011) Target Genes, Consensus Binding Site, and Role of Phosphorylation for the Response Regulator MtrA of *Corynebacterium glutamicum*. *J Bacteriol* **193**: 1237-1249.
- Buckler, D.R., Y. Zhou & A.M. Stock, (2002) Evidence of intradomain and interdomain flexibility in an OmpR/PhoB homolog from *Thermotoga maritima*. *Structure* **10**: 153-164.
- Bunet, R., M.V. Mendes, N. Rouhier, X. Pang, L. Hotel, P. Leblond & B. Aigle, (2008) Regulation of the synthesis of the angucyclinone antibiotic alpomycin in *Streptomyces ambofaciens* by the autoregulator receptor AlpZ and its specific ligand. *J Bacteriol* **190**: 3293-3305.
- Burbulys, D., K.A. Trach & J.A. Hoch, (1991) Initiation of sporulation in *B. subtilis* is controlled by a multicomponent phosphorelay. *Cell* **64**: 545-552.
- Burman, J.D., R.L. Harris, K.A. Hauton, D.M. Lawson & R.G. Sawers, (2004) The iron-sulfur cluster in the L-serine dehydratase TdcG from *Escherichia coli* is required for enzyme activity. *FEBS Letters* **576**: 442-444.
- Bush, M.J., M.J. Bibb, G. Chandra, K.C. Findlay & M.J. Buttner, (2013) Genes required for aerial growth, cell division, and chromosome segregation are targets of WhiA before sporulation in *Streptomyces venezuelae*. *mBio* **4**: e00684-00613.
- Butler, A.R., C. Glidewell & M. Li, (1988) Nitrosyl complexes of iron-sulfur clusters. *Adv Inorg Chem* **32**: 335-393.
- Butler, A.R. & R. Nicholson, (2003) *Life, Death and Nitric Oxide*. Royal Society of Chemistry, Cambridge.
- Bystrykh, L.V., M.A. Fernandez-Moreno, J.K. Herrema, F. Malpartida, D.A. Hopwood & L. Dijkhuizen, (1996) Production of Actinorhodin-Related "Blue Pigments" by *Streptomyces coelicolor* A3(2) *Journal of Bacteriology* **178**: 2238-2244
- Chandra, G. & K.F. Chater, (2013) Developmental biology of *Streptomyces* from the perspective of 100 actinobacterial genome sequences. *FEMS Microbiol Rev* **38**: 345-379.
- Chandramouli, K. & M.K. Johnson, (2006) HscA and HscB stimulate [2Fe-2S] cluster transfer from IscU to apoferredoxin in an ATP-dependent reaction. *Biochemistry* **45**: 11087-11095.
- Chater, K.F., (1999) Developmental decisions during sporulation in the aerial mycelium in *Streptomyces*. In: Prokaryotic development. Y.V.a.S. Brun, L.J. (ed). Washington, D.C.: ASM Press, pp. 33-48.
- Chater, K.F., S. Biró, K.J. Lee, T. Palmer & H. Schrempf, (2009) The complex extracellular biology of *Streptomyces*. *FEMS Microbiology Reviews* **34**: 171 - 198.

- Chater, K.F., C.J. Bruton, K.A. Plaskitt, M.J. Buttner, C. Mendez & J.D. Helmann, (1989) The developmental fate of *S. coelicolor* hyphae depends upon a gene product homologous with the motility sigma factor of *B. subtilis*. *Cell* **59**: 133-143.
- Chater, K.F. & G. Chandra, (2006) The evolution of development in *Streptomyces* analysed by genome comparisons. *FEMS Microbiol Rev* **30**: 651-672.
- Chater, K.F. & R. Losick, (1997) Mycelial life style of *Streptomyces coelicolor* A3(2) and its relatives. In: *Bacteria as multicellular organisms*. J.A.a.D. Shapiro, M. (ed). New York, N.Y.: Oxford university press, pp. 149-182.
- Choi, P.S., Z. Naal, C. Moore, E. Casado-Rivera, H.D. Abruna, J.D. Helmann & J.P. Shapleigh, (2006) Assessing the impact of denitrifier-produced nitric oxide on other bacteria. *Appl Environ Microbiol* **72**: 2200-2205.
- Claessen, D., W. de Jong, L. Dijkhuizen & H.A. Wosten, (2006) Regulation of *Streptomyces* development: reach for the sky! *Trends Microbiol* **14**: 313-319.
- Claessen, D., H.A. Wosten, G. van Keulen, O.G. Faber, A.M. Alves, W.G. Meijer & L. Dijkhuizen, (2002) Two novel homologous proteins of *Streptomyces coelicolor* and *Streptomyces lividans* are involved in the formation of the rodlet layer and mediate attachment to a hydrophobic surface. *Mol Microbiol* **44**: 1483-1492.
- Cole, S.T., R. Brosch, J. Parkhill, T. Garnier, C. Churcher, D. Harris, S.V. Gordon, K. Eiglmeier, S. Gas, C.E. Barry, 3rd, F. Tekaia, K. Badcock, D. Basham, D. Brown, T. Chillingworth, R. Connor, R. Davies, K. Devlin, T. Felwell, S. Gentles, N. Hamlin, S. Holroyd, T. Hornsby, K. Jagels, A. Krogh, J. McLean, S. Moule, L. Murphy, K. Oliver, J. Osborne, M.A. Quail, M.A. Rajandream, J. Rogers, S. Rutter, K. Seeger, J. Skelton, R. Squares, S. Squares, J.E. Sulston, K. Taylor, S. Whitehead & B.G. Barrell, (1998) Deciphering the biology of *Mycobacterium tuberculosis* from the complete genome sequence. *Nature* **393**: 537-544.
- Cole, S.T., K. Eiglmeier, J. Parkhill, K.D. James, N.R. Thomson, P.R. Wheeler, N. Honore, T. Garnier, C. Churcher, D. Harris, K. Mungall, D. Basham, D. Brown, T. Chillingworth, R. Connor, R.M. Davies, K. Devlin, S. Duthoy, T. Felwell, A. Fraser, N. Hamlin, S. Holroyd, T. Hornsby, K. Jagels, C. Lacroix, J. Maclean, S. Moule, L. Murphy, K. Oliver, M.A. Quail, M.A. Rajandream, K.M. Rutherford, S. Rutter, K. Seeger, S. Simon, M. Simmonds, J. Skelton, R. Squares, S. Squares, K. Stevens, K. Taylor, S. Whitehead, J.R. Woodward & B.G. Barrell, (2001) Massive gene decay in the leprosy bacillus. *Nature* **409**: 1007-1011.
- Cosma, C.L., D.R. Sherman & L. Ramakrishnan, (2003) The secret lives of the pathogenic mycobacteria. *Annual review of microbiology* **57**: 641-676.
- Crack, J.C., C.D. den Hengst, P. Jakimowicz, S. Subramanian, M.K. Johnson, M.J. Buttner, A.J. Thomson & N.E. Le Brun, (2009) Characterization of [4Fe-4S]-Containing and Cluster-Free Forms of *Streptomyces* WhiD. *Biochemistry* **48**: 12252-12264.
- Crack, J.C., A.A. Gaskell, J. Green, M.R. Cheesmant, N.E. Le Brun & A.J. Thomson, (2008) Influence of the environment on the [4Fe-4S](2+) to [2Fe-2S](2+) cluster switch in the transcriptional regulator FNR. *Journal of the American Chemical Society* **130**: 1749-1758.
- Crack, J.C., J. Green, M.I. Hutchings, A.J. Thomson & N.E. Le Brun, (2012) Bacterial iron-sulfur regulatory proteins as biological sensor-switches. *Antioxidants & redox signaling* **17**: 1215-1231.
- Crack, J.C., L.J. Smith, M.R. Stapleton, J. Peck, N.J. Watmough, M.J. Buttner, R.S. Buxton, J. Green, V.S. Oganessian, A.J. Thomson & N.E. Le Brun, (2011) Mechanistic insight into the nitrosylation of the [4Fe-4S] cluster of WhiB-like proteins. *J Am Chem Soc* **133**: 1112-1121.
- Crane, B.R., J. Sudhamsu & B.A. Patel, (2010) Bacterial Nitric Oxide Synthases. *Annu. Rev. Biochem* **79**: 445-470.

- Crawford, M.J. & D.E. Goldberg, (1998) Role for the Salmonella flavohemoglobin in protection from nitric oxide. *Journal of Biological Chemistry* **273**: 12543-12547.
- Curcic, R., S. Dhandayuthapani & V. Deretic, (1994) Gene expression in mycobacteria: transcriptional fusions based on xylE and analysis of the promoter region of the response regulator mtrA from Mycobacterium tuberculosis. *Mol Microbiol* **13**: 1057-1064.
- Davis, N.K. & K.F. Chater, (1990) Spore colour in Streptomyces coelicolor A3(2) involves the developmentally regulated synthesis of a compound biosynthetically related to polyketide antibiotics. *Mol Microbiol* **4**: 1679-1691.
- den Hengst, C.D. & M.J. Buttner, (2008) Redox control in actinobacteria. *Biochim Biophys Acta* **1780**: 1201-1216.
- Ditkowski, B., N. Holmes, J. Rydzak, M. Donczew, M. Bezulska, K. Ginda, P. Kedzierski, J. Zakrzewska-Czerwinska, G.H. Kelemen & D. Jakimowicz, (2013) Dynamic interplay of ParA with the polarity protein, Scy, coordinates the growth with chromosome segregation in Streptomyces coelicolor. *Open biology* **3**: 130006.
- Donadio, S., M. Sosio & G. Lancini, (2002) Impact of the first Streptomyces genome sequence on the discovery and production of bioactive substances. *Appl Microbiol Biotechnol* **60**: 377-380.
- Errington, J., R.A. Daniel & D.J. Scheffers, (2003) Cytokinesis in bacteria. *Microbiol Mol Biol Rev* **67**: 52-65.
- Fang, F.C., (2004) Antimicrobial reactive oxygen and nitrogen species: Concepts and controversies. *Nature Reviews Microbiology* **2**: 820-832.
- Feitelson, J.S., F. Malpartida & D.A. Hopwood, (1985) Genetic and biochemical characterization of the red gene cluster of Streptomyces coelicolor A3(2). *Journal of general microbiology* **131**: 2431-2441.
- Fileenko, N., S. Spiro, D.F. Browning, D. Squire, T.W. Overton, J. Cole & C. Constantinidou, (2007) The NsrR regulon of Escherichia coli K-12 includes genes encoding the hybrid cluster protein and the periplasmic, respiratory nitrite reductase. *J Bacteriol* **189**: 4410-4417.
- Flårdh, K., E. Leibovitz, M.J. Buttner & K.F. Chater, (2000) Generation of a non-sporulating strain of Streptomyces coelicolor A3(2) by the manipulation of a developmentally controlled ftsZ promoter. *Mol Microbiol* **38**: 737-749.
- Flatley, J., J. Barrett, S.T. Pullan, M.N. Hughes, J. Green & R.K. Poole, (2005) Transcriptional responses of Escherichia coli to S-nitrosoglutathione under defined chemostat conditions reveal major changes in methionine biosynthesis. *Journal of Biological Chemistry* **280**: 10065-10072.
- Fleischhacker, A.S., A. Stubna, K.L. Hsueh, Y. Guo, S.J. Teter, J.C. Rose, T.C. Brunold, J.L. Markley, E. Munck & P.J. Kiley, (2012) Characterization of the [2Fe-2S] cluster of Escherichia coli transcription factor IscR. *Biochemistry* **51**: 4453-4462.
- Flårdh, K., (2010) Cell polarity and the control of apical growth in Streptomyces. *Curr Opin Microbiol* **13**: 758-765.
- Flårdh, K. & M.J. Buttner, (2009) Streptomyces morphogenetics: dissecting differentiation in a filamentous bacterium. *Nature Reviews Microbiology* **7**: 36-49.
- Flårdh, K., K.C. Findlay & K.F. Chater, (1999) Association of early sporulation genes with suggested developmental decision points in Streptomyces coelicolor A3(2). *Microbiology* **145 (Pt 9)**: 2229-2243.
- Flårdh, K., E. Leibovitz, M.J. Buttner & K.F. Chater, (2000) Generation of a non-sporulating strain of Streptomyces coelicolor A3(2) by the manipulation of a developmentally controlled ftsZ promoter. *Molecular Microbiology* **38**: 737-749.
- Flårdh, K. & G.P. van Wezel, (2003) Cell division during growth and development in Streptomyces. *Recent Res. Dev. Bacteriol.* **1**: 71-90.

- Fol, M., A. Chauhan, N.K. Nair, E. Maloney, M. Moomey, C. Jagannath, M.V. Madiraju & M. Rajagopalan, (2006) Modulation of Mycobacterium tuberculosis proliferation by MtrA, an essential two-component response regulator. *Mol Microbiol* **60**: 643-657.
- Fontecave, M. & S. Ollagnier-De-Choudens, (2008) Iron-sulfur cluster biosynthesis in bacteria: Mechanisms of cluster assembly and transfer. *Archives of Biochemistry and Biophysics* **474**: 226-237.
- Fowler-Goldsworthy, K., B. Gust, S. Mouz, G. Chandra, K.C. Findlay & K.F. Chater, (2011) The actinobacteria-specific gene wblA controls major developmental transitions in *Streptomyces coelicolor* A3(2). *Microbiology* **157**: 1312–1328.
- Friedland, N., T.R. Mack, M. Yu, L.W. Hung, T.C. Terwilliger, G.S. Waldo & A.M. Stock, (2007) Domain orientation in the inactive response regulator Mycobacterium tuberculosis MtrA provides a barrier to activation. *Biochemistry* **46**: 6733-6743.
- Fukuchi, K., Y. Kasahara, K. Asai, K. Kobayashi, S. Moriya & N. Ogasawara, (2000) The essential two-component regulatory system encoded by yycF and yycG modulates expression of the ftsAZ operon in *Bacillus subtilis*. *Microbiology* **146 (Pt 7)**: 1573-1583.
- Fukushima, T., H. Szurmant, E.J. Kim, M. Perego & J.A. Hoch, (2008) A sensor histidine kinase co-ordinates cell wall architecture with cell division in *Bacillus subtilis*. *Mol Microbiol* **69**: 621-632.
- Fuqua, C., M.R. Parsek & E.P. Greenberg, (2001) Regulation of gene expression by cell-to-cell communication: acyl-homoserine lactone quorum sensing. *Annual review of genetics* **35**: 439-468.
- Galperin, M.Y., (2006) Structural Classification of Bacterial Response Regulators: Diversity of Output Domains and Domain Combinations. *Journal of Bacteriology* **188**: 4169-4182.
- Gao, R., T. Mack & A.M. Stock, (2007) Bacterial response regulators: versatile regulatory strategies from common domains. *Trends in Biochemical Sciences* **32**: 225-234.
- Gardner, P.R., A.M. Gardner, L.A. Martin & A.L. Salzman, (1998) Nitric oxide dioxygenase: an enzymic function for flavohemoglobin. *Proc Natl Acad Sci U S A* **95**: 10378-10383.
- Giel, J.L., A.D. Nesbit, E.L. Mettert, A.S. Fleischhacker, B.T. Wanta & P.J. Kiley, (2013) Regulation of iron-sulphur cluster homeostasis through transcriptional control of the Isc pathway by [2Fe-2S]-IscR in *Escherichia coli*. *Mol Microbiol* **87**: 478-492.
- Giel, J.L., D. Rodionov, M. Liu, F.R. Blattner & P.J. Kiley, (2006) IscR-dependent gene expression links iron-sulphur cluster assembly to the control of O₂-regulated genes in *Escherichia coli*. *Mol Microbiol* **60**: 1058-1075.
- Gilberthorpe, N.J., M.E. Lee, T.M. Stevanin, R.C. Read & R.K. Poole, (2007) NsrR: a key regulator circumventing *Salmonella enterica* serovar Typhimurium oxidative and nitrosative stress in vitro and in IFN-gamma-stimulated J774.2 macrophages. *Microbiology* **153**: 1756-1771.
- Gomez-Escribano, J.P.S., L. Fox, D. J. Yeo, V. Bibb, M. J. and Challis, G.L. , (2012) Structure and biosynthesis of the unusual polyketide alkaloid coelimycin P1, a metabolic product of the cpk gene cluster of *Streptomyces coelicolor* M145. *Chemical Science* **3**: 2716-2720.
- Gottelt, M., S. Kol, J.P. Gomez-Escribano, M. Bibb & E. Takano, (2010) Deletion of a regulatory gene within the cpk gene cluster reveals novel antibacterial activity in *Streptomyces coelicolor* A3(2). *Microbiology* **156**: 2343-2353.
- Grantcharova, N., U. Lustig & K. Flärdh, (2005) Dynamics of FtsZ assembly during sporulation in *Streptomyces coelicolor* A3(2). *J Bacteriol* **187**: 3227-3237.
- Grantcharova, N., W. Ubhayasekera, S.L. Mowbray, J.R. McCormick & K. Flärdh, (2003) A missense mutation in ftsZ differentially affects vegetative and developmentally

- controlled cell division in *Streptomyces coelicolor* A3(2). *Mol Microbiol* **47**: 645-656.
- Grebe, T.W. & J.B. Stock, (1999) The histidine protein kinase superfamily. *Advances in microbial physiology* **41**: 139-227.
- Greendyke, R., M. Rajagopalan, T. Parish & M.V. Madiraju, (2002) Conditional expression of *Mycobacterium smegmatis* dnaA, an essential DNA replication gene. *Microbiology* **148**: 3887-3900.
- Gregory, M.A., R. Till & M.C. Smith, (2003) Integration site for *Streptomyces* phage phiBT1 and development of site-specific integrating vectors. *J Bacteriol* **185**: 5320-5323.
- Grosset, J., (2003) *Mycobacterium tuberculosis* in the extracellular compartment: an underestimated adversary. *Antimicrob Agents Chemother* **47**: 833-836.
- Gusarov, I., M. Starodubtseva, Z.Q. Wang, L. McQuade, S.J. Lippard, D.J. Stuehr & E. Nudler, (2008) Bacterial nitric-oxide Synthases operate without a dedicated redox partner. *Journal of Biological Chemistry* **283**: 13140-13147.
- Gushchin, I., V. Gordeliy & S. Grudinin, (2013) Two distinct states of the HAMP domain from sensory rhodopsin transducer observed in unbiased molecular dynamics simulations. *PLoS One* **8**: e66917.
- Gust, B., T. Kieser & K. Chater, (2002) *PCR targeting system in Streptomyces coelicolor* A3(2). John Innes Centre, Norwich Research Park, Colney, Norwich, NR47UH.
- Hakenbeck, R. & J.B. Stock, (1996) Analysis of Two-Component Signal Transduction Systems Involved in Transcriptional Regulation. *Methods in Enzymology* **273**: 281-300.
- Hanahan, D., (1983) Studies on transformation of *Escherichia coli* with plasmids. *J Mol Biol* **166**: 557-580.
- Heichlinger, A., M. Ammelburg, E.M. Kleinschnitz, A. Latus, I. Maldener, K. Flärdh, W. Wohlleben & G. Muth, (2011) The MreB-like protein Mbl of *Streptomyces coelicolor* A3(2) depends on MreB for proper localization and contributes to spore wall synthesis. *J Bacteriol* **193**: 1533-1542.
- Hempel, A.M., S. Cantlay, V. Molle, S.B. Wang, M.J. Naldrett, J.L. Parker, D.M. Richards, Y.G. Jung, M.J. Buttner & K. Flärdh, (2012) The Ser/Thr protein kinase AfsK regulates polar growth and hyphal branching in the filamentous bacteria *Streptomyces*. *Proc Natl Acad Sci U S A* **109**: E2371-2379.
- Hempel, A.M., S.B. Wang, M. Letek, J.A. Gil & K. Flärdh, (2008) Assemblies of DivIVA mark sites for hyphal branching and can establish new zones of cell wall growth in *Streptomyces coelicolor*. *J Bacteriol* **190**: 7579-7583.
- Henares, B., S. Kommineni, O. Chumsakul, N. Ogasawara, S. Ishikawa & M.M. Nakano, (2014) The ResD Response Regulator, through Functional Interaction with NsrR and Fur, Plays Three Distinct Roles in *Bacillus subtilis* Transcriptional Control. *J Bacteriol* **196**: 493-503.
- Heurlier, K., M.J. Thomson, N. Aziz & J.W.B. Moir, (2008) The nitric oxide (NO)-Sensing repressor NsrR of *Neisseria meningitidis* has a compact regulon of genes involved in NO synthesis and detoxification. *Journal of Bacteriology* **190**: 2488-2495.
- Hewitson, K.S., J.E. Baldwin, N.M. Shaw & P.L. Roach, (2000) Mutagenesis of the proposed iron-sulfur cluster binding ligands in *Escherichia coli* biotin synthase. *Febs Letters* **466**: 372-376.
- Hoch, J.A. & T.J. Silhavy, (1995) Two-Component Signal Transduction. In.: American Society for Microbiology Press, pp.
- Hodgson, D.A., (2000) Primary metabolism and its control in streptomycetes: a most unusual group of bacteria. *Advances in microbial physiology* **42**: 47-238.
- Holmes, N.A., J. Walshaw, R.M. Leggett, A. Thibessard, K.A. Dalton, M.D. Gillespie, A.M. Hemmings, B. Gust & G.H. Kelemen, (2013) Coiled-coil protein Scy is a key

- component of a multiprotein assembly controlling polarized growth in *Streptomyces*. *Proc Natl Acad Sci U S A* **110**: E397-406.
- Hong, H.J., M.I. Hutchings, J.M. Neu, G.D. Wright, M.S. Paget & M.J. Buttner, (2004) Characterization of an inducible vancomycin resistance system in *Streptomyces coelicolor* reveals a novel gene (*vanK*) required for drug resistance. *Mol Microbiol* **52**: 1107-1121.
- Hopwood, D.A., (2007a) How do antibiotic-producing bacteria ensure their self-resistance before antibiotic biosynthesis incapacitates them? *Mol Microbiol* **63**: 937-940.
- Hopwood, D.A., (2007b) *Streptomyces*. In: Nature and Medicine. New York: Oxford University Press, pp.
- Hopwood, D.A., M. Bibb, K. Chater, K. T, C.J. Bruton, H. Kieser, D.J. Lydiate, C.P. Smith, J.M. Ward & H. Schrempf, (1985) *Genetic Manipulation of Streptomyces. A Laboratory Manual*. John Innes Foundation, Norwich.
- Hoskisson, P.A. & M.I. Hutchings, (2006) MtrAB-LpqB: a conserved three-component system in actinobacteria? *Trends Microbiol* **14**: 444-449.
- Hutchings, M.I., J.C. Crack, N. Shearer, B.J. Thompson, A.J. Thomson & S. Spiro, (2002) Transcription Factor FnrP from *Paracoccus denitrificans* Contains an Iron-Sulfur Cluster and Is Activated by Anoxia: Identification of Essential Cysteine Residues. *JOURNAL OF BACTERIOLOGY* **184**: 503–508.
- Hutchings, M.I., P.A. Hoskisson, G. Chandra & M.J. Buttner, (2004) Sensing and responding to diverse extracellular signals? Analysis of the sensor kinases and response regulators of *Streptomyces coelicolor* A3(2). *Microbiology* **150**: 2795–2806.
- Hutchings, M.I., T. Palmer, D.J. Harrington & I.C. Sutcliffe, (2009) Lipoprotein biogenesis in Gram-positive bacteria: knowing when to hold 'em, knowing when to fold 'em. *Trends Microbiol* **17**: 13-21.
- Imlay, J.A., (2006) Iron-sulphur clusters and the problem with oxygen. *Mol Microbiol* **59**: 1073-1082.
- Imlay, J.A., (2008) Cellular defenses against superoxide and hydrogen peroxide. *Annu Rev Biochem* **77**: 755-776.
- Isabella, V.M., J.D. Lapek, Jr., E.M. Kennedy & V.L. Clark, (2009) Functional analysis of NsrR, a nitric oxide-sensing Rrf2 repressor in *Neisseria gonorrhoeae*. *Mol Microbiol* **71**: 227-239.
- Jakimowicz, D., K. Chater & J. Zakrzewska-Czerwinska, (2002) The ParB protein of *Streptomyces coelicolor* A3(2) recognizes a cluster of *parS* sequences within the origin-proximal region of the linear chromosome. *Mol Microbiol* **45**: 1365-1377.
- Jakimowicz, D. & G.P. van Wezel, (2012) Cell division and DNA segregation in *Streptomyces*: how to build a septum in the middle of nowhere? *Mol Microbiol* **85**: 393-404.
- Jakimowicz, D., P. Zydek, A. Kois, J. Zakrzewska-Czerwinska & K.F. Chater, (2007) Alignment of multiple chromosomes along helical ParA scaffolding in sporulating *Streptomyces* hyphae. *Mol Microbiol* **65**: 625-641.
- Jakimowicz, P., M.R. Cheesman, W.R. Bishai, K.F. Chater, A.J. Thomson & M.J. Buttner, (2005) Evidence That the *Streptomyces* Developmental Protein WhiD, a Member of the WhiB Family, Binds a [4Fe-4S] Cluster. *THE JOURNAL OF BIOLOGICAL CHEMISTRY* **280**: 8309–8315.
- Johnson, D.C., D.R. Dean, A.D. Smith & M.K. Johnson, (2005) Structure, function, and formation of biological iron-sulfur clusters. *Annual Review of Biochemistry* **74**: 247-281.
- Johnson, M.K., (1994) *Encyclopedia of Inorganic Chemistry*. Wiley, New York.
- Johnston, A.W.B., J.D. Todd, A.R. Curson, S. Lei, N. Nikolaidou-Katsaridou, M.S. Gelfand & D.A. Rodionov, (2007) Living without Fur: the subtlety and complexity of iron-

- responsive gene regulation in the symbiotic bacterium *Rhizobium* and other alpha-proteobacteria. *Biometals* **20**: 501-511.
- Jones-Carson, J., J. Laughlin, M.A. Hamad, A.L. Stewart, M.I. Voskuil & A. Va'zquez-Torres, (2008) Inactivation of [Fe-S] Metalloproteins Mediates Nitric Oxide-Dependent Killing of *Burkholderia mallei*. *PLoS ONE* **3**: e1976.
- Joshi, M., X. Rong, S. Moll, J. Kers, C. Franco & R. Loria, (2007) *Streptomyces turgidiscabies* secretes a novel virulence protein, Nec1, which facilitates infection. *Molecular plant-microbe interactions : MPMI* **20**: 599-608.
- Justino, M.C., J.B. Vicente, M. Teixeira & L.M. Saraiva, (2005) New genes implicated in the protection of anaerobically grown *Escherichia coli* against nitric oxide. *Journal of Biological Chemistry* **280**: 2636-2643.
- Jyothikumar, V., E.J. Tilley, R. Wali & P.R. Herron, (2008) Time-lapse microscopy of *Streptomyces coelicolor* growth and sporulation. *Appl Environ Microbiol* **74**: 6774-6781.
- Kanamaru, K., H. Aiba, S. Mizushima & T. Mizuno, (1989) Signal transduction and osmoregulation in *Escherichia coli*. A single amino acid change in the protein kinase, EnvZ, results in loss of its phosphorylation and dephosphorylation abilities with respect to the activator protein, OmpR. *J Biol Chem* **264**: 21633-21637.
- Karrasch, S., D. Typke, T. Walz, M. Miller, G. Tsiotis & A. Engel, (1996) Highly ordered two-dimensional crystals of photosystem I reaction center from *Synechococcus* sp: Functional and structural analyses. *Journal of Molecular Biology* **262**: 336-348.
- Kaufmann, S.H. & A.J. McMichael, (2005) Annulling a dangerous liaison: vaccination strategies against AIDS and tuberculosis. *Nature medicine* **11**: S33-44.
- Kawamoto, S., H. Watanabe, A. Hesketh, J.C. Ensign & K. Ochi, (1997) Expression analysis of the *ssgA* gene product, associated with sporulation and cell division in *Streptomyces griseus*. *Microbiology* **143 (Pt 4)**: 1077-1086.
- Keon, R.G., R.D. Fu & G. Voordouw, (1997) Deletion of two downstream genes alters expression of the *hmc* operon of *Desulfovibrio vulgaris* subsp. *vulgaris* Hildenborough. *Archives of Microbiology* **167**: 376-383.
- Kers, J.A., K.D. Cameron, M.V. Joshi, R.A. Bukhalid, J.E. Morello, M.J. Wach, D.M. Gibson & R. Loria, (2005) A large, mobile pathogenicity island confers plant pathogenicity on *Streptomyces* species. *Mol Microbiol* **55**: 1025-1033.
- Kieser, T., M. Bibb, M. Buttner, K. Chater & D.A. Hopwood, (2000) *Practical Streptomyces Genetics*. The John Innes Foundation.
- Kindt, T.J., R.A. Goldsby & B.A. Osbourne, (2007) Immune response to infectious diseases In: *Immunology*.: W.H. Freeman and Company, pp.
- Kleinschnitz, E.M., A. Heichlinger, K. Schirner, J. Winkler, A. Latus, I. Maldener, W. Wohlleben & G. Muth, (2011) Proteins encoded by the *mre* gene cluster in *Streptomyces coelicolor* A3(2) cooperate in spore wall synthesis. *Mol Microbiol* **79**: 1367-1379.
- Kommineni, S., A. Lama, B. Popescu & M.M. Nakano, (2012) Global Transcriptional Control by NsrR in *Bacillus subtilis*. *Journal of Bacteriology* **194**: 1679-1688.
- Kommineni, S., E. Yukl, T. Hayashi, J. Delepine, H. Geng, P. Moënne-Loccoz & M.M. Nakano, (2010) Nitric oxide-sensitive and -insensitive interaction of *Bacillus subtilis* NsrR with a ResDE-controlled promoter. *Mol Microbiol* **78**: 1280-1293.
- Koretke, K.K., A.N. Lupas, P.V. Warren, M. Rosenberg & J.R. Brown, (2000) Evolution of two-component signal transduction. *Molecular biology and evolution* **17**: 1956-1970.
- Kramer, R., (2009) Osmosensing and osmosignaling in *Corynebacterium glutamicum*. *Amino acids* **37**: 487-497.
- Kwak, J., A.J. Dharmatilake, H. Jiang & K.E. Kendrick, (2001) Differential regulation of *ftsZ* transcription during septation of *Streptomyces griseus*. *J Bacteriol* **183**: 5092-5101.

- Labeda, D.P., (2011) Multilocus sequence analysis of phytopathogenic species of the genus *Streptomyces*. *International journal of systematic and evolutionary microbiology* **61**: 2525-2531.
- Lee, K.C., W.S. Yeo & J.H. Roe, (2008) Oxidant-responsive induction of the suf operon, encoding a Fe-S assembly system, through Fur and IscR in *Escherichia coli*. *J Bacteriol* **190**: 8244-8247.
- Leonard, T.A., P.J. Butler & J. Lowe, (2005a) Bacterial chromosome segregation: structure and DNA binding of the Soj dimer--a conserved biological switch. *The EMBO journal* **24**: 270-282.
- Leonard, T.A., J. Moller-Jensen & J. Lowe, (2005b) Towards understanding the molecular basis of bacterial DNA segregation. *Philosophical transactions of the Royal Society of London. Series B, Biological sciences* **360**: 523-535.
- Letek, M., M. Fiuza, E. Ordonez, A.F. Villadangos, K. Flårdh, L.M. Mateos & J.A. Gil, (2009) DivIVA uses an N-terminal conserved region and two coiled-coil domains to localize and sustain the polar growth in *Corynebacterium glutamicum*. *FEMS Microbiol Lett* **297**: 110-116.
- Li, Y., J. Zeng & Z.G. He, (2010a) Characterization of a functional C-terminus of the *Mycobacterium tuberculosis* MtrA responsible for both DNA binding and interaction with its two-component partner protein, MtrB. *J Biochem* **148**: 549-556.
- Li, Y., J. Zeng, H. Zhang & Z.-G. He, (2010b) The characterization of conserved binding motifs and potential target genes for *M. tuberculosis* MtrAB reveals a link between the two-component system and the drug resistance of *M. smegmatis*. *BMC Microbiology* **10**.
- Lill, R., (2009) Function and biogenesis of iron-sulphur proteins. *Nature* **460**: 831-838.
- Loiseau, L., S. Ollagnier-de-Choudens, L. Nachin, M. Fontecave & F. Barras, (2003) Biogenesis of Fe-S cluster by the bacterial Suf system: SufS and SufE form a new type of cysteine desulfurase. *J Biol Chem* **278**: 38352-38359.
- Loria, R., J. Kers & M. Joshi, (2006) Evolution of plant pathogenicity in *Streptomyces*. *Annual review of phytopathology* **44**: 469-487.
- Lovenburg, W., (1973) *Iron-Sulphur cluster proteins*. Academic Press, New York.
- Luti, K.J. & F. Mavituna, (2011) Elicitation of *Streptomyces coelicolor* with dead cells of *Bacillus subtilis* and *Staphylococcus aureus* in a bioreactor increases production of undecylprodigiosin. *Appl Microbiol Biotechnol* **90**: 461-466.
- Lutkenhaus, J. & S.G. Addinall, (1997) Bacterial cell division and the Z ring. *Annu Rev Biochem* **66**: 93-116.
- MacNeil, D.J., K.M. Gewain, C.L. Ruby, G. Dezeny, P.H. Gibbons & T. MacNeil, (1992) Analysis of *Streptomyces avermitilis* genes required for avermectin biosynthesis utilizing a novel integration vector. *Gene* **111**: 61-68.
- Madigan, M.T. & J.M. Martinko, (2006) *Person-To-Person Microbial Diseases* In: Brock Biology Of Microorganisms. . Pearson Prentice Hall, pp.
- Margolin, W., (2000) Themes and variations in prokaryotic cell division. *FEMS Microbiol Rev* **24**: 531-548.
- Martins, B.M., H. Dobbek, I. Cinkaya, W. Buckel & A. Messerschmidt, (2004) Crystal structure of 4-hydroxybutyryl-CoA dehydratase: Radical catalysis involving a [4Fe-4S] cluster and flavin. *Proceedings of the National Academy of Sciences of the United States of America* **101**: 15645-15649.
- Mazza, P., E.E. Noens, K. Schirner, N. Grantcharova, A.M. Mommaas, H.K. Koerten, G. Muth, K. Flårdh, G.P. van Wezel & W. Wohlleben, (2006) MreB of *Streptomyces coelicolor* is not essential for vegetative growth but is required for the integrity of aerial hyphae and spores. *Mol Microbiol* **60**: 838-852.

- McCormick, J.R. & K. Flärdh, (2012) Signals and regulators that govern *Streptomyces* development. *FEMS Microbiol Rev* **36**: 206-231.
- McCormick, J.R., E.P. Su, A. Driks & R. Losick, (1994) Growth and viability of *Streptomyces coelicolor* mutant for the cell division gene *ftsZ*. *Mol Microbiol* **14**: 243-254.
- Membrillo-Hernandez, J., M.D. Coopamah, M.F. Anjum, T.M. Stevanin, A. Kelly, M.N. Hughes & R.K. Poole, (1999) The flavohemoglobin of *Escherichia coli* confers resistance to a nitrosating agent, a "nitric oxide releaser," and paraquat and is essential for transcriptional responses to oxidative stress. *Journal of Biological Chemistry* **274**: 748-754.
- Meyer, J., (2008) Iron-sulfur protein folds, iron-sulfur chemistry, and evolution. *Journal of Biological Inorganic Chemistry* **13**: 157-170.
- Migueluez, E.M., C. Hardisson & M.B. Manzanal, (1999) Hyphal death during colony development in *Streptomyces antibioticus*: Morphological evidence for the existence of a process of cell deletion in a multicellular prokaryote. *Journal of Cell Biology* **145**: 515-525.
- Möker, N., M. Brocker, S. Schaffer, R. Kramer, S. Morbach & M. Bott, (2004) Deletion of the genes encoding the MtrA-MtrB two-component system of *Corynebacterium glutamicum* has a strong influence on cell morphology, antibiotics susceptibility and expression of genes involved in osmoprotection. *Mol Microbiol* **54**: 420-438.
- Möker, N., J. Kramer, G. Uden, R. Kramer & S. Morbach, (2007a) In vitro analysis of the two-component system MtrB-MtrA from *Corynebacterium glutamicum*. *J Bacteriol* **189**: 3645-3649.
- Möker, N., P. Reihlen, R. Kramer & S. Morbach, (2007b) Osmosensing properties of the histidine protein kinase MtrB from *Corynebacterium glutamicum*. *J Biol Chem* **282**: 27666-27677.
- Molle, V., W.J. Palframan, K.C. Findlay & M.J. Buttner, (2000) WhiD and WhiB, homologous proteins required for different stages of sporulation in *Streptomyces coelicolor* A3(2). *J Bacteriol* **182**: 1286-1295.
- Morris, R.P., L. Nguyen, J. Gatfield, K. Visconti, K. Nguyen, D. Schnappinger, S. Ehrt, Y. Liu, L. Heifets, J. Pieters, G. Schoolnik & C.J. Thompson, (2005) Ancestral antibiotic resistance in *Mycobacterium tuberculosis*. *Proc Natl Acad Sci U S A* **102**: 12200-12205.
- Moseley, J.B. & B.L. Goode, (2006) The yeast actin cytoskeleton: from cellular function to biochemical mechanism. *Microbiol Mol Biol Rev* **70**: 605-645.
- Mukhopadhyay, P., M. Zheng, L.A. Bedzyk, R.A. LaRossa & G. Storz, (2004) Prominent roles of the NorR and Fur regulators in the *Escherichia coli* transcriptional response to reactive nitrogen species. *Proceedings of the National Academy of Sciences of the United States of America* **101**: 745-750.
- Myronovskyi, M., E. Welle, V. Fedorenko & A. Luzhetskyy, (2011) Beta-glucuronidase as a sensitive and versatile reporter in actinomycetes. *Appl Environ Microbiol* **77**: 5370-5383.
- Nachin, L., L. Loiseau, D. Expert & F. Barras, (2003) SufC: an unorthodox cytoplasmic ABC/ATPase required for [Fe-S] biogenesis under oxidative stress. *The EMBO journal* **22**: 427-437.
- Nesbit, A.D., J.L. Giel, J.C. Rose & P.J. Kiley, (2009) Sequence-specific binding to a subset of IscR-regulated promoters does not require IscR Fe-S cluster ligation. *J Mol Biol* **387**: 28-41.
- Nguyen, H.T., K.A. Wolff, R.H. Cartabuke, S. Ogwang & L. Nguyen, (2010) A lipoprotein modulates activity of the MtrAB two-component system to provide intrinsic multidrug resistance, cytokinetic control and cell wall homeostasis in *Mycobacterium*. *Mol Microbiol* **76**: 348-364.

- Nielsen, J.B. & J.O. Lampen, (1982) Glyceride-cysteine lipoproteins and secretion by Gram-positive bacteria. *J Bacteriol* **152**: 315-322.
- Noens, E.E., V. Mersinias, J. Willemsse, B.A. Traag, E. Laing, K.F. Chater, C.P. Smith, H.K. Koerten & G.P. van Wezel, (2007) Loss of the controlled localization of growth stage-specific cell-wall synthesis pleiotropically affects developmental gene expression in an *ssgA* mutant of *Streptomyces coelicolor*. *Mol Microbiol* **64**: 1244-1259.
- Nowak, E., S. Panjikar, P. Konarev, D.I. Svergun & P.A. Tucker, (2006) The structural basis of signal transduction for the response regulator PrrA from *Mycobacterium tuberculosis*. *J Biol Chem* **281**: 9659-9666.
- Ollagnier-de Choudens, S., Y. Sanakis, K.S. Hewitson, P. Roach, J.E. Baldwin, E. Munck & M. Fontecave, (2000) Iron-sulfur center of biotin synthase and lipoate synthase. *Biochemistry* **39**: 4165-4173.
- Outten, F.W., O. Djaman & G. Storz, (2004) A *suf* operon requirement for Fe-S cluster assembly during iron starvation in *Escherichia coli*. *Mol Microbiol* **52**: 861-872.
- Outten, F.W., M.J. Wood, F.M. Munoz & G. Storz, (2003) The SufE protein and the SufBCD complex enhance SufS cysteine desulfurase activity as part of a sulfur transfer pathway for Fe-S cluster assembly in *Escherichia coli*. *J Biol Chem* **278**: 45713-45719.
- Overton, T.W., R. Whitehead, Y. Li, L.A.S. Snyder, N.J. Saunders, H. Smith & J.A. Cole, (2006) Coordinated regulation of the *Neisseria gonorrhoeae*-truncated denitrification pathway by the nitric oxide-sensitive repressor, NsrR, and nitrite-insensitive NarQ-NarP. *Journal of Biological Chemistry* **281**: 33115-33126.
- Parkinson, J.S., (2010) Signaling mechanisms of HAMP domains in chemoreceptors and sensor kinases. *Annual review of microbiology* **64**: 101-122.
- Partridge, J.D., D.M. Bodenmiller, M.S. Humphrys & S. Spiro, (2009) NsrR targets in the *Escherichia coli* genome: new insights into DNA sequence requirements for binding and a role for NsrR in the regulation of motility. *Mol Microbiol* **73**: 680-694.
- Payne, W.J., (1983) Bacterial denitrification: asset or defect. *Bioscience* **33**: 319-325.
- Perego, M. & J.A. Hoch, (1996) Protein aspartate phosphatases control the output of two-component signal transduction systems. *Trends in genetics : TIG* **12**: 97-101.
- Plocinska, R., G. Purushotham, K. Sarva, I.S. Vadrevu, E.V. Pandeeti, N. Arora, P. Plocinski, M.V. Madiraju & M. Rajagopalan, (2012) Septal localization of the *Mycobacterium tuberculosis* MtrB sensor kinase promotes MtrA regulon expression. *J Biol Chem* **287**: 23887-23899.
- Poole, R.K., (2005) Nitric oxide and nitrosative stress tolerance in bacteria. *Biochem Soc Trans* **33**: 176-180.
- Poole, R.K., M.F. Anjum, J. MembrilloHernandez, S.O. Kim, M.N. Hughes & V. Stewart, (1996) Nitric oxide, nitrite, and *fnr* regulation of *hmp* (Flavo-hemoglobin) gene expression in *Escherichia coli* K-12. *Journal of Bacteriology* **178**: 5487-5492.
- Py, B. & F. Barras, (2010) Building Fe-S proteins: bacterial strategies. *Nature reviews. Microbiology* **8**: 436-446.
- Py, B., P.L. Moreau & F. Barras, (2011) Fe-S clusters, fragile sentinels of the cell. *Curr Opin Microbiol* **14**: 218-223.
- Rajagopalan, S., S.J. Teter, P.H. Zwart, R.G. Brennan, K.J. Phillips & P.J. Kiley, (2013) Studies of IscR reveal a unique mechanism for metal-dependent regulation of DNA binding specificity. *Nature structural & molecular biology* **20**: 740-747.
- Rao, P.V. & R.H. Holm, (2004) Synthetic analogues of the active sites of iron-sulfur proteins. *Chemical Reviews* **104**: 527-559.
- Raulfs, E.C., I.P. O'Carroll, P.C. Dos Santos, M.C. Unciuleac & D.R. Dean, (2008) In vivo iron-sulfur cluster formation. *Proc Natl Acad Sci U S A* **105**: 8591-8596.

- Redenbach, M., H.M. Kieser, D. Denapaita, A. Eichner, J. Cullum, H. Kinashi & D.A. Hopwood, (1996) A set of ordered cosmids and a detailed genetic and physical map for the 8 Mb *Streptomyces coelicolor* A3(2) chromosome. *Mol Microbiol* **21**: 77-96.
- Richardson, D., H. Felgate, N. Watmough, A. Thomson & E. Baggs, (2009) Mitigating release of the potent greenhouse gas N₂O from the nitrogen cycle - could enzymic regulation hold the key? *Trends in biotechnology* **27**: 388-397.
- Rico, S., R.I. Santamaria, A. Yepes, H. Rodriguez, E. Laing, G. Bucca, C.P. Smith & M. Diaz, (2014) Deciphering the regulon of the *Streptomyces coelicolor* AbrC3, a positive response regulator of antibiotic production. *Appl Environ Microbiol*.
- Rigali, S., F. Titgemeyer, S. Barends, S. Mulder, A.W. Thomae, D.A. Hopwood & G.P. van Wezel, (2008) Feast or famine: the global regulator DasR links nutrient stress to antibiotic production by *Streptomyces*. *EMBO reports* **9**: 670-675.
- Rincon-Enriquez, G., P. Crete, F. Barras & B. Py, (2008) Biogenesis of Fe/S proteins and pathogenicity: IscR plays a key role in allowing *Erwinia chrysanthemi* to adapt to hostile conditions. *Mol Microbiol* **67**: 1257-1273.
- Robinson, V.L., T. Wu & A.M. Stock, (2003) Structural analysis of the domain interface in DrrB, a response regulator of the OmpR/PhoB subfamily. *J Bacteriol* **185**: 4186-4194.
- Rock, J.D., M.J. Thomson, R.C. Read & J.W.B. Moir, (2007) Regulation of denitrification genes in *Neisseria meningitidis* by nitric oxide and the repressor NsrR. *Journal of Bacteriology* **189**: 1138-1144.
- Rodionov, D.A., I.L. Dubchak, A.P. Arkin, E.J. Alm & M.S. Gelfand, (2005) Dissimilatory Metabolism of Nitrogen Oxides in Bacteria: Comparative Reconstruction of Transcriptional Networks. *PLoS Computational Biology* **1**: e55.
- Rodriguez-Garcia, A., A. Sola-Landa, K. Apel, F. Santos-Beneit & J.F. Martin, (2009) Phosphate control over nitrogen metabolism in *Streptomyces coelicolor*: direct and indirect negative control of *glnR*, *glnA*, *glnII* and *amtB* expression by the response regulator PhoP. *Nucleic Acids Research* **37**: 3230-3242.
- Rogstam, A., J.T. Larsson, P. Kjelgaard & C. von Wachenfeldt, (2007) Mechanisms of Adaptation to Nitrosative Stress in *Bacillus subtilis*. *JOURNAL OF BACTERIOLOGY*, **189**: 3063–3071.
- Rose, A., S.J. Schraegle, E.A. Stahlberg & I. Meier, (2005) Coiled-coil protein composition of 22 proteomes--differences and common themes in subcellular infrastructure and traffic control. *BMC Evol Biol* **5**: 66.
- Rothfield, L., S. Justice & J. Garcia-Lara, (1999) Bacterial cell division. *Annual review of genetics* **33**: 423-448.
- Rousset, C., M. Fontecave & S.O. de Choudens, (2008) The [4Fe-4S] cluster of quinolinate synthase from *Escherichia coli*: Investigation of cluster ligands. *Febs Letters* **582**: 2937-2944.
- Ryding, N.J., G.H. Kelemen, C.A. Whatling, K. Flärdh, M.J. Buttner & K.F. Chater, (1998) A developmentally regulated gene encoding a repressor-like protein is essential for sporulation in *Streptomyces coelicolor* A3(2). *Mol Microbiol* **29**: 343-357.
- Saini, V., A. Farhana & A.J.C. Steyn, (2011) *Mycobacterium tuberculosis* WhiB3: a novel iron-sulphur cluster protein that regulates redox homeostasis and virulence. *Antioxidants & redox signaling* **16**: 687-697.
- Schaberle, T.F., A. Orland & G.M. König, (2013) Enhanced production of undecylprodigiosin in *Streptomyces coelicolor* by co-cultivation with the coralopyronin A-producing myxobacterium, *Corallococcus coralloides*. *Biotechnology letters*.
- Schorey, J.S., M.C. Carroll & E.J. Brown, (1997) A macrophage invasion mechanism of pathogenic mycobacteria. *Science* **277**: 1091-1093.

- Schreiber, F., M. Beutler, D. Enning, M. Lamprecht-Grandio, O. Zafra, J.E. Gonzalez-Pastor & D. de Beer, (2011) The role of nitric-oxide-synthase-derived nitric oxide in multicellular traits of *Bacillus subtilis* 3610: biofilm formation, swarming, and dispersal. *BMC Microbiol* **11**: 111.
- Schwartz, C.J., J.L. Giel, T. Patschkowski, C. Luther, F.J. Ruzicka, H. Beinert & P.J. Kiley, (2001) IscR, an Fe-S cluster-containing transcription factor, represses expression of *Escherichia coli* genes encoding Fe-S cluster assembly proteins. *Proc Natl Acad Sci U S A* **98**: 14895-14900.
- Schwedock, J., J.R. McCormick, E.R. Angert, J.R. Nodwell & R. Losick, (1997) Assembly of the cell division protein FtsZ into ladder-like structures in the aerial hyphae of *Streptomyces coelicolor*. *Mol Microbiol* **25**: 847-858.
- Shu, D., L. Chen, W. Wang, Z. Yu, C. Ren, W. Zhang, S. Yang, Y. Lu & W. Jiang, (2009) afsQ1-Q2-sigQ is a pleiotropic but conditionally required signal transduction system for both secondary metabolism and morphological development in *Streptomyces coelicolor*. *Appl Microbiol Biotechnol* **81**: 1149-1160.
- Stewart, V., (2014) The HAMP signal-conversion domain: static two-state or dynamic three-state? *Mol Microbiol*.
- Steyn, A.J., J. Joseph & B.R. Bloom, (2003) Interaction of the sensor module of *Mycobacterium tuberculosis* H37Rv KdpD with members of the Lpr family. *Mol Microbiol* **47**: 1075-1089.
- Studier, F.W. & B.A. Moffatt, (1986) Use of bacteriophage T7 RNA polymerase to direct selective high-level expression of cloned genes. *J Mol Biol* **189**: 113-130.
- Sutcliffe, I.C. & R.R. Russell, (1995) Lipoproteins of gram-positive bacteria. *J Bacteriol* **177**: 1123-1128.
- Szukics, U., E. Hackl, S. Zechmeister-Boltenstern & A. Sessitsch, (2009) Contrasting response of two forest soils to nitrogen input: rapidly altered NO and N₂O emissions and nirK abundance. *Biology and Fertility of Soils* **45**: 855-863.
- Szurmant, H., T. Fukushima & J.A. Hoch, (2007a) The essential YycFG two-component system of *Bacillus subtilis*. *Methods Enzymol* **422**: 396-417.
- Szurmant, H., M.A. Mohan, P.M. Imus & J.A. Hoch, (2007b) YycH and YycI interact to regulate the essential YycFG two-component system in *Bacillus subtilis*. *J Bacteriol* **189**: 3280-3289.
- Szurmant, H., K. Nelson, E.J. Kim, M. Perego & J.A. Hoch, (2005) YycH regulates the activity of the essential YycFG two-component system in *Bacillus subtilis*. *J Bacteriol* **187**: 5419-5426.
- Tahlan, K., S.K. Ahn, A. Sing, T.D. Bodnaruk, A.R. Willems, A.R. Davidson & J.R. Nodwell, (2007) Initiation of actinorhodin export in *Streptomyces coelicolor*. *Mol Microbiol* **63**: 951-961.
- Tanous, C., O. Soutourina, B. Raynal, M.F. Hullo, P. Mervelet, A.M. Gilles, P. Noirot, A. Danchin, P. England & I. Martin-Verstraete, (2008) The CymR Regulator in Complex with the Enzyme CysK Controls Cysteine Metabolism in *Bacillus subtilis*. *Journal of Biological Chemistry* **283**: 35551-35560.
- Tian, Y., K. Fowler, K. Findlay, H. Tan & K.F. Chater, (2007) An unusual response regulator influences sporulation at early and late stages in *Streptomyces coelicolor*. *J Bacteriol* **189**: 2873-2885.
- Tillotson, R.D., H.A. Wosten, M. Richter & J.M. Willey, (1998) A surface active protein involved in aerial hyphae formation in the filamentous fungus *Schizophillum commune* restores the capacity of a bald mutant of the filamentous bacterium *Streptomyces coelicolor* to erect aerial structures. *Mol Microbiol* **30**: 595-602.

- Todd, J.D., G. Sawers & A.W.B. Johnston, (2005) Proteomic analysis reveals the wide-ranging effects of the novel, iron-responsive regulator RirA in *Rhizobium leguminosarum* bv. *viciae*. *Molecular Genetics and Genomics* **273**: 197-206.
- Traag, B.A., G.H. Kelemen & G.P. Van Wezel, (2004) Transcription of the sporulation gene *ssgA* is activated by the IclR-type regulator SsgR in a whi-independent manner in *Streptomyces coelicolor* A3(2). *Mol Microbiol* **53**: 985-1000.
- Tucker, N.P., M.G. Hicks, T.A. Clarke, J.C. Crack, G. Chandra, N.E. Le Brun, R. Dixon & M.I. Hutchings, (2008) The transcriptional repressor protein NsrR senses nitric oxide directly via a [2Fe-2S] cluster. *PLoS One* **3**: e3623.
- Tucker, N.P., N.E. Le Brun, R. Dixon & M.I. Hutchings, (2010) There's NO stopping NsrR, a global regulator of the bacterial NO stress response. *Trends in Microbiology*.
- van Wezel, G.P., J. van der Meulen, S. Kawamoto, R.G. Luiten, H.K. Koerten & B. Kraal, (2000) *ssgA* is essential for sporulation of *Streptomyces coelicolor* A3(2) and affects hyphal development by stimulating septum formation. *J Bacteriol* **182**: 5653-5662.
- Via, L.E., R. Curcic, M.H. Mudd, S. Dhandayuthapani, R.J. Ulmer & V. Deretic, (1996) Elements of signal transduction in *Mycobacterium tuberculosis*: in vitro phosphorylation and in vivo expression of the response regulator MtrA. *J Bacteriol* **178**: 3314-3321.
- Volkman, B.F., D. Lipson, D.E. Wemmer & D. Kern, (2001) Two-State Allosteric Behavior in a Single-Domain Signaling Protein. *Science* **291**.
- Walshaw, J., M.D. Gillespie & G.H. Kelemen, (2010) A novel coiled-coil repeat variant in a class of bacterial cytoskeletal proteins. *Journal of structural biology* **170**: 202-215.
- Wang, S.B., S. Cantlay, N. Nordberg, M. Letek, J.A. Gil & K. Flärdh, (2009) Domains involved in the in vivo function and oligomerization of apical growth determinant DivIVA in *Streptomyces coelicolor*. *FEMS Microbiol Lett* **297**: 101-109.
- Warner, D.F. & V. Mizrahi, (2007) The survival kit of *Mycobacterium tuberculosis*. *Nature medicine* **13**: 282-284.
- Watmough, N.J., G. Butland, M.R. Cheesman, J.W. Moir, D.J. Richardson & S. Spiro, (1999) Nitric oxide in bacteria: synthesis and consumption. *Biochim Biophys Acta* **1411**: 456-474.
- Willems, A.R., K. Tahlan, T. Taguchi, K. Zhang, Z.Z. Lee, K. Ichinose, M.S. Junop & J.R. Nodwell, (2008) Crystal structures of the *Streptomyces coelicolor* TetR-like protein ActR alone and in complex with actinorhodin or the actinorhodin biosynthetic precursor (S)-DNPA. *J Mol Biol* **376**: 1377-1387.
- Willemse, J., J.W. Borst, E. de Waal, T. Bisseling & G.P. van Wezel, (2011) Positive control of cell division: FtsZ is recruited by SsgB during sporulation of *Streptomyces*. *Genes Dev* **25**: 89-99.
- Willemse, J., A.M. Mommaas & G.P. van Wezel, (2012) Constitutive expression of *ftsZ* overrides the whi developmental genes to initiate sporulation of *Streptomyces coelicolor*. *Antonie van Leeuwenhoek* **101**: 619-632.
- Willey, J., J. Schwedock & R. Losick, (1993) Multiple extracellular signals govern the production of a morphogenetic protein involved in aerial mycelium formation by *Streptomyces coelicolor*. *Genes Dev* **7**: 895-903.
- Willey, J.M., L.M. Sherwood & C.J. Woolverton, (2008) Bacteria: The High G + C Gram Positives In: Prescott, Harley, and Klein's Microbiology. McGraw-Hill Higher Education, pp.
- Winkler, M.E. & J.A. Hoch, (2008) Essentiality, bypass, and targeting of the YycFG (VicRK) two-component regulatory system in gram-positive bacteria. *J Bacteriol* **190**: 2645-2648.
- Wolanin, P.M., P.A. Thomason & J.B. Stock, (2002) Histidine protein kinases: key signal transducers outside the animal kingdom. *Genome biology* **3**: REVIEWS3013.

- Wolanski, M., R. Wali, E. Tilley, D. Jakimowicz, J. Zakrzewska-Czerwinska & P. Herron, (2011) Replisome trafficking in growing vegetative hyphae of *Streptomyces coelicolor* A3(2). *J Bacteriol* **193**: 1273-1275.
- Wright, G.D., (2007) The antibiotic resistome: the nexus of chemical and genetic diversity. *Nature reviews. Microbiology* **5**: 175-186.
- Xian, J.A., H. Guo, B. Li, Y.T. Miao, J.M. Ye, S.P. Zhang, X.B. Pan, C.X. Ye, A.L. Wang & X.M. Hao, (2013) Measurement of intracellular nitric oxide (NO) production in shrimp haemocytes by flow cytometry. *Fish Shellfish Immunol.*
- Xu, Y., A. Willems, C. Au-Yeung, K. Tahlan & J.R. Nodwell, (2012) A two-step mechanism for the activation of actinorhodin export and resistance in *Streptomyces coelicolor*. *mBio* **3**: e00191-00112.
- Yang, K., L. Han & L.C. Vining, (1995) Regulation of jadomycin B production in *Streptomyces venezuelae* ISP5230: involvement of a repressor gene, *jadR2*. *J Bacteriol* **177**: 6111-6117.
- Yeo, W.S., J.H. Lee, K.C. Lee & J.H. Roe, (2006) IscR acts as an activator in response to oxidative stress for the *suf* operon encoding Fe-S assembly proteins. *Mol Microbiol* **61**: 206-218.
- Yukl, E.T., M.A. Elbaz, M.M. Nakano & P. Moenne-Loccoz, (2008) Transcription Factor NsrR from *Bacillus subtilis* Senses Nitric Oxide with a 4Fe-4S Cluster. *Biochemistry* **47**: 13084-13092.
- Zahrt, T.C. & V. Deretic, (2000) An essential two-component signal transduction system in *Mycobacterium tuberculosis*. *J Bacteriol* **182**: 3832-3838.
- Zeng, J., X. Zhang, Y. Wang, C. Ai, Q. Liu & G. Qiu, (2008) Glu43 is an essential residue for coordinating the [Fe₂S₂] cluster of IscR from *Acidithiobacillus ferrooxidans*. *FEBS Lett* **582**: 3889-3892.
- Zhang, G., Y. Tian, K. Hu, C. Feng & H. Tan, (2010) SCO3900, co-transcribed with three downstream genes, is involved in the differentiation of *Streptomyces coelicolor*. *Curr Microbiol* **60**: 268-273.

Chapter 9: Appendix

9.1. Results from MtrA Project

9.1.1 Strategy for Producing Mutants

Prior to working on this project the cosmid StE33, containing *lpqB*, *mtrB*, *mtrA* and *sco3014* had already been targeted by the redirect system to produce the knock out cosmids: *sco3014:apr*, *mtrA:apr*, *mtrB:hyg* and *lpqB:apr*. These mutant cosmids had then successfully been conjugated into *Streptomyces coelicolor* M145 and double crossovers had been screened to reveal the knock out mutant strains. However any phenotype or work carried out with these mutants may reveal changes due to polar effects caused by inserting the resistance cassette. Therefore in order to determine whether phenotype was due to a direct mutation of the gene then the resistance cassette had to be removed.

The redirect system was therefore implemented by using the flp recombinase sites, which were introduced when the disruption cassette replaced the target genes. Therefore the flp recombinase (FRT) sites within the *sco3014:apr*, *mtrA:apr*, *mtrB:hyg* and *lpqB:apr* cosmids were used to remove the resistance cassette, by placing the knock out cosmids in an *E.coli* strain BT340 containing the flp recombinase plasmid. When flp recombinase was expressed cleavage occurred at the FRT sites causing the resistance cassette to be excised to leave an 81 bp scar at the site. Successful in-frame cosmids (designated Δ *sco3014*, Δ *mtrA*, Δ *mtrB* and Δ *lpqB*) were checked by digestion and conjugated into the knock out strains in order to identify double crossover mutants by apramycin / hygromycin sensitivity screening instead of resistance.

9.1.2. Making In-Frame Mutants

Previously made knock out cosmids were transformed into *E. coli* BT340 and grown to induce flp recombinase expression. Inducing flp recombinase would remove the apramycin or hygromycin cassette from the knock out cosmids due to the flanking FRT sites. Once flp recombinase was expressed in order to identify whether flp recombination was successfully colonies were then screened for apramycin or kanamycin sensitivity due to the desired loss of the resistance cassette. Potential candidates, which were sensitive to apramycin or hygromycin but resistant to kanamycin were tested by isolating and digesting the cosmids. The fragment sizes, that were produced to identify $\Delta sco3014$, $\Delta mtrA$, $\Delta mtrB$ and $\Delta lpqB$ cosmids were successfully produced are displayed in tables 9.1 and 9.2.

Tables 9.1 and 9.2 reveal the desired fragment sizes in the $\Delta sco3014$, $\Delta mtrA$, $\Delta mtrB$ and $\Delta lpqB$ cosmids. To identify whether successful cosmids were made for *lpqB* the EcoRI and SacI digests were undertaken, where the desired 743 bp EcoRI fragment was seen. Also a SacI digest of $\Delta lpqB$ confirmed production of the $\Delta lpqB$ cosmid was successful. The $\Delta lpqB$ candidates were also checked by PCR to confirm they contained the correct cosmid, which showed that the $\Delta lpqB$ candidates contained the desired 369 bp fragment. Meaning each of these strains contained the $\Delta lpqB$ cosmid. Once this was discovered the strains were prepared for spores stocks and used for subsequent experiments.

The $\Delta mtrB$ had to be identified and was checked by restriction digestion where, like *lpqB*, the fragment sizes are displayed in tables 9.1 and 9.2. The desired 743 bp fragment produced by digesting $\Delta mtrB$ with EcoRI was observed. This revealed that the $\Delta mtrB$ cosmid was correct. Especially when the SacI digestion of the same cosmid produced the desired 8457 bp and 3908 bp fragments.

Potential $\Delta mtrA$ candidates were first tested by restriction digestion. The results of *mtrA* cosmids being digested with either EcoRI or SacI isolated the desired fragments displayed in tables 9.1 and 9.2. Therefore the $\Delta mtrA$ cosmid was successfully created. The potential strains were also tested by PCR where the candidates were successful and spore stocks were created.

The $\Delta sco3014$ cosmid was tested by digesting with EcoRI or SacI, where the desired EcoRI fragment of 743 bp was seen. Also the 8457 bp and 3908 bp fragments digested with SacI were observed. Therefore the successful cosmid was stored and successful strains were also stored for future work.

Table 9.1: A comparison of fragment sizes (bp) produced when cosmids were digested with EcoRI for identification. Unique fragments in in-frame mutant cosmids (Δ) are highlighted in red.

StE33	<i>lpqB: apra</i>	Δ<i>lpqB - oriT</i>	Δ<i>lpqB</i>	<i>mtrB: hyg</i>	Δ<i>mtrB- oriT</i>	Δ<i>mtrB</i>	<i>mtrA: apra</i>	Δ<i>mtrA- oriT</i>	Δ<i>mtrA</i>	<i>3014: apra</i>	Δ<i>3014- oriT</i>	Δ<i>3014</i>
25667	25195	23906	23906	12823	23653	23653	40537			25900	24611	24611
				12367			26353	25064	25604			
6792	6792	6792	6644	6792	6792	6644	6792	6792	6644	6792	6792	6644
3879	3879	3879	3877	3879	3879	3877	3879	3879	3877	3879	3879	3877
2462	2462	2462	2464	2462	2462	2464	2462	2462	24964	2462	2462	2464
1051	1051	1051	1051	1051	1051	1051	1051	1051	1051	1051	1051	1051
-	-	-	743	-	-	743	-	-	743	-	-	743

Table 9.2: Comparison of fragment sizes (bp) produced when cosmids were digested with SacI for identification. Unique fragments in in-frame mutant cosmids (Δ) strains are highlighted in red.

StE33	<i>lpqB:</i> <i>apra</i>	Δ<i>lpqB</i> - <i>oriT</i>	Δ<i>lpqB</i>	<i>mtrB:</i> <i>hyg</i>	Δ<i>mtrB</i>- <i>oriT</i>	Δ<i>mtrB</i>	<i>mtrA:</i> <i>apra</i>	Δ<i>mtrA</i>- <i>oriT</i>	Δ<i>mtrA</i>	<i>3014:</i> <i>apra</i>	Δ<i>3014</i>- <i>oriT</i>	Δ<i>3014</i>
22074	14927	20313	20313	12958	20060	20060	12180	21471	21471	11764	21018	21018
11764	11764	11764		11764	11764		9923	11764		11033	11764	
				8639			9829			10523		
-	-	-	8451	-	-	8451	-	-	8451	-		8451
	5924											
4313	4313	4313	4313	4313	4313	4313	4313	4313	4313	4313	4313	4313
-	-	-	3908	-	-	3908	-	-	3908	-	-	3908
							1841					
1700	1700	1700	1700	1700	1700	1700	1700	1700	1700	1700	1700	1700
	751						751			751		

9.1.3. Complementing the *sco3014-mtrAB-lpqB* Mutants

Even though removal of the resistance cassette within the $\Delta mtrA$, $\Delta mtrB$ and $\Delta lpqB$ strains prevented polar effects being observed the question remained whether results seen were due to the loss of *mtrA*, *mtrB* and *lpqB*. Therefore in order to verify these mutations, the removed genes needed to be complemented. To achieve this complementation plasmids were constructed. This began with individual constructs being synthesised from Genscript into pUC57. The genes *mtrA*, *mtrB* and *lpqB* were flanked by EcoRI and XbaI. The position of the restriction sites in relation to the *lpqB*, *mtrB* and *mtrA* can be seen in figures 9.1, 9.3 and 9.5 respectively.

Figure 9.2 displays the plasmid pUC57 *lpqB*, which was designed in order to subclone the genes of interest into pSET152. Other plasmids designed in order to subclone into pSET152 are pUC57 *mtrB* (figure 9.4) and pUC57 *mtrA* (figure 9.6) This was achieved by digesting the fragments out of pUC57 plasmids using EcoRI and XbaI. The digested fragments were isolated using Qiagen gel extraction and ligated into pSET152. However due to the presence of two EcoRI sites within pSET152 the digestion time was adjusted accordingly in order to isolate the vector containing the desired EcoRI site being excised. This took a number of attempts until the correctly digested pSET152 was isolated.

In order to check whether ligation was successful colonies which exhibited Apramycin resistance had their plasmids isolated. By isolating the plasmids the presence of successfully cloned inserts could be detected. This was achieved by digesting prospective candidates with EcoRI and XbaI.

Figures 9.2, 9.4 and 9.6 also show successful pSET152 plasmids containing *lpqB*, *mtrB* and *mtrA* inserts, respectively. These plasmids were then renamed pL11912, pB11912 and pA11912 due to the day successful plasmids were discovered. The complementation plasmids were conjugated into the respective mutant strains to form the complementation

strains Δ/pqB grey (pL11912), Δ/pqB white (pL11912), $\Delta mtrB$ (pB11912) and $\Delta mtrA$ (pA11912). These complementation strains were then used to compare phenotypes of the mutants. If the wild type phenotype was successfully restored then the change in phenotype could be confirmed as due to the loss in the gene of interest, the results of which can be seen in section 4.2.

GAATTC **TCA**CCCCGGATAGACCGGCGCGGTCCCCTCCGTCACCTTCTGCCACTGCAGCCCGGA
 CGGCAGCCGCACGATGAGGTCTCCGAATACGCCACCAGCGGCAGCCGCTCGTCTCGGTGCG
 GCGATCTCCTTGACTCCGGTCAGGGCCGCGGGCACCGATGCCTCCGGCGTCGAGCCGTCGAC
 CTGGACGTACCCGATCTGCTGGACGCCCCCGGCTCGCGCCCCACCACGACGAGCCGGGCGTC
 GCCGGCCAGGACATGGCCGTGACCTCCTCCAGCTCGGGGGTCGCGGAACGCAGTTCGAGCAC
 GGTGACCGCGGGCACGTGCCCCGCTTCCCGTCCCGTTCGATCCGCCCGATGAGCAGCGACCG
 CTTGCCGTCTTCTCCACCAGAGCGGATCCGCACCCCGTCGGCGGGCCACCCGCACGGCCTG
 GACGCGCCCATCGAGGCCTGGGGTCCGCACCTCCACCGGATCGCCCGCGCCCTCCTTCAGCAG
 CAGCAACC CGGGTTCGGCCGGGTTGCGGTTCGGCTATCCACAGGTGCCTTCGCGATCCCAGCT
 GGGCGGGGTCAGCCGGTCCGACTCCGCTTGGCCCTGGCTTGCCAGCACGGGGTCGCCGAGCGA
 ACCGCCGACACCAGCGAGCCGACGTACAGCAACTTGTGTCGAGACCGATTCCGGCCGCGCT
 GTGCTCGTCGCGGACACCGCCACCGACCGCAGGGCCTGATGACCCTCGCCAGCGGGCCGGG
 CACGGGTTCCGGCCCGGGTCCCCTTGTGCGGGCCGCGATCCGCACCAGGCGGTCTGGTCGTC
 GACGAAGTACAGGTAGTCGGGCCGCTGCGCGGAGCCGCGGGTAGCGACCGTCTCGGCGCGGT
 CTCGGAGAGCGAACACAACACTGCTCACCGCCCAGCGCAGCTCGACCTCCTGCACCGCCGGGGT
 GAGGTTCTGCAGCGTGAACAGGAGCTGTGCGGCCATCTCGTCGCACCTGTCCGCGCCGGCCCG
 CGCCGCTTGTGCTTACGCGGGACGGTCAGCTTGTGCGGTTCGCGGGGCCAGCGAGCCGGC
 GTTCTTCGCCAGTGCCGTCCCGGTCCGGAAAGCTCGACCTGACCACGGGGCCAGCAGGCTCGT
 CGGCCCGCTGAGCAGGGAACGCACCACCTGGGTCATCGGGTCCACCCGCCGGCGCACGTAGAC
 GGGATCGGCGACGGCCCGGCTCCCGCACCGGTCCCCTCTCGGCGGGCCCGCCGCACCGGGT
 GTTCGAGGCGAAGTAGTACCGGTTGACCGACATGTAGTTGCGCTGGAAGTCCGACTTGCCCAT
 GACGACGCCCGGCGGCAGCGAATCGATGCGCCACTGCTTGGACTTGCCGTCCCTCGTGAGGTG
 CACCGACTCGCGGTACACGCCGTCGGCCGGCGGTACGACTGCTGCGCGTCGACCGTGGCGAC
 CCTGGTGC CGGTACGGGTGACCGAGTAGTCGTTGGCGTCTCGCGGTTGCCCGAGTGGTCGGA
 CTCCGTTCCC GGCCCGCCGGCGAGCACCGTCGCCGACTCGTCCGGCCGCCAGCTCTTCGCGGC
 GTCGCCCGGTACGGTACTTGCGCGCCGCTCTCGTAGTGCGGATCGTCACTGGTCAGCGCCTCCAG
 GAAGCCCTGCACGATGTCGGCGGGCGGGGCGTCTCCC GCGGGCCATCGCGAACACCCGCAC
 CTGCGGGTCTGCGGGGCGTGGACTCCACGCCCTGAGGTCCC CGCTGTCGGGCATGGCCGC
 ACACCCGGCCAGCAGTACGACACCGCCGACGGCGTACGCCACCACGCGTGCCGGCCTCCGCCG
 ACCGCCCTCCCGGGTCA GCGGCCACGCGGTTCAGTCTGCCCCCTGTACGACGGACAATTGAA
 GGTGCGCAGCCCCTACCGCGCCCGGTCCGCACCCGACGCCCCCATGGCACGATGGCTGCCAAC
 CCGCCGCCCGACCGCGGACGCGCACCGTGAAGGAGCGACGATGAACGACACTCCGGGCTGGG
 CATCGCCCCGATCCGCCCCGTCGACGGGCACGAGCCCGGCGCGTCCGGCCCCGCCGACCGG
 CCGACCGCCCCGCCGGCCCCGACCAGCCCGCGCCCGCCGCGACCGGCCGATGCGGAACCGA
 CGAGCCCCGGCATCTAGA

Figure 9.1: DNA sequence used to complement the $\Delta lpqB$ mutation. This insert was synthesised by genscript to include the *lpqB* gene (orange), 300 bp of the upstream region of *sco3014* (grey) and flanked by the restriction enzymes EcoRI and XbaI for cloning into pSET152 to produce the complementation plasmid pL11912. The sequence is reverse complemented due to the strand in which the *lpqB* gene is encoded within the *S. coelicolor* genome.

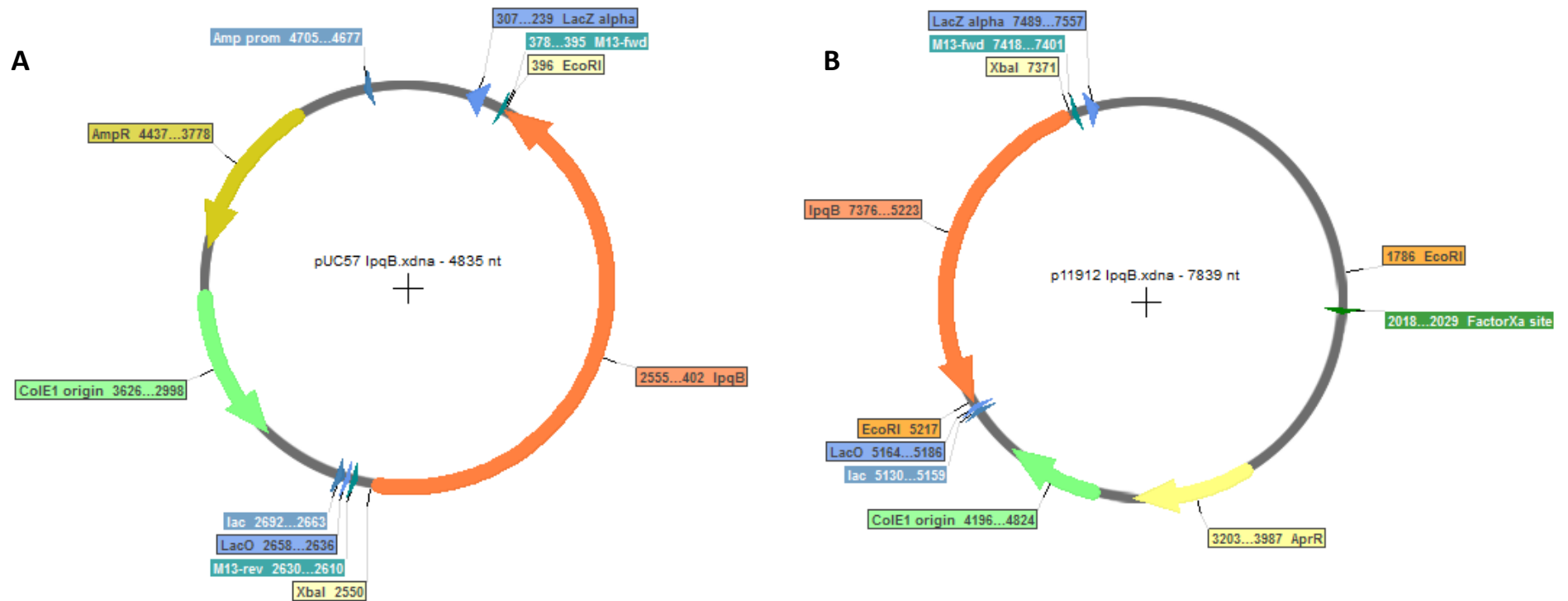


Figure 9.2: Plasmids used to complement the $\Delta lpqB$ mutant. (A) Plasmid pUC57 *lpqB* obtained from genscript containing the *lpqB* gene along with 300 bp of the upstream region of *sco3014*, thought to contain the native promoter of the *sco3014-mtrAB-lpqB* operon. The *lpqB* insert was excised via EcoRI and XbaI, which were synthesised at the flanking regions of the insert (figure 9.1). (B) The *lpqB* insert was ligated into pSET152, which contains an integrase. This plasmid was then deemed pL11912 as used to complement the $\Delta lpqB$ mutant.

GAATTC **TCAGCGCCACGAGATGCCTCCCCCTGCCTGCTCGAGTCTCGGGACCGGGCTCTG**
CCGGCCCGCCCTCCGGTGCCGGCCACCGTCTGTCTCCGCGCCCCGACACGGGCTCGG
TACCACGCGCGCCGTTGCCCGCAGTGCCGTGGGATCCGCCGTGGGTGCCACCGTGGCCTG
CCGCGGCGTTATCGGCCCCCGCGGAGACCTGCCCGCCGGCACCTGCGCCGGGACGCCGAC
CGACTTGTCCGCGCCCGCCACCGCCGGTTCGGCGAGGCCCGCGTCTGTTGAGCCCGCGGTT
GCGGCGGAGTCCGTCCGCTCCAGCGGTATCGGCGACCCCTGAGCGGCTCGTCCGCCGTCT
GGGACGCGTCCAGCCGGAACGCGAGCCACCGCCGGGCTCGCCCCAGGCCTGCAGCCAGCCACC
GTGCAGCCGCGCTCTCCAGGGCGATCGACAGCCCGAGCCCCGTGCCGCCGGTGGTACGCGC
GCGTGCCGGGTCCGCCCGCAGAAGCGGCTGAAGACCCGGGTGGCCTCGCCCCGCTTGTAGTCC
GACGCCGTAGTCCGCGACCGCGACGGCGACGGCGCCCCCGGCCGCGGGGAGCTTACGACGAC
GTCCCGGCCCTCGCCGTGCTCGACGGCGTTGACGACGAGGTTGCGCAGCACACGCTCGACCCG
CCGGGCGTCCGCCCTCGGCGACGACGGGCTGCTGGTCCCGACCACGCGTATCCCCGTGCCCTT
GCGTCCGGCGAGCGGCTCCGCGCCGCTGACGACGCGCCGGACGACCTCCCTGAGGTCTATCGG
CTCCGCCCTCCAGCGCGGCGCGCCCGCGTCAAGCGGCTGATCTCCAGCAGGTCCGGCGAGCAG
CGTCTCGAACCGGTCCAGCTGGTCCGGCGAGCAGTTCGGCCGACCGCGCGGTACCAGGATCGAA
GTCCACGCGCGCGTCTGAATGACGTCGGCCGCCATCCGCACGGTCTGTCAGTGGGGTGGCAG
CTCGTGGACACGTCGGAGACGAACCGCCGCTGCATCCGCGACAGGTCTCCAGCTGGCTGAT
CTTGTGAGCTGGAGGTTCTGCGCCATCTTGTGAAGGCTCGCCGAGCCGGGCGATGTCGCTCTC
GCCGGTGACCTTCATCCGTTCCCTGCAACCGCCCCGCGGACAGCCGCTCGGCGATGTCGCCGC
CATCCGTACCGGGGTGACGACCTGGCGCACACGAGCCAGGCGATGGCCCCGAGCAGCACGAC
CACGAACAGACCGGCGGTCCAGTGTGCCCTGACCAGGCTGAGCGACTTCTCCTCCTGAGT
GAGCGGGAAGAGGTAGTACAGCTGGTACGGCTCGCCGTTCCGGTTCGTTGACCTGCTTGGCGAT
GACCAGTCCCGGCTGGGACGGCTGGTCCGAGTTGTAGACGATCCGGGTGTAGCTCTGGGCGGC
CGCGGTGTCCCGTTCGATCCGCTCCCGCAGGGCCTCGGGGACGCTCACCGCCAGTCCGACCGA
TCCGGAGGCGCGCGGACCGCGTCCGCTGCCGCTCTCCCCGCCATGGGGAGCGTGACCACGTC
GAACGCGCTCTGGCCACCGCTGGAGAGCGACTTACCAGCTCGCTCATCCACTGGATGACGTT
CTGCGAGGGACGCCCGTCCGCGGGGGTCCCGTTCGTCGCGGTTGGTCTCGCCGCTCCTCGGC
CTTCTGCTTGGCCGCCGTGAAACCACCGGTGGCCTGGCTCTGGGAGGCCTTACCTTGGCGTC
CAGCAGCCCGTTGCGGACCTGCCCGATCACACGAAGCCGAGCAGCAGCACCACCCCGAGCGA
CATCAGCAGGGTGGTGGCGACGACCTTGTGAGCTGGATGTTGCGCCGCCACAGCCGCATGACCGG
CAGCAGGGGGCGGCGCACCCAGCGCATGAACAGGCGGAGCACCGGGGCTGCCCTGCACCCGCC
GTGCAGCAGCCCGCCCTCCAGCACACGGCCGAAGAGACGGGAGCCGACGCTCCGGTGGCCGAC
AGGCCGTCCGGCGCGGGCCCCGACCCGGGCGCCGAAGCGGCACTGTCCCTGGCCATGCGGTC
AGTCTGCCCCCTGTACGACGGACAATTGAAGGTGCGCAGCCCCACCAGCGCCCGGTCCGCACC
CGACGCCCCCATGGCACGATGGCTGCCAACCCGCCCGCGACCGCGGACGCGCACCGTGAAG
GAGCGACGATGAACGACACTCCGGGCTGGGCATCGCCCGGATCCGCCCGTCCGACGGGCACG
AGCCCGGCGCGTCCGGCCCCCGGACCGGCCGACCGCCCCGCGGCCCGGACCGCCCGCGC
CGCCCCGCGGACCGGCCGATGCGGAACCGACGAGCCCCGGCATCTAGA

Figure 9.3 DNA sequence used to complement the *ΔmtrB* mutation. This insert was synthesised by genscript to include the *mtrB* gene (purple), 300 bp of the upstream region of *sco3014* (grey) and flanked by the restriction enzymes EcoRI and XbaI for cloning into pSET152 to produce the complementation plasmid pB11912. The sequence is reverse complemented due to the strand in which the *mtrB* gene is encoded within the *S. coelicolor* genome.

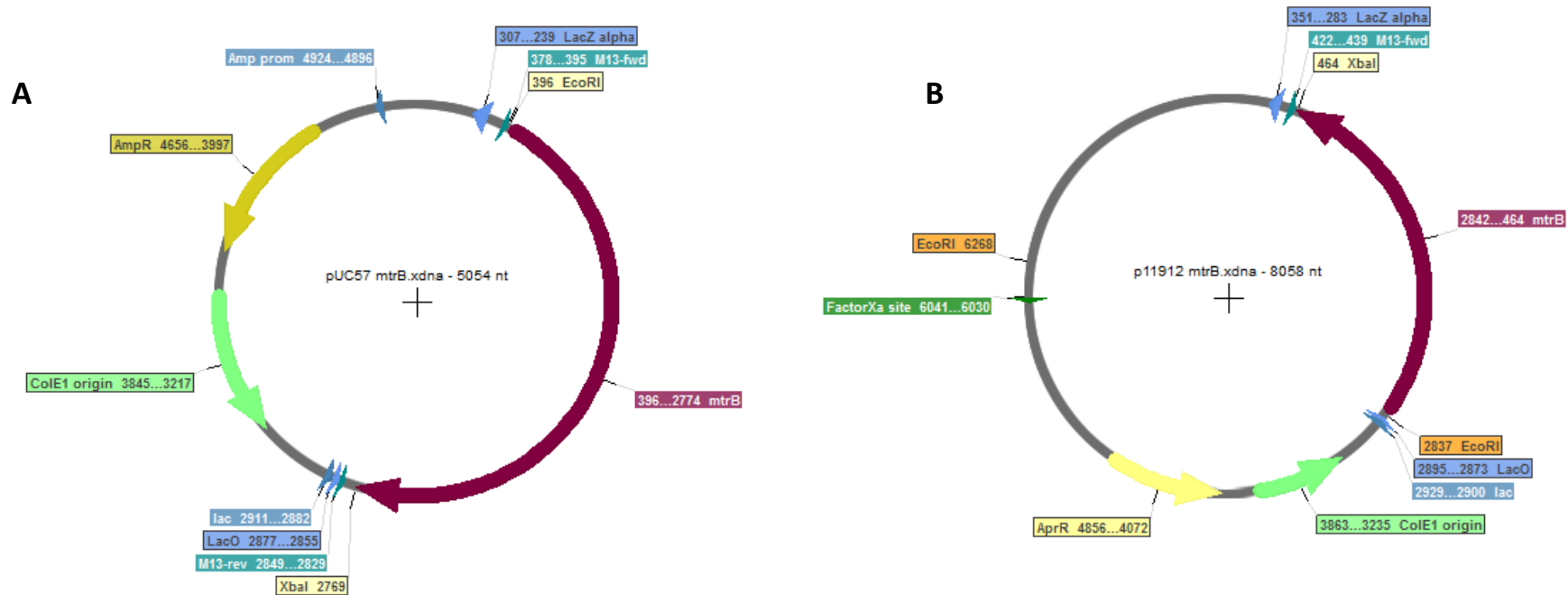


Figure 9.4: Plasmids used to complement the $\Delta mtrB$ mutant. (A) Plasmid pUC57 *mtrB* obtained from genscript containing the *mtrB* gene along with 300 bp of the upstream region of *sco3014*, thought to contain the native promoter of the *sco3014-mtrAB-lpqB* operon. The *mtrB* insert was excised via EcoRI and XbaI, which were synthesised at the flanking regions of the insert (figure 9.3). (B) The *mtrB* insert was ligated into pSET152, which contains an integrase. This plasmid was then deemed pB11912 as used to complement the $\Delta mtrB$ mutant.

GAATTC **TCAGCTCGGTCCGGCCTTG TAGCCGACGCCGGACGGTCACCACGATCTCCGGCTT**
CTCCGGTTCCTTCTCGACCTTGGAGCGCAGCCGCTGGACGTGCACGTTGACCAGGCGGGTGTG
GGCGCGTGCCGGTAGCCCCAGACCTGCTCGAGGAGCACCTCGCGGTGAACACCTGCCACGG
CTTGCGGGCCAGCGCCACCAGCAGGTCGAACTCCAGCGGCGTCAGCGGATCGACTGCCCGTC
CCGCTTACGGAGTGACCGGCCACGTGATGACCAGGTCGCCTATGGCGAGCTGCTCCGGCGC
CGGTTCTCCGACCTGCGCAGCCGCGCCCGGATCCGGGCCACCAGCTCCTTCGGCTTGAACGG
CTTACAGATGTAGTCGTGCGGCCCGACTCCAGACCCACCACGACGTGACGGTGTGCTCTT
CGCCGTCAGCATCACGATCGGCACACCCGACTCCGCCCTGATCAGGCGGCACACCTCGATGCC
GTCCCGTCCGGGCAGCATCAGGTCGAGCAGCACCAGGTCGGCTTGGTCTCCCGAAGGCGGC
CAGCGCCTTGTCGCCGTGCGCTACGAAAGACGGCTCAAAACCTCACCACGCAGCACAATGCC
GAGCATCTCGGCCAGTGCGGTGTGTCGTGTCGACGACAAGGACTCGTCCCTTCATAAACGACAT
CAT GCGGTCAGTCTGCCCCCTGTACGACGGACAATTGAAGGTGCGCAGCCCCCTACCGCGCCCG
 GTCCGCACCCGACGCCCCCATGGCACGATGGCTGCCAACCCGCCGCCGACCGCGGACGCGC
 ACCGTGAAGGAGCGACGATGAACGACACTCCGGGCTGGGCATCGCCCCGATCCGCCCCGTCCG
 ACGGGCACGAGCCCGGCGCGTCCGGCCCCGCCGGACCGGCCGACCGCCCCGCCGGCCCCGACC
 AGCCCCGCGCCCGCCGCGGACCGGCCGGATGCGGAACCGACGAGCCCCGGCATCTAGA

Figure 9.5 DNA sequence used to complement the $\Delta mtrA$ mutation. This insert was synthesised by genscript to include the *mtrA* gene (pink), 300 bp of the upstream region of *sco3014* (grey) and flanked by the restriction enzymes EcoRI and XbaI for cloning into pSET152 to produce the complementation plasmid pA11912. The sequence is reverse complemented due to the strand in which the *mtrA* gene is encoded within the *S. coelicolor* genome.

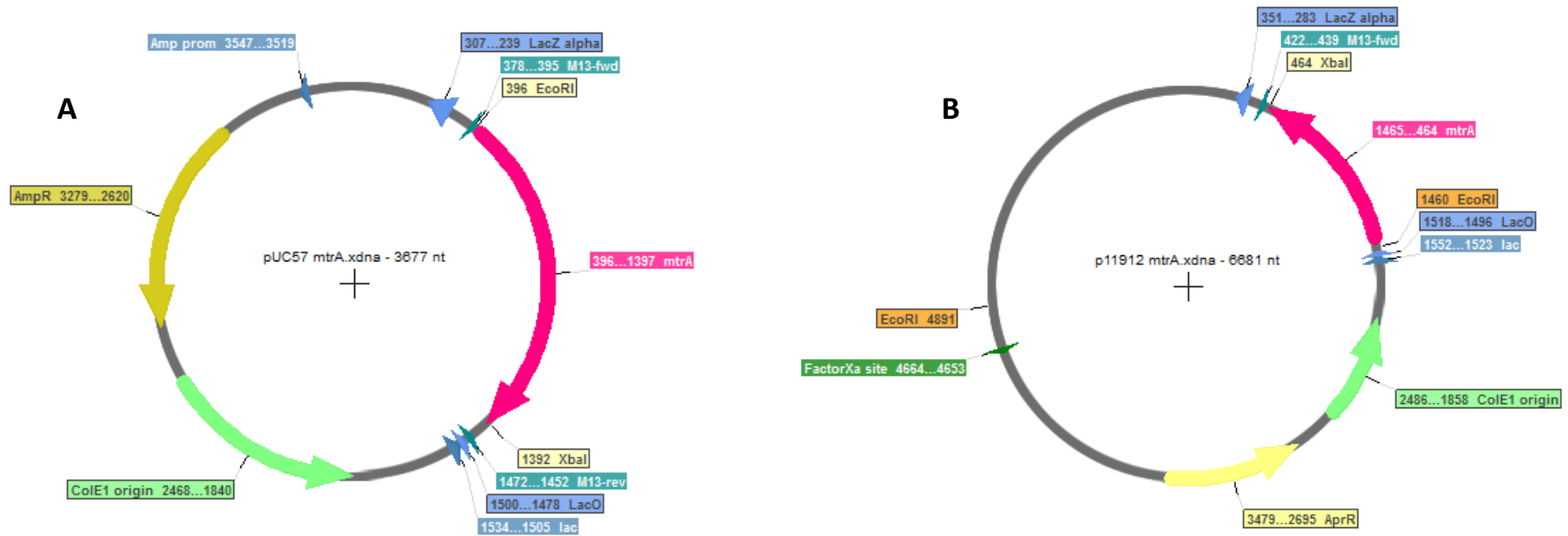


Figure 9.6: Plasmids used to complement the $\Delta mtrA$ mutant. (A) Plasmid pUC57 *mtrA* obtained from genscript containing the *mtrA* gene along with 300 bp of the upstream region of *sco3014*, thought to contain the native promoter of the *sco3014-mtrAB-lpqB* operon. The *mtrA* insert was excised via EcoRI and XbaI, which were synthesised at the flanking regions of the insert (figure 9.5). (B) The *mtrA* insert was ligated into pSET152, which contains an integrase. This plasmid was then deemed pA11912 as used to complement the $\Delta mtrA$ mutant.

9.1.4 Pigmented Antibiotic Production

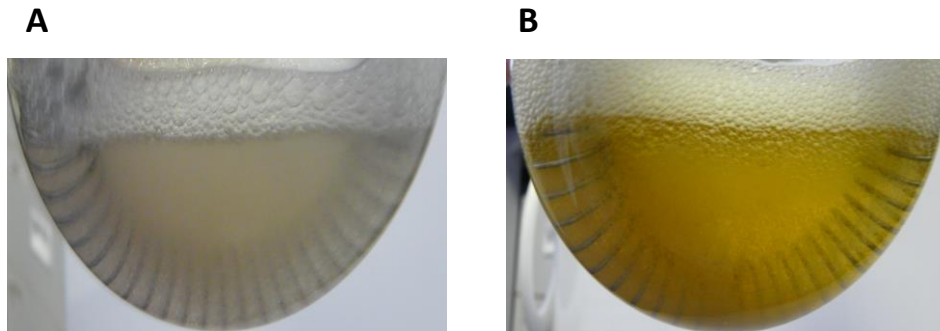


Figure 9.7: Pigmentation seen in *S. coelicolor* cultures grown in SMM for 20 hours at 30 °C. (A) No yellow pigmentation was observed in wild type culture. (B) Yellow pigmentation seen in $\Delta mtrA$ culture grown under these conditions.

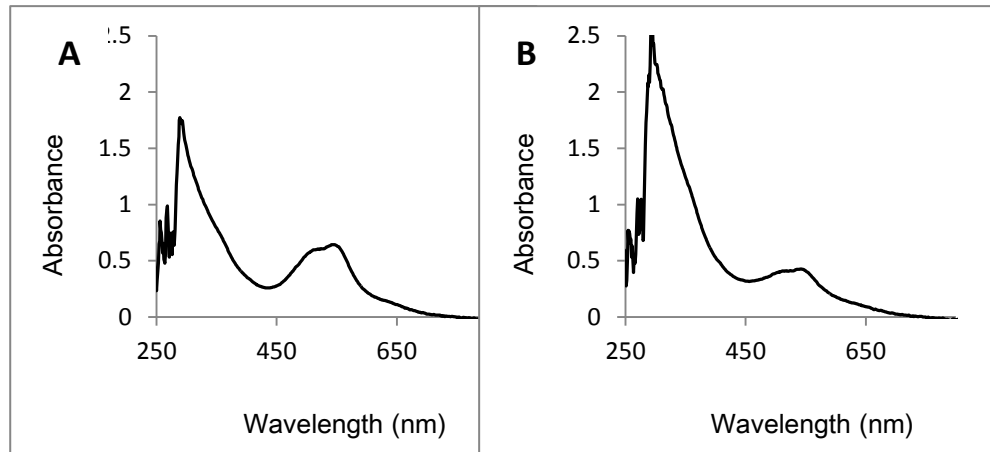


Figure 9.8: UV visible spectrum of yellow pigmented supernatant produced by $\Delta mtrB$ and $\Delta mtrA$ strains grown for 39 hours in liquid SMM at 30 °C, in comparison to UV visible spectrum of CpK producing strains that exhibit a distinctive 460 nm peak. (A) UV visible spectrum of supernatant from the $\Delta mtrB$ strain, where no 460 nm peak can be seen. (B) UV visible spectrum of supernatant from the $\Delta mtrA$ strain where no 460 nm peak can be seen.

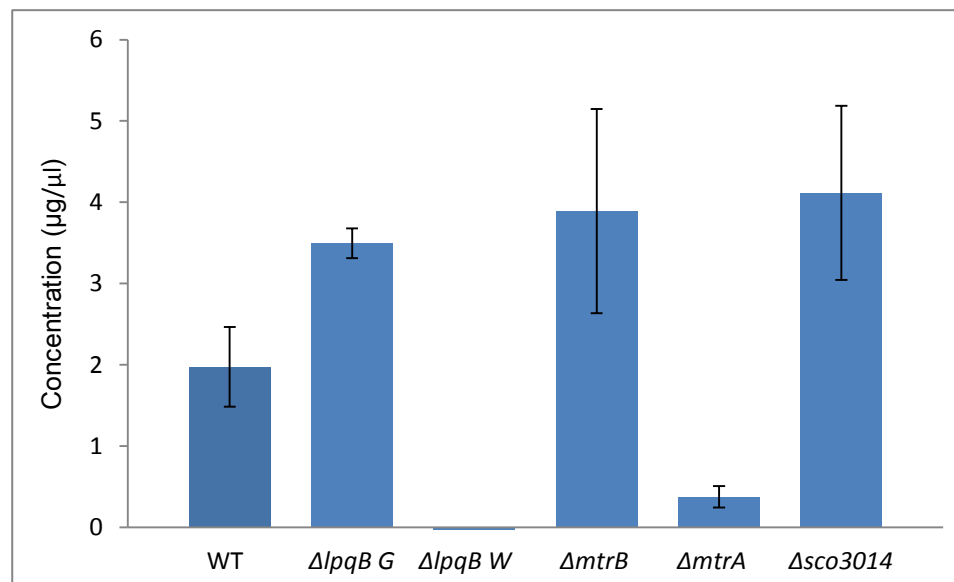


Figure 9.9: : Actinorhodin produced by the wild type, $\Delta lpqB$ grey, $\Delta lpqB$ white, $\Delta mtrB$, $\Delta mtrA$ and $\Delta sco3014$ strains. No actinorhodin production was detected in the $\Delta lpqB$ white strain.

9.2 Results from NsrR Project

9.2.1 Strategy for Producing an *nsrR* Mutant

In order to construct an *nsrR* mutant the PCR targeting system 'Redirect' was adopted. The *nsrR* gene was replaced by a resistance cassette, which in this case was Apramycin. The disruption cassette therefore contained apramycin, an *oriT* site, flp recombinase (FRT) sites as well as sequence for both upstream and downstream of the *nsrR* gene. This disruption cassette was introduced into cosmid DNA by way of homologous recombination within an *E. coli* strain expressing λ RED recombinase. Successful recombinants were identified in order to be conjugated into wild type *S. coelicolor* M145. Conjugation occurred due to the knock out cosmid being placed within a methylation deficient *E. coli* strain, which allowed the cosmid DNA to be introduced into M145 without being degraded. Double crossovers were then selected for by replica plating in order to identify strains which had become desirably apramycin resistant and sensitive in turn to kanamycin, which was due to cosmid resistance. Successful double crossover mutants were screened and successful candidates were saved by isolating and freezing spore stocks.

Once an apramycin marked mutation was produced an in-frame mutation was made to prove any phenotype changes were not due to polar effects caused by introducing the resistance gene. Therefore the apramycin gene was removed from the *nsrR:apr* cosmid by placing it within an *E.coli* strain expressing flp recombinase. Due to the presence of flp recombinase sites flanking the apramycin gene within the cosmid this could then be excised from the *nsrR:apr* cosmid. This excision would leave an 81 bp scar sequence within the resultant $\Delta nsrR$ cosmid that were selected by exhibiting apramycin sensitivity while being resistant to kanamycin unlike the *nsrR:apr* cosmid. Successful $\Delta nsrR$ cosmids were also conjugated into *Streptomyces coelicolor* and identified by screening double crossovers. Both *nsrR:apr* and $\Delta nsrR$ mutants were used to study the role of *nsrR* in *S. coelicolor*.

9.2.2 Making an *nsrR:apr* mutant

In order to construct an *nsrR:apr* mutant the apramycin cassette was amplified by PCR. Once this product was isolated the correct cosmid need to be identified in order to introduce this apramycin resistance cassette.

The potential cosmid St6D11 was digested with both BamHI and SacI separately in order to check the digestion pattern for identification. Both digests with BamHI or SacI revealed that the 6D11 was the correct cosmid. Once identified the apramycin cassette was introduced into the 6D11 cosmid in order to replace the *nsrR* contained within it.

One check used to determine whether a successful *nsrR:apr* cosmid had been created was PCR where amplification of the apramycin cassette or *nsrR* gene. The PCR to identify apramycin or *nsrR* revealed that the wild type cosmid 6D11 contained *nsrR* but lacked the apramycin cassette. In contrast apramycin was identified in the *nsrR:apr* cosmid at the expense of the *nsrR* gene. These results were also seen in the wild type and mutant *S. coelicolor* strains. Therefore both an *nsrR:apr* cosmid and *nsrR:apr* strain were made successfully (figure 9.10).

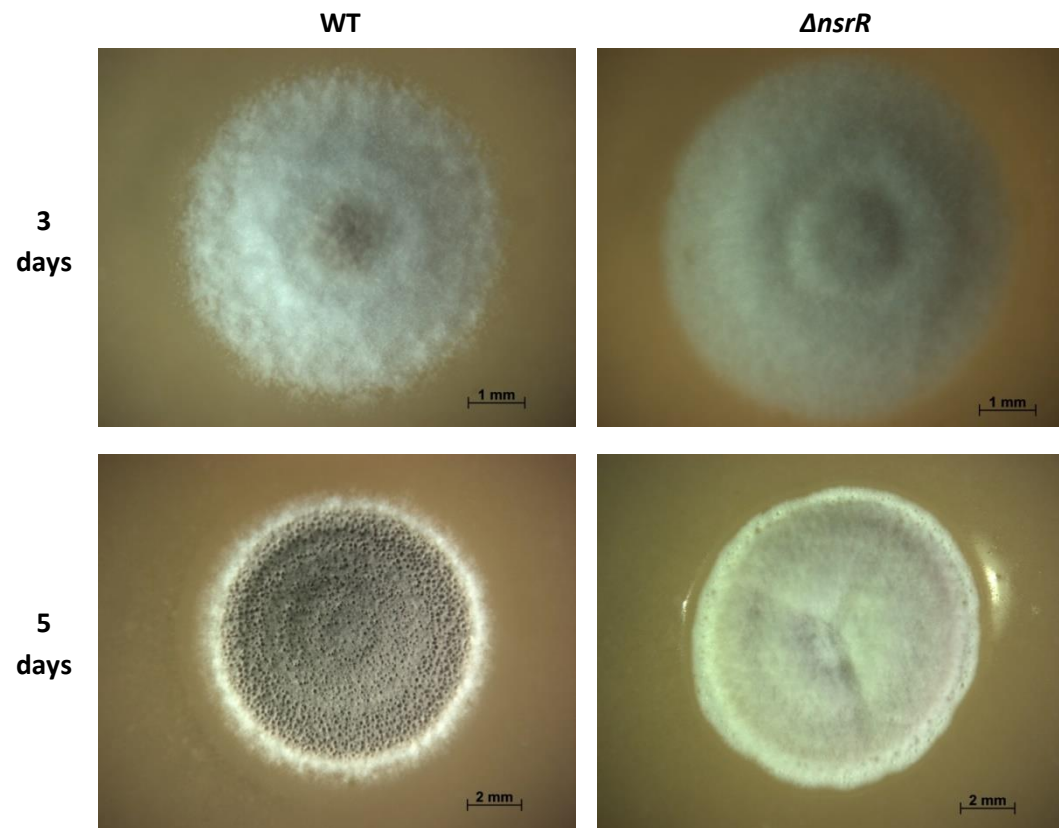


Figure 9.10: Phenotypic comparison of *S.coelicolor* wild type and *nsrR:apra* mutant colonies grown on SFM at 30 °C for 3 or 5 days then visualised using a light microscope.

9.2.3 Making an *nsrR* In-Frame Mutant

Once an *nsrR:apr* mutant had been made a $\Delta nsrR$ mutant was required to show that any changes seen within the mutant were due to the absence of *nsrR* and not due to polar effects. The in-frame cosmid was made by placing the *nsrR:apr* cosmid within an *E. coli* strain that expressed flp recombinase. The expression of flp recombinase excised the apramycin cassette from the marked cosmid producing the $\Delta nsrR$ cosmid. This $\Delta nsrR$ -*oriT* cosmid then had an *oriT* site added to produce the $\Delta nsrR$ cosmid in order to introduce the cosmid into *S.coelicolor*. These in-frame cosmids were tested by EcoRI or SacI restriction digestion, which revealed the $\Delta nsrR$ and $\Delta nsrR$ -*oriT* cosmids were produced

Once this was determined the $\Delta nsrR$ -*oriT* cosmid was introduced and screened for in *S. coelicolor* forming the $\Delta nsrR$ mutant and tested for the absence of *nsrR* using PCR where no *nsrR* was detected in the mutant cosmid and $\Delta nsrR$ candidate. This in combination with screening for apramycin sensitivity and kanamycin resistance revealed that a successful $\Delta nsrR$ mutant was produced in order to work with further.

9.2.4 Complementing the *nsrR* Mutation

When *nsrR* mutants were successfully made, complementing the *nsrR* mutant was important to observe if the *nsrR* phenotype was restored. A complementation strain was constructed by using a TOPO cloning system. The *nsrR* gene was amplified and inserted into the PCRII-TOPO vector. The remaining PCR product then had overhanging adenines added at either end via PCR. Once the adenines were added the gene could then be inserted into PCRII-TOPO using the topoisomerase within the TOPO cloning kit. Once vector had insert ligated in successful clones were identifies by blue / white selection. Plasmid candidates were sent to sequencing to check the presence of the insert (figure 9.11).

The sequencing results revealed a point mutation had been introduced into the *nsrR* gene during PCR amplification. This point mutation was the change of a guanine for an adenine within the *nsrR* sequence. Therefore in order to establish whether this mutation was silent the amino acid sequence of both NsrR and NsrR created from this G-A mutation (figure 9.11). This comparison of amino acid sequences revealed the point mutation of guanine to adenine to be a silent one. Both DNA sequences produce a Serine at this codon and therefore the mutation within *nsrR* was silent. Therefore this *nsrR* insert within the newly created TOPO *nsrR* vector (figure 9.12) was used to complement the *nsrR* mutation.

Once a useable *nsrR* sequence was detected within the TOPO *nsrR* vector (figure 9.11) this was subcloned into pMS82, so *nsrR* could integrate into the mutant chromosome. Therefore the TOPO *nsrR* vector and pMS82 were excised by restriction digest in preparation for cloning. Once ligation was successful the complementation vector named p26712 was produced (figure 9.12). The p26712 vector was then transformed into the $\Delta nsrR$ mutant causing integration of the *nsrR* gene. The complementation of *nsrR* would reveal if replacing the gene would restore the loss of function observed within the mutant.

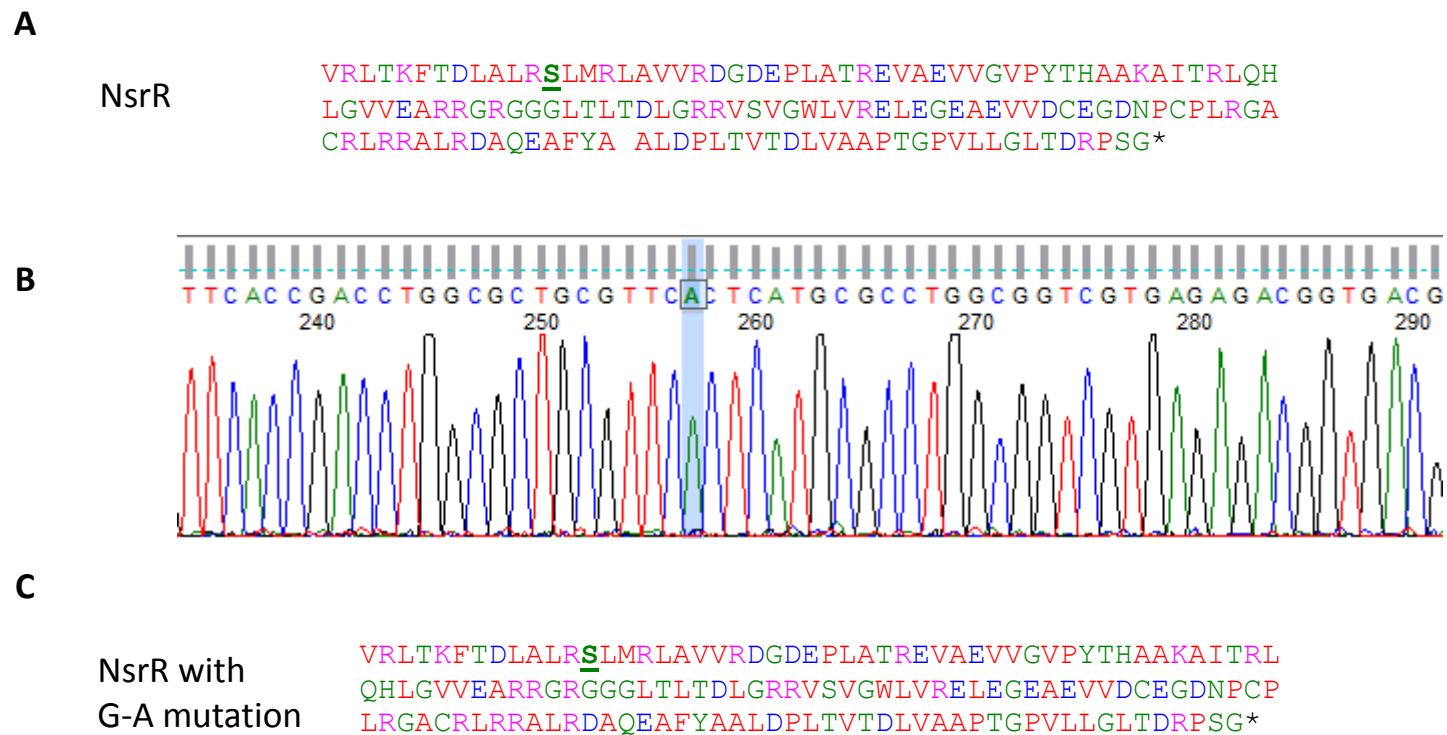
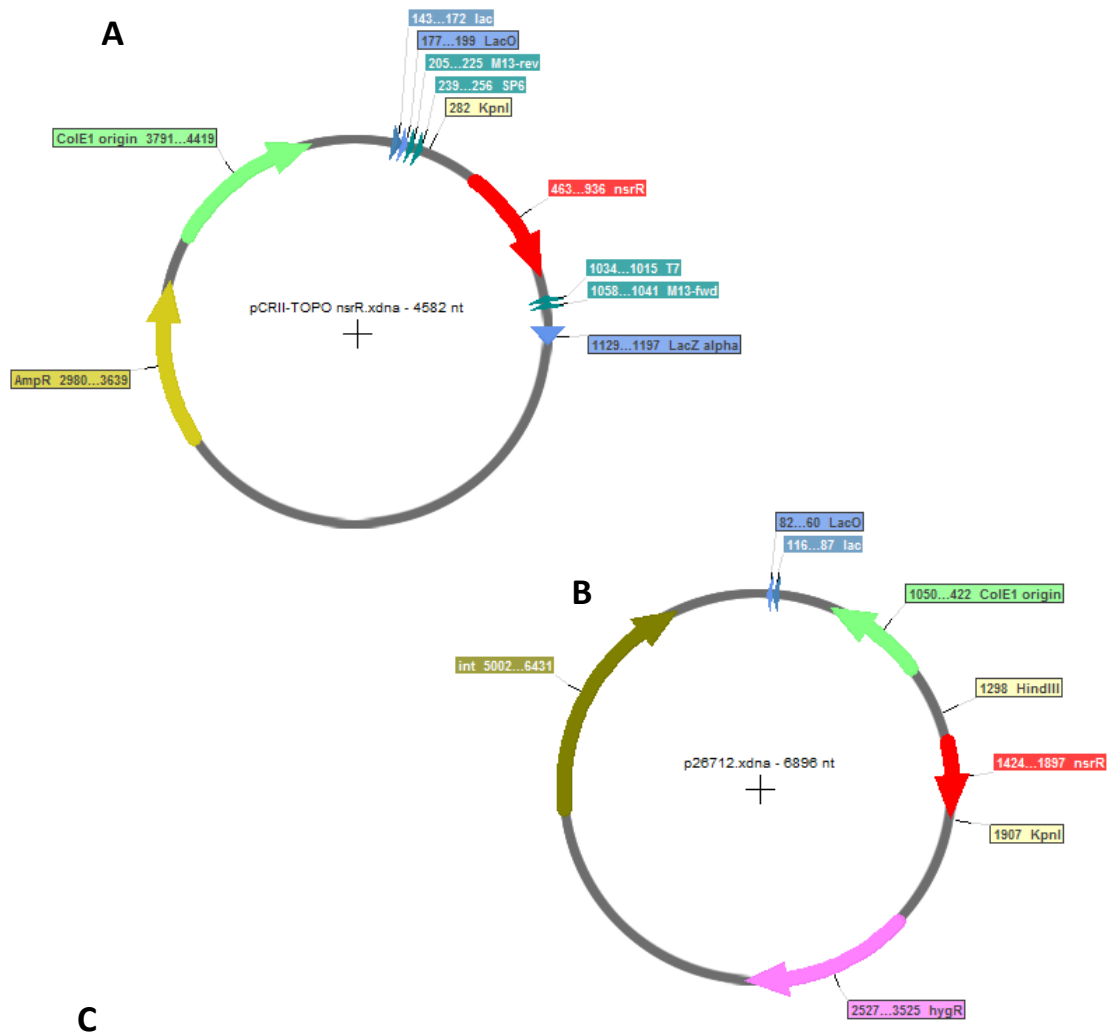


Figure 9.11: Sequencing results of *nsrR* inserted into the PCRII-TOPO vector amplified using the M13F and T7R primers. (A) The wild type NsrR amino acid sequence. (B) The chromatogram depicting the silent point mutation where the replacement of guanine with an adenine is highlighted. (C) The NsrR amino acid sequence that resulted from the point mutation. The affected amino acid underlined in both amino acid sequences, which revealed that point mutation is silent mutation as Serine is present in both.



AAGCTTTCAGGTGCCGCCGTTCCGTGTGCCCGACCGTGCCCGTACGCCGCCCCGTTGAGC
 GTCCCGTGCCGGGGCGGCCGGTCCAGTGACGCACCGCACAGGCTCAGTACCCCGGGTAAA
 GGCAACCTAGCATGCGCATTGATAGCGTCCCTGGT **GTGCGGTTGACGAAGTTCACCGAC**
CTGGCGCTGCGTTCACTCATGCGCCTGGCGGTCGTGAGAGACGGTGACGAACCACTGGCC
 ACCCGAGAGGTGGCCGAGGTCGTGGGGTGCCGTACACGCACGCGGCGAAGGCCATCACC
 CGCCTGCAGCACCTGGGTGTGGTGGAGGCGGACGCGGTCGCGGGCGGGGCTGACGCTG
 ACCGACCTGGGCCGGCGCTCTCCGTGGGCTGGCTGGTGCCTGAACTCGAGGGCGAGGCC
 GAGGTGGTCGACTGCGAGGGCGACAACCCCTGCCCGCTGCGCGGGCCCTGCCGGCTGCGG
 CGTGCCTGCGCGACGCCAGGAGGCGTTCTACGCGGCACTCGACCACTGACCGTGACC
 GACCTGGTGGCCGCACCGACCGGCCCGGTTCTGCTCGGCC **TGA**CGGACCGCCCTCGGGA
TGAGGTACC

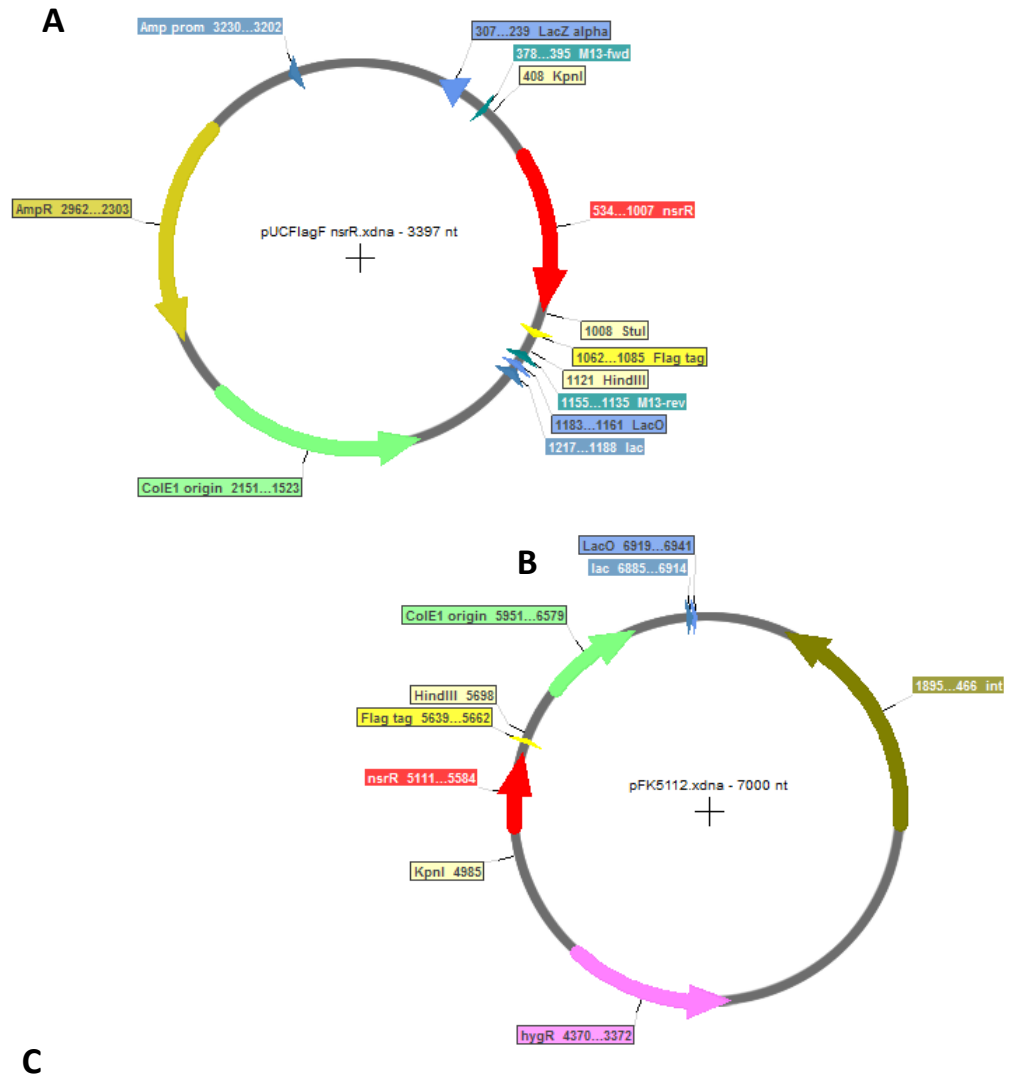
Figure 9.12: The plasmids and DNA sequence used to complement the $\Delta nsrR$ mutant. (A) The sequenced pCRII-TOPO vector containing the correct *nsrR* sequence. (B) The *nsrR* sequence was inserted into pMS82 via the KpnI and HindIII restriction sites the plasmid was then deemed pN26712. (C) The *nsrR* PCR product used to complement the $\Delta nsrR$ mutant. Where the *nsrR* sequence (red) contained the silent point mutation (blue) discovered when the pCRII-TOPO *nsrR* plasmid was sequenced (figure 9.11). The stop codon (bold), primers (underlined), 150 bp upstream region and restriction sites (green) are also shown.

9.2.5 Making an *nsrR* 3XFlag Strain

In order to investigate the targets of NsrR a 3XFlag tag strain needed to be constructed. This was achieved by amplifying the *nsrR* gene along with its native promoter but excluding the stop codon (figure 9.13). Once the gene was amplified it was then cloned into the KpnI and NdeI digested plasmid pUCflagF (figure 9.13) in order to insert *nsrR*. Prospective plasmids were tested by restriction digestion. These vectors were deemed pUCflagF *nsrR* and the map of this plasmid is shown in figure 9.13. This map shows when *nsrR* is inserted into the pUCflagF plasmid a C-terminal 3XFlag tag. The 3XFlag tag, contained within the pUCflagF plasmid, were GC rich for use in *S. coelicolor*. The successfully cloned plasmid was transformed into *E. coli* and tested by PCR. Four prospective colonies contained *nsrR* and were isolated for further testing.

Plasmids were isolated from these strains and checked for the presence of the desired insert by restriction enzyme digestion. Three plasmids contained the *nsrR* 3XFlag insert and were sequenced. The results of which were correct, where the *nsrR* gene was successfully inserted with no mutations. Two pUCflagF plasmids were digested in order to insert the *nsrR* 3XFlag sequence into pMS82 (figure 9.13), which was then deemed pN5112.

Potential pN5112 plasmids were isolated and tested by restriction enzyme digestion where the *nsrR*-FLAG fragment (707 bp) was cleaved from pN5112 using KpnI and HindIII. Therefore these pN5112 plasmids were conjugated into the *S. coelicolor nsrR* mutant. As pFK5112 contains integrase the *nsrR* 3XFlag gene would be inserted into the $\Delta nsrR$ chromosome, forming the $\Delta nsrR$ (pN5112) strain. When successful conjugants were identified the strain was used for ChIP-seq analysis.



GGTACCGAGCGGTCCGTGCCGGGGCGGCCGGTCCAGTGACGCACCGCACAGGCTCAGTACCCCGGG
 TAAAGGCGAACCTAGCATGCGCATTTGATAGCGTCTCTG GTGTGCGGTTGACGAAGTTCACCGACCT
GGCGCTGCGTTCGCTCATGCGCTGGCGGTCTGAGAGACGGTGACGAACCACTGGCCACCCGAGA
GGTGGCCGAGGTCGTGGGGGTGCCGTACACGCACGCGGCGAAGGCCATCACCCGCTGCAGCACCT
GGGTGTGGTGGAGGCGGACGCGGTCCGCGGCGCGGGCTGACGCTGACCGACCTGGGCCGGCGCGT
CTCCGTGGGCTGGCTGGTGCCTGAAGTTCGAGGGCGAGGCCGAGGTGGTTCGACTGCGAGGGCGACAA
CCCTGCCCGCTGCGCGGGGCTGCCGGCTGCCGCTGCGCTGCGCGACGCCAGGAGGCGTTCTA
CGCGGCACTCGACCACTGACCGTGACCGACCTGGTGGCCGACCGACCGGCCCGGTTCTGCTCGG
CTGACGGACCGCCCTCGGGAAGGCCTCTCGAG GACTACAAGGACCACGACGGCGACTACAAGGA
CCACGACATCGACTACAAGGACGATGACGACAAGTAGGGGGATCCTCTAGAGTCGACCTGCAGGCA
TGCAAGCTT

Figure 9.13: The plasmids and DNA sequence used to make the *nsrR* flag strain $\Delta nsrR$ (pN5112).
(A) The vector pUCflagF containing the inserted *nsrR*. The *nsrR* gene was inserted into pUCflagF at the KpnI and StuI restriction sites. By inserting *nsrR* into this vector the sequence for a flag tag, containing *Streptomyces* GC rich changes, is downstream of the *nsrR* gene. **(B)** Plasmid map of pN5112, which was constructed with C terminal flag tagged *nsrR* being ligated into pMS82. This plasmid contains an integrase so that the C terminus flag tagged *nsrR* can integrate into the $\Delta nsrR$ chromosome. **(C)** The DNA sequence inserted into pMS82 containing the *nsrR* gene (red), *S. coelicolor* flag tag sequence taken from pUCflagF (yellow), where restriction sites (green) and primers (underlined) are also displayed.

9.2.6 Constructing pGUS Vectors for Analysing Promoter Activity

Once NsrR targets were identified by CHIP-seq binding of NsrR to target promoters was tested by conducting a GUS assay. Target Promoters were inserted upstream and in-frame of the β -glucuronidase gene in the vector pGUS so that promoter activity could be visualised by observing β -glucuronidase production. The 500 bp upstream region of *sco7426*, *nsrR* and *hmpA1* were amplified by PCR. Amplified *sco7426*, *nsrR* and *hmpA1* promoter regions were cloned into pGEMT and prospective transformants were identified by blue/white screening; vectors were tested by restriction digestion.

As successful clones were identified the pGUS vector was digested with KpnI and XbaI and fragments were sub-cloned into pGUS, which were tested by restriction digestion. The 500 bp promoter fragment was isolated from pGUS vectors that had been successfully cloned. As the pGUS *SCO7426*, pGUS *nsrR* and pGUS *hmpA1* vectors had been made successfully they were then conjugated them into *S. coelicolor* wild type and Δ *nsrR* so target expression could be compared in the presence (wild type) and absence (Δ *nsrR*) of NsrR.

A TCTAGACGCCTCCTGGGCGTCGCGCAGCGCACGCCGAGCCGGCAGGCCCGCGCAGCGGGCAGGG
 GTTGTGCCCCTCGCAGTCGACCACCTCGGCCTCGCCCTCGAGTTCACGCACCAGCCAGCCCACGGA
 GACGCGCCGGCCAGGTTCGGTCAGCGTCAGCCCGCCGCGACCCGCTCGCGCTCCACCACACC
 CAGGTGCTGCAGGCGGGTGATGGCCTTCGCCGCGTGCGTGTACGGCACCCCCACGACCTCGGCCAC
 CTCTCGGGTGGCCAGTGGTTCGTCACCGTCTCTCACGACCGCCAGGCGCATGAGCGAACGCAGCGC
 CAGGTTCGGTGAACCTTCGTCAACCGCACACCAGGACGCTATCAAATGCGCATGCTAGGTTTCGCCTTT
 ACCCGGGTACTGAGCCTGTGCGGTGCGTCACTGGACCGGCCGCCCGGCACGGACCGCTCAACGG
 GCGGCGTACGGGCACGGTCGGGCACACGGAACGGCGGCACCTGGTACCATGGCAGCGGAAGACG
 GCGGCTCCCCGGGCACTGCGGGCC

B TCTAGAAGGTACGTACCCCGTCCGGCCCGGCGAGGACGGCCCGGGTTCGAGCCGTGCGGCAGCCAG
 GTCAAAACGCCCCGCGCGCAGTGGGTGCTCGCCGTGCTCGAGTCGAGGCGGGCCGACCCCTCGAGG
 ACGAGGAGCAGGACGTTCGAGGTTCGGCTCGGTGTGGGTGTCCACCCGGCCGCCGGGGAGGCGG
 ACGACGTTGGCGTCGAGCTGCCGGCCGGGTTCCGCCAGCTTCCACAGGGCGCCGGCCGGCGGTCG
 CCGCCAGGGACAGGAGCTCCGCCGTGTCGCACAGCACCCGGGGGAGGGGAGGGCCCGCAGTGCCC
 GGGGAGCCGCCGCTTCCGCTGCCATCAGGTGCCGCCGTTCCGTGTGCCCGACCGTGCCCGTACGC
 CGCCCCGTTGAGCGGTCCGTGCCGGGGCGGCCGGTCCAGTGACGCACCCGCACAGGCTCAGTACCC
 GGGTAAAGGCGAACCTAGCATGCGCATTTGATAGCGTCCTGGTGGTACCCTGCGGTTGACGAAGTT
 CACCGACCTGGCGCTGCGTTCGCTCATGCGCCTGGCGGTTCGTG

C TCTAGACGACCTGGGCGTGCCTTCGCTCATGCGCCTGGCGGTTCGTGAGAGACGGTGACGAACCACT
 GGCCACCCGAGAGGTGGCCGAGGTTCGTGGGGTGCCTACACGCACGCGGCGAAGGCCATCACCCG
 CCTGCAGCACCTGGGTGTGGTGGAGGCGCGACGCGGTTCGCGGCGGGGCTGACGCTGACCGACCT
 GGGCCGGCGCGTCTCCGTGGGCTGGCTGGTGCCTGAACTCGAGGGCGAGGCCGAGGTGGTTCGACTG
 CGAGGGCGACAACCCCTGCCCGCTGCGCGGGGCTGCCGGCTGCGGCGTGCCTGCGCGACGCCCA
 GGAGGCGTTCTACGCGGCACTCGACCCACTGACCGTGACCGACCTGGTGGCCGCACCGACCGGCC
 GGTTCGTGCTCGGCCTGACGGACCGCCCCCTCGGGATGACGGGCGGCGGCCCCCTGAGGCCGTGAGC
 TGTGGCCTAAAACACGAATATCATCTACCAATTAAGGAGTTCGCTGGTACCCTGCTCTCCGAACAGT
 CCGTTCGGTGGTCCGAGCCACC

Figure 9.14: The promoter sequences of *sco7426*, *nsrR* and *hmpA1* cloned into the reporter construct pGUS (Myronovsky *et al.*, 2011). (A) Promoter region of *sco7426* (green) was amplified using primers (underlined) and inserted into pGUS using XbaI and KpnI (yellow). (B) Promoter region of *nsrR* (red) was amplified using primers (underlined) and inserted into pGUS using XbaI and KpnI (yellow). (C) Promoter region of *hmpA1* (blue) was amplified using primers (underlined) and inserted into pGUS using XbaI and KpnI (yellow).